

SPECTRUM FATIGUE LIFETIME AND RESIDUAL STRENGTH  
FOR FIBERGLASS LAMINATES

by

Neil Kelly Wahl

A dissertation submitted in partial fulfillment  
of the requirements for the degree

of

Doctor of Philosophy

in

Mechanical Engineering

MONTANA STATE UNIVERSITY  
Bozeman, Montana

July 2001

APPROVAL

of a dissertation submitted by

Neil Kelly Wahl

This dissertation has been read by each member of the dissertation committee and has been found to be satisfactory regarding content, English usage, format, citations, bibliographic style, and consistency, and is ready for submission to the College of Graduate Studies.

Dr. John F. Mandell

\_\_\_\_\_  
Co-Chairman, Graduate Committee

\_\_\_\_\_  
Date

Dr. Douglas S. Cairns

\_\_\_\_\_  
Co-Chairman, Graduate Committee

\_\_\_\_\_  
Date

Approved for the Department of Mechanical Engineering

Dr. Vic A. Cundy

\_\_\_\_\_  
Head, Dept of Mechanical & Industrial  
Engineering

\_\_\_\_\_  
Date

Approved for the College of Graduate Studies

Dr. Bruce R. McLeod

\_\_\_\_\_  
Graduate Dean

\_\_\_\_\_  
Date

STATEMENT OF PERMISSION TO USE

In presenting this dissertation in partial fulfillment of the requirements for a doctoral degree at Montana State University, I agree that the Library shall make it available to borrowers under rules of Library. I further agree that copying of this thesis is allowable only for scholarly purposes, consistent with "fair use" as prescribed in the U.S. Copyright Law. Requests for extensive copying or reproduction of this dissertation should be referred to Bell & Howell Information and Learning, 300 North Zeeb Road, Ann Arbor, Michigan 48106, to whom I have granted "the exclusive right to reproduce and distribute my dissertation in and from microform along with the non-exclusive right to reproduce and distribute my abstract in any format in whole or in part."

Signature \_\_\_\_\_

Date \_\_\_\_\_

## ACKNOWLEDGMENTS

This work evolved over the past six years and would not have been completed without the guidance of Drs. John Mandell, Douglas Cairns and Herb Sutherland and most certainly would not have been successful without the assistance and friendship of Mr. Daniel Samborsky. I offer them, my sincere appreciation and acknowledge their contributions.

Further thanks are extended to Mr. Samborsky for his photographic contributions to this dissertation.

This study was supported by Sandia National Laboratories through subcontracts AN-0412 and BC 7159, and the U. S. Department of Energy and the State of Montana under the EPSCoR Program, Contract DE-FC02-91ER75681.

## TABLE OF CONTENTS

LIST OF TABLES .....	viii
LIST OF FIGURES .....	ix
ABSTRACT .....	xvii
1. INTRODUCTION .....	1
2. FATIGUE OF MATERIALS .....	6
Background .....	6
Metals .....	10
Fiberglass Laminates .....	21
Laminate Fatigue Description .....	22
Fatigue Trends of Fiberglass Laminates .....	24
3. LIFETIME PREDICTION MODELS FOR COMPOSITE MATERIALS .....	29
Miner's Linear Damage Rule .....	30
Residual Strength Based Models .....	32
Residual Stiffness Based Models .....	34
4. EXPERIMENTAL PROGRAM .....	37
Laminate Selection .....	38
Coupon Design .....	41
Tension-Tension Coupons .....	41
Compression-Compression Coupons .....	45
Reverse Loading Coupons .....	47
Testing Equipment .....	49
Control Software .....	53
Wind Turbine Data Acquisition System .....	54
5. CONSTANT AMPLITUDE FATIGUE TESTING AND RESULTS .....	56
Constant Amplitude Test Results .....	56
Residual Strength of Laminate Under Fatigue .....	69

6. BLOCK SPECTRUM FATIGUE TESTING AND RESULTS .....	73
Sequence Effects .....	74
Two-Block Fatigue Testing .....	77
Multi-Block Fatigue Testing .....	91
7. RANDOM SPECTRUM FATIGUE TESTING AND RESULTS .....	94
WISPER and WISPERX .....	94
WISPERX Modifications .....	96
Modified WISPERX Spectrum Test Results .....	100
Unmodified WISPERX Spectrum Test Results .....	103
8. LIFETIME PREDICTIONS .....	105
Constant Amplitude Fatigue Life Predictions .....	106
Block Spectrum Fatigue Life Prediction Mechanics .....	107
Miner's Rule Lifetime Prediction Methodology .....	107
Residual Strength Rule Based Lifetime Prediction Methodology .....	108
Two-Block Spectrum Fatigue Life Predictions .....	110
General Observations .....	111
Comparison of Residual Strength Based Lifetime Prediction Rules .....	112
Fatigue Model Selection Effect on Predictions .....	113
Three and Six-Block Spectrum Fatigue Life Predictions .....	114
Modified WISPERX Spectra Fatigue Life Predictions .....	116
Block or Cycle Damage Contributions .....	121
Unmodified WISPERX Spectrum Fatigue Life Predictions .....	127
9. SUMMARY, CONCLUSIONS AND RECOMMENDATIONS .....	132
Lifetime Observations and Application to Blade Design .....	133
Comments on Spectrum Effects .....	134
Stress Level Sequencing Effects .....	135
Fatigue Model Selection .....	136
Recommendations for Future Work .....	137
Spectrum Considerations .....	137
Compressive Residual Strength .....	137
Failure Mode Transition .....	138
Residual Strength Model Refinement .....	138
High Cycle Spectrum Fatigue Testing .....	139
REFERENCES CITED .....	140

APPENDICES .....	146
Appendix A - Spectrum Fatigue Database .....	147
Appendix B - Constant Amplitude Fatigue Test Summary .....	167
Appendix C - Multi-Block Fatigue Test Summary .....	180
Appendix D - WISPERX Fatigue Test Summary .....	191
Appendix E - Wind Turbine Blade Strain Data Acquisition System .....	194
Appendix F - Programs for Lifetime Prediction .....	223

## LIST OF TABLES

Table	Page
1. Summary of Ply Orientation Effect on Fatigue Trends . . . . .	28
2. Fiberglass Laminates . . . . .	38
3. Instron 8800 Controller Tuning Parameters . . . . .	50
4. Exponential Regression Analysis Parameters for Constant Amplitude Fatigue . .	60
5. Power Law Regression Analysis Parameters for Constant Amplitude Fatigue . .	62
6. Two-Block Testing Campaigns . . . . .	77
7. Three-Block Test Results . . . . .	91
8. Six-Block Spectrum . . . . .	92
9. Six-Block Test Results . . . . .	92
10. Exponential Regression Analysis Parameters for WISPERX Fatigue . . . . .	100
11. Power Law Regression Analysis Parameters for WISPERX Fatigue . . . . .	101
12. Descriptive Statistics for Constant Amplitude Miner's Sum . . . . .	106
13. Lifetime Prediction Methods . . . . .	110
14. Three-Block Spectrum Fatigue Life Predictions . . . . .	114
15. Six-Block Spectrum Fatigue Life Predictions . . . . .	115



## LIST OF FIGURES

Figure	Page
1. Constant Amplitude Load History . . . . .	2
2. Portion of European Standard Variable Amplitude Fatigue Load History . . . . .	3
3. Micon 65/13 Wind Turbine Blade Edge Bending Moment History . . . . .	4
4. Cyclic Loading Test Parameters . . . . .	7
5. Load Regimes and R-Values . . . . .	7
6. S-N Curve for 7075-T6 Aluminum Alloy, Fully Reversed (R-value = -1) Axial Loading . . . . .	8
7. Goodman Diagram . . . . .	9
8. Hydro-Turbine Shaft Failure . . . . .	11
9. Stress Intensity Factor and Crack Growth Rate Trends . . . . .	14
10. Crack Growth Based Predictions of S-N Fatigue for 7075-T6 Aluminum Plotted on Log-Log Coordinates (Constant Amplitude) . . . . .	15
11. Crack Growth Based Predictions of S-N Fatigue for 7075-T6 Aluminum Plotted on Linear Stress - Log Cycles Coordinates (Constant Amplitude) . . . . .	16
12. Typical Two-Block Spectrum, Second Block Continued Until Failure . . . . .	18
13. Crack Growth Prediction for Two-Block Fatigue of 7075-T6 Aluminum Second Block Continued Until Failure . . . . .	19
14. Calculated Two-Block Fatigue Crack Growth Curves for 7075-T6 Aluminum, Repeated Blocks . . . . .	20
15. Typical Fracture Mechanics Based Predictions for 7075-T6 Aluminum Two-Block Fatigue Miner's Sums . . . . .	21
16. Schematic representation of the development of damage during the fatigue life of a composite laminate . . . . .	23

List of Figures - continued

Figure	Page
17. Comparison of Exponential and Power Law Constant Amplitude Laminate Fatigue Trends on Semi-Log Plot . . . . .	25
18. Laminate Fatigue Trends for Tensile, Compressive and Reversing Constant Amplitude Loads . . . . .	26
19. Normalized Goodman Diagram for Fiberglass Laminates Based on the MSU/DOE Data Base . . . . .	27
20. Effect of Exponent on Residual Miner’s Sum Model (Constant Amplitude Fatigue) . . . . .	32
21. Effect of Exponent on Residual Strength Model (Constant Amplitude Fatigue) . . . . .	34
22. Laminate Residual Stiffness Experimental Trend (Constant Amplitude Fatigue, Carbon/Epoxy) . . . . .	35
23. DD11 Constant Amplitude Fatigue, Preliminary Tests for Scatter, R = 0.1 . . . .	39
24. DD16 Laminate Dry Fabrics . . . . .	40
25. Pin Router . . . . .	42
26. Test Coupon Configurations . . . . .	43
27. Tensile Coupon Failure Examples . . . . .	44
28. Compressive Coupon Failure Examples . . . . .	45
29. Compressive Coupons at Runout . . . . .	47
30. Reversing Coupon Failure Examples . . . . .	48
31. Instron 8872 . . . . .	50
32. Load Demand and Feedback Signals . . . . .	51
33. Constant Amplitude Fatigue Test Results for R = 0.1 . . . . .	57

## List of Figures - continued

Figure	Page
34. Constant Amplitude Fatigue Test Results for $R = 0.5$ .....	57
35. Constant Amplitude Fatigue Test Results for $R = -1$ .....	58
36. Constant Amplitude Fatigue Test Results for $R = 10$ .....	58
37. Constant Amplitude Fatigue Test Results for $R = 2$ .....	59
38. Goodman Diagram Based Upon Exponential Regression Analysis, Including All Data .....	63
39. Goodman Diagram Based Upon Exponential Regression Analysis, Excluding Static Data .....	64
40. Goodman Diagram Based Upon Power Law Regression Analysis, Including All Data .....	64
41. Goodman Diagram Based Upon Power Law Regression Analysis, Excluding Static Data .....	65
42. Normalized Fatigue Models, Exponential Regression, Including All Data .....	65
43. Normalized Fatigue Models, Exponential Regression, Excluding Static Data .....	66
44. Normalized Fatigue Models, Power Law Regression, Including All Data .....	66
45. Normalized Fatigue Models, Power Law Regression, Excluding Static Data .....	67
46. Exponential Fatigue Regression Models For All R-Values, Including All Data .....	67
47. Exponential Fatigue Regression Models For All R-Values, Excluding Static Data .....	68
48. Power Law Fatigue Regression Models For All R-Values,	

Including All Data . . . . . 68

List of Figures - continued

Figure	Page
49. Power Law Fatigue Regression Models For All R-Values, Excluding Static Data . . . . .	69
50. Residual Strength Data for R = 0.1 . . . . .	71
51. Residual Strength Data for R = 0.5 . . . . .	72
52. Excerpt of WISPER Spectrum . . . . .	73
53. Two-Block Sequences (Blocks Repeated to Failure) . . . . .	74
54. Two-Block Sequence Test . . . . .	75
55. Overall Two-Block Miner's Sum, Stresses 325 and 207 MPa, High Amplitude Cycle Ratio of 0.01 . . . . .	76
56. Two-Block Test Results for R = 0.1, 414 & 325 MPa; Exponential Fatigue Model With Linear and Nonlinear Residual Strength and Miner's Rule Lifetime Predictions . . . . .	80
57. Two-Block Test Results for R = 0.1, 414 & 325 MPa; Power Law Fatigue Model With Linear and Nonlinear Residual Strength and Miner's Rule Lifetime Predictions . . . . .	80
58. Two-Block Test Results for R = 0.1, 414 & 235 MPa; Exponential Fatigue Model With Linear and Nonlinear Residual Strength and Miner's Rule Lifetime Predictions . . . . .	81
59. Two-Block Test Results for R = 0.1, 414 & 235 MPa; Power Law Fatigue Model With Linear and Nonlinear Residual Strength and Miner's Rule Lifetime Predictions. . . . .	81
60. Two-Block Test Results for R = 0.1, 325 & 235 MPa; Exponential Fatigue Model With Linear and Nonlinear Residual Strength and Miner's Rule Lifetime Predictions . . . . .	82
61. Two-Block Test Results for R = 0.1, 325 & 235 MPa; Power Law Fatigue Model With Linear and Nonlinear Residual	

Strength and Miner’s Rule Lifetime Predictions . . . . . 82

List of Figures - continued

Figure	Page
62. Two-Block Test Results for R = 0.1, 325 & 207 MPa; Exponential Fatigue Model With Linear and Nonlinear Residual Strength and Miner’s Rule Lifetime Predictions . . . . .	83
63. Two-Block Test Results for R = 0.1, 325 & 207 MPa; Power Law Fatigue Model With Linear and Nonlinear Residual Strength and Miner’s Rule Lifetime Predictions . . . . .	83
64. Two-Block Test Results for R = 0.1, 235 & 207 MPa; Exponential Fatigue Model With Linear and Nonlinear Residual Strength and Miner’s Rule Lifetime Predictions . . . . .	84
65. Two-Block Test Results for R = 0.1, 235 & 207 MPa; Power Law Fatigue Model With Linear and Nonlinear Residual Strength and Miner’s Rule Lifetime Predictions . . . . .	84
66. Two-Block Test Results for R = 0.5, 414 & 325 MPa; Exponential Fatigue Model With Linear and Nonlinear Residual Strength and Miner’s Rule Lifetime Predictions . . . . .	85
67. Two-Block Test Results for R = 0.5, 414 & 325 MPa; Power Law Fatigue Model With Linear and Nonlinear Residual Strength and Miner’s Rule Lifetime Predictions . . . . .	85
68. Two-Block Test Results for R = 0.5, 414 & 235 MPa; Exponential Fatigue Model With Linear and Nonlinear Residual Strength and Miner’s Rule Lifetime Predictions . . . . .	86
69. Two-Block Test Results for R = 0.5, 414 & 235 MPa; Power Law Fatigue Model With Linear and Nonlinear Residual Strength and Miner’s Rule Lifetime Predictions . . . . .	86
70. Two-Block Test Results for R = 0.5, 325 & 235 MPa; Exponential Fatigue Model With Linear and Nonlinear Residual Strength and Miner’s Rule Lifetime Predictions . . . . .	87
71. Two-Block Test Results for R = 0.5, 325 & 235 MPa; Power Law	

Fatigue Model With Linear and Nonlinear Residual  
Strength and Miner’s Rule Lifetime Predictions . . . . . 87

List of Figures - continued

Figure	Page
72. Two-Block Test Results for R = 10, -275 & -207 MPa; Exponential Fatigue Model With Linear and Nonlinear Residual Strength and Miner’s Rule Lifetime Predictions . . . . .	88
73. Two-Block Test Results for R = 10, -275 & -207 MPa; Power Law Fatigue Model With Linear and Nonlinear Residual Strength and Miner’s Rule Lifetime Predictions . . . . .	88
74. Two-Block Test Results for R = 10, -325 & -207 MPa; Exponential Fatigue Model With Linear and Nonlinear Residual Strength and Miner’s Rule Lifetime Predictions . . . . .	89
75. Two-Block Test Results for R = 10, -325 & -207 MPa; Power Law Fatigue Model With Linear and Nonlinear Residual Strength and Miner’s Rule Lifetime Predictions . . . . .	89
76. Two-Block Test Results for R = -1, 173 & 104 MPa; Exponential Fatigue Model With Linear and Nonlinear Residual Strength and Miner’s Sum Lifetime Predictions . . . . .	90
77. Two-Block Test Results for R = -1, 173 & 104 MPa; Power Law Fatigue Model With Linear and Nonlinear Residual Strength and Miner’s Sum Lifetime Predictions . . . . .	90
78. WISPERX Spectrum . . . . .	95
79. Scaled WISPERX Spectrum . . . . .	96
80. Modified WISPERX Spectrum Example . . . . .	97
81. Mod 1 Spectrum for R = 0.1 . . . . .	98
82. Mod 1 Spectrum for R = 0.5 . . . . .	99
83. Mod 2 Spectrum for R = 0.1 . . . . .	99

84. Mod 1 Spectrum Fatigue S-N Curve, R = 0.1 . . . . . 101

85. Mod 1 Spectrum Fatigue S-N Curve, R = 0.5 . . . . . 102

List of Figures - continued

Figure	Page
86. Mod 2 Spectrum Fatigue S-N Curve, R = 0.1 . . . . .	102
87. Unmodified WISPERX Spectrum Fatigue S-N Curve . . . . .	103
88. Miner’s Sum Lifetime Prediction Methodology . . . . .	108
89. Lifetime Prediction Cycle Trace, Residual Strength Models . . . . .	109
90. Mod 1 Spectrum Lifetime Prediction, R = 0.1, Exponential Fatigue Model Including All Data . . . . .	118
91. Mod 1 Spectrum Lifetime Prediction, R = 0.1, Power Law Fatigue Model Including All Data . . . . .	118
92. Mod 1 Spectrum Lifetime Prediction, R = 0.5, Exponential Fatigue Model Including All Data . . . . .	119
93. Mod 1 Spectrum Lifetime Prediction, R = 0.5, Power Law Fatigue Model Including All Data . . . . .	119
94. Mod 2 Spectrum Lifetime Prediction, Exponential Fatigue Model Including All Data . . . . .	120
95. Mod 2 Spectrum Lifetime Prediction, Power Law Fatigue Model Including All Data . . . . .	120
96. Two-Block Stress Level Damage Contributions . . . . .	122
97. WISPERX Spectrum Cycle Count . . . . .	123
98. Stress Level Damage Contributions, Mod 1 Spectrum, R = 0.5, 414 MPa . . . .	124
99. Stress Level Damage Contributions, Mod 1 Spectrum, R = 0.5, 241 MPa . . . .	125
100. Two-Block Load Level Sensitivity, Low-Block Amplitude as Percent	

of High-Block Amplitude (nonlinear residual strength model prediction with $\hat{r} = 0.265$ , exponential fatigue model) . . . . .	126
101. Transition From Tensile to Compressive Failure Mode, Constant Amplitude . . . . .	127

List of Figures - continued

Figure	Page
102. Unmodified WISPERX Spectrum Lifetime Predictions, Exponential Fatigue Model Including All Data . . . . .	130
103. Unmodified WISPERX Spectrum Lifetime Predictions, Power Law Fatigue Model Including All Data . . . . .	130
104. Comparison of WISPERX Lifetime Predictions . . . . .	131
105. Data Acquisition System . . . . .	197
106. Data Acquisition GUI . . . . .	198
107. Playback Software Screen . . . . .	206
108. Goodman Diagram . . . . .	224



## ABSTRACT

Engineering design of cyclically loaded mechanical components requires an understanding of the ability of the chosen material to fulfill a desired lifetime that is dictated by the fatigue properties of the material. Present fatigue lifetime prediction models for fiberglass laminates are non-conservative, prompting inefficient designs and this investigation for improved models.

This dissertation addresses the effects of spectrum loading on lifetime and residual strength of a typical fiberglass laminate configuration used in wind turbine blade construction. Over 1100 tests have been run on laboratory specimens under a variety of load sequences. Repeated block loading at two or more load levels, either tensile-tensile, compressive-compressive, or reversing, as well as more random standard spectra have been studied. Data have been obtained for residual strength at various stages of the lifetime. Several lifetime prediction theories have been applied to the results.

The repeated block loading data show lifetimes that are usually shorter than predicted by the most widely used linear damage accumulation theory, Miner's sum. Actual lifetimes are in the range of 10-20 percent of predicted lifetime in many cases. Linear and nonlinear residual strength models tend to fit the data better than Miner's sum, with the nonlinear providing a better fit of the two. Direct tests of residual strength at various fractions of the lifetime are consistent with the residual strength models. Load sequencing effects are found to be insignificant. The more a spectrum deviates from constant amplitude, the more sensitive predictions are to the damage law used. The nonlinear model provided improved correlation with test data for a modified standard wind turbine spectrum. When a single, relatively high load cycle was removed, all models provided similar, though somewhat non-conservative correlation with the experimental results. Predictions for the full spectrum, including tensile and compressive loads were slightly non-conservative relative to the experimental data, and accurately captured the trend with varying maximum load. The nonlinear residual strength based prediction with a power law S-N curve extrapolation provided the best fit to the data in most cases. The selection of the constant amplitude fatigue regression model becomes important at the lower stress / higher cycle loading cases.

The residual strength models may provide a more accurate estimate of blade lifetime than Miner's rule for some loads spectra. They have the added advantage of providing an estimate of current blade strength throughout the service life.

## CHAPTER 1

### INTRODUCTION

One of the many tasks in the design process for any engineered product has to be the consideration of component life. Life for these products is defined as the length of time that the component is capable of performing its intended service. The lifetime may be limited to a short life of a one time use or cycle in something as simple as a kitchen match. Conversely, a product may experience many millions of cycles of loading, such as that endured by rotating power generation machinery. Such long-life equipment that is subjected to cyclical loading and unloading is susceptible to fatigue failure.

Engineers need some fatigue lifetime estimating tools to assist in the design of products for consumer or industrial use. These tools can provide insight into material selection, size and shape, all to allow the product to achieve a desired lifetime. Development of estimating tools, also termed rules or laws, has proven to be quite successful for metals. A concise history of the evolution of the fatigue work in metals is contained in Reference 1, tracing the evolution from stress-cycle diagrams to linear elastic fracture mechanics and fatigue crack growth life predictions. References 2 and 3 also provide a history of the development of models for metal fatigue.

The development of predictive design tools for fiberglass laminates has lagged that of metals for a number of reasons, one of which is the anisotropic nature of the laminates. While metals have the single damage metric or parameter of crack size, composites have

many more complicated failure modes. Failure of composites may include matrix cracking, delamination, fiber debonding, fiber pullout, fiber buckling, ply delamination, ply failure, and fiber fracture; a typical failure may involve a complex contribution of some or all these possible mechanisms. Although rules based upon nearly every laminate property have been proposed, many seem to have limited validity, with theoretical and actual lifetimes sometimes decades apart [4]. The more complicated models do not seem to yield better results than the linear damage accumulation law first proposed by M. A. Miner in the 1940's [3, 5, 6]. Despite this law's shortcomings, it is used throughout the wind industry, for estimating laminate wind turbine blade lifetimes, e.g., Sandia National Laboratories' computer code LIFE2 [7-9], as well as by many researchers in laminate fatigue [10-12].

Fatigue testing of fiberglass laminates typically involves the constant amplitude sinusoidal loading of a specimen until failure. Illustrated in Figure 1 is data, captured by use

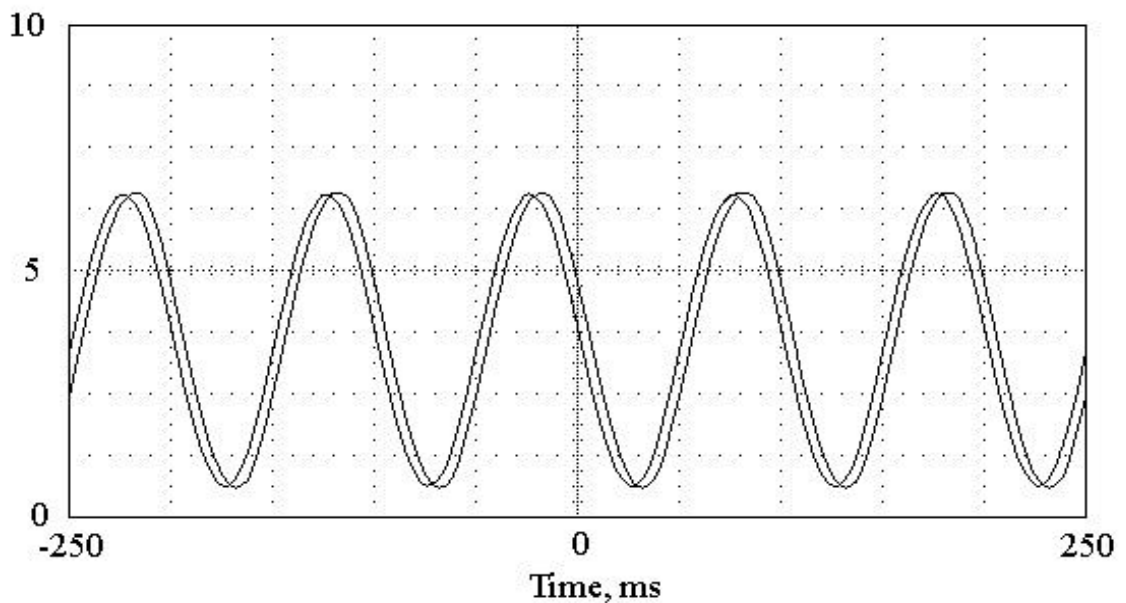


Figure 1. Constant Amplitude Load History

of a digital storage oscilloscope. The data is typical of load cycles used in constant amplitude fatigue testing. In the test; the cycle rate was 10 Hz, with maximum and minimum loads of 6.4 and 0.64 kN, respectively. Shown on the oscilloscope screen capture are both the demand and feedback signals from the test machine controller. The demand signal slightly leads the feedback signal. There is a slight amplitude deviation between the demand and feedback of approximately 1 percent in this example. The variation is a function of the laminate, test frequency, load levels and controller tuning.

Data such as found in References 13 and 14, which consist of the results of constant amplitude testing, are readily available. Unfortunately, constant amplitude testing and the Miner's rule ignore any possibility of load interaction and load sequence effects, which may be particularly important for load spectra that are random in nature. Shown in Figures 2 and 3 are variable amplitude spectrum loading histories for wind turbine blades. Figure 2 is a portion of a European standard loading spectrum [15, 16]; note the single, relatively large

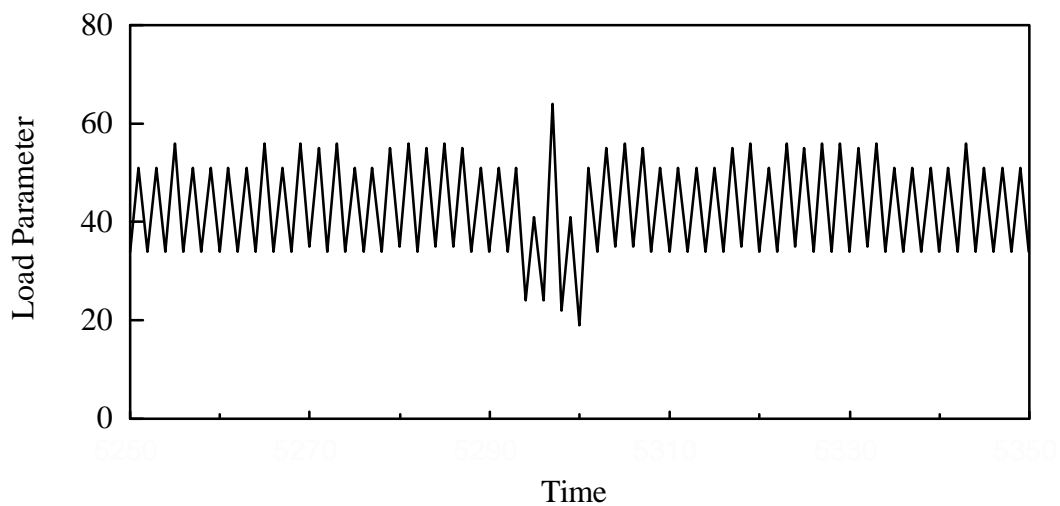


Figure 2. Portion of European Standard Variable Amplitude Fatigue Load History

cycle of higher stress that must be considered in any fatigue model. This European spectrum is a distillation of flap load data collected from near the root of the blades of nine wind turbines in Europe. A portion of the edge bending moment loading of a blade of a Micon 65/13 wind turbine in California is shown in Figure 3 [17]. This loading is typical of a variable amplitude loading spectrum that may be encountered in industry. An arbitrary time scale is shown, as the frequency can be set by the operator when applying these load histories in a laboratory testing program.

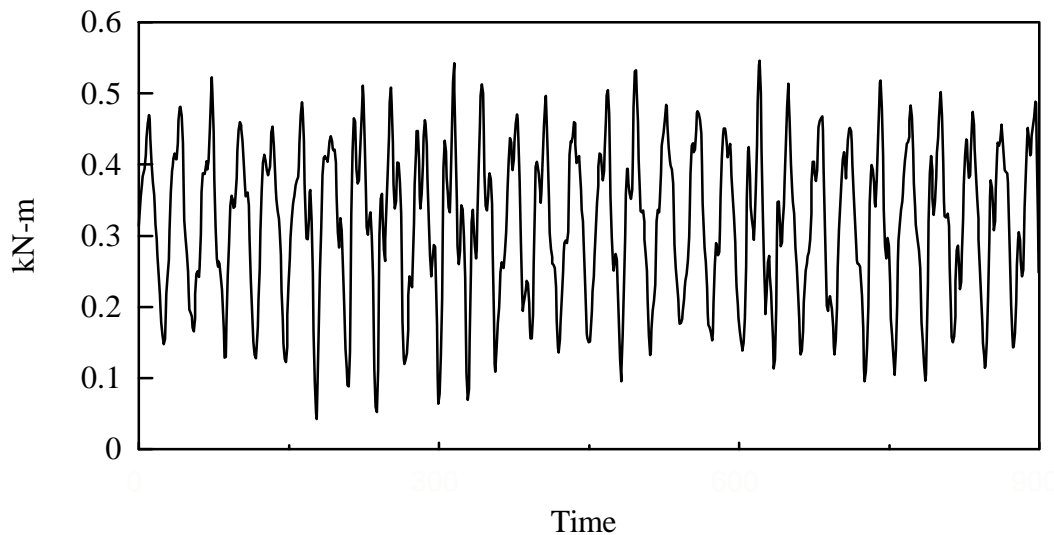


Figure 3. Micon 65/13 Wind Turbine Blade Edge Bending Moment History

Researchers and wind energy industry authorities have spelled out a need for improved life estimating rules and for the study of variable amplitude or spectrum loading [4, 8, 18]. The goal of the research presented by this dissertation was to investigate improvements to lifetime prediction rules for fiberglass laminates used in the construction of wind turbine blades. Any model that would be readily accepted must be easy to use,

contain a minimum of parameters, and be accurate [19].

Very few researchers have undertaken an investigation of lifetime prediction models that started at the simplest of fatigue cases and logically progressed through an ever increasing complexity. Most research efforts can be characterized as a study of constant amplitude fatigue followed by the development of a lifetime prediction model, and, finally, an attempt to verify the model by analyzing the fatigue of specimens subjected to a two-block spectrum, with the second block run to failure. Sendekyj [19] and Bond [20] itemized a research program that would lead to the development of a rational life prediction model. The work, herein summarized, attempts to follow those guidelines [19]; namely,

1. establish an experimental program to investigate the damage process of the laminate
2. determine a valid damage measurement method (metric)
3. develop a life prediction rule based upon the established metric
4. experimentally validate the life prediction rule.

The experimental program should begin with constant amplitude fatigue testing and progress to block spectra fatigue testing [20].

## CHAPTER 2

## FATIGUE OF MATERIALS

Fatigue is typically defined as the failure of a material due to repeated loading at levels below the ultimate strength. The general nature of fatigue for the two common materials, metals and fiberglass laminates, will be reviewed in this chapter along with some fundamentals of fatigue testing.

Background

Fatigue of materials subjected to cyclic loading (Figures 1, 2 and 3) is dependent upon not only the maximum stress level encountered, but also the range of the stresses applied. Generally, the greater the maximum stress, and the greater the range, greater damage is encountered. Although there are a variety of methods for describing each cycle of loading of a specimen, the method normally accepted for laminates is the maximum stress and R-value.

$$R - value = R = \frac{\mathbf{s}_{\min}}{\mathbf{s}_{\max}} \quad (1)$$

where  $\sigma_{\min}$  is the minimum stress level  
 $\sigma_{\max}$  is the maximum stress level

Summarized in Figure 4 are the basic descriptions of the various cycle stress parameters.

Displayed in Figure 5 are a grouping of typical R-values as well as an identification of the primary loading regimes.

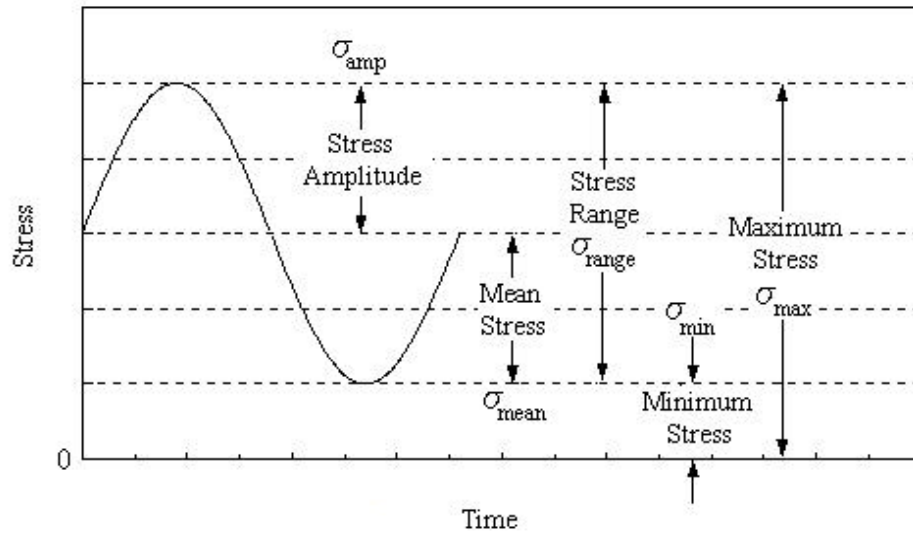


Figure 4. Cyclic Loading Test Parameters

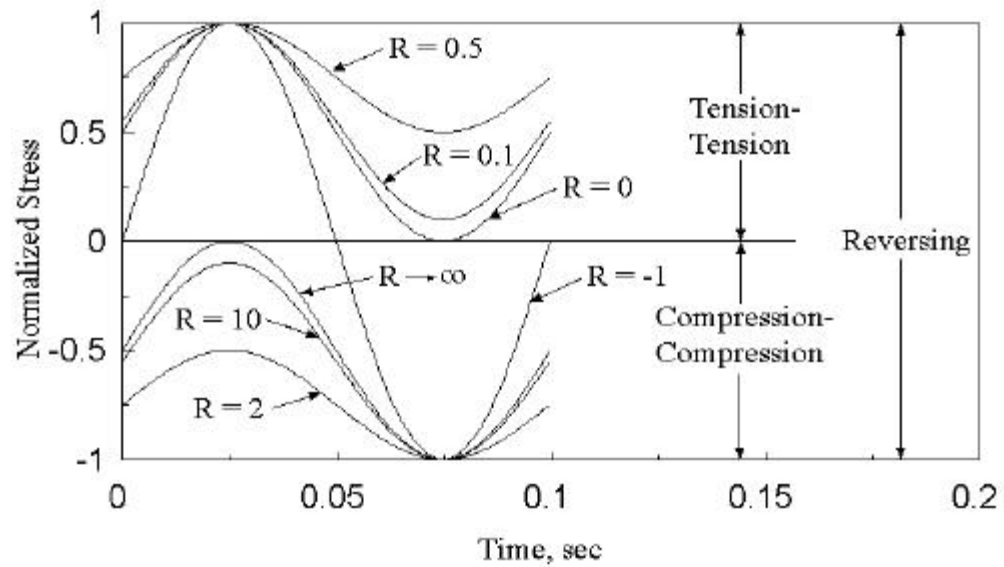


Figure 5. Load Regimes and R-Values



Constant amplitude testing of a material at a constant R-value, but at a family of maximum stress levels is typically summarized in stress-cycle (S-N) diagrams. The information displayed on an S-N diagram is usually the maximum stress level as a function of the number of cycles to failure on a semi-log plot. Figure 6 [3] is a typical S-N diagram and for 7075-T6 aluminum.

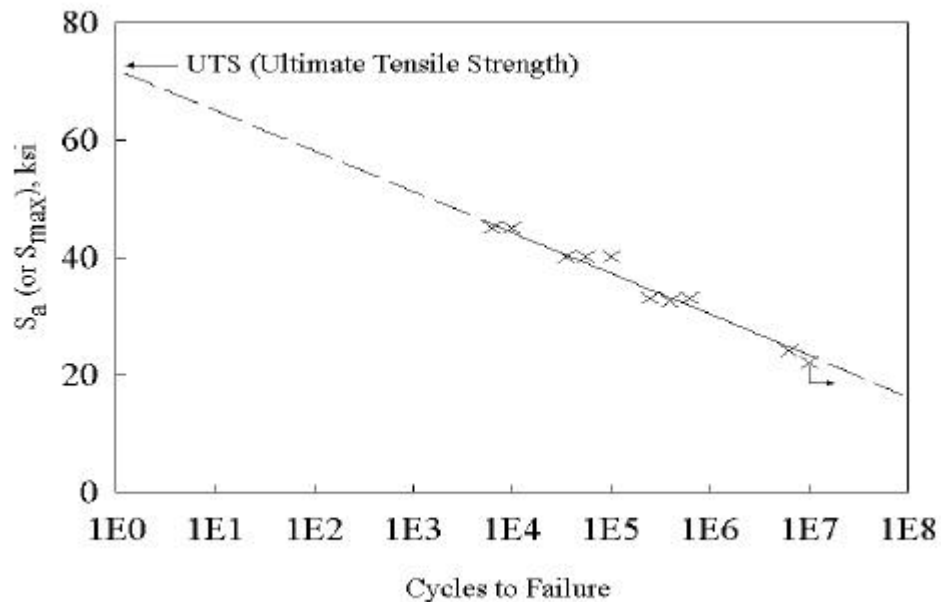


Figure 6. S-N Curve for 7075-T6 Aluminum Alloy, Fully Reversed (R-value = -1) Axial Loading [3]

Constant amplitude testing at a variety of R-values can be summarized within a Goodman diagram, see Figure 7, relating the alternating stress to the mean stress. Each set of tests at a constant R-value is represented by a straight line as defined in Equation 2. Small amplitude and consequently, longer tests are closer to the origin on any selected radial line

of constant R-value.

$$s_{alt} = \frac{1-R}{1+R} * s_{mean} \tag{2}$$

where  $\hat{\sigma}_{alt}$  is the alternating stress value =  $\hat{\sigma}_{amp}$

R = R-value

$\hat{\sigma}_{mean}$  = mean stress level

A slope of zero represents the ultimate tensile strength test, while a slope of 180° represents an ultimate compressive strength test.

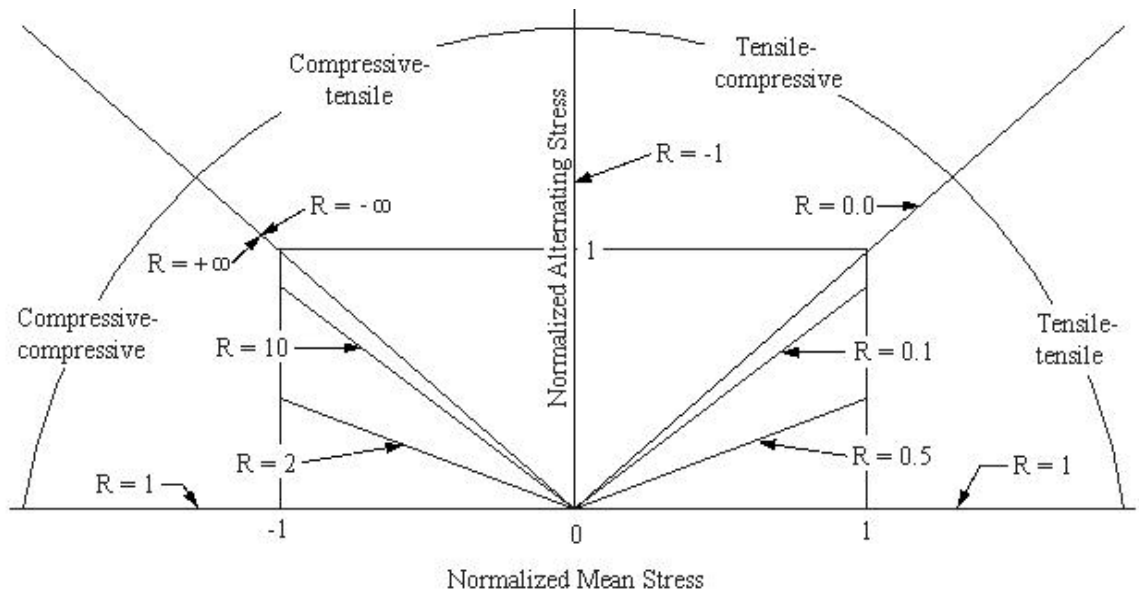


Figure 7. Goodman Diagram

Metals

This author performed repairs of Montana Power Company's failed hydro-turbine shafts at the Madison Plant in southwestern Montana. The turbine shafts of these 2.5 MW units were horizontal and supported vertically at three journal bearings. The general shape of the shaft was quite involved, yet failures occurred at the minimum diameters near the bearing surfaces. The fracture surface exhibited an initiation point at a surface flaw and crack growth from that point until catastrophic failure due to insufficient strength to support the applied torsional load. Typical "beach mark" bands or striations were visible in the region where the crack had progressed. These striations occur when a high cyclic stress causes a rapid crack growth. Reference Figure 8 during the following description of the fracture surface. The fracture surface in the crack growth region was relatively smooth, due to working of the surfaces as the crack opened and closed. The fracture surface in the region of final failure exhibited some ductile characteristics of localized yielding of the material. Failure of the input shaft of Montana Power Company's Colstrip Unit #1A boiler feed pump was nearly identical to the hydro-turbine shaft. In this case, the crack initiation point was at the root of a key slot. The failure surface was again comprised of essentially three regions; crack initiation, crack growth and final failure.



Figure 8. Hydro-Turbine Shaft Failure

Historically, the first serious concern for fatigue failure in metals came with the expansion of the railway industry in the mid 19<sup>th</sup> century. Early investigations by Wöhler led to the summary of constant amplitude fatigue in diagrams relating stress and life (S-N diagrams). These diagrams can be considered a means for life prediction for metals subjected to constant amplitude loading. Estimates of S-N diagrams can be developed from fundamental material properties, thereby speeding the design process by minimizing laboratory fatigue testing. Other investigators, Gerber and Goodman [1], researched the effects of the mean and range of stresses upon lifetimes. For a given maximum stress level, the greater the stress range the greater the cyclic damage. Diagrams relating the mean and

alternating stresses bear the names of these gentlemen.

Palmgren proposed [21] and Miner developed [5] the first cumulative damage rule in attempts to account for variable amplitude cyclic loading. Frequently, the “Miner’s rule” is called a linear model, relating to the linear addition of damage contributions of each cycle of loading. Each cycle is considered to contribute damage in the amount of the fractional amount of life expended at that cycle’s constant amplitude equivalent.

$$\text{Miner's Sum} = \sum_i \frac{n_i}{N_i} \quad (3)$$

where  $i$  is the cycle sequential index

$n_i$  is the number of cycles at stress level  $\sigma_i$

$N_i$  is the number of constant amplitude cycles to failure at stress level  $\sigma_i$

Miner’s work in aluminum revealed a wide variation in the predictive capability of this linear damage rule. The rule is incapable of accounting for any sequence effects for a variable amplitude load spectrum. Sequencing effects or load interactions such as work hardening and “overstressing” are not addressed by this rule [5]. Overstressing is the loading sequence of first applying high loads and then cycling the material to failure at lower loads. The rule also cannot satisfy the consequences of a single large cycle that can cause catastrophic failure with little contribution to the damage rule.

Irwin can be considered the father of linear elastic fracture mechanics (LEFM) and fatigue crack growth lifetime predictions. During the last half of the 20<sup>th</sup> century, failure of aircraft and bridges due to crack growth led to the development and acceptance of fracture mechanics for lifetime predictions [1, 2, 22, 23].

It is generally understood and approximated that the crack growth rate is a function

of the stress intensity factor as the Paris law [2, 22, 23].

$$\frac{da}{dN} = C\Delta K^m \quad (4)$$

where  $a$  is the crack size

$N$  is the number of cycles of loading

$\Delta K$  is the stress intensity factor range

$C$  and  $m$  are constants for the material

This equation is valid over a portion of the lifetime or crack growth history. The relationship fits the middle range of the overall S-shaped crack growth rate versus  $\Delta K$  curve on a double logarithmic plot as shown in Figure 9 [24]. At the low stress intensity factors of region I, crack growth is extremely slow, leading to the postulate that crack growth does not occur below some threshold value,  $K_{th}$ . Region II covers a major portion of the crack growth and is modeled as the Paris law, equation 4. Rapid crack growth occurs in region III, as the maximum stress intensity factor approaches some critical stress intensity factor  $K_c$ .

The stress intensity factor,  $K$ , is approximated with Equation 5 [2, 22, 23].

$$K = S_a Y \sqrt{\pi a} \quad (5)$$

where  $S_a$  is the applied stress

$Y$  is a geometric factor

$a$  is the crack length

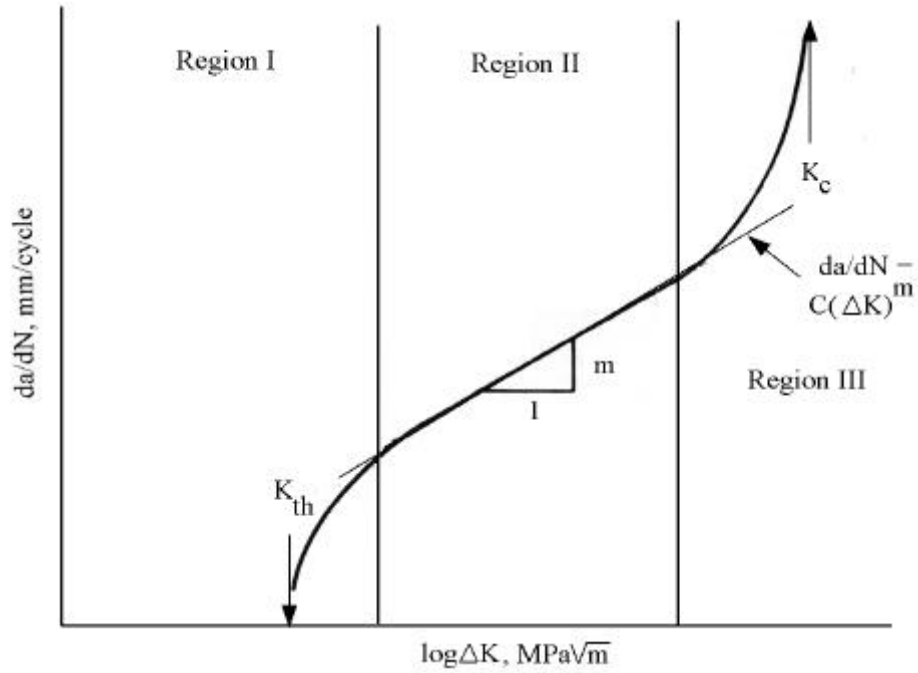


Figure 9. Stress Intensity Factor and Crack Growth Rate Trends

Substitutions, rearrangement and integration of the above two equations results in an expression relating the number of cycles required to grow a crack between two sizes ( $Y$  is taken as 1.0):

$$N = \frac{1}{CS_a^m} \left( \frac{2}{-m+2} \right) a_i^{\frac{-m+2}{2}} \Big|_{a_d}^{a_i}, \quad (m \neq 2) \quad (6)$$

where  $a_d$  is the minimum detectable crack size  
 $a_i$  is some increased crack size  
 $N$  represents the number of required cycles  
 $S_a$  is the applied stress  
 $C$  and  $m$  are constants for the material

The LEFM method was used to estimate lifetimes for a 7075-T6 aluminum alloy using properties as found in References [1] and [22]. Estimates were made for constant amplitude and two-block loading spectra. Depicted in Figure 10 is an S-N summary of the results of calculations for the constant amplitude loading case. Note the relative effect of the variation of the R-value (equation 1) on the fatigue of the material. The greater the stress range the more damaging the loading, just as will be seen for fiberglass laminates. Displaying the results on a semi-log plot, Figure 11, rather than log-log (or power) plot reveals the appearance of a flattening at high cycles, which could be interpreted as approaching an endurance limit, or more properly, a threshold value for the stress intensity factor, below which crack growth would not be present.

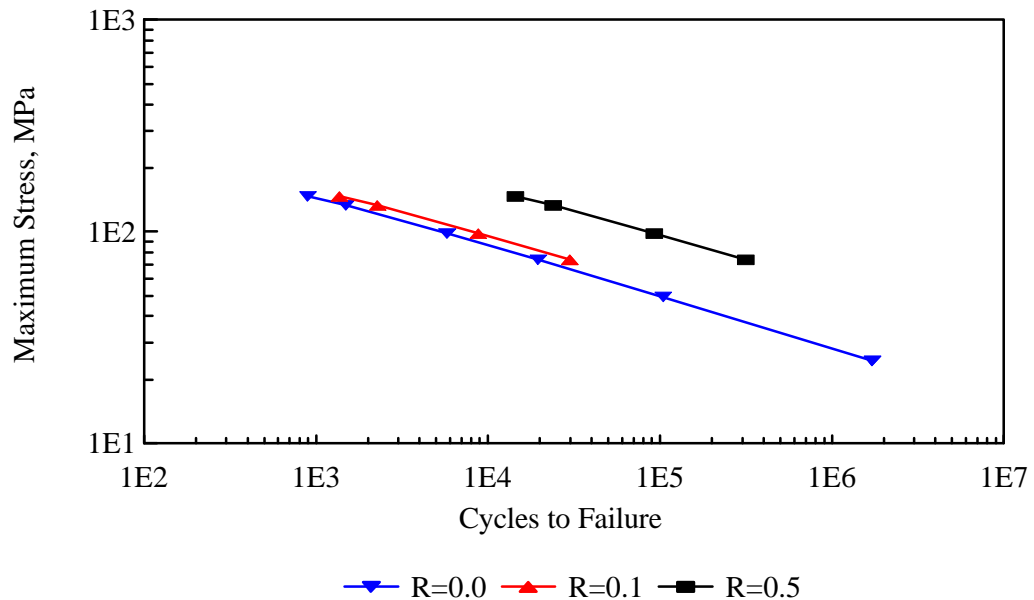


Figure 10. Crack Growth Based Predictions of S-N Fatigue for 7075-T6 Aluminum Plotted on Log-Log Coordinates (Constant Amplitude)



Load sequencing effects can be important in the fatigue of metals. Crack growth in constant amplitude fatigue has been found to be slowed by a high load cycle or overload [22]. The type of overload has a great effect on the crack growth rate or retardation. Tensile overloads can retard crack growth whereas compressive overloads will offer little effect by themselves or will cause a reduction of the beneficial retardation of a prior tensile overload. The amount of retardation is dependent upon the size of the plastic zone created at the crack tip during a tensile high load cycle. Upon relaxation of the high load, the material in the plastic zone will be in compression. The following “normal” cycles must cause the crack to progress through this compressed zone before continuing at the faster rate.

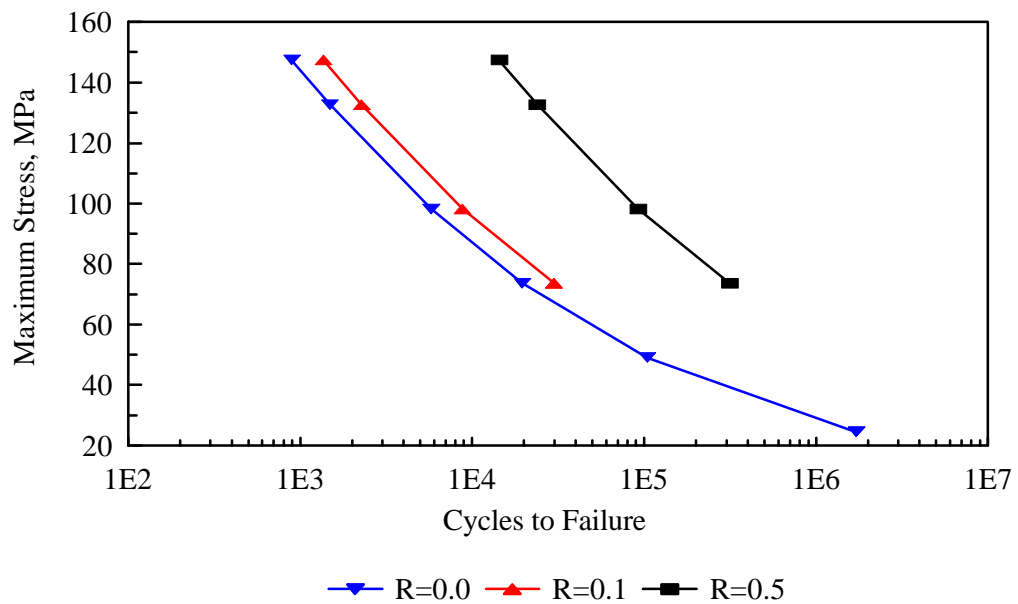


Figure 11. Crack Growth Based Predictions of S-N Fatigue for 7075-T6 Aluminum Plotted on Linear Stress - Log Cycles Coordinates (Constant Amplitude)

Models for retardation are discussed in References [2] and [22]. The Wheeler

retardation model was applied in the following fatigue calculations for variable amplitude spectra. Software was developed (Appendix F) to speed calculations. The Wheeler model was chosen to allow verification of the software calculations by comparison to examples in Reference [22].

The plastic zone size was approximated by

$$r_p = C \frac{K^2}{\sigma_{ys}^2} \quad (7)$$

where  $r_p$  is the plastic zone size  
 $K$  is the stress intensity factor  
 $\sigma_{ys}$  is the yield strength  
 $C$  is a constant

This equation was used to determine the size of the overload plastic zone and the zone during crack extension under “normal” load cycles.

The retardation factor was determined from

$$f = \left( \frac{r_{pi}}{l} \right)^m \quad (8)$$

where  $\ddot{o}$  is the retardation factor  
 $r_{pi}$  is the plastic zone size for the  $i^{\text{th}}$  cycle  
 $\ddot{e}$  is the remaining distance the crack must travel to pass through the plastic overload plastic zone  
 $m$  is a material property

The retardation factor ( $\leq 1$ ) converges towards unity as the crack moves through the overload plastic zone.  $\ddot{o}$  is applied to the crack growth rate,  $da/dN$ , thereby modeling the slower crack growth.

Once the baseline calculations for constant amplitude fatigue were established, spectra containing two blocks, similar to that shown in Figure 12, were considered.

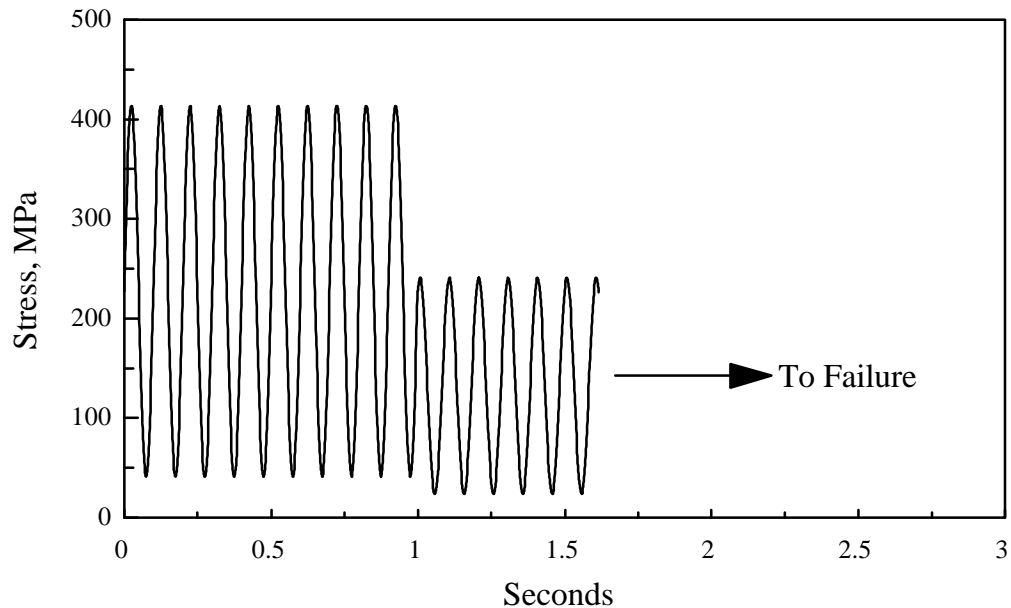


Figure 12. Typical Two-Block Spectrum, Second Block Continued Until Failure

This prompted the addition of crack retardation within the linear elastic fracture mechanics model to include the influence of load interactions. The Wheeler crack retardation model [22, 23] was implemented during the calculations involving two-block spectra. The results of a typical two-block calculation, with the second block run until a critical crack size ( $a_c$  based on  $K_{Ic}$ ) are shown in Figure 13. The example case is comprised of a first block of 1000 cycles of 130 MPa (R-value = 0) followed by 2447 cycles of 100 MPa (R=0) stress level. The transition between the two blocks is evident by the discontinuity in slope at the 1000 cycle point. The calculated Miner's sum for this case was 1.09. Retardation played little role in this case in that the two stress levels were relatively close, thereby allowing the cycles of

the second block to rapidly progress through the plastic zone created by the “overload” of the last cycle of the first block.

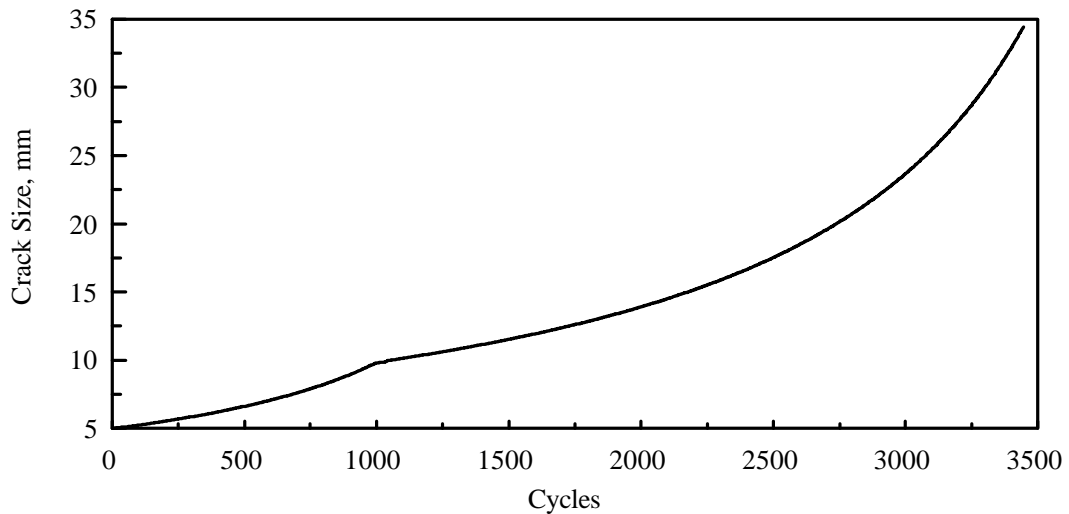


Figure 13. Crack Growth Prediction for Two-Block Fatigue of 7075-T6 Aluminum  
Second Block Continued Until Failure

Another method of applying two-block spectra was to set the sizes of both blocks and repeat the series of blocks until the fatigue model indicated a critical crack size had been reached. Depicted in Figure 14 are three cases of block sizes; 10 high amplitude cycles followed by 1000 low amplitude cycles (10/1000) as well as 10/100 and 10/10. The Miner’s sums at failure for these cases were 0.9, 0.84, and 1.1 respectively for the block sizes of 10/1000, 10/100 and 10/10.

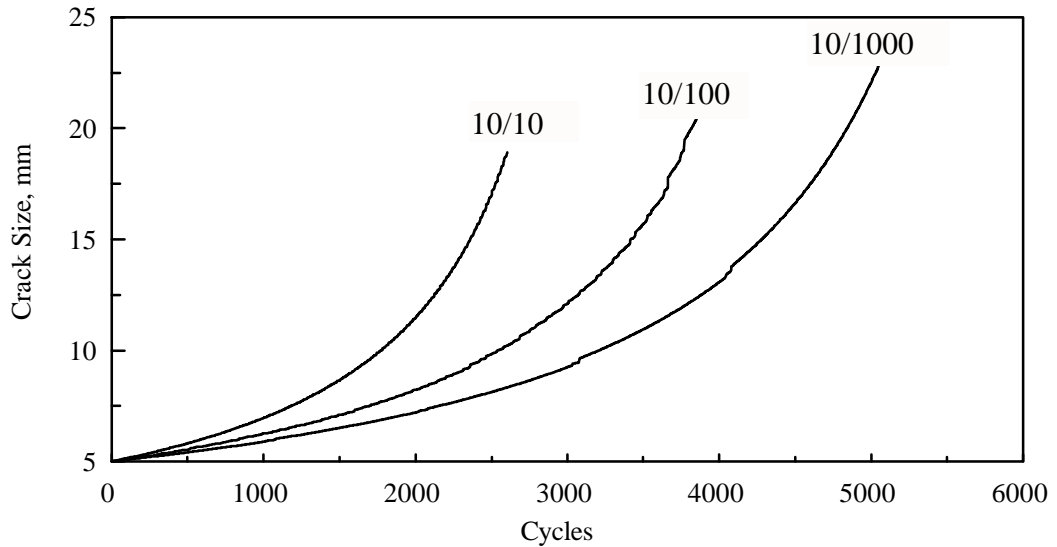


Figure 14. Calculated Two-Block Fatigue Crack Growth Curves for 7075-T6 Aluminum, Repeated Blocks

Figure 15 is an alternate method (that will be used extensively for the fiberglass laminate presentations) of representing the Miner's sum for these two-block spectra. The general shape of the Miner's sum curves are probably dependent upon the amount of retardation due to the relative differences between the high and low amplitude cycles. Note for the case of the greater difference, 130/70 MPa, retardation seemed to have slowed the crack growth to the point of benefitting the life and hence Miner's sums trending greater than one. The second case of 130/100 MPa, seems to have little retardation of the crack growth rate and in fact there seemed to be a detrimental interaction of these two loads. The former case was not seen in the laboratory testing, nor for the prediction rule calculations for fiberglass laminates, while the latter was nearly universally present.

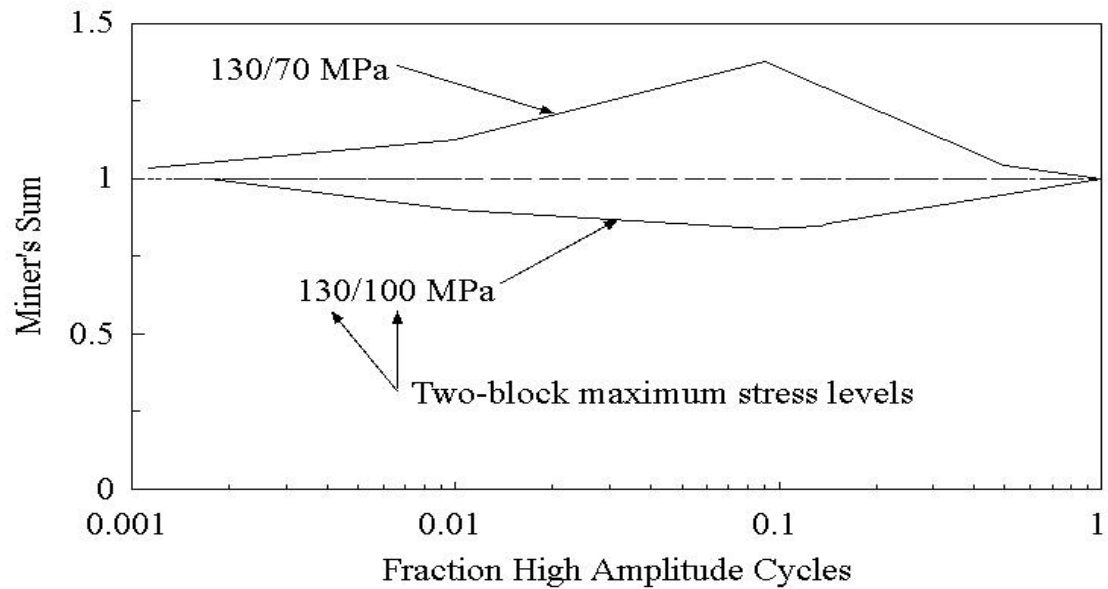


Figure 15. Typical Fracture Mechanics Based Predictions for 7075-T6 Aluminum Two-Block Fatigue Miner's Sums

### Fiberglass Laminates

The damage metric of metals is chiefly that of crack growth, whereas for laminates there is no clear, dominant metric. Damage can be attributed to a variety of contributors, such as fiber breakage, matrix cracking, fiber debonding and pullout and delamination.

The laminate under consideration in this research was comprised of E-glass (electrical grade) reinforcement and a thermoset matrix. Each of these constituents play roles in the strength and fatigue resistance of the laminate. The tensile properties for loading in the fiber direction are fiber dominated, while compressive properties are matrix dominated [24].

### Laminate Fatigue Description

The following description of the progression of fatigue damage of laminates is summarized from References 24 and 25. Reifsnider [24] provided a detailed analysis of the progression of fatigue damage in laminates as shown in Figure 16. This analysis considers both tensile and compressive loads as well as a variety of laminate ply orientations. Upon initial tensile cyclic loading, at levels below the ultimate strength, matrix cracks in the off-axis plies occur first. This cracking will continue until a pattern or spacing of the matrix cracking becomes saturated. This spacing is dictated by the ability of the laminate to redistribute the loads to the material between cracks. This degree of damage has been termed a characteristic damage state, which also signals a transition from one stage of damage development to another.

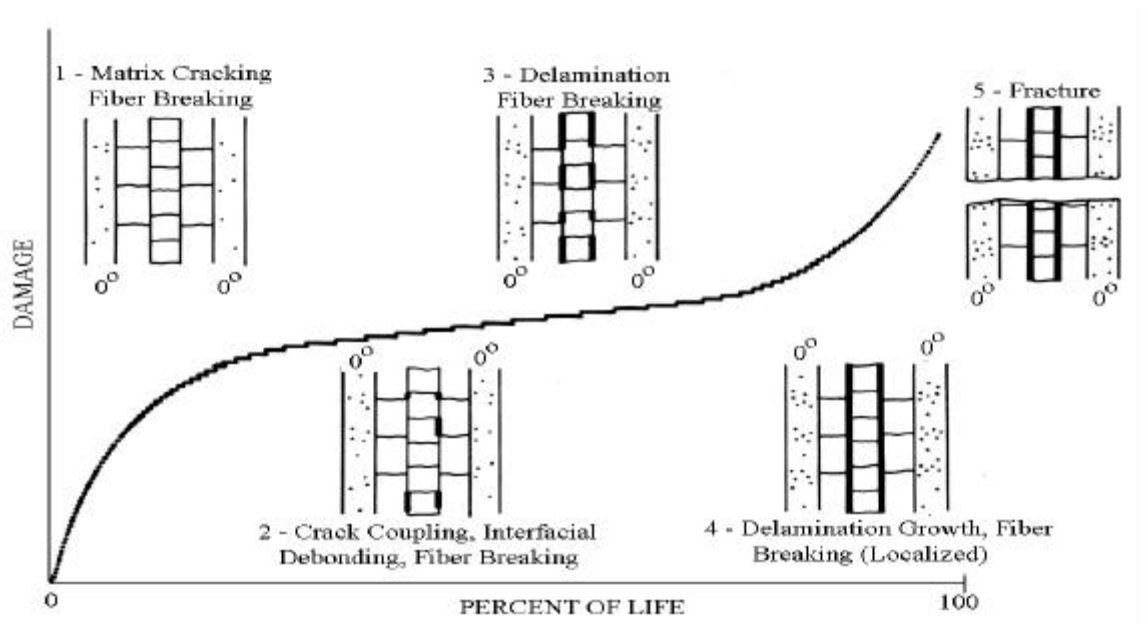


Figure 16. Schematic representation of the development of damage during the fatigue life of a composite laminate [24]

Upon continued cyclic loading, matrix cracking continues, but may develop in

interlaminar areas and along axial fibers, causing a coalescing and interdependence of cracking, ultimately leading to localized delamination. Compressive excursions will promote this delamination process, not providing a damage retardation as was discussed for fatigue in metals.

Continued cycling will cause a spreading of and interaction of localized damage. Loads will be redistributed causing some fiber damage, breakage, debonding and delamination growth. With continuation of cycling, the load carrying capacity will be reduced to levels that can no longer support the applied load. The failure is sudden and catastrophic, with fiber breakage and pull out described as “brooming”.

The damage manifests itself in changes of bulk properties such as stiffness and residual or remaining strength of the laminate. After initiation of damage (analogous to loading metals at stresses that produce a stress intensity factor above its threshold) the damage accumulates rapidly at first and then accumulates more slowly. This acceleration and deceleration of damage is not consistent with the continual increase of damage accumulation (crack length) in metals (Figures 13 and 14). The damage accumulation in laminates is consistent with the initial rapid loss of stiffness and then a slowing of the stiffness reduction [26, 27]. This is also proposed in Chapter 3 as related to the loss of residual strength of laminates.



Constant amplitude fatigue testing of laminates is generally summarized in stress-cycle (S-N) diagrams and represented in models as either linear on semi-log (equation 9) or log-log (equation 10) plots for exponential or power law trends, respectively.

$$\frac{\mathbf{s}}{\mathbf{s}_0} = C_1 - b * \log(N) \quad (9)$$

$$\frac{\mathbf{s}}{\mathbf{s}_0} = C_2 * N^{-1/m} \quad (10)$$

where  $\sigma$  is the maximum applied stress  
 $\sigma_0$  the ultimate strength  
 N the number of cycles to failure  
 $C_1, C_2, b$  and  $m$  are regression parameters

Rearrangement of equations 9 and 10 to solve for N, led to equations 11 and 12. Equation 11 is exponential in form, while equation 12 is of the power law form.

$$N = 10^A \quad (11)$$

where  $A = \left[ \frac{C_1 - \frac{\mathbf{s}}{\mathbf{s}_0}}{b} \right]$

$$N = \left( \frac{s}{C_2 s_0} \right)^{-m} \quad (12)$$

Typical S-N curves for these fatigue regression analyses are shown in Figure 17.

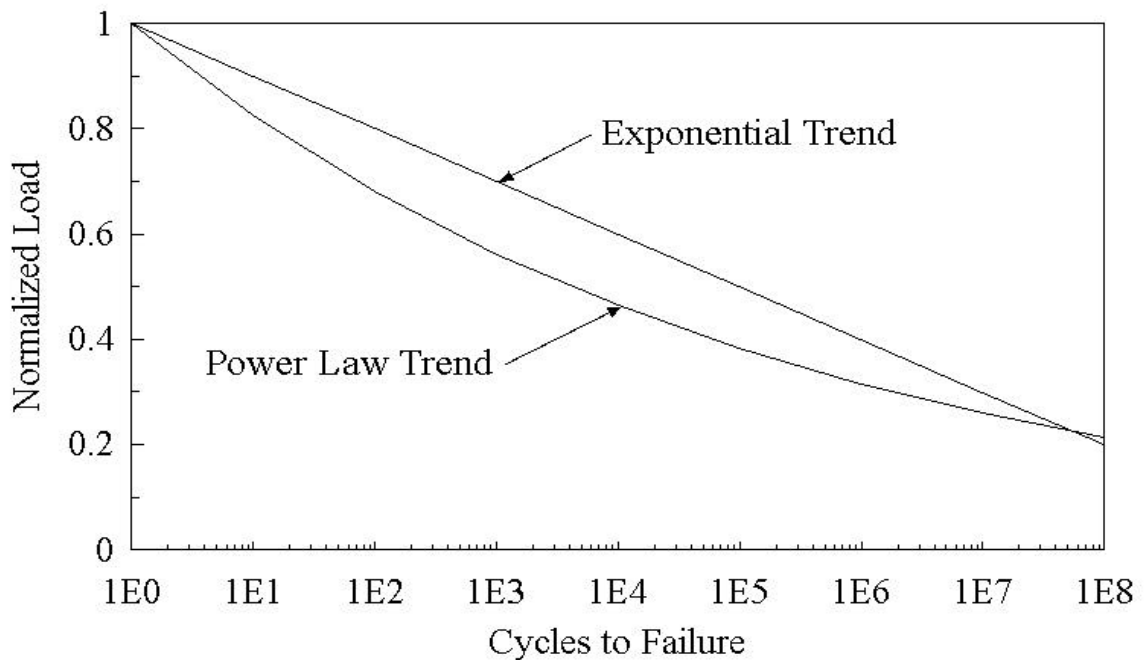


Figure 17. Comparison of Exponential and Power Law Constant Amplitude Laminate Fatigue Trends on Semi-Log Plot

Much of the early work used exponential fits and semi-log plots, with the power law representation and log-log plots becoming popular with the advent of high cycle testing. Questions have arisen as to which is the better fatigue model (regression equation) for use in lifetime prediction methods involving extrapolation to higher cycles [4, 9, 28-32]. The selection of the “best” fit may be the cause of a shift in the failure prediction at some fraction

of the laminate's life [33]. This seems somewhat subject to the material, type of loading and the fraction of life expended.

A general rule has been promoted for quick comparison of the fatigue sensitivity of various laminates comprised of  $0^\circ$  and off axis plies. The stress or strain normalized slope,  $b$ , of the exponential regression has frequently been touted as 0.1 (10 percent per decade) for “good” fiberglass laminates in tension ( $R = 0.1$ ), while a slope of 0.14 has been considered a “poor” material response [13, 34]. The general trend for the better laminates in compression ( $R = 10$ ) is 0.07 (7 percent per decade), while the poorer laminates follow a fatigue trend of 0.11 (11 percent per decade) [34]. Reversing load ( $R = -1$ ) fatigue response ranges from 0.12 to 0.18 (12 to 18 percent per decade). These fatigue trends are summarized in Figure 18.

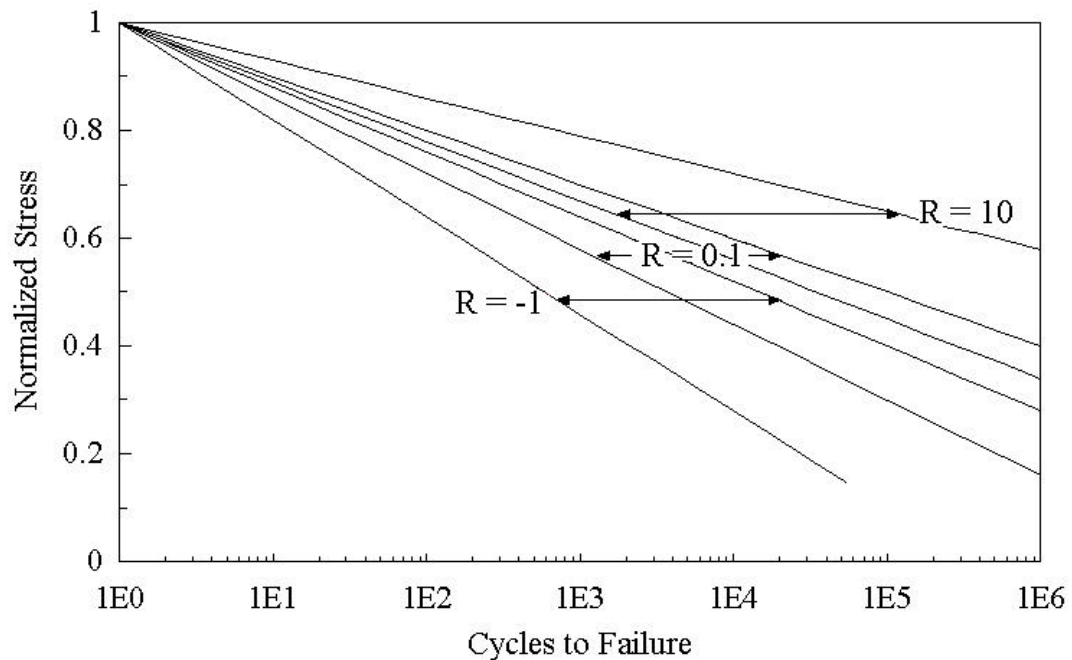


Figure 18. Laminate Fatigue Trends for Tensile, Compressive and Reversing Constant Amplitude Loads

Sutherland and Mandell [9] compiled a Goodman diagram, Figure 19, based upon the data of Reference 13. Note the asymmetry, relating to the differences in the tensile and compressive fatigue properties.

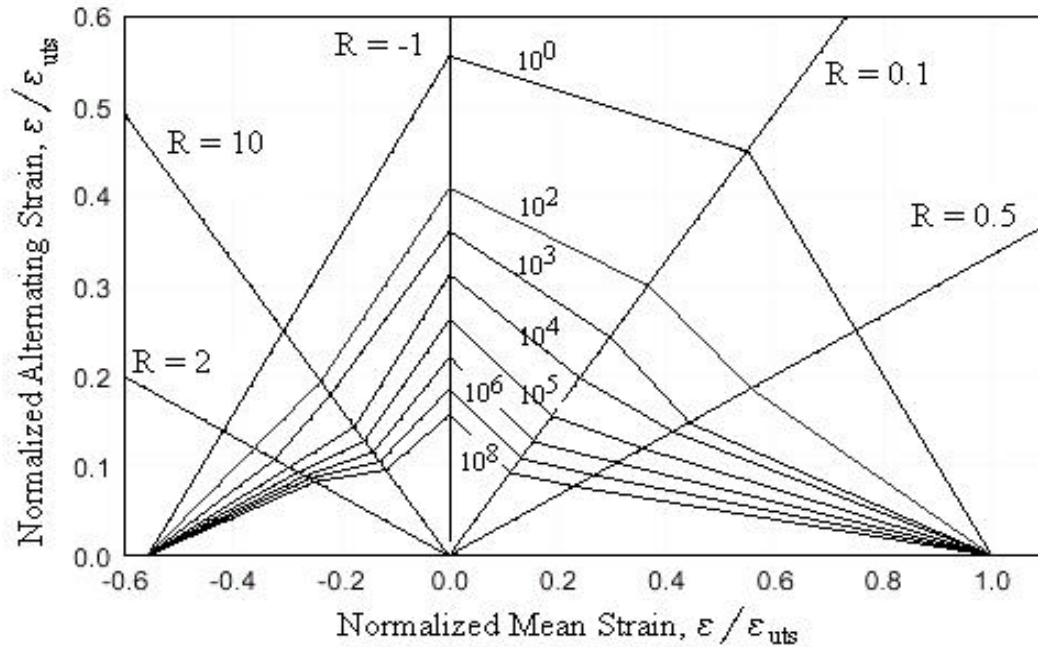


Figure 19. Normalized Goodman Diagram for Fiberglass Laminates Based on the MSU/DOE Data Base [9]

The fatigue sensitivity of unidirectional laminates does vary with fiber volume fraction, with the increase in fiber volume fraction resulting in increased magnitudes for the exponential regression parameter  $b$ . This is ostensibly due to the increased likelihood of fiber-to-fiber contact damage with the increased fiber volume. The fiber volume range summarized in Reference 34 was from 0.3 to approximately 0.6.

The effect of the content of  $0^\circ$  plies of the laminate is summarized in Table 1 [13]. The tensile fatigue trend is poorer in the laminates containing combinations of  $0^\circ$  and  $\pm 45^\circ$

plies and improves at the extremes of contents of these orientations. The compressive fatigue trend improves with greater 0° ply content.

Table 1. Summary of Ply Orientation Effect on Fatigue Trends

Percent 0° Plies	b, R = 10	b, R = 0.1
0, ( $\pm 45^\circ$ only)	0.106	0.113
16	0.114	0.116
24	0.115	0.128
28	0.088	0.124
39	0.095	0.128
50	0.089	0.128
55-63	-	0.121
69-85	0.072	0.118
100 (0° only)	0.073	0.111

The laminate studied in this research will be compared to the above laminate fatigue trends in Chapter 5.

## CHAPTER 3

## LIFETIME PREDICTION MODELS FOR COMPOSITE MATERIALS

Lifetime prediction models for laminates have been developed from the basis of nearly every conceivable property of the materials. Engineering mechanical properties such as stiffness and/or compliance [35-37], natural frequency [38], damping [38, 39], and residual strength [40-46] as well as micromechanical properties such as crack density [24], fiber-matrix debonding and pullout, and delamination [47] have been applied towards development of lifetime prediction models. Other models are based upon properties determined by simple fatigue tests of laminates and more evolved statistical analyses [40] of the material. Some researchers have applied linear elastic fracture mechanics, a method considered appropriate for isotropic materials such as metals, to the analysis of fatigue in composites. Regardless of the efforts expended upon the development of reliable models, and of the model's complexity, most researchers still compare the results of their work to the simple, linear model proposed by Miner [5]. The leap from the theoretical, advanced models to their practical use seems to be daunting. Computer codes that have been developed for the fatigue lifetime analysis for wind turbine blade design still use the first model, Miner's linear damage rule [7, 8, 40, 48], and have not applied the newer, and reportedly more reliable models. Practicing engineers prefer simple, easy to apply models, for their use in the design of components.

### Miner's Linear Damage Rule

The early work on aluminum by Miner [5] resulted in a simple linear damage accumulation rule that was based upon constant amplitude fatigue test results. The basis of this rule is that the damage contribution of each load level is equal to its cycle ratio, which is the number of cycles experienced at that load level divided by the number of constant amplitude cycles to failure at that same load level. The damage contributions of each load level are algebraically added to allow determining an overall damage level. Symbolically this can be represented as

$$D = \sum \text{Cycle Ratios} = \sum_i \frac{n_i}{N_i} \quad (13)$$

where  $D$  is a quantified damage accumulation parameter previously termed Miner's sum in equation 3

$i$  is the indexing parameter related to the number of different load levels

$n_i$  is the number of cycles experienced at a  $\sigma_i$  maximum stress level

$N_i$  is the number of constant amplitude cycles to failure at the stress level  $\sigma_i$ .

Typically, failure is taken to occur when  $D$  reaches unity, as originally proposed by Miner.

The crack growth model discussed earlier for metals used Miner's rule to accumulate crack extension, but failure was considered from the point of view of reaching a critical stress intensity factor. For future reference and comparison to other lifetime prediction models,  $D_R$  is defined as the residual Miner's sum.

$$D_R = 1 - D \quad (14)$$

Miner's original work with aluminum exhibited a range of values for  $D$  from 0.61 to 1.49, but with an average of 1.0 and a standard deviation of 0.25. Miner reported that his

model did not include any provisions to account for the possibility of load interactions such as related to work hardening. The Miner's rule has limitations in that it does not account for any possible sequencing effects or the fact that the component may fail upon a significant large event that does not numerically contribute greatly to  $D$ . The latter is sometimes referred to as a "sudden death behavior," such as reaching  $K_c$  in the metals crack growth example.

Several researchers have proposed modifications to Miner's rule to coax the damage parameter,  $D$ , closer to unity. Performing a square root, or for that matter any other root, forces the damage parameter closer to unity [12, 20, 40, 49]. Others merely acknowledge that the damage parameter may not be unity, and propose values other than one, such as 0.1 [48]. Any superiority of these modifications is often due to fitting of model constants to particular experimental data [3].

Graphically, Miner's rule can be viewed as shown in Figure 20. The straight line relationship represents the Miner's original linear rule, whereas the line lying below represents a prediction based upon applying a square root to the linear rule. The upper line represents the prediction should an exponent greater than one be applied.

This model has been tested by application of a two stress level spectrum of loads [10, 41]. The first set of cycles at a constant stress level constitutes a loading block. The second block of cycles at a second stress level was run to specimen failure. Empirical results for testing of fiberglass laminate (13 plies of  $0^\circ$  and  $90^\circ$  oriented e-glass fibers in an epoxy matrix) indicated a range of 0.29 to 1.62 for Miner's sum [41]. The general observation was that for a block of high amplitude cycles followed by a block of low amplitude cycles would



result in Miner's sums greater than one. The opposite sequencing of a low amplitude block followed by a high amplitude block resulted in Miner's sum less than one.

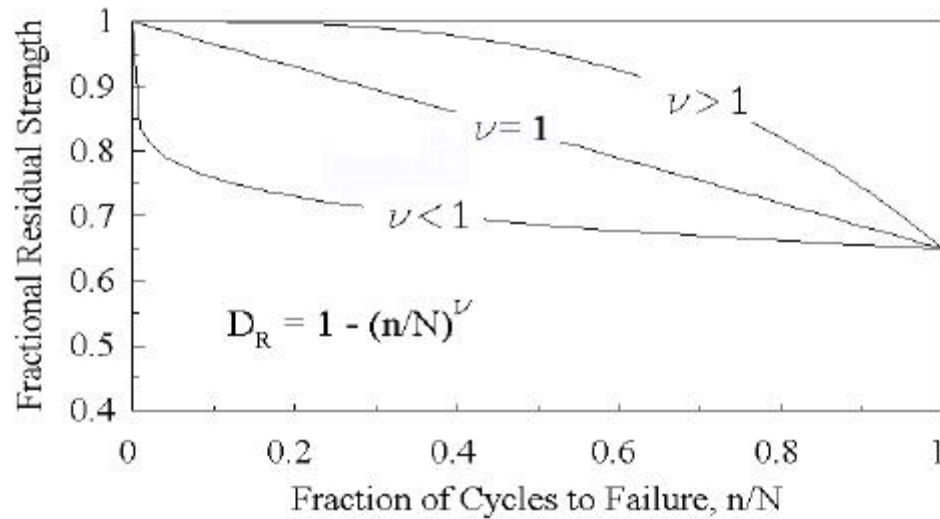


Figure 20. Effect of Exponent on Residual Miner's Sum Model (Constant Amplitude Fatigue)

### Residual Strength Based Models

A concept of a material's progressive loss of strength during fatigue has led several researchers to investigate models with this basis [10, 19, 38, 41-46]. In a sense, this parallels the crack growth model for metals with failure when  $K$  reaches  $K_c$ . Broutman and Sahu [41] were one of the earliest to develop a model founded upon residual strength changes during fatigue. Their model was based upon a linear loss of strength with cycles of fatigue, as represented by:

$$\mathbf{s}_R = \mathbf{s}_0 + \frac{\mathbf{s}_i - \mathbf{s}_0}{N} * n \quad (15)$$

where  $\sigma_R$  is the residual strength  
 $\sigma_i$  is the maximum applied stress level  
 $\sigma_0$  is the static strength of the specimen  
 $N$  is the number of constant amplitude cycles to failure at the stress level of  $\sigma_i$   
 $n$  is the number of cycles experienced at stress level  $\sigma_i$

Broutman and Sahu [41] reported the residual strength lifetime prediction rule also satisfies the sequencing effects of high/low and low/high blocks of constant amplitude cycles. Spectra of a high amplitude block followed by a low amplitude block exhibited Miner's sums greater than one if the second block is run to failure. The opposite spectrum of a low followed by a high amplitude block yielded Miner's sums less than one.

Many investigators of residual strength and/or residual stiffness have argued that the residual strength is not a linear function of the number of cycles, but rather non-linear [10, 19, 42-44, 46]. This prompted a modification of the residual strength model to include non-linear possibilities:

$$s_R = s_0 + (s_i - s_0) * \left(\frac{n}{N}\right)^{\lambda} \quad (16)$$

where the parameter,  $\lambda$ , is termed the strength degradation parameter [42-44]. Strength degradation parameters greater than one define laminates that exhibit little loss of strength throughout most of their life and suffer a sudden failure at the end of life. Parameters less than one represent laminates that suffer the greater damage in their early life. A value of unity for  $\lambda$  reduces equation 16 to the linear model of equation 15.

The general shape of the residual strength curve, Figure 21, is uncertain. Upon considering a simple link between residual stiffness and residual strength, researchers have shown all possible ranges of the strength degradation parameter. This variation leads one

to consider that the strength degradation parameter is a material property and hence variable from laminate to laminate.

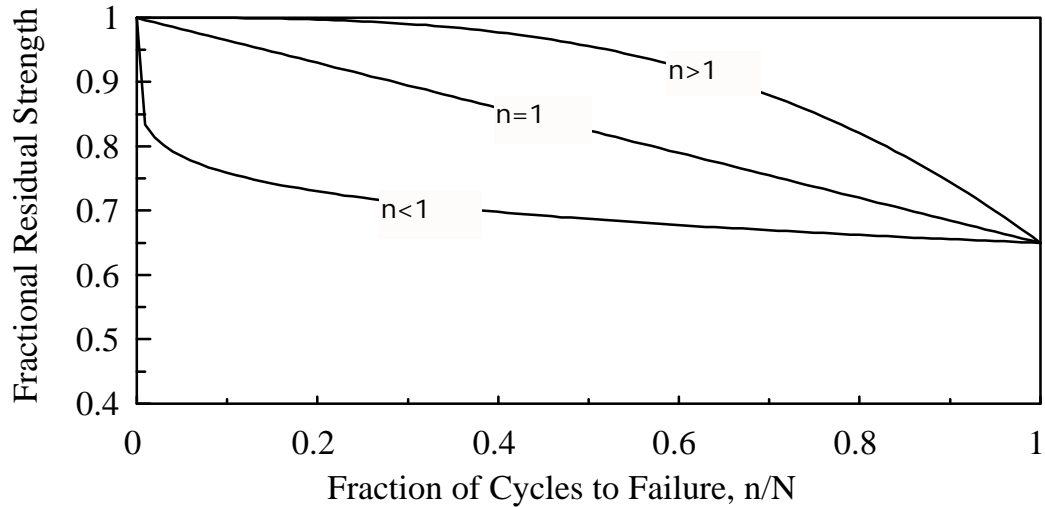


Figure 21. Effect of Exponent on Residual Strength Model (Constant Amplitude Fatigue)

### Residual Stiffness Based Models

Another proposed model, similar to the residual strength model, is one based upon the change in stiffness,  $E$ , of a material undergoing fatigue [19, 35-37, 45, 50]. The residual stiffness prediction model represented by Equation 17 was proposed by Yang, et. al. [35] and is similar to the nonlinear residual strength model proposed by Schaff and Davidson [42-44]

$$E(n) = E(0) - \left[ E(0) - E(n_k) \right] * \left( \frac{n}{n_k} \right)^{\nu(k)} \quad (17)$$

where  $E(n)$  and  $E(n_k)$  are the stiffnesses at cycles  $n$  and  $n_k$  respectively  
 $E(0)$  is the initial stiffness  
 $\nu(k)$  is the fitting parameter.

The fitting parameter is considered to be a function of the applied stress level and perhaps even the number of cycles experienced. Experimental results for a graphite laminate of  $[90/\pm 45/0]_s$  layup were  $E(0) = 53.8$  GPa,  $E(10,000) = 42$  GPa, and  $\nu(10,000) = 0.162$  (dimensionless). These data were used to generate a graphical representation, Figure 22, of the change in the normalized stiffness over a normalized life.

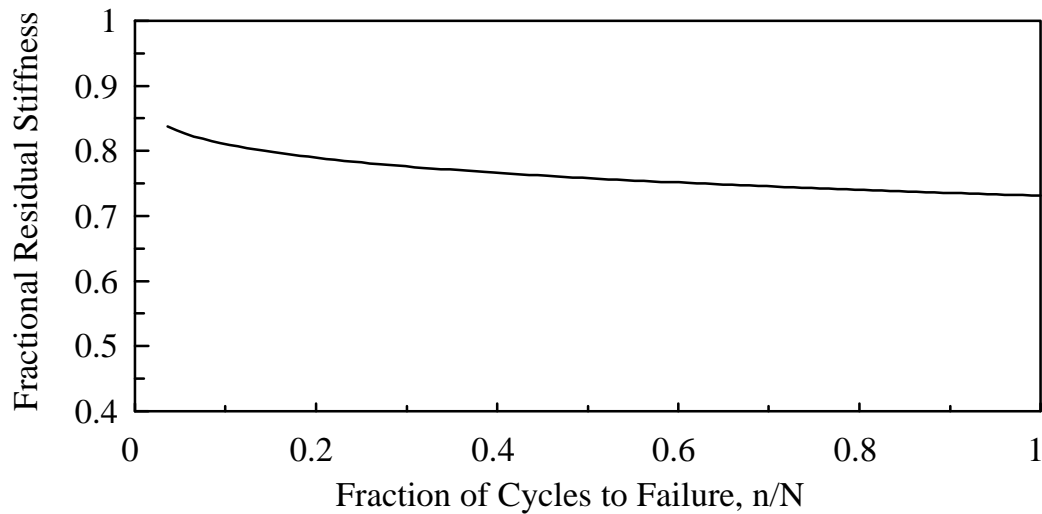


Figure 22. Laminate Residual Stiffness Experimental Trend  
 (Constant Amplitude Fatigue, Carbon/Epoxy)

Note the similarities of the graphs, Figures 21 and 22. The nonlinear residual strength model based upon a strength degradation parameter less than one presents a similar trend as the results of residual stiffness testing by Yang, et. al. [35] and Bach [36].

## CHAPTER 4

## EXPERIMENTAL PROGRAM

A laboratory test program was developed in attempts to ensure the performance of meaningful fatigue tests. This program included the selection of a typical wind turbine blade fiberglass laminate, design of test specimens, test of laboratory equipment capability, and the execution of planned fatigue tests. The underlying goal was to first perform constant amplitude tests that could be compared with the results of other investigators and then methodically increase the complexity of the loading spectrum.

Investigation of variable amplitude fatigue, including that of two-block load levels can be hampered by the scatter of the testing results. The scatter in constant amplitude fatigue data can be due to testing techniques, specimen preparation, variation in the material itself and the variability of fatigue mechanisms. For data presented in References 1 and 3 there appears to be less scatter at the higher stress tests than at the lower stress tests; this may be due to a “flattening” of the S-N trend. With large scatter of data, the fatigue contribution of each load level in multi-load level testing becomes indistinguishable. Effects of several of these contributing factors can be minimized with proper design of test procedures and fabrication techniques.

Laminate Selection

The choice of the fiberglass laminate was to be one that would be typical of those used in wind turbine blade construction and one that would yield meaningful fatigue test results. The laminate materials and configuration or lay-up can have an effect on the statistical results of fatigue testing. Three different laminates were considered for testing; DD5, DD11 and DD16. The laminate designations are described in References 13 and 34 and in Table 2.

Table 2. Fiberglass Laminates

Material	Percent Fiber Volume	Ply Configuration	Matrix	Fabric Description
DD5	38	$[0/\pm 45/0]_S$	P	0's - D155 45's - DB120
DD11	31	$[0/\pm 45/0]_S$	P	0's - A130 45's - DB120
DD16	36	$[90/0/\pm 45/0]_S$	P	0's & 90's - D155 45's - DB120
P - orthopolyester matrix, CoRezyn 63-AX-051 by Interplastics Corp. A130, D155 & DB120 - Owens Corning Fabrics				

Since this research was to consider spectrum loading effects on the fatigue life of fiberglass laminates, the statistical scatter of constant amplitude load testing was to be minimized. A related factor, the tendency of some coupons to fail near the grip, was also to

be minimized under various loading conditions; the addition of 90° outside plies helped in this respect. Of the three laminates listed in Table 2, upon testing, the DD16 was chosen to be best suited for variable amplitude testing. Summarized in Figure 23 are preliminary constant amplitude fatigue test results for the material DD11. Note the unacceptable scatter in the life for the material when loaded to a maximum stress level of slightly greater than 400 MPa. The life for the material when subjected to fatigue at a stress level of 414 MPa was indistinguishable from that at the higher stress level of 475 MPa. The nearly two decades of scatter in the cycles to failure at the 414 MPa load level were deemed unacceptable, and would have been undoubtedly even greater for lower stress tests. Similar, but not as pronounced results were also observed for test results of the DD5 material fatigue. In retrospect, the scatter has since been found to also depend on the variations in the particular reinforcing fabric [34].

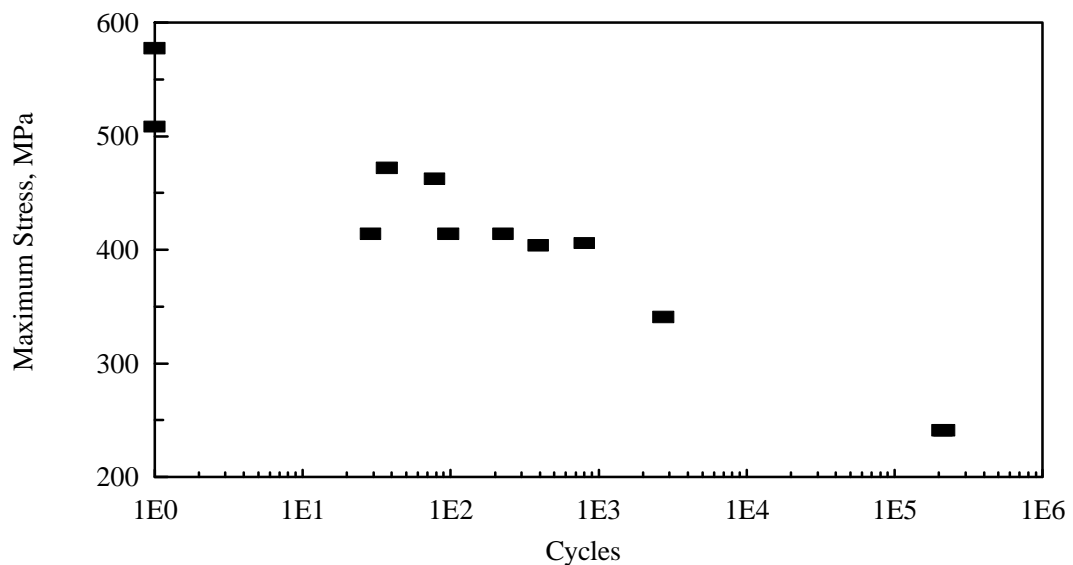


Figure 23. DD11 Constant Amplitude Fatigue, Preliminary Tests for Scatter,  $R = 0.1$



The material that produced acceptable scatter results was termed DD16 in the database of Reference 13. DD16 was comprised of Owens Corning D155 (stitched unidirectional) and DB120 (stitched  $\pm 45^\circ$ ) fabrics in a  $[90/0/\pm 45/0]_S$  lay-up for a total of ten plies and eight layers of fabric. The  $90^\circ$  plies on the outside were thought to produce more reliable gage-section failures, as noted earlier. Photographs of the fabrics are shown in Figure 24. Plates of this material were fabricated by a resin transfer molding (RTM) process with Interplastics Corporation CoRezyn 63-AX-051 orthopolyester matrix to an average fiber volume of 0.36. Details can be found in References 13 and 34.

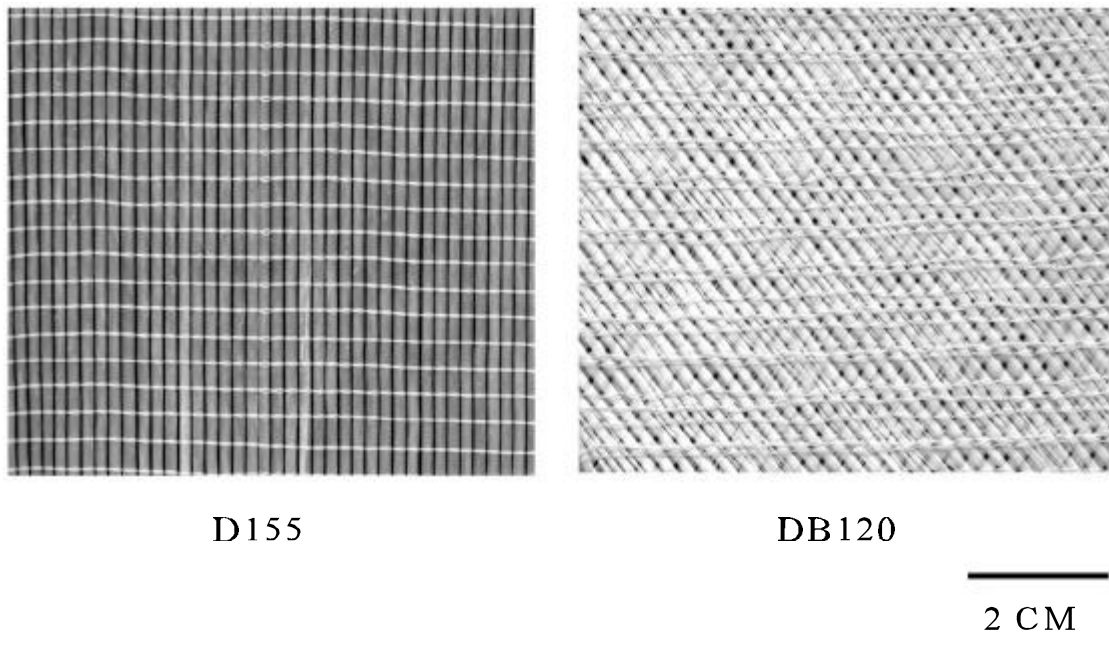


Figure 24. DD16 Laminate Dry Fabrics

### Coupon Design

Coupons were designed for the type of load testing to be fulfilled, whether for tensile-tensile (T-T), compressive-compressive (C-C), or reverse loading. These regimes of loading and their respective R-values are detailed in Figure 5 of Chapter 2. The location and mode of failure was the factor used to determine the acceptability of the specimen design. The failure mode was to be attributed to the fatigue loading, and not to other factors such as thermal degradation, elastic buckling or gripping effects. Similarly, the location of the failure should be in the gage section as opposed to in or adjacent to the grips. The long history of test coupon geometry development for various fiberglass materials can be found in References 13 and 34.

#### Tension-Tension Coupons

Tensile-tensile specimen blanks were rectangular in shape, typically 12.7 mm wide by 4 mm thick and 64 to 75 mm long. These blanks were then individually machined to a dog-bone style with a pin router, clamping jig, and master pattern as shown in Figure 25. The profile of each edge was machined sequentially. Machined surfaces were then cleaned with sanding screen to remove any fiber “burrs”. Sanding screen was also used to roughen the grip areas in preparation for the addition of tab material. G10 fiberglass tab material, manufactured by International Paper, Inc., was attached to facilitate distribution of testing machine gripping forces. The tabs were 1.6 mm thick with length and width varying dependent upon the test type, as shown in Figure 26. Attempts to perform tensile tests

without tabs were not successful, due to laminate failure in the grips of the testing machine. Specimens with straight sides, with or without tabs, were also deemed not acceptable; failures occurred in the grips.

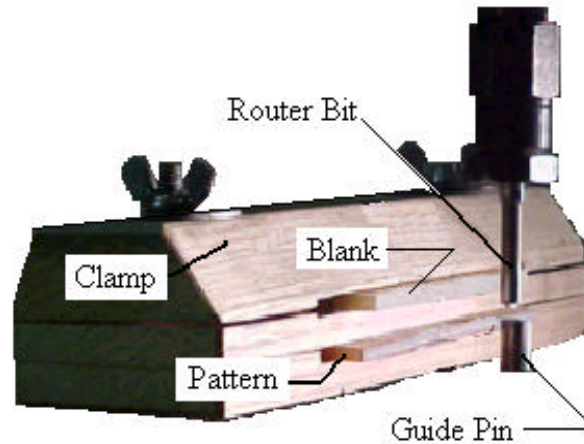


Figure 25. Pin Router

Specimens with a gage section and tabs, Figure 26, were tested and found to be a successful coupon design. Typical examples of fatigue failures of these tensile specimen are shown in Figure 27. Failures occurred in the gage section and were typical of laminate tensile fatigue failures; the matrix material was severely fractured, fibers were pulled out, broken and “brooming” at the failure. This final design for a tensile test specimen is similar to that for metal-matrix specimen as per ASTM Standard D 3552, rather than the ASTM Standard D 3039 for polymeric-matrix specimens [51].

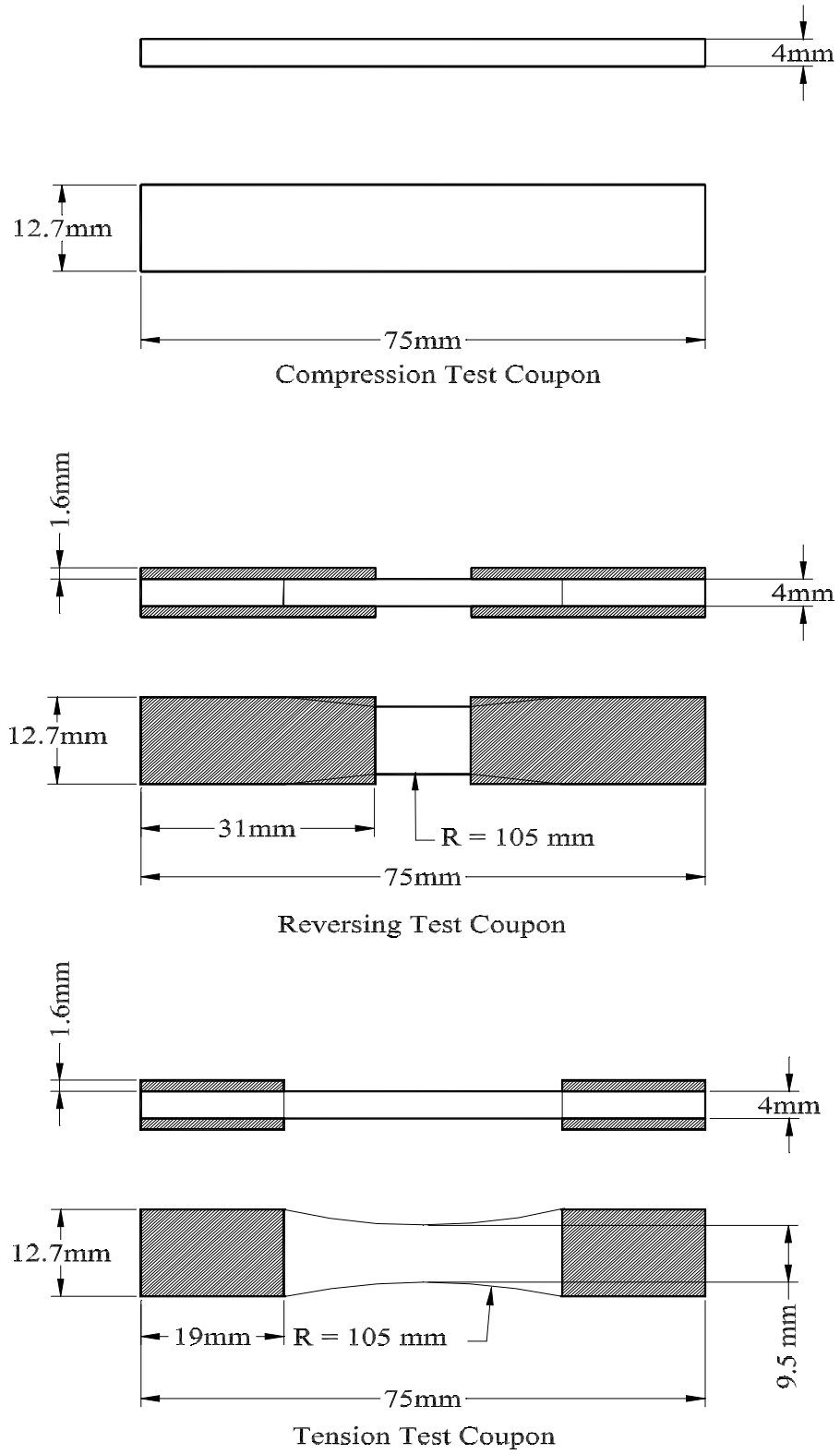


Figure 26. Test Coupon Configurations



Coupon number 555 in Figure 27 was a tensile fatigue test performed at an R-value of 0.1 and a constant amplitude maximum stress level of 207 MPa. Coupon 716 was tested with an R-value of 0.1, but under a variable amplitude loading spectrum and with a maximum stress of 245 MPa. Coupon 773 was subjected to a variable amplitude loading spectrum, but with R-values of both 0.1 and 0.5 and a maximum stress of 245 MPa. The bottom coupon, number 774, was subjected to an ultimate tensile test. All coupons displayed the severe fracturing of the matrix, some even to the point of total wasting of the matrix around the 45 degree plies. All examples also exhibit the “brooming” of the fibers that occurred with this explosive type of failure.

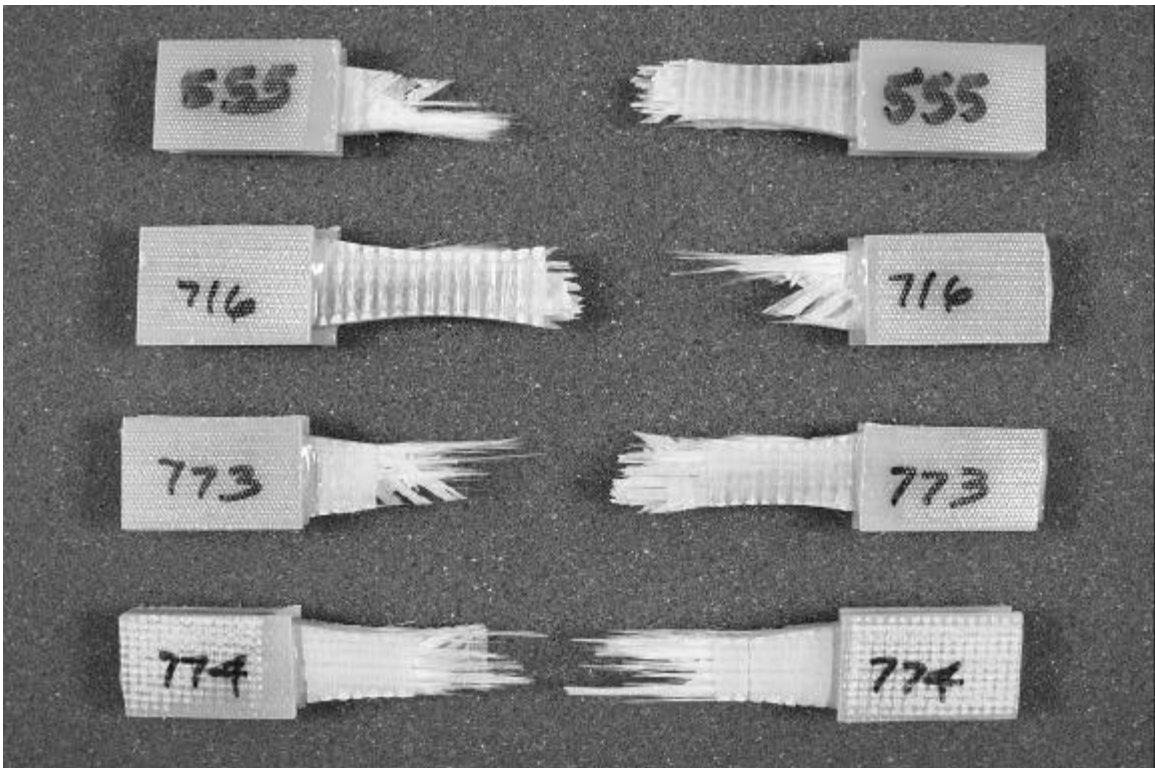


Figure 27 . Tensile Coupon Failure Examples

### Compression-Compression Coupons

The specimens designed for the tensile fatigue testing were first considered for compression testing. Unfortunately, buckling was evident due to slight misalignment caused by the variation in tab material thicknesses and also due to the length of the gage section. A workable compression specimen was a simple rectangularly shaped laminate without any tab material. The gage section was held to 12.7 mm by the grips, to preclude buckling. The overall dimensions were the same as those of the tensile specimen blanks. The failure mode of the compression specimen tests was matrix fracture and destruction, resultant fiber debonding, delamination and crushing or buckling of the fibers, Figure 28. Final crushing was relatively symmetrical on each face in the thickness direction, indicating an absence of elastic buckling or misalignment [13, 34].

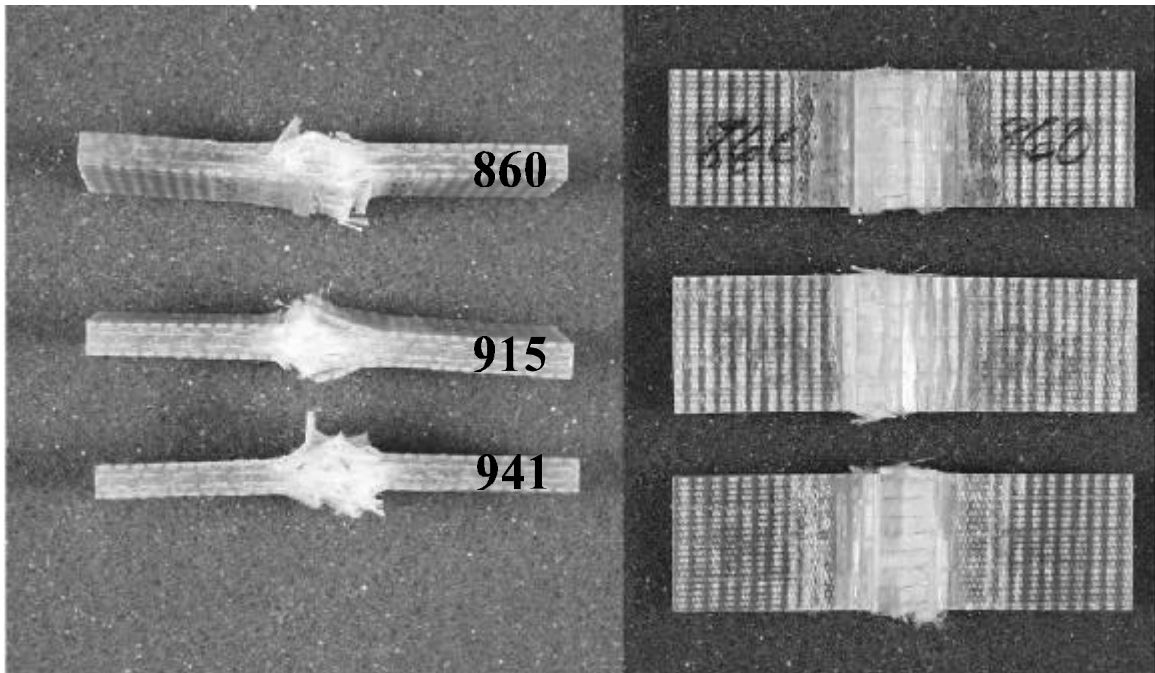


Figure 28. Compressive Coupon Failure Examples

Coupon number 860 in Figure 28 was subjected to constant amplitude loading spectrum at an R-value of 10 and with a minimum (maximum negative) stress of -207 MPa. Number 915 was subjected to a constant amplitude loading spectrum at an R-value of 2 and a minimum stress of -325 MPa. The bottom example in Figure 28 was subjected to a two-block spectrum with minimum stress levels of -325 and -207 MPa and at an R-value of 10. Each of these examples exhibited the failure mode of matrix cracking, delamination, and final buckling of the fibers due to loss of lateral support with the disintegration of the matrix material.

Figure 29 depicts the delamination that occurred during the compressive cyclic loading of coupons 906, 908 and 893 top to bottom respectively. All three tests were performed at an R-value of 10, with tests 906 and 908 at a maximum compressive stress of 245 MPa and test 898 at 275 MPa. The lower stress tests were terminated at approximately ten million cycles and were considered run-out, or cases that could run for a longer period of time. Coupon 893 was terminated at roughly 60,000 cycles as an example of delamination response. All three coupons display signs of delamination growth from the edges. Had the cycling continued until failure, undoubtedly, the delamination would have progressed from each side, eventually joining. The weakened laminate would have had reduced buckling resistance and failed similarly to the examples shown in Figure 28.



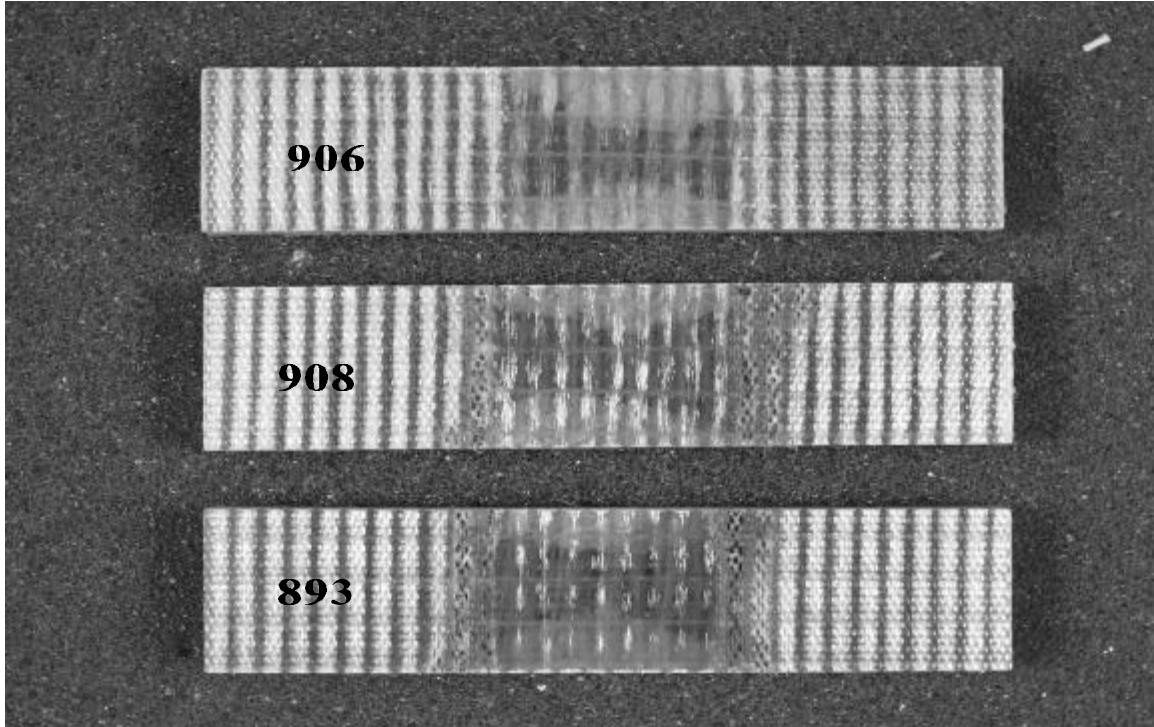


Figure 29. Compressive Coupons at Runout

#### Reverse Loading Coupons

Specimens for reverse loading, R-value of -1, are subjected to both tensile and compressive loads and consequently show diverse and complex failure modes. Static tensile and compressive ultimate strengths are considerably different due to the different failure modes and mechanisms. Also, for a given maximum stress level, the reversing load case may be more detrimental to a laminate than either the tensile-tensile or compressive-compressive cases [13]. As a result, both the tensile-tensile and compressive-compressive coupon designs were considered for the reversing coupon design. A slightly modified tensile-tensile specimen proved successful in use for reverse loading fatigue tests. The elongated tabs aided in buckling resistance while providing a 12.7 mm gage section. The compressive-compressive design could not withstand the tensile loading portion of the

reversing cycle due to grip failures.

Failure of these specimens were similar to that observed for the tensile only case.

Figure 30 is a representation of failures of coupons subjected to reversing load spectra.

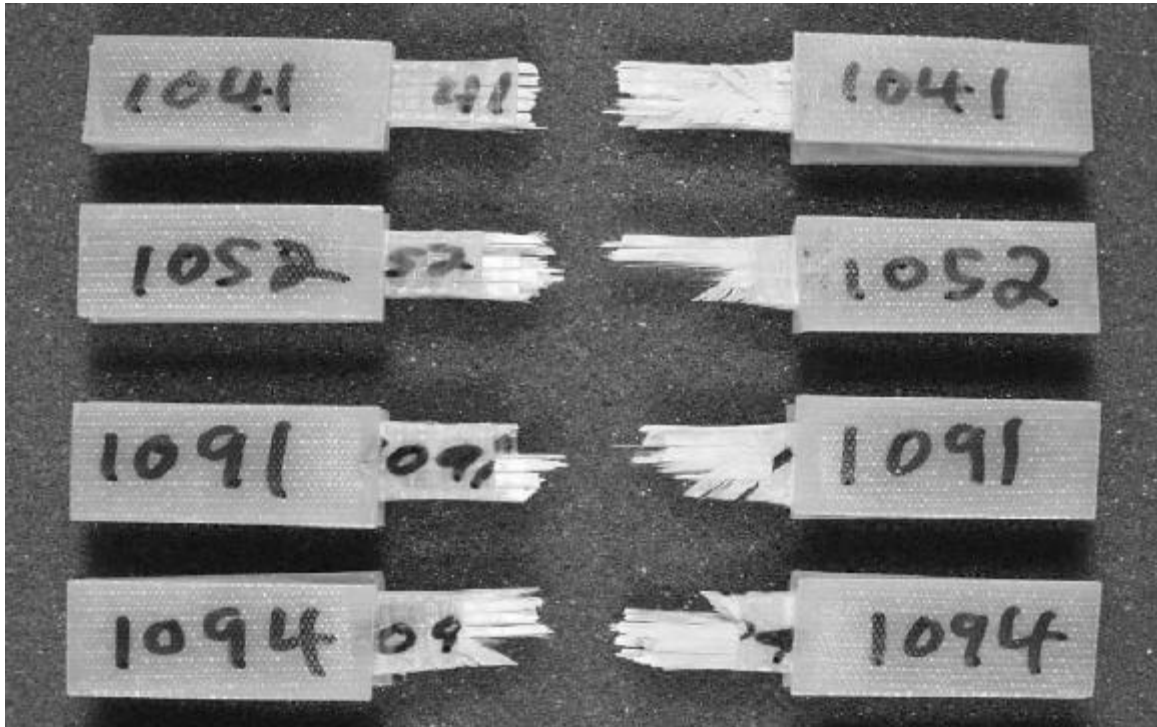


Figure 30. Reversing Coupon Failure Examples

Coupon number 1041 in Figure 30 was subjected to a constant amplitude reversing spectrum with a maximum and minimum stresses of  $\pm 103$  MPa. The remaining three examples were specimens subjected to two-block reversing spectra; with the two maximum stress levels of 172 and 103 MPa for the two blocks. The top specimen could have possibly been a compressive failure, yet was separated upon failure reaction of the testing machine. The bottom three examples exhibit similar failure characteristics of the tensile examples of

Figure 27. None of the reversing failures were similar in appearance to the compressive failures of Figure 28.

### Testing Equipment

An Instron 8872 hydraulic testing machine with an Instron 8800 controller was used to subject the specimen to the spectrum loads. This testing machine, shown in Figure 31, was capable of producing  $\pm 20$  kN of force over a displacement of  $\pm 51$  mm, with a 0.64 L/s servo-valve operating at 3000 psi. Specimens were affixed vertically between a stationary grip at the bottom and a moveable one at the top. These hydraulically actuated grips retain the specimen by wedging paired knurled grip faces towards each other, trapping the specimen. The upper set of grips could be moved vertically by means of varying hydraulic pressures within a cylinder. Pressure, in turn, was varied by regulating the flow of hydraulic fluid into and out of the cylinder by means of a servo valve. The servo valve received control signals from a microprocessor based controller of typical linear proportional, integral, and derivative design. Either position or load can be controlled. A variable differential transformer, LVDT, was used to measure position and a load cell to measure the force. Tuning or selection of the proportional, integral and derivative controller gains, was performed manually for different testing campaigns. A tuning method developed by Ziegler and Nichols [52] was used and resulted in the values shown in Table 3.

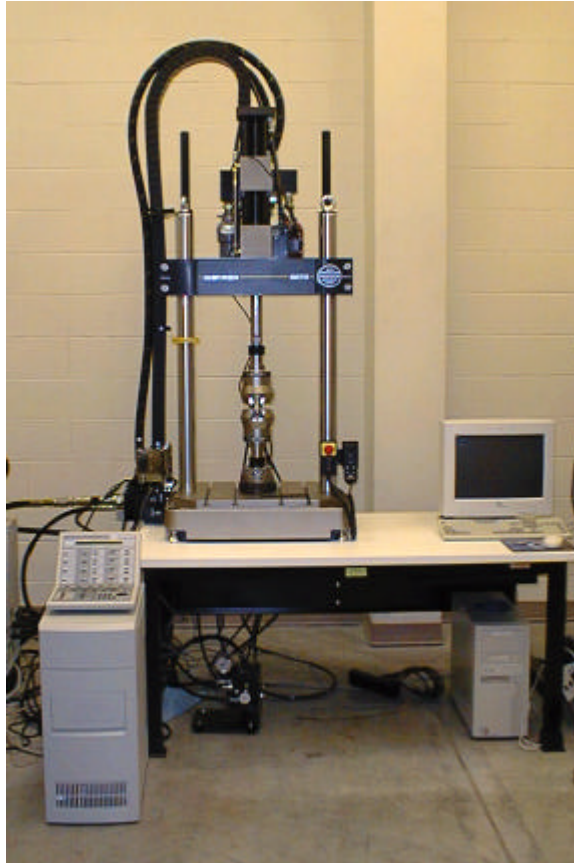


Figure 31. Instron 8872

Table 3. Instron 8800 Controller Tuning Parameters

Testing Regime	Proportional Gain, dB	Integral Gain, s <sup>-1</sup>	Derivative Gain, s	Lag, s
Tensile-tensile	-0.25	1.0	0.0	0.8
Compressive-compressive	+2.5	30.0	0.0	0.8
Reversing	+2.5	30.0	0.0	0.8
Amplitude control was not used.				

Performance of the hydraulic machine was dependent upon the frequency of cyclic motion or loading, as well as to the tuning of the controller, the material being tested, and the type of test. As with most systems, the greater the frequency of operation, the lower the amplitude capability.

Frequency response capability of the machine, along with concern for thermal degradation of the laminate under fatigue, led to performing tests at ten Hertz and less. Secondary measurement and recording of the actual loading waveforms, as shown in Figure 32, were favorably compared to that available from the Instron testing equipment.

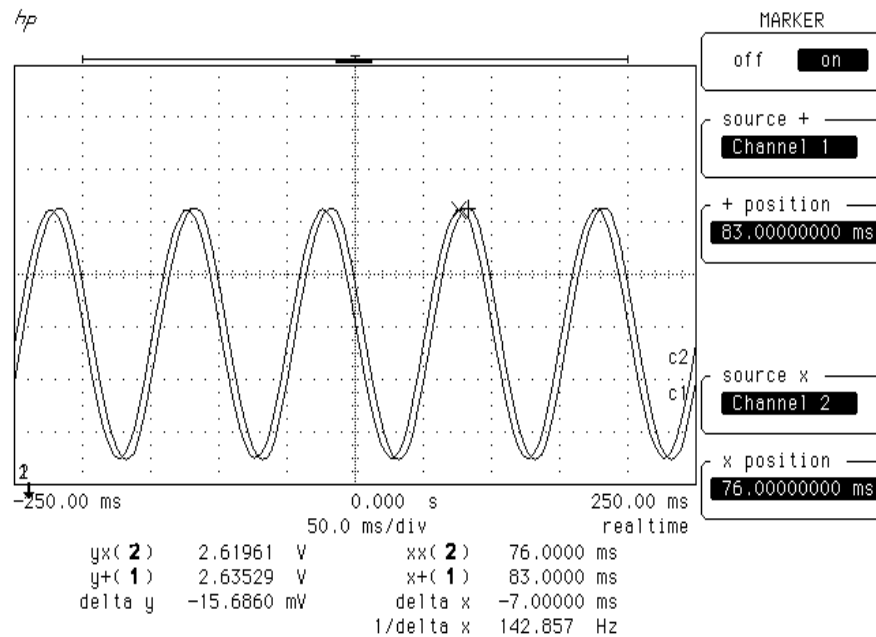


Figure 32. Load Demand and Feedback Signals

The maximum variation of the constant amplitude peak stress for R-values of 0.5, was within 1.5 percent of the mean, whereas the maximum variation of the constant

amplitude valley stress was within 0.2 percent. Typical maximum stress and standard deviation for a 241 MPa constant amplitude fatigue test was 239.4 MPa and 0.338 MPa respectively. The maximum stress level generally decreased with time, due to the increased compliance of the specimen; consequently, greater motion was required to attain the loads.

The two-block tests performed with the block loading software exhibited a low error in the maximum stress upon a change from a low amplitude cycle to a high amplitude cycle. Upon a change from a low stress level block to a high stress level block, the typical maximum variation of the peak value of stress was 0.2 percent. This relatively low error was probably achieved by the fact a ramp from one cycle mean to the next cycle mean was used to progress from one block to the next. Two-block testing performed with the random loading software exhibited a higher error upon a change from a low amplitude stress cycle to a high amplitude stress level. The maximum error was 4 percent and occurred at the initiation of the test with the first cycle. Following errors were typically on the order of 2 percent.

Analysis of random spectrum loading revealed the greatest error (difference between demand and feedback) was upon start-up of the test; well removed from the maximum applied stress. The maximum error was less than 4 percent. The difference between the demand and feedback at the maximum stress cycle was less than 2 percent. Based upon the machine performance analysis, the Instron hydraulic testing apparatus was deemed acceptable for spectrum fatigue testing.

Control Software

Instron WaveEditor<sup>®</sup> (Version 6.2.00) and WaveRunner<sup>®</sup> (Version 6.4.0) software packages were primarily developed for block loading type of fatigue testing. The WaveEditor program was used to create the loading files that were subsequently used by the WaveRunner program for control of the hydraulic test machine.

Blocks of loading profiles could be defined as either ramps or sinusoids via WaveEditor. A ramp block was one in which a change in load from one level to another was specified to occur in a user entered amount of time. A sinusoidal block was one that was sinusoidal in shape, where the frequency, number of cycles, load mean and load amplitude were defined. Blocks could be specified to control either position or load. A constant amplitude test was prepared by the use of only one sinusoidal block, that was repeated until specimen failure. A spectrum of more than one sinusoidal loading block was prepared by a sequence of blocks, typically:

- a) block one was a ramp from zero load to the mean of the first sinusoidal loading block; this was taken as a starter block
- b) block two was a sinusoidal block
- c) block three was a ramp from the mean load level of the block two to a mean load of the upcoming block four
- d) block four was a second sinusoidal block
- e) block five was a ramp from the mean of the fourth block to the mean of the second block.

Blocks two through five were then repeated until specimen failure. Additional blocks could be added when more than two load levels were desired. Once loading files were specified by the use of WaveEditor, actual control was accomplished by the use of WaveRunner.

The Instron software package, RANDOM<sup>®</sup>, was used to subject specimens to, as the name implies, random loading spectra. The function of the software was to sinusoidally load a specimen to a random spectrum when given a succession of peak and valley reversal points. A file containing the succession of peaks and valleys was created by use of a BASIC language program. Each line of the file contained a single reversal point. The contents of the file were scaled to a maximum (or minimum) value of one and signed for tension or compression. The entries format was “+#.#####”, signed and four significant digits. Block loading could therefore easily be accomplished by the use of the RANDOM software package.

Early in fatigue testing, use of the WaveEditor and WaveRunner was discontinued since the RANDOM package would be required for the random spectrum fatigue testing and could also accomplish block fatigue testing. This was done to help preclude any anomalies that might be introduced by differences in software execution.

### Wind Turbine Data Acquisition System

Insight into the actual loading of wind turbine blades was useful in developing a laboratory testing program. Data such as that shown in Figures 2 and 3 were collected from moving blades by means of digital data telemetering systems. A system that was developed



for this purpose and use in this research is documented in Appendix E. Software that was developed for control of this system is also included in Appendix E..

## CHAPTER 5

## CONSTANT AMPLITUDE FATIGUE TESTING AND RESULTS

The fatigue testing in this research program, outlined previously, began with constant amplitude testing and progressed towards the implementation of more complex spectra. This first round of testing provided a set of baseline data that was compared to the results of other researchers and was used in the implementation of various life prediction models. Constant amplitude testing was performed at R-values of 0.1, 0.5, -1, 1, 2 and 10 to reasonably cover the significant regions of a Goodman diagram, reference Figure 7 of Chapter 2. The results of the constant amplitude fatigue tests were reduced to stress-cycle (S-N) diagrams. Regression analysis was performed for each data set assuming either an exponential (equation 9) or power law (equation 10) trend. The regression equations are hereafter referred to as the fatigue models.

Constant Amplitude Test Results

The results of constant amplitude testing are recorded in raw and reduced form in Appendix B. Results at each R-value are summarized in a graphical form of stress-cycle (S-N) diagrams; Figures 33 through 37 are representations (on semi-log plots) of the constant amplitude fatigue of the laminate coupons for R-values of 0.1, 0.5, -1, 10 and 2.

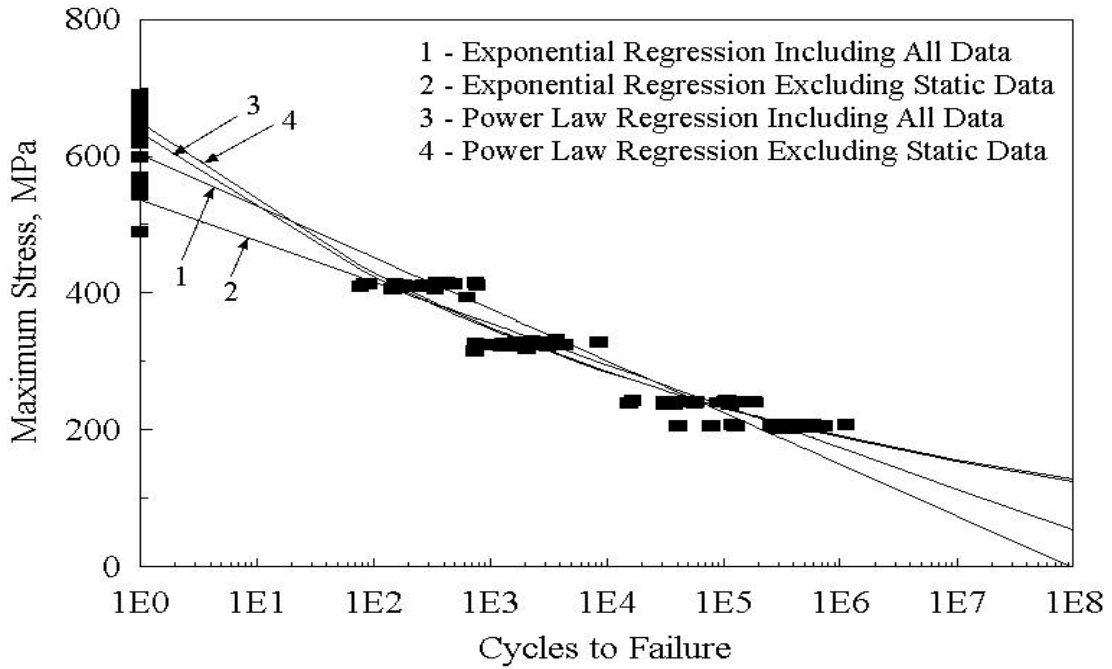


Figure 33. Constant Amplitude Fatigue for  $R = 0.1$

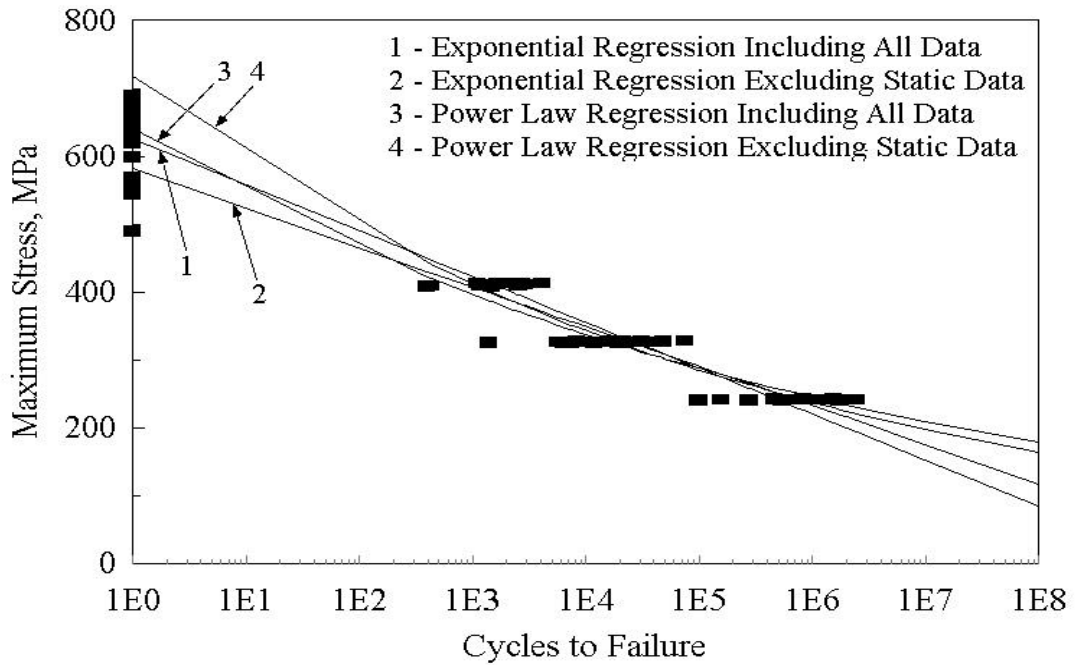
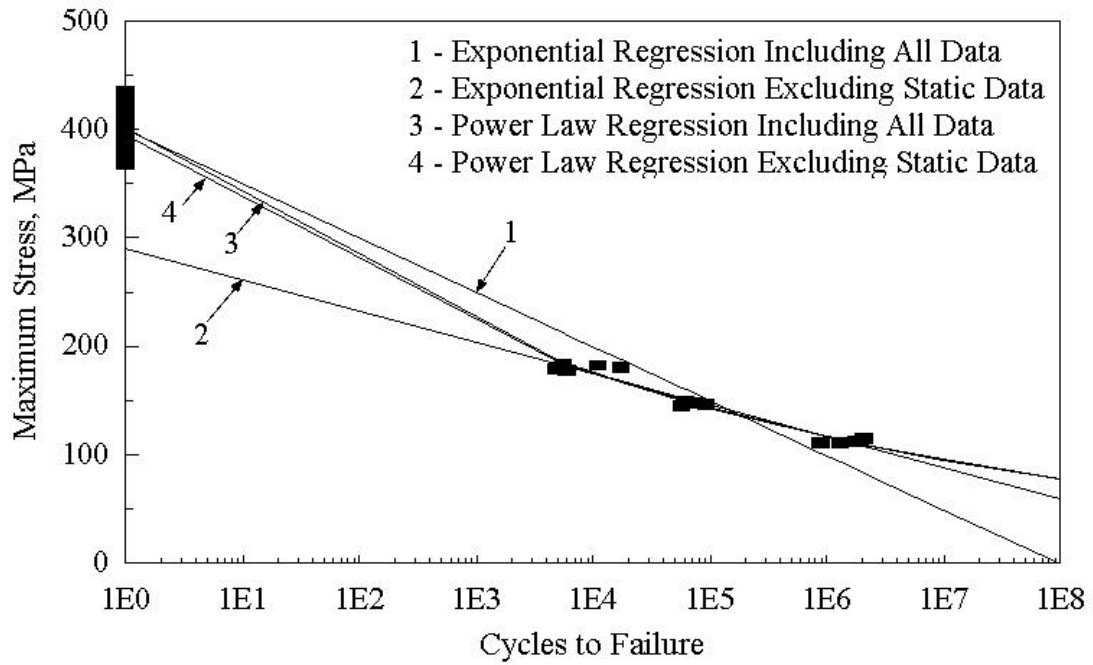
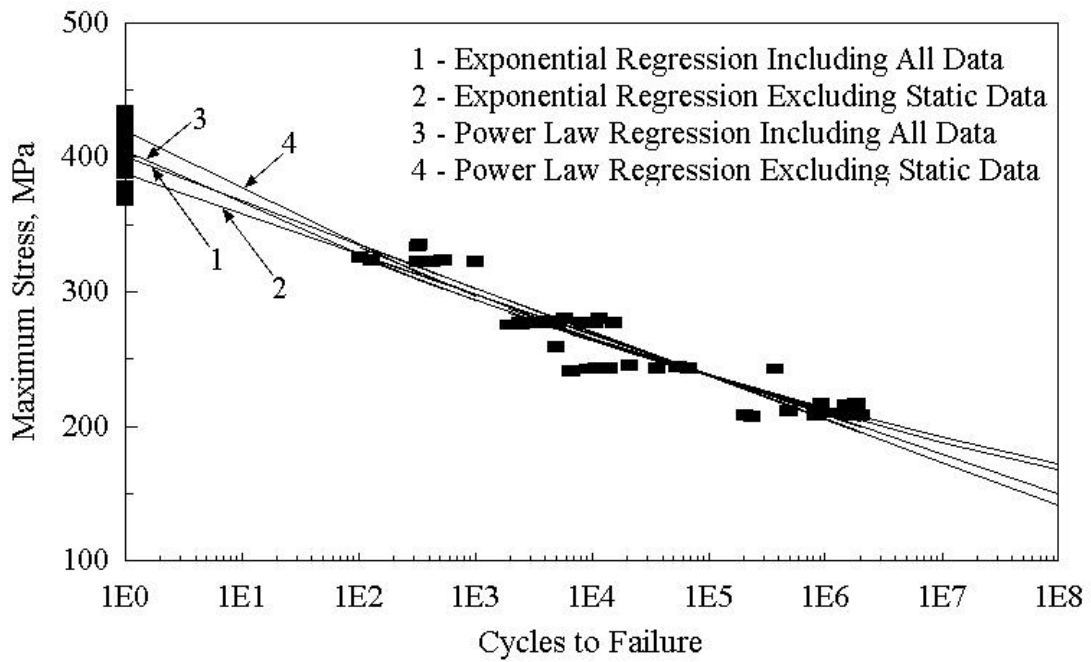


Figure 34. Constant Amplitude Fatigue for  $R = 0.5$

Figure 35. Constant Amplitude Fatigue for  $R = -1$ Figure 36. Constant Amplitude Fatigue for  $R = 10$

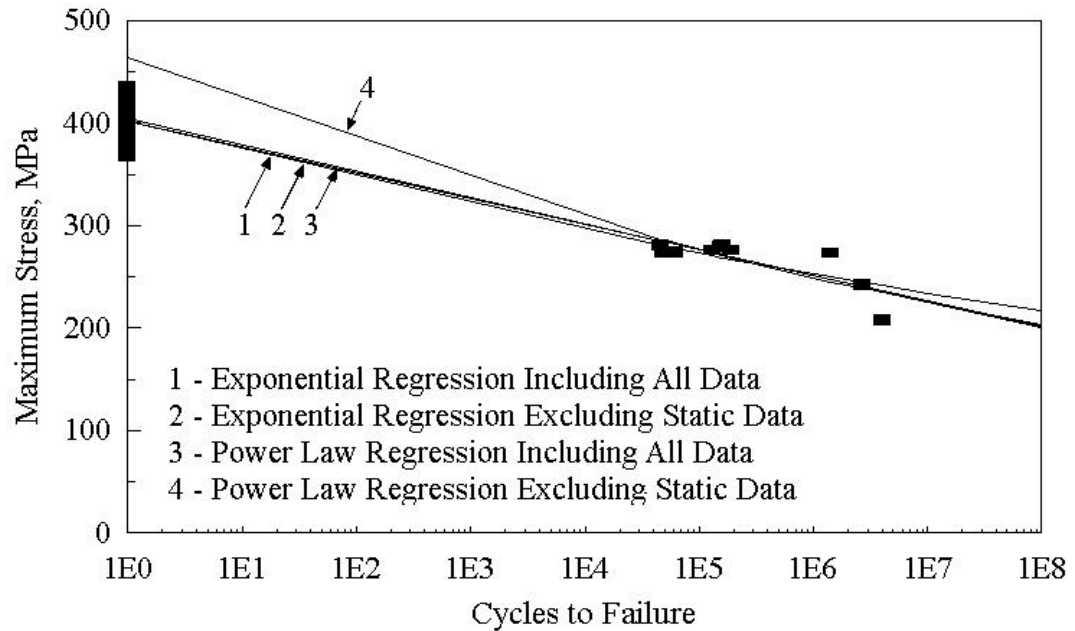


Figure 37. Constant Amplitude Fatigue for R = 2

Each S-N diagram was reduced to two fatigue models by performing both an exponential and power law regression of the respective data sets. The fatigue models were used in subsequent lifetime prediction rules or laws. These fatigue models take on the generic forms of equations 9 and 10, which are repeated here for convenience, for the exponential and power law models, respectively

$$\frac{s}{s_0} = C_1 - b \cdot \log(N) \quad (9)$$

where  $\acute{o}$  = maximum applied stress, MPa  
 $\acute{o}_0$  = static strength, MPa  
 $C_1$  = regression parameter, typically forced through unity  
 $N$  = number of cycles to failure

b = regression parameter related to the reduction in maximum applied stress for each decade increase in cycles

and

$$\frac{s}{s_0} = C_2 N^{-(1/m)} \quad (10)$$

where  $C_2$  = regression parameter

m = regression parameter, similar [30, 33] to the exponent in the fatigue crack growth equation 4

Table 4 contains the exponential regression parameters for each R-value as well as a comparison to the work of Samborsky [34] with the same laminate construction, yet from a different batch and specimen geometry.

Table 4. Exponential Regression Analysis Parameters for Constant Amplitude Fatigue

MPa	Range of Applicability	Regression Coefficients	R-Value, Equation 1				
			0.1	0.5	-1	10	2
Present Work UTS=632 UCS=400	1 to 10 <sup>7</sup> Cycles	C <sub>1</sub>	0.955	0.990	0.994	0.994	1.000
		b	0.120	0.107	0.125	0.081	0.062
		Correlation	0.938	0.942	0.975	0.955	0.927
	10 to 10 <sup>7</sup> Cycles	C <sub>1</sub>	0.849	0.920	0.722	0.963	1.006
		b	0.096	0.092	0.072	0.074	0.063
		Correlation	0.921	0.860	0.959	0.889	0.624
Reference [34]	1 to 10 <sup>6</sup> Cycles	C <sub>1</sub>	1	-	-	-	-
		b	0.12	-	-	-	-
UTS=672 UCS=418	-	-	-	-	-	-	-
	-	-	-	-	-	-	-

Comparison of the work reported in Reference [34] and this present work revealed no significant difference for the fatigue trend, b, for tests at R-values of 0.1. The ultimate

tensile strengths were within 5.5% and the ultimate compressive strengths were within 4%.

The DD16 laminate used in this research may be considered to have an average fatigue sensitivity when compared to a family of similar laminates [13] comprised of E-glass and a polyester matrix and with a lay-up of zero and off-axis plies, reference Table 1, Chapter 2. The fatigue sensitivity (regression parameter  $b$  of equation 9) in tension was reported in Chapter 2, to range from 0.1 to 0.14. The tension fatigue sensitivity of the DD16 material was 0.12 as shown in Table 4. The compression fatigue sensitivity of 0.08 falls in the range of 0.07 to 0.11 for the family of similar laminates. The DD16 reversing load fatigue sensitivity of 0.125 again falls in the range of 0.12 to 0.18 for similar cross-ply laminates.

The fiber volume fraction of the DD16 laminate was 36%, placing this laminate in the class of better laminates' fatigue performance for this fiber volume fraction. The surface 90° plies of the DD16 laminate offered little in the material properties; their main purpose was aiding in mitigating grip effects. Discounting these surface plies places this laminate in the region of high 0° ply content (69 - 85 percent) where the fatigue trends of this laminate are in good agreement with that of similar laminates summarized in Table 1.

Table 5 contains the results of power law regressions at each R-value and comparisons to results of tests of uniaxial fiber lay-up material as reported by Sutherland [28]. Due to the difference in material, direct comparisons are not possible, yet trends can be compared and are similar.

Table 5. Power Law Regression Analysis Parameters for Constant Amplitude Fatigue

MPa	Range of Applicability	Regression Coefficients	R-Value , Equation 1				
			0.1	0.5	-1	10	2
Present Work UTS=632 UCS=400	1 to 10 <sup>7</sup> Cycles	C <sub>2</sub>	1.005	1.013	0.998	1.005	1.000
		m	11.478	14.400	11.158	21.550	29.820
		Correlation	0.966	0.946	0.993	0.961	0.933
	10 to 10 <sup>7</sup> Cycles	C <sub>2</sub>	1.026	1.135	0.981	1.043	1.155
		m	11.214	12.490	11.343	20.089	22.249
		Correlation	0.936	0.872	0.964	0.906	0.61
Reference [28] UTS=1422 UCS=720	1 to 10 <sup>8</sup> Cycles	C <sub>2</sub>	1	1	1	1	1
		m	11.3	15.4	14.9	18.0	31.2
	10 <sup>3</sup> to 10 <sup>8</sup> Cycles	C <sub>2</sub>	0.969	0.977	1.124	0.862	0.859
		m	11.6	16.0	13.2	22.5	47.8
	10 <sup>5</sup> to 10 <sup>8</sup> Cycles	C <sub>2</sub>	0.740	0.977	1.124	0.802	0.802
		m	14.3	16.0	13.2	24.9	61.7
Reference [53] UTS=392 UCS=298	10 <sup>3</sup> to 10 <sup>8</sup> Cycles	C <sub>2</sub>	1.30	-	1.64	-	1.26
		m	10.5	-	9.34	-	21.7
-	-	-	-	-	-	-	
-	-	-	-	-	-	-	

The data of Tables 4 and 5 were also reduced to the graphical form of Goodman diagrams, Figures 38 through 41, and to the graphical form of regression lines, Figures 42 through 49. Note, in Figure 42, the relative order of the R-values, with the reversing condition being the more damaging (more rapid loss of life), followed by the tensile and lastly by the compressive load cases. This is consistent with the information displayed in the Goodman diagrams; note the closer spacing of the constant cycle lines for the compressive case, with the spacing increasing first for the tensile and lastly for the reversing.

Important information can be gleaned from a regression of the fatigue models, but not in a normalized format. Notice in Figures 46 through 49, that for moderate stress levels,



there is a crossing of the curves for the tensile and compressive cases. At a given high absolute stress, compression is more damaging, while at low stresses, tension is more damaging.

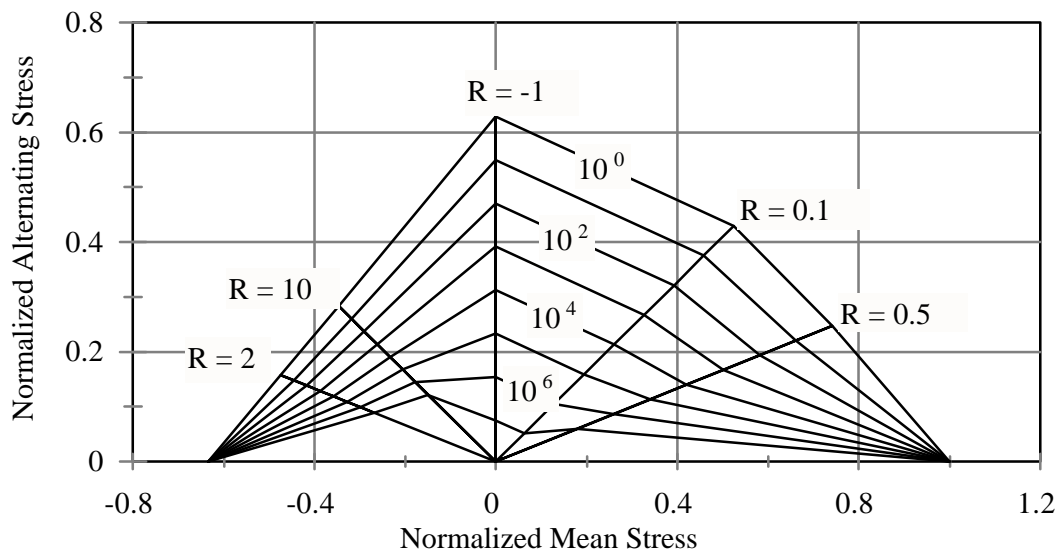


Figure 38. Goodman Diagram Based Upon Exponential Regression Analysis, Including All Data

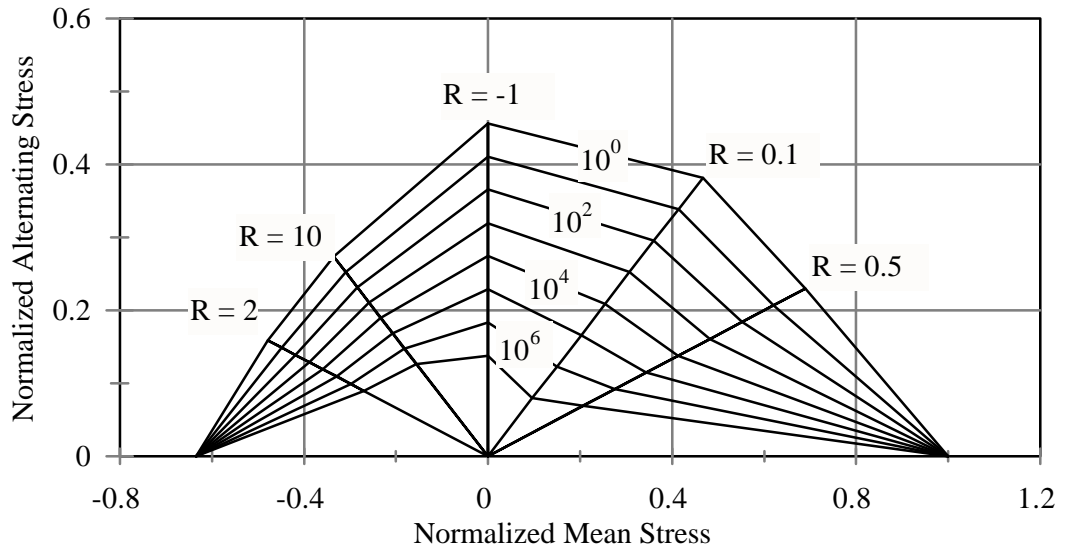


Figure 39. Goodman Diagram Based Upon Exponential Regression Analysis, Excluding Static Data

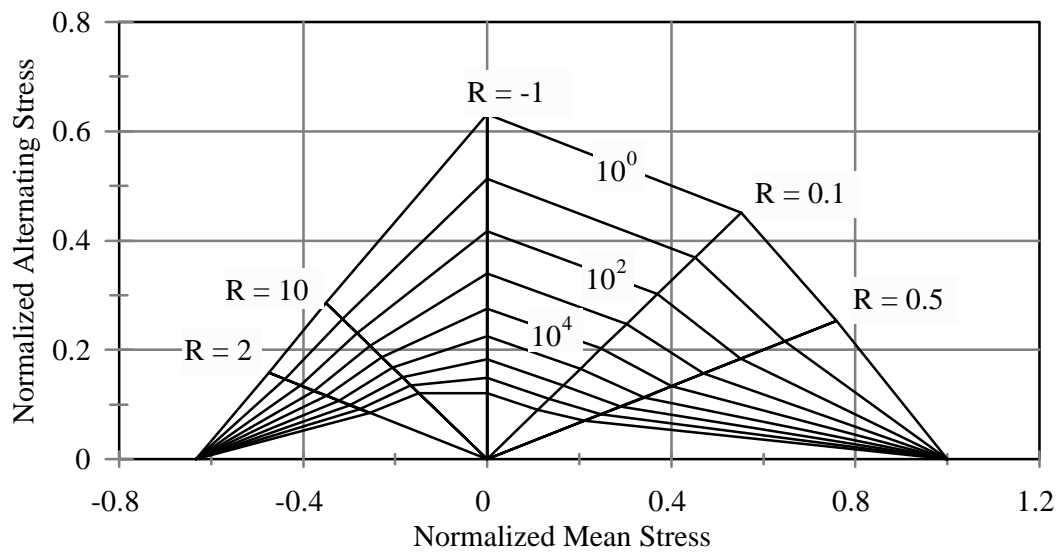


Figure 40. Goodman Diagram Based Upon Power Law Regression Analysis, Including All Data

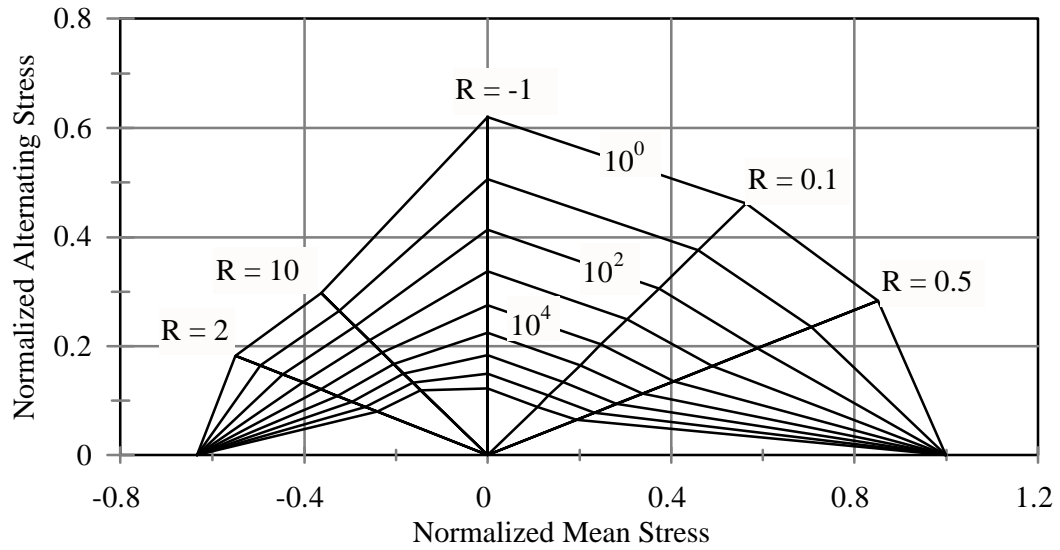


Figure 41. Goodman Diagram Based Upon Power Law Regression Analysis, Excluding Static Data

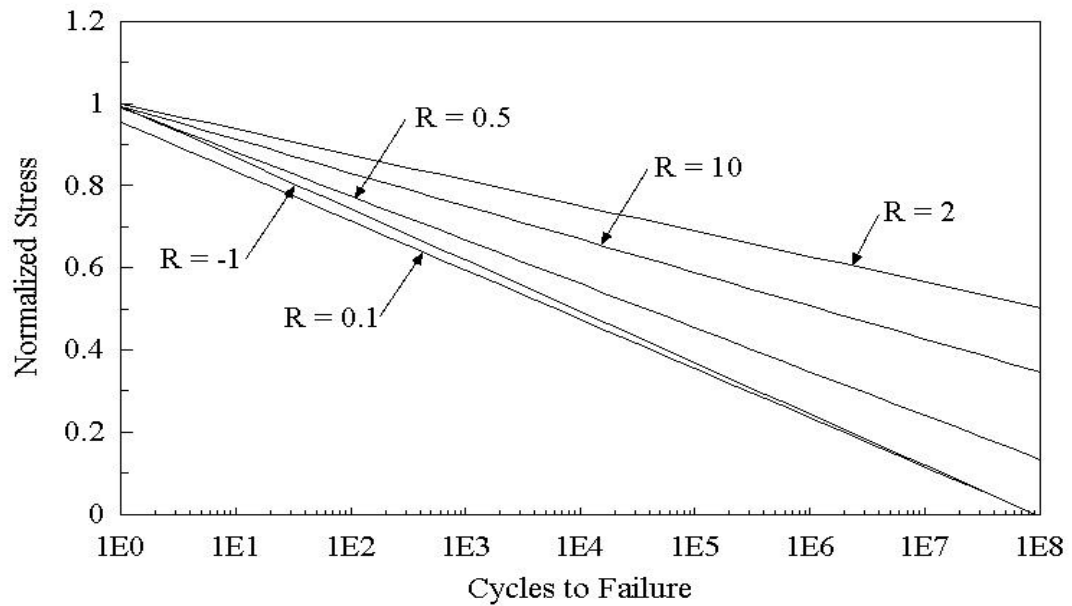


Figure 42. Normalized Fatigue Models, Exponential Regression Including All Data

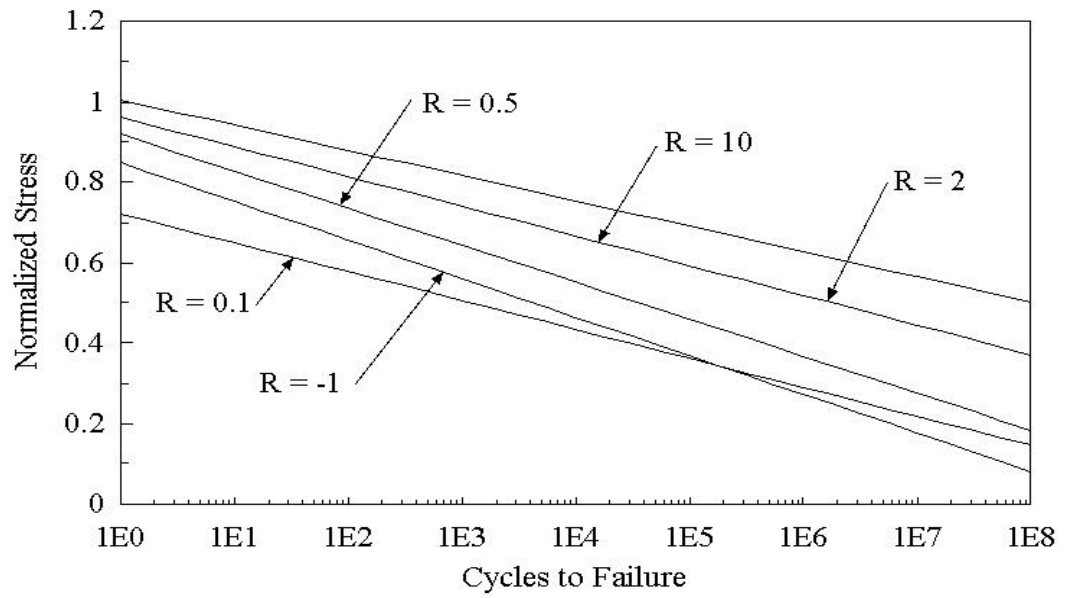


Figure 43. Normalized Fatigue Models, Exponential Regression Excluding Static Data

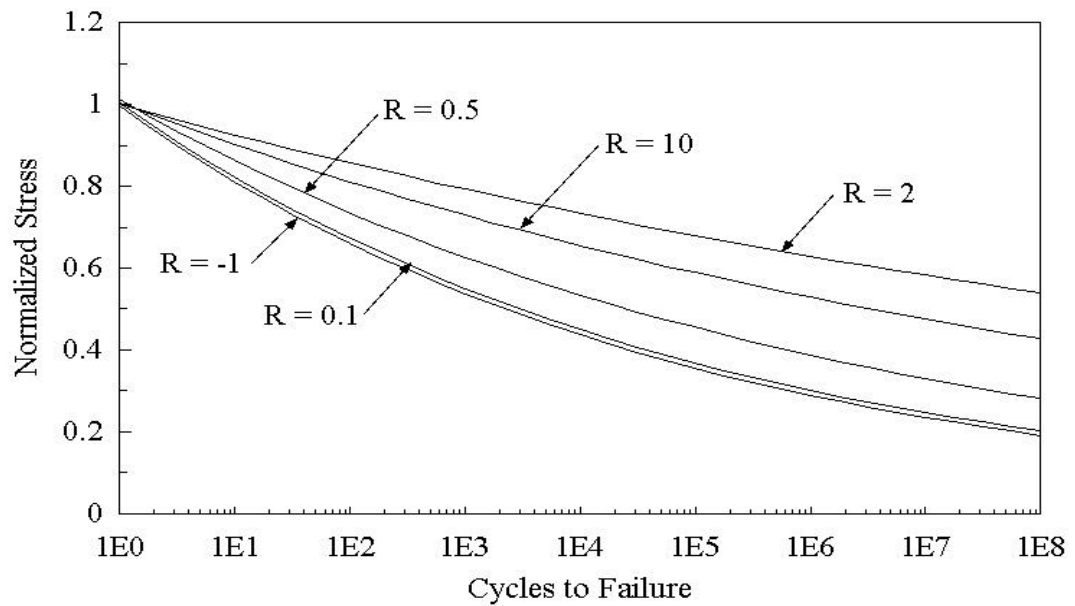


Figure 44. Normalized Fatigue Models, Power Law Regression Including All Data

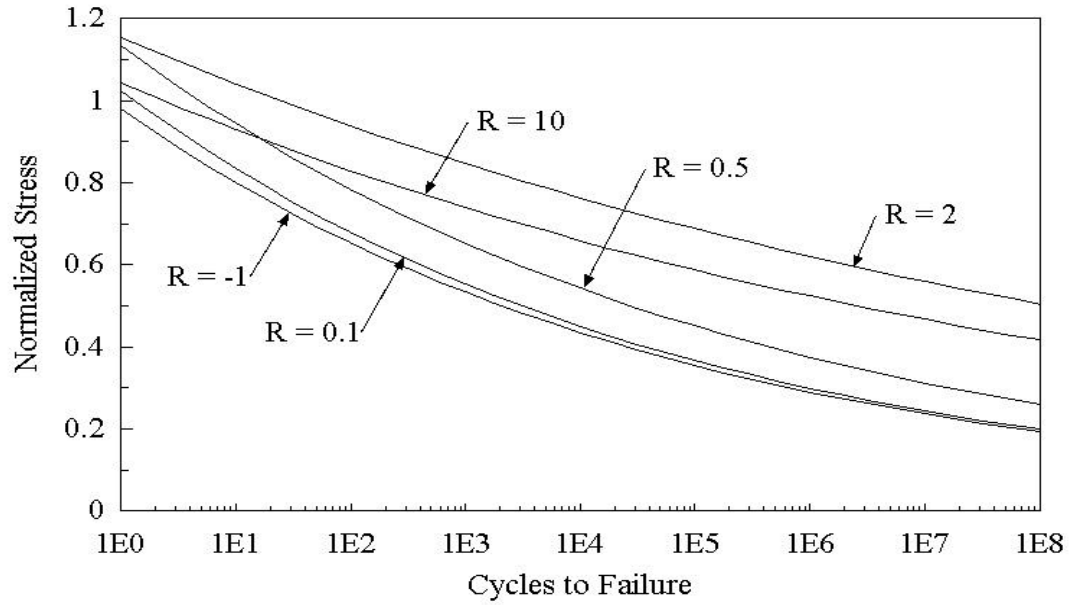


Figure 45. Normalized Fatigue Models, Power Law Regression Excluding Static Data

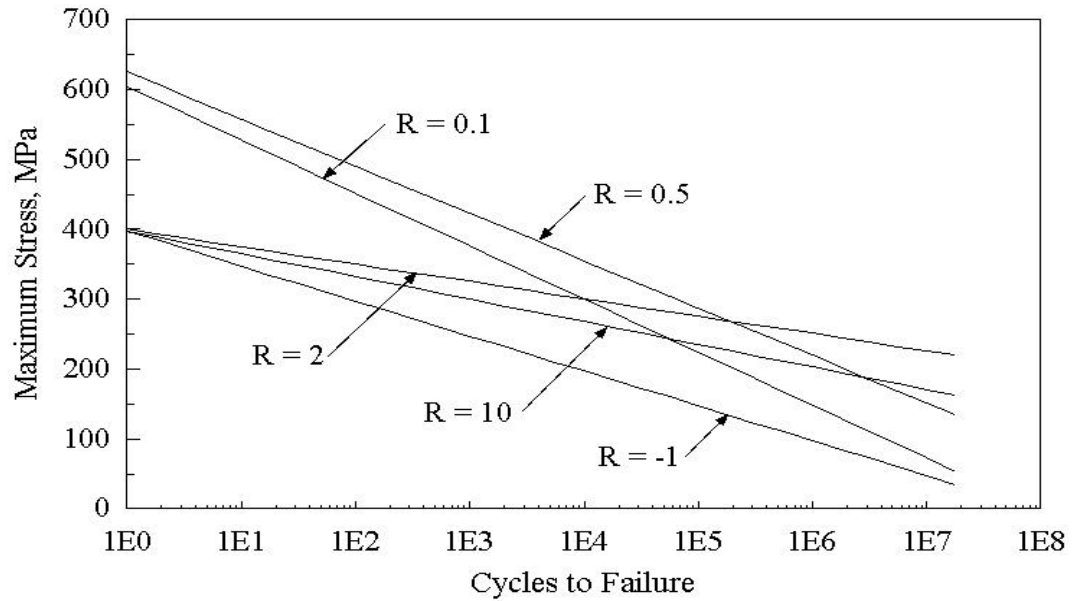


Figure 46. Exponential Fatigue Regression Models For All R-Values Including All Data

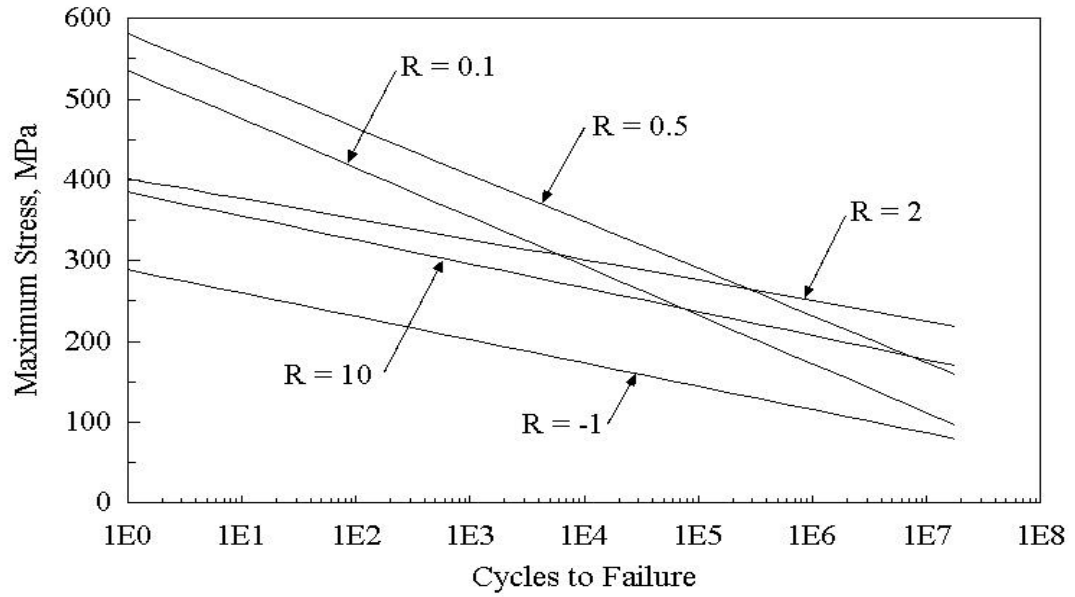


Figure 47. Exponential Fatigue Regression Models For All R-Values Excluding Static Data

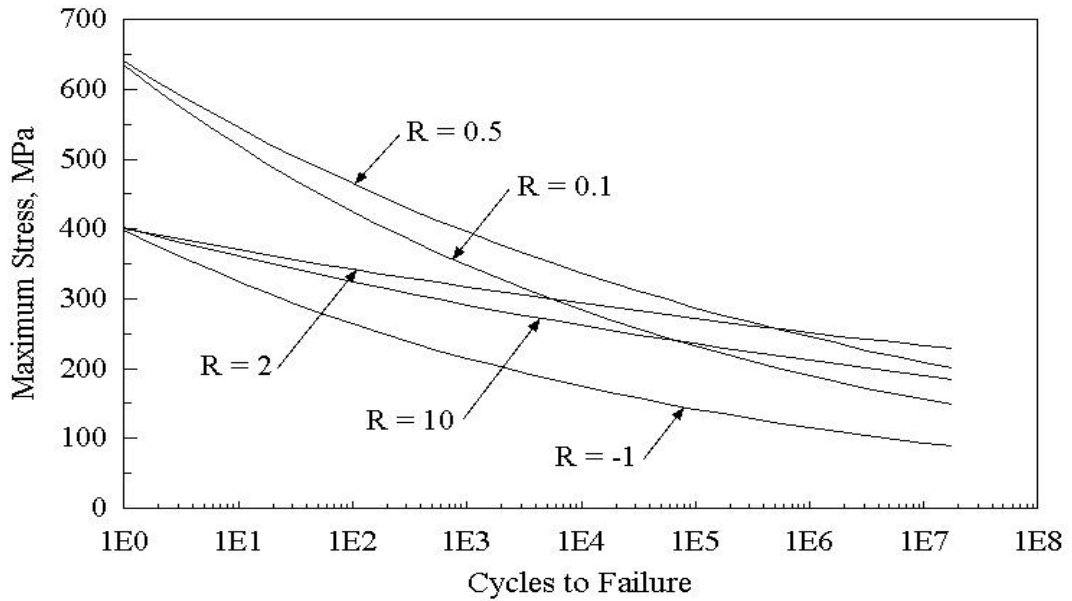


Figure 48. Power Law Fatigue Regression Models For All R-Values Including All Data

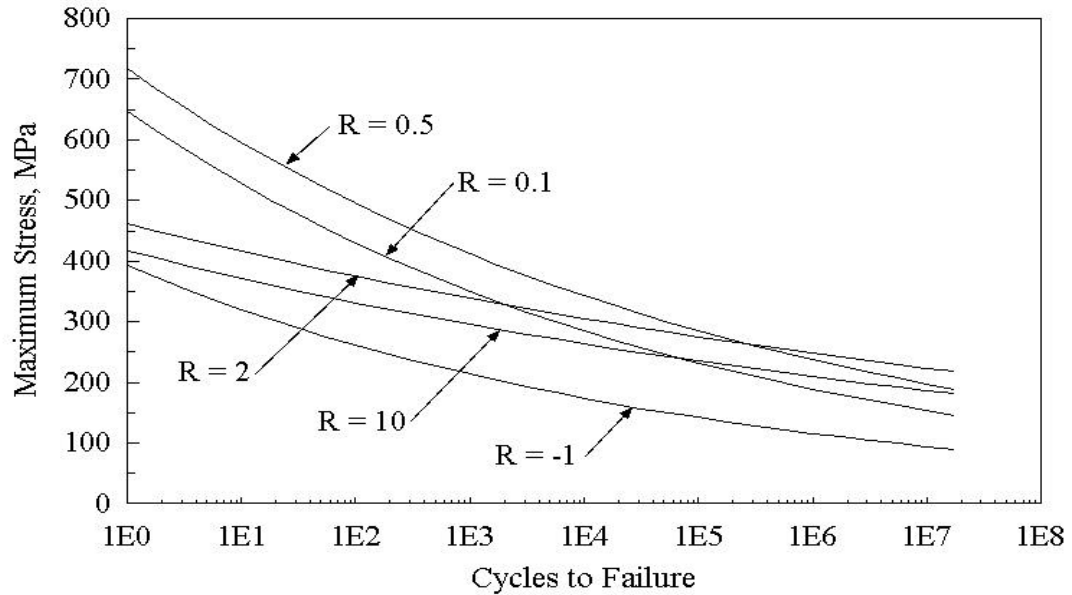


Figure 49. Power Law Fatigue Regression Models For All R-Values Excluding Static Data

### Residual Strength of Laminate Under Fatigue

The general trend of the residual strength of a laminate over its life was discussed in Chapter 3. Recall that the shape of the strength curve, as related to the number of cycles experienced, can drastically affect lifetime predictions. Attempts were made to perform partial fatigue tests in order to ascertain the residual strength parameter,  $\hat{\sigma}$ . Specimens were subjected to selected constant amplitude stress levels for a fixed number of cycles. The ultimate strengths of the cycled specimens were measured and compared with the ultimate strength of virgin, un-fatigued, specimens. Residual strength tests have been run for specimens subjected to fatigue at R-values of 0.1 and 0.5.

Figure 50 presents the residual strength results for the laminate subjected to 241 MPa

with an R-value of 0.1. Tabulated data were taken from Reference [34] and placed into the graphical form of Figure 50. Specimens were fatigued to cycle accumulations at three different levels, 50,000, 100,000, and 200,000 cycles. Some specimens failed prior to achieving the desired cycle level and are so noted. Also shown and labeled as S-N fatigue, are the results of specimens cycled until failure as well as the virgin material ultimate tensile strength test results. It is evident from the residual strength data collected, that the residual strength parameter,  $\hat{\sigma}$ , is not greater than unity. The premature failure of specimens before reaching the desired number of cycles complicates the analysis of a reasonable value for  $\hat{\sigma}$ . Regardless, upon investigating the residual strength results for both R-values of 0.1 and of 0.5, a factor of less than one was considered appropriate. The residual strength tests, summarized in Figure 51, were performed at a maximum stress level of 325 MPa and at an R-value of 0.5.

The general shape of the residual strength lifetime curves (equations 15 and 16) is uncertain. An error analysis of the residual strength data shown in Figure 50 indicates the nonlinear strength degradation curve yields a mean absolute minimum error of 23 percent with a degradation parameter,  $\hat{\sigma}$ , of 0.265. The linear residual strength curve analysis indicated a mean absolute error of 37 percent. The results of this work and that of Reference [34] indicate that the nonlinear parameter,  $\hat{\sigma}$ , is not greater than one. Broutman and Sahu [41] data seems to indicate that a linear residual strength degradation is valid; while Yang and Jones [35] indicate (without data) that a nonlinear strength degradation parameter greater than one is reasonable. This parameter may be a function of the laminate as well as the stage of life of the material.



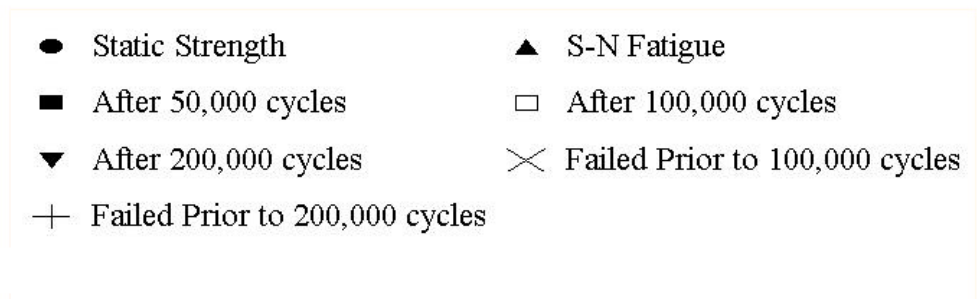
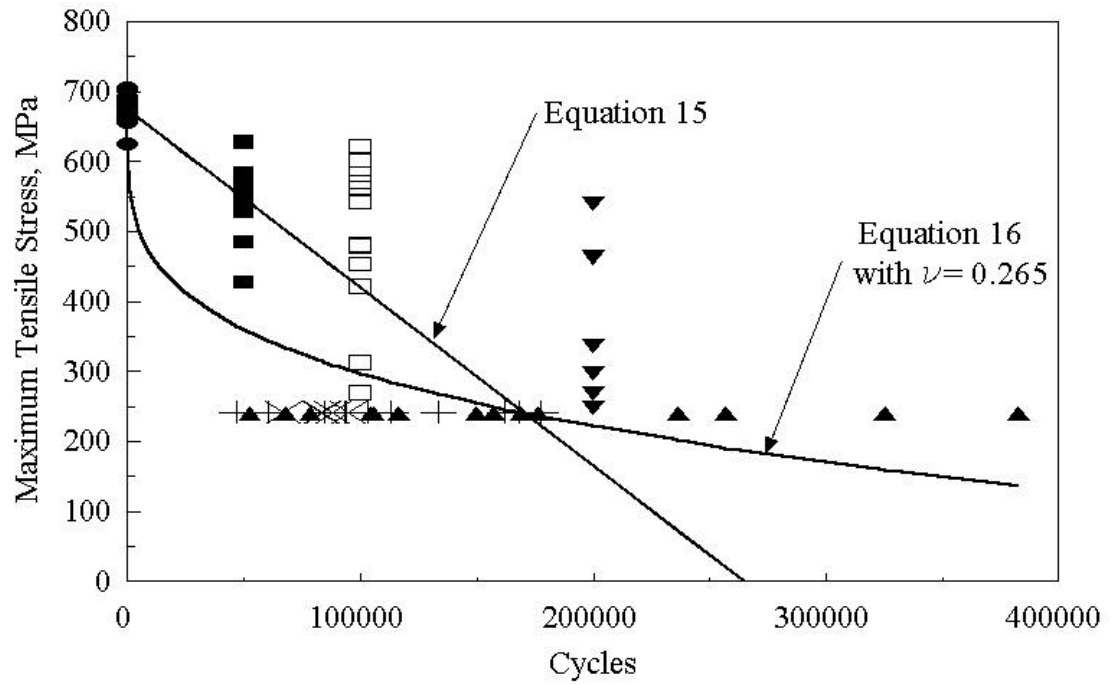


Figure 50. Residual Strength Data For R = 0.1 [34]

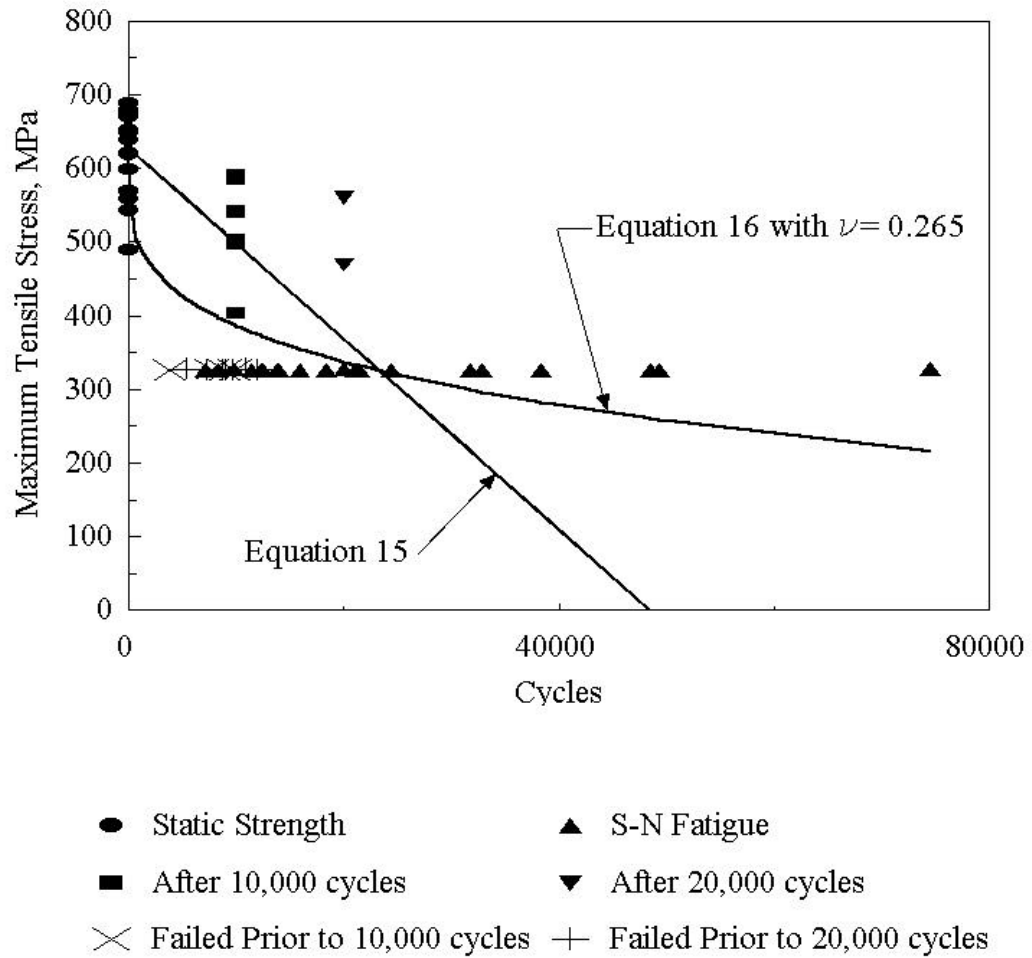


Figure 51. Residual Strength Data For R = 0.5

## CHAPTER 6

## BLOCK SPECTRUM FATIGUE TESTING AND RESULTS

An investigation into variable amplitude fatigue testing logically begins with two amplitudes or stress levels before considering more complex spectra. Other researchers have also taken this approach, implementing a spectrum of one block of constant amplitude cycles followed by a second block of different constant amplitude cycles. The second block was run until specimen failure in tests by Yang, et. al. [10].

Testing in this format is not considered representative of a realistic spectrum; consequently, an alternate application of two-block testing was considered for this research. Upon considering a standard European spectrum for wind turbine blades, it is evident that a repetition of blocks would be more appropriate. Note the obvious repetitions in the time-compressed European spectrum WISPER [15, 16] shown in Figure 52.

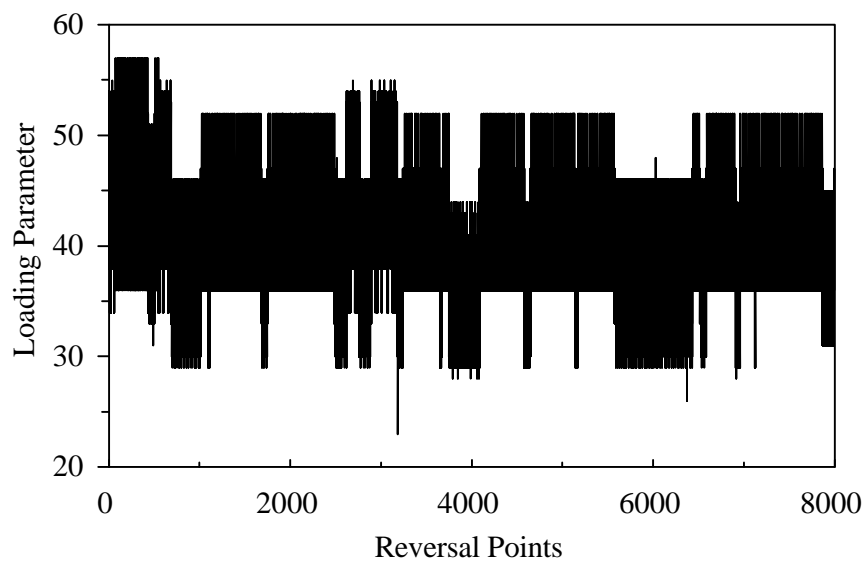


Figure 52. Excerpt of WISPER Spectrum

### Sequence Effects

When entering into studies of fatigue at two different load levels, thought must be given to possible effects of the sequencing of the cycles. This is prompted by the result of fatigue analysis in metals by linear elastic fracture mechanics [22]. In metals, a high load can create a compressed region at the crack tip, thereby retarding crack growth at lower loads, and consequently extending fatigue life.

Three separate spectra containing the same number of cycles at each stress level were developed for investigation of possible sequence effects in the fatigue of this laminate. The three spectra are shown in Figure 53. The first contains a block of one high amplitude cycle followed by 100 low amplitude cycles. These two blocks are shown repeated ten times to create a spectrum of 1010 cycles in length. The second spectrum was comprised of ten high amplitude cycles followed by 1000 low amplitude cycles. The third was constructed to

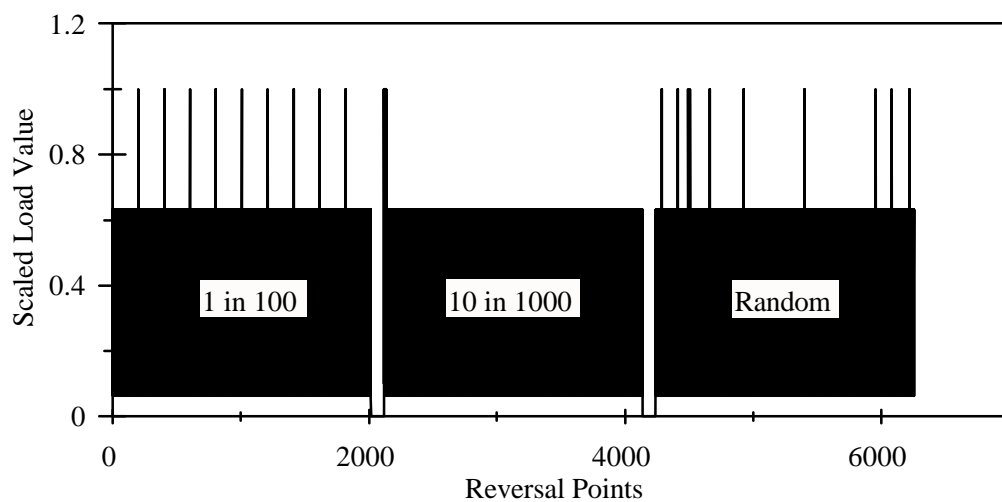


Figure 53. Two-Block Sequences (Blocks Repeated to Failure)

contain ten high amplitude cycles randomly interspersed within 1000 low amplitude cycles. The high amplitude cycle fraction is defined as the number of high amplitude cycles divided by the total number of cycles. Each of these spectra, then, had a fraction of approximately 0.01.

High amplitude cycles were set at an R-value of 0.1 and had a maximum stress of 325 MPa. Low amplitude cycles were also set at an R-value of 0.1, but at a maximum stress of 207 MPa. Figure 54 details the results of 120 tests, 82 two-block and 38 reference constant amplitude tests. The fraction of specimen failures is displayed against the total number of cycles experienced. All of the specimens are from the same batch of fabric reinforcement, and tests were randomly interspersed between the different sequences and the constant amplitude cases.

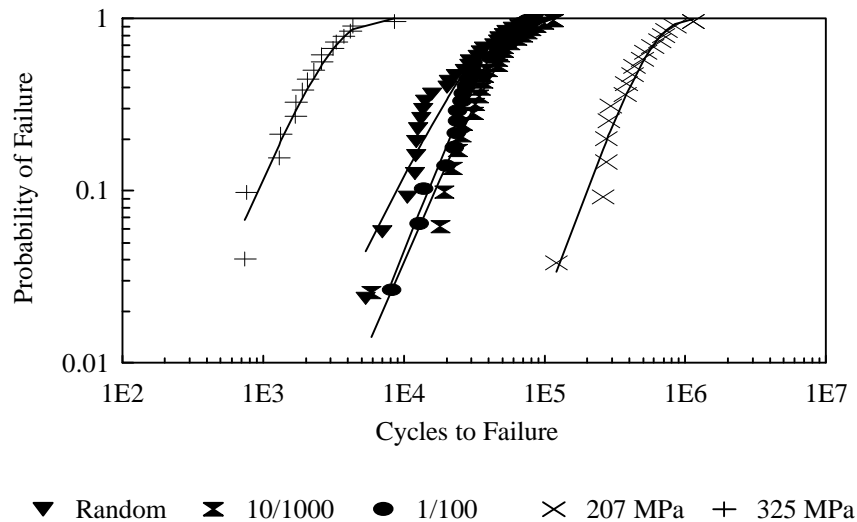


Figure 54. Two-Block Sequence Test

Within confidence limits of 0.95, there is no statistical difference among the three sequences. Consequently, sequencing was not considered important and ignored for the remainder of the testing.

Only four of the 82 sequencing effect tests achieved Miner's sums greater than unity. In fact the average Miner's sum is slightly less than 0.3, as evident in Figure 55. Compare this against the average Miner's sum of 1.0 for the constant amplitude fatigue tests and it becomes evident that spectral loading does not produce failure at a Miner's sum averaging 1.0. This phenomenon will be investigated further in Chapter 8, which deals with predictions of service lifetimes.

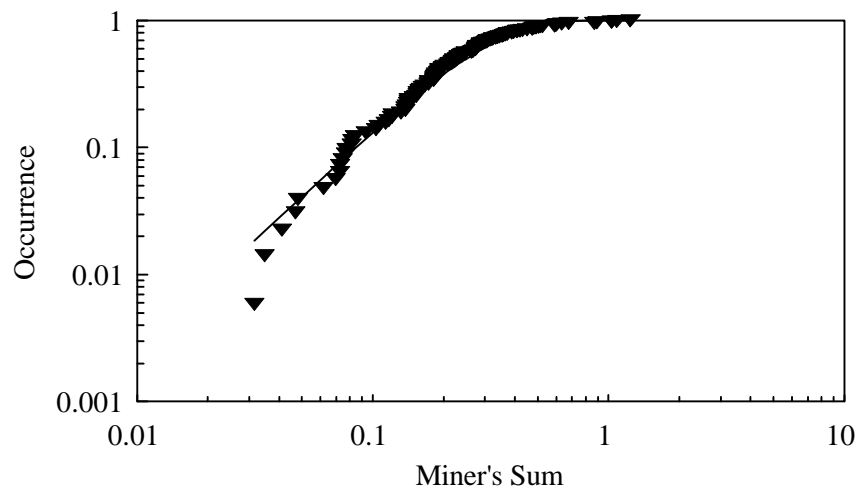


Figure 55. Overall Two-Block Miner's Sum, Stresses 325 and 207 MPa, High Amplitude Cycle Ratio of 0.01

Two-Block Fatigue Testing

Two-block testing was performed at several combinations of stress levels as well as for different R-values. Testing was performed for cases in which the two stress levels were relatively close as well as distant. Test campaigns are identified in Table 6. The cycles column gives the number of cycles per block; blocks are repeated until failure in all cases.

Table 6. Two-Block Testing Campaigns

High Stress Block			Low Stress Block		
$\sigma_{\max}$ , MPa	R-value	cycles	$\sigma_{\max}$ , MPa	R-value	cycles
414	0.1	10	325	0.1	10, 90, 100, 990, 1K, 9K
414	0.1	10	235	0.1	10, 90, 100, 112, 1K, 10K
325	0.1	10	235	0.1	10, 100, 500, 1K, 3K, 5K
325	0.1	10	207	0.1	10, 50, 90, 100, 1K, 3K, 5K, 10K, 20K, 33K, 50K, 60K
235	0.1	10, 20	207	0.1	10, 90, 100, 990, 1K, 9K, 33K, 50K, 60K
414	0.5	10	325	0.5	10, 50, 100, 1K
414	0.5	10	235	0.5	10, 100, 1K, 10K
325	0.5	10	235	0.5	10, 90, 100, 1K, 10K
235	0.5	10	207	0.5	90

Table 6. Two-Block Testing Campaigns - continued

High Stress Block			Low Stress Block		
$\sigma_{\max}$ , MPa	R-value	cycles	$\sigma_{\max}$ , MPa	R-value	cycles
-276	10	10, 1K, 10K	-207	10	10, 100, 1K, 10K
-325	10	10	-207	10	10, 100, 1K, 10K
173	-1	10	104	-1	10, 100, 1K, 10K

One would expect that as the two stress levels approached each other in magnitude, any effects on fatigue would diminish, the limiting case being of constant amplitudes. Tests were arranged to allow investigation of this possibility.

Results of two-block fatigue testing have been summarized into graphical form (Figures 56 - 77) relating the Miner's sum to the fraction of high amplitude cycles. A fraction of high amplitude cycles of zero would, in reality, be a constant amplitude test of the lower stress level. Conversely, a fraction of one would indicate a constant amplitude test at the higher stress level. In each of the following two-block graphs, the abscissa has been broken into two parts, the extreme left is of a linear scale, allowing the zero fraction to be displayed; the remainder of the scale to the right is logarithmic. Included in each graph are lifetime predictions that will be discussed in Chapter 8. Within the legend of each graph, NRSD and LRSD refer to a nonlinear and linear lifetime residual strength prediction models, respectively the NRSD cases were all run with  $\dot{\epsilon} = 0.265$ ). The graphs are presented in pairs, on one page, with the upper displaying the lifetime predictions based upon an exponential



fatigue model (equation 9); the lower represents lifetime predictions based upon a power law fatigue model (equation 10).

Note, in most of these figures that the trend of Miner's number varies from one at the left hand margin (low stress level constant amplitude fatigue test) to less than one and finally back towards an average of one at the right hand margin (high stress level constant amplitude fatigue test). This was also observed, in Figure 15, for specific load cases in the linear elastic fracture mechanics analysis, including retardation, of two-block load spectrum calculations for metals. There does not appear to be a retardation effect observable in the multi-block fatigue of the tested laminate.

The degrading effect of load interaction (Miner's sums below 1.0) was most prevalent in the tensile tests at R-values of 0.1 and 0.5, with the effect greater for the larger spread of the applied maximum stress levels. The effect was also observed in the reversing load cases, and R-value of -1; and to a much lesser extent in the compressive cases of the R-values of 2 and 10.

A tabulated form of the test results and calculations for all two-block testing campaigns can be found in Appendix C.

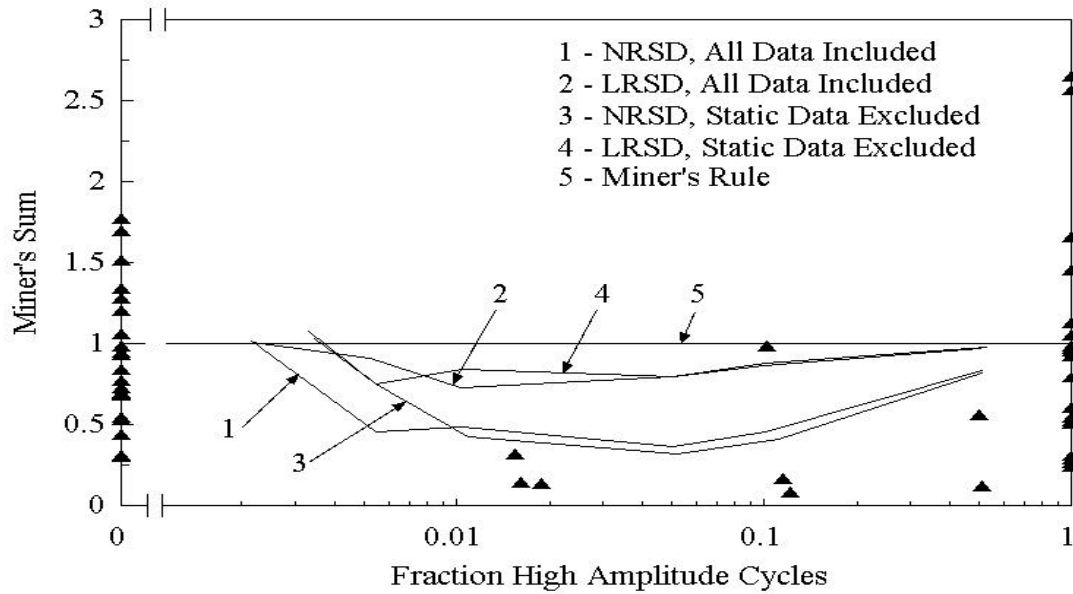


Figure 56. Two-Block Test Results for R = 0.1, 414 & 325 MPa; Exponential Fatigue Model With Linear and Nonlinear Residual Strength and Miner's Rule Lifetime Predictions

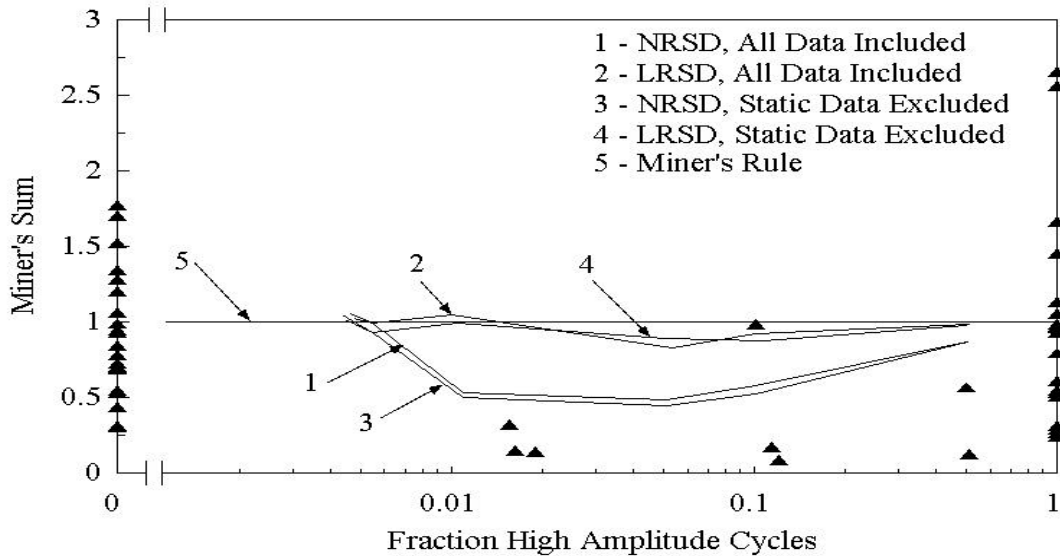


Figure 57. Two-Block Test Results for R = 0.1, 414 & 325 MPa; Power Law Fatigue Model With Linear and Nonlinear Residual Strength and Miner's Rule Lifetime Predictions

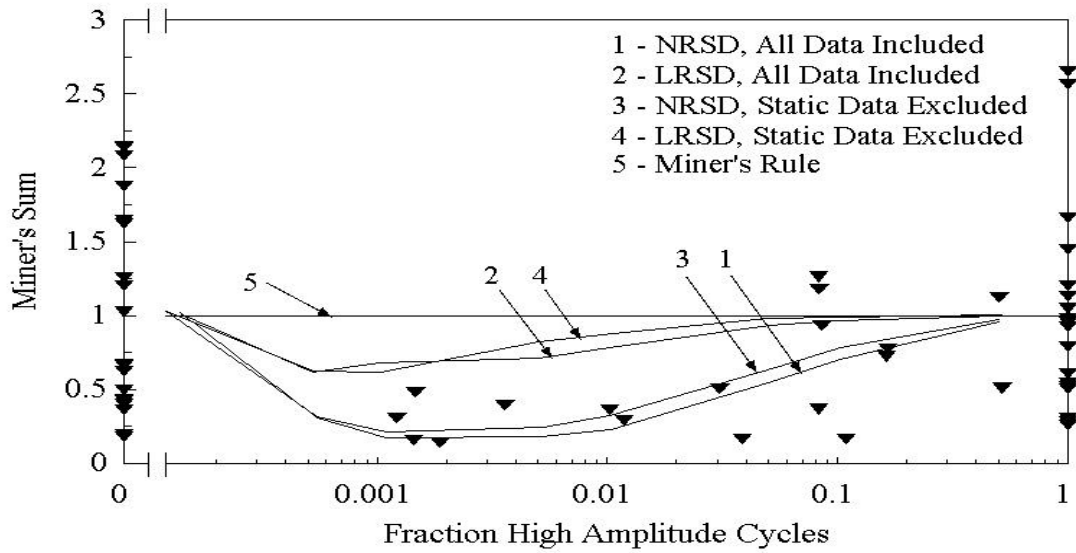


Figure 58. Two-Block Test Results for R = 0.1, 414 & 235 MPa; Exponential Fatigue Model With Linear and Nonlinear Residual Strength and Miner's Rule Lifetime Predictions

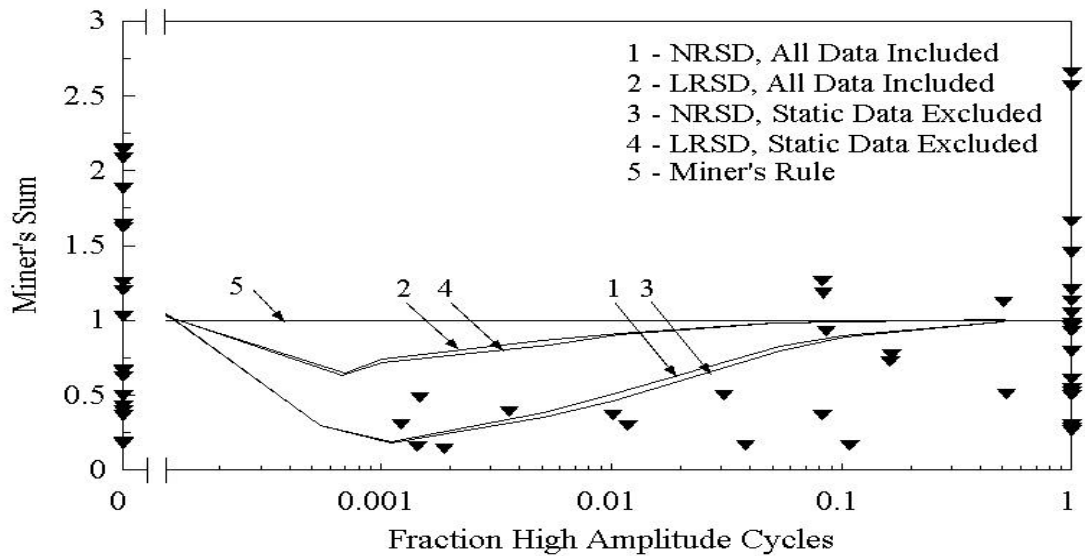


Figure 59. Two-Block Test Results for R = 0.1, 414 & 235 MPa; Power Law Fatigue Model With Linear and Nonlinear Residual Strength and Miner's Rule Lifetime Predictions

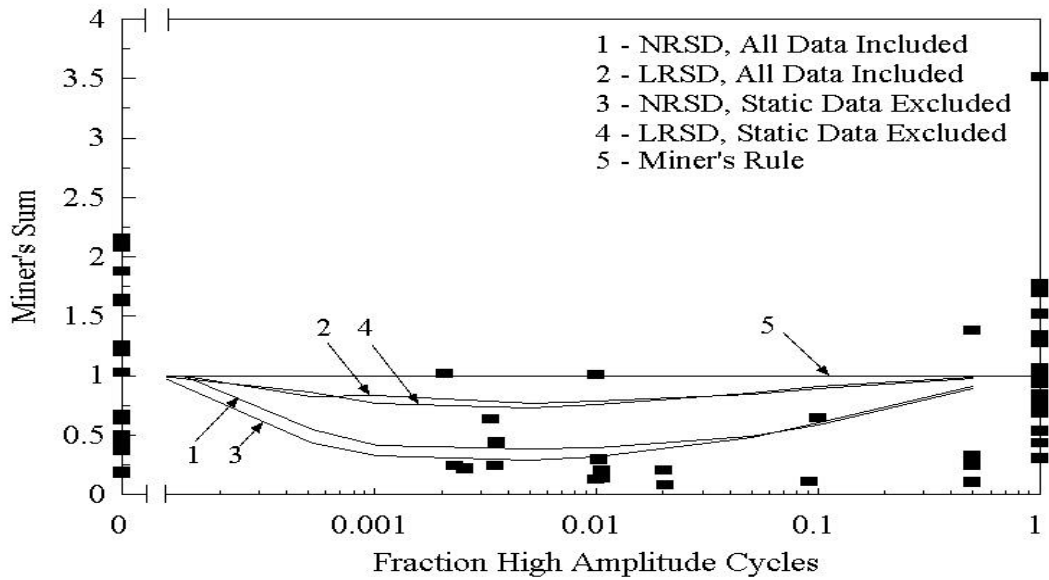


Figure 60. Two-Block Test Results for  $R = 0.1$ , 325 & 235 MPa; Exponential Fatigue Model With Linear and Nonlinear Residual Strength and Miner's Rule Lifetime Predictions

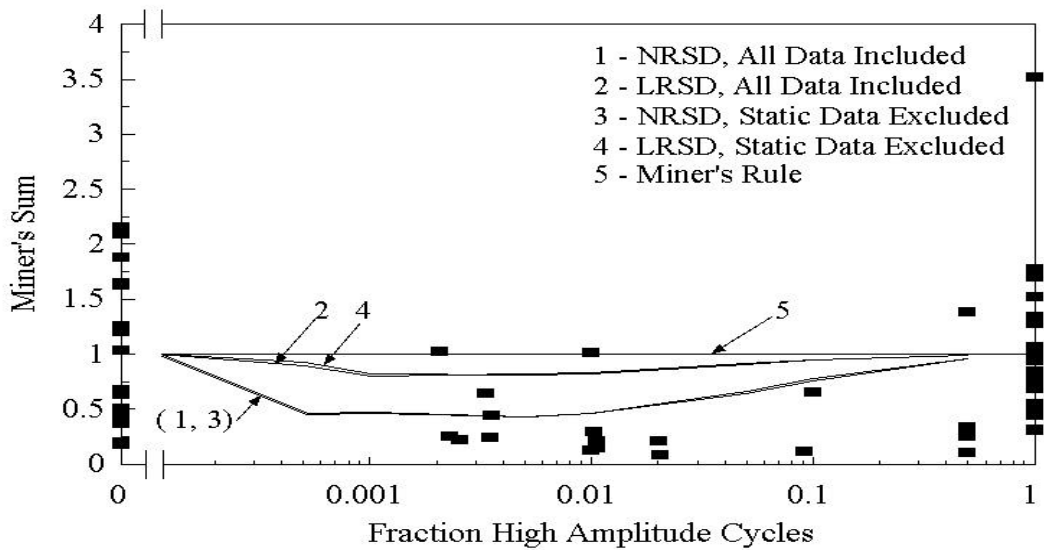


Figure 61. Two-Block Test Results for  $R = 0.1$ , 325 & 235 MPa; Power Law Fatigue Model With Linear and Nonlinear Residual Strength and Miner's Rule Lifetime Predictions

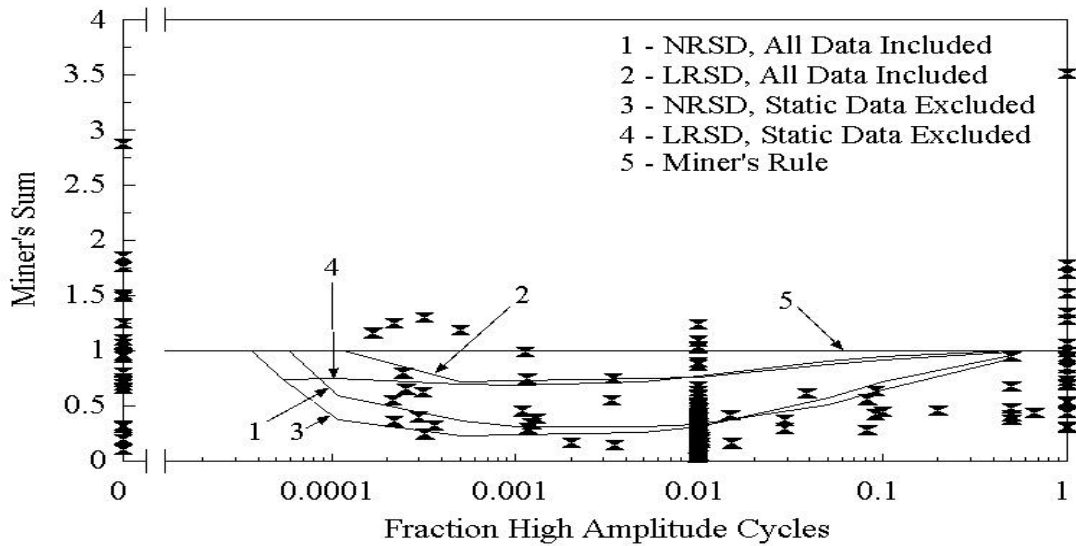


Figure 62. Two-Block Test Results for R = 0.1, 325 & 207 MPa; Exponential Fatigue Model With Linear and Nonlinear Residual Strength and Miner's Rule Lifetime Predictions

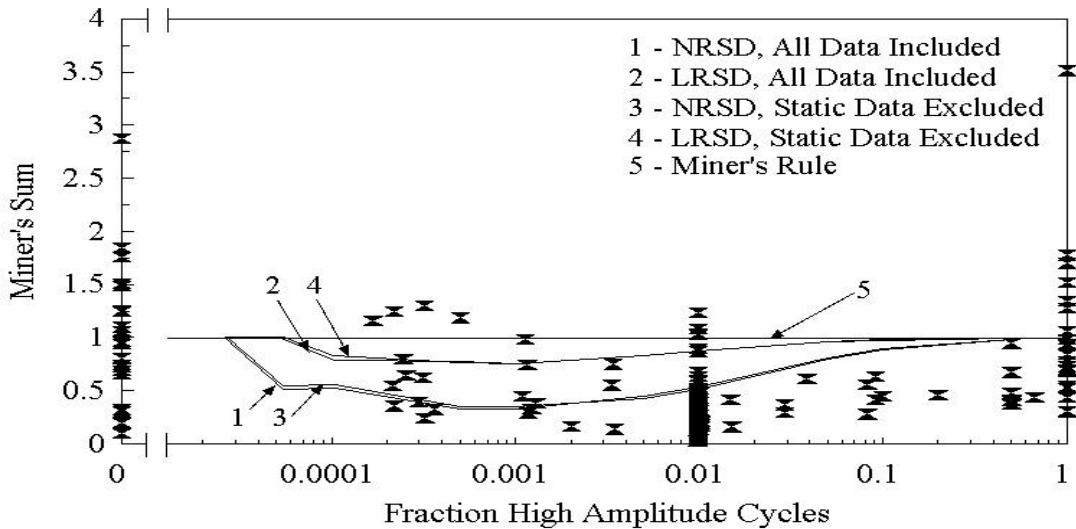


Figure 63. Two-Block Test Results for R = 0.1, 325 & 207 MPa; Power Law Fatigue Model With Linear and Nonlinear Residual Strength and Miner's Rule Lifetime Predictions

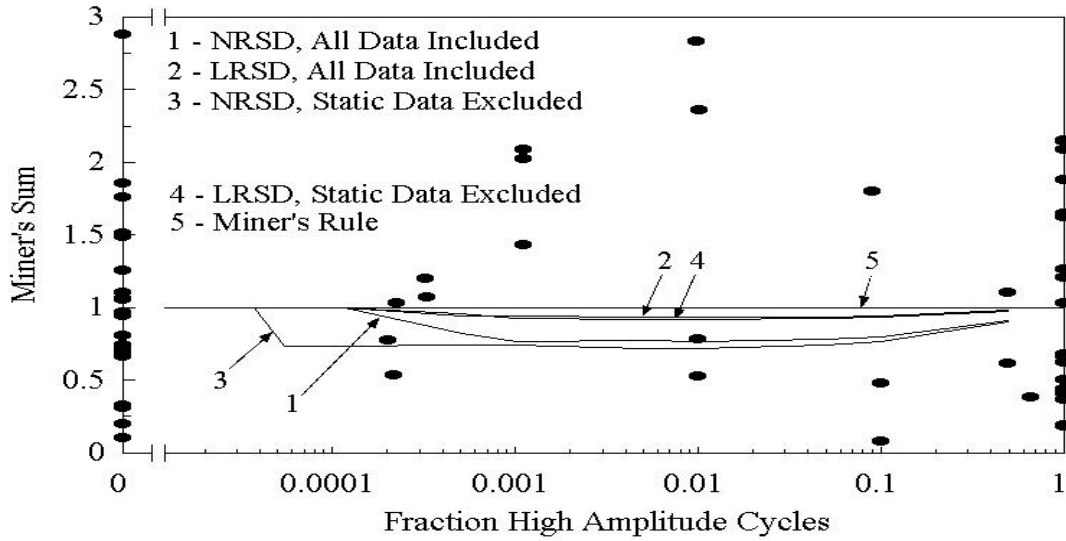


Figure 64. Two-Block Test Results for  $R = 0.1$ , 235 & 207 MPa; Exponential Fatigue Model With Linear and Nonlinear Residual Strength and Miner's Rule Lifetime Predictions

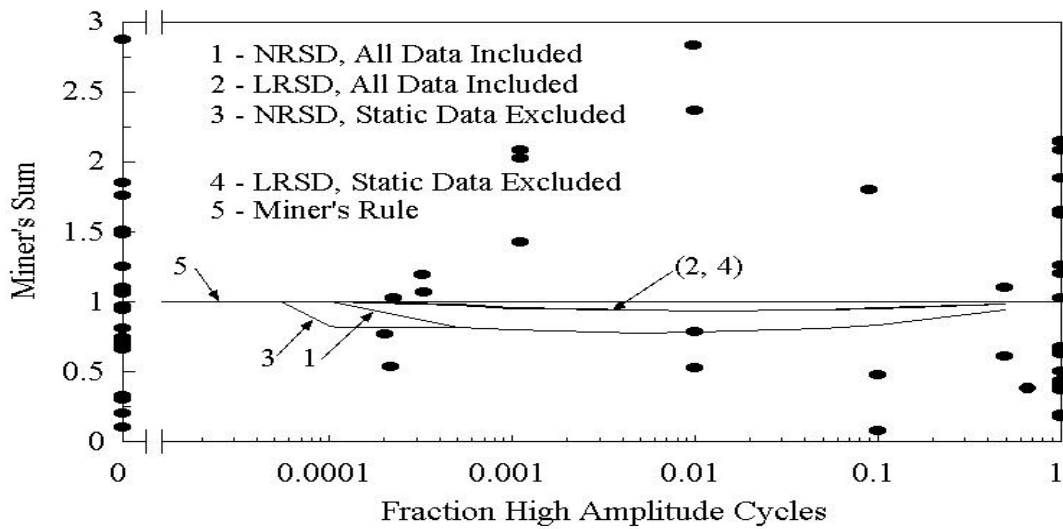


Figure 65. Two-Block Test Results for  $R = 0.1$ , 235 & 207 MPa; Power Law Fatigue Model With Linear and Nonlinear Residual Strength and Miner's Rule Lifetime Predictions

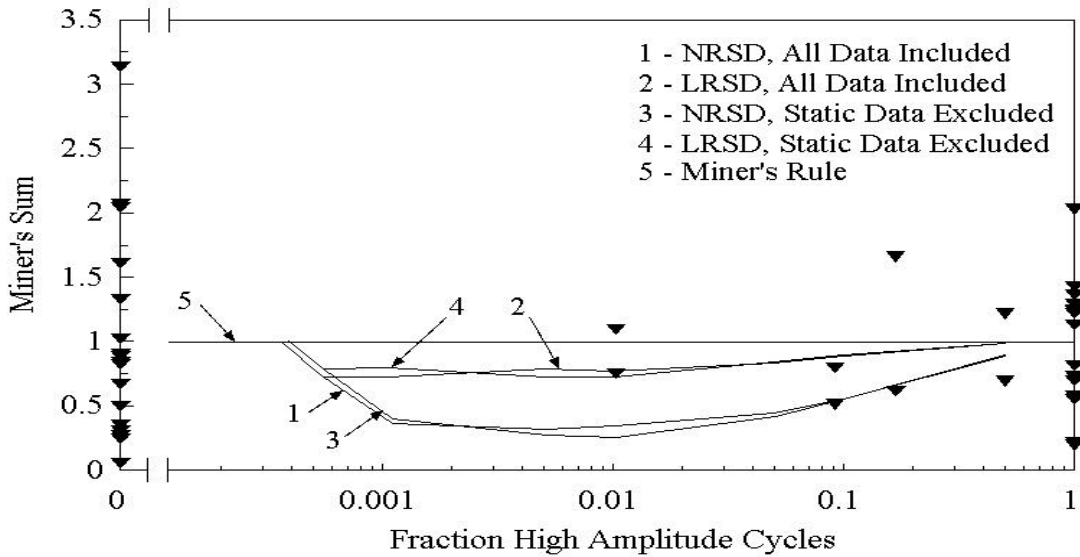


Figure 66. Two-Block Test Results for R = 0.5, 414 & 325 MPa; Exponential Fatigue Model With Linear and Nonlinear Residual Strength and Miner's Rule Lifetime Predictions

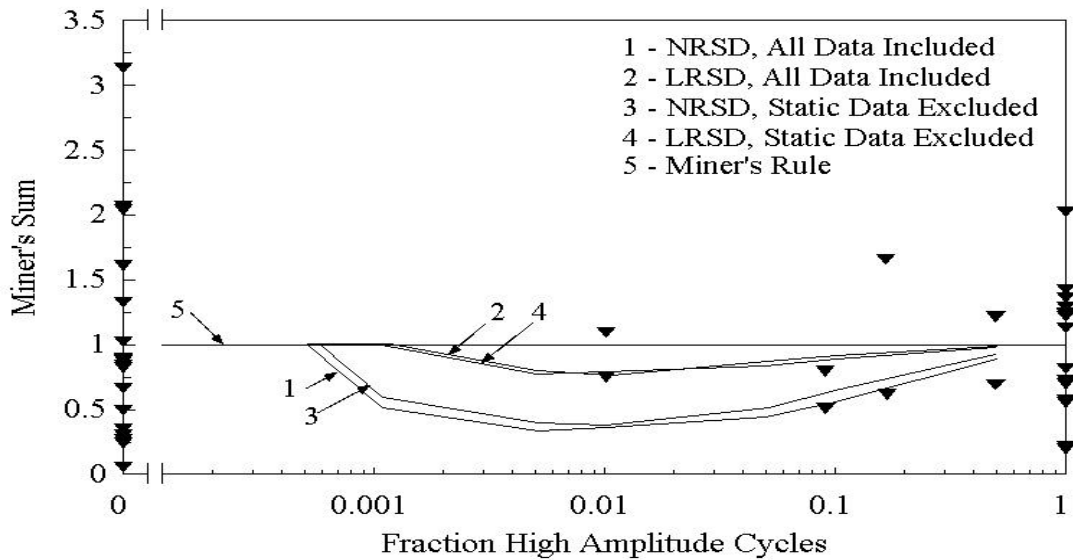


Figure 67. Two-Block Test Results for R = 0.5, 414 & 325 MPa; Power Law Fatigue Model With Linear and Nonlinear Residual Strength and Miner's Rule Lifetime Predictions

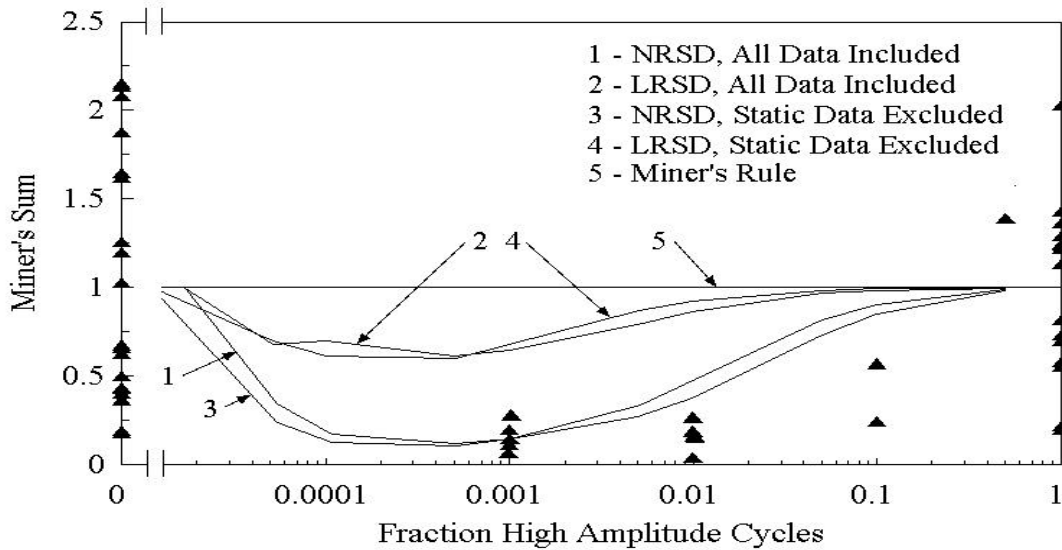


Figure 68. Two-Block Test Results for R = 0.5, 414 & 235 MPa; Exponential Fatigue Model With Linear and Nonlinear Residual Strength and Miner's Rule Lifetime Predictions

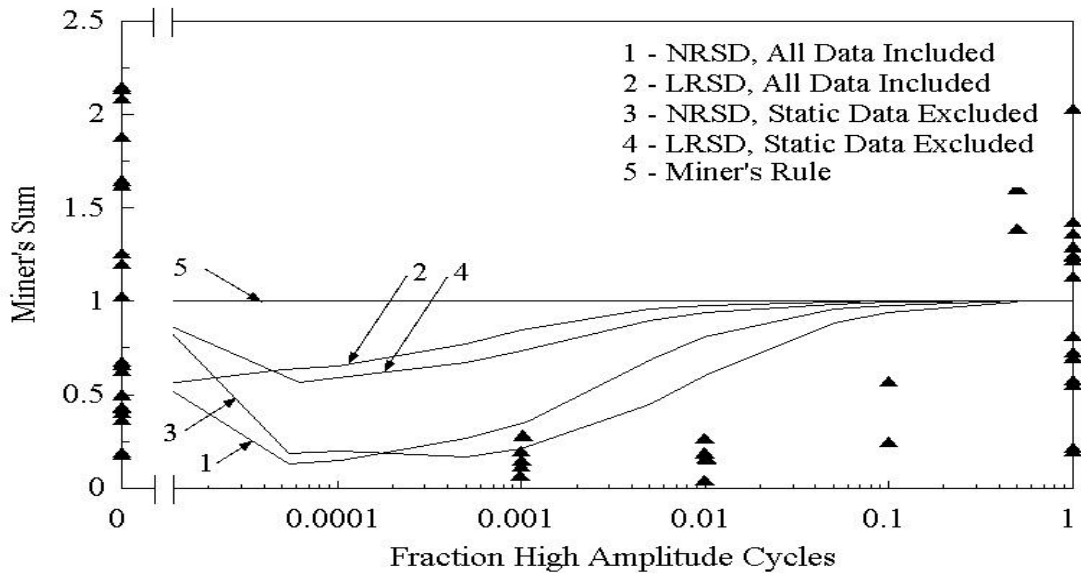


Figure 69. Two-Block Test Results for R = 0.5, 414 & 235 MPa; Power Law Fatigue Model With Linear and Nonlinear Residual Strength and Miner's Rule Lifetime Predictions



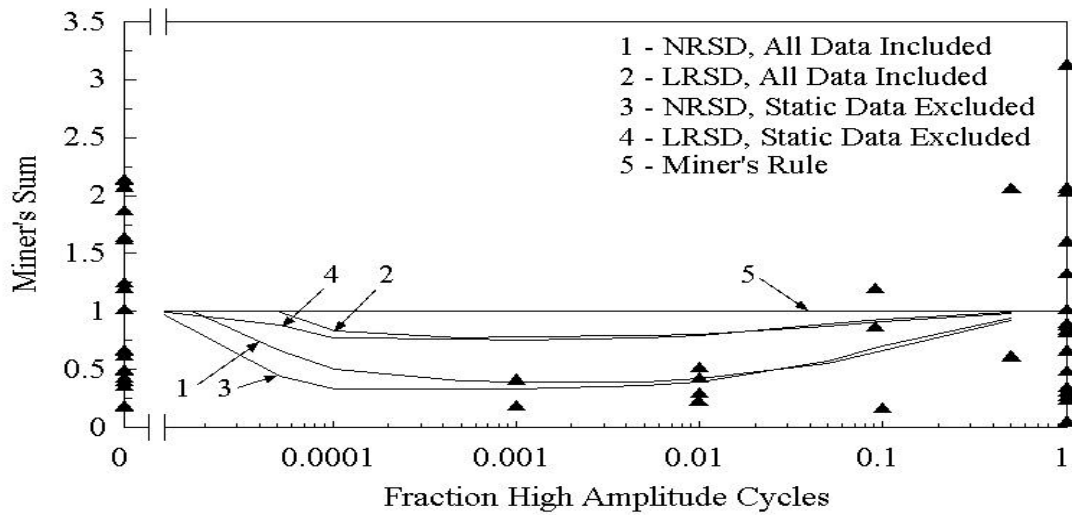


Figure 70. Two-Block Test Results for R = 0.5, 325 & 235 MPa; Exponential Fatigue Model With Linear and Nonlinear Residual Strength and Miner's Rule Lifetime Predictions

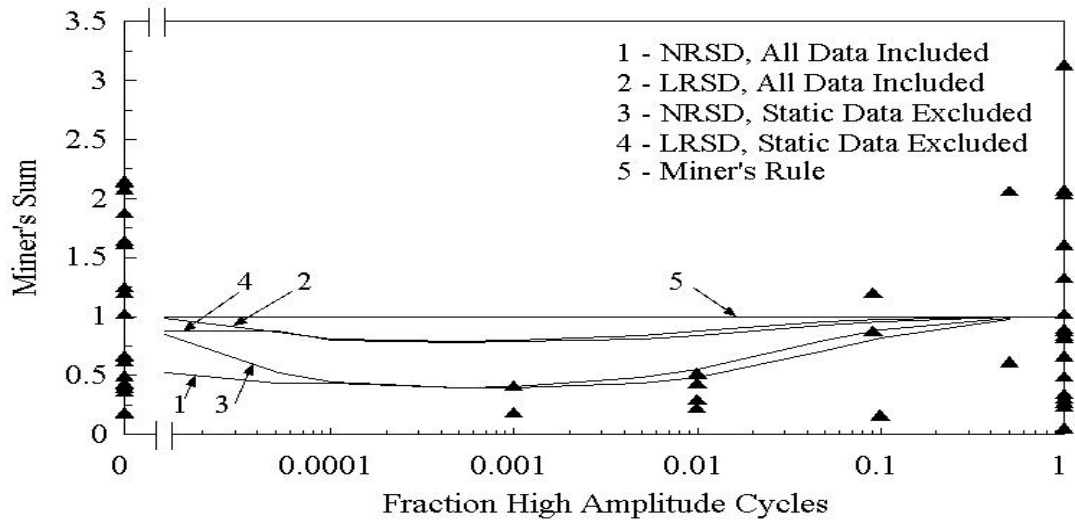


Figure 71. Two-Block Test Results for R = 0.5, 325 & 235 MPa; Power Law Fatigue Model With Linear and Nonlinear Residual Strength and Miner's Rule Lifetime Predictions

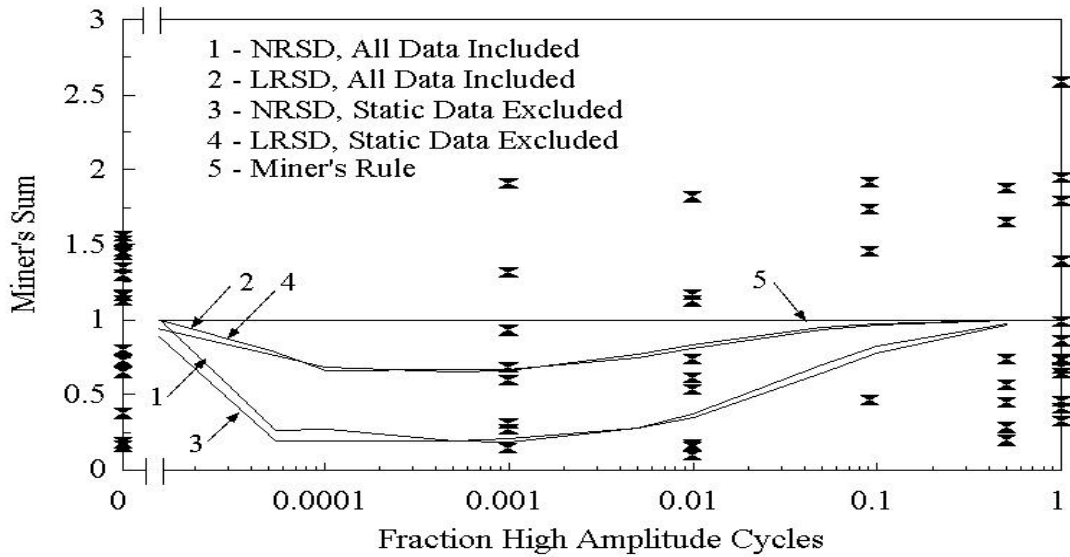


Figure 72. Two-Block Test Results for R = 10, -275 & -207 MPa; Exponential Fatigue Model With Linear and Nonlinear Residual Strength and Miner's Rule Lifetime Predictions

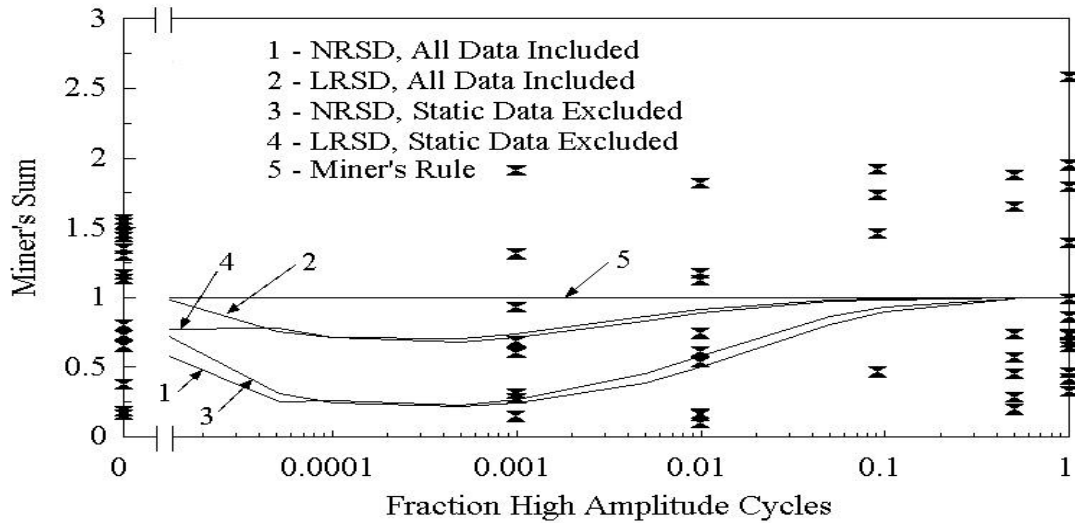


Figure 73. Two-Block Test Results for R = 10, -275 & -207 MPa; Power Law Fatigue Model With Linear and Nonlinear Residual Strength and Miner's Rule Lifetime Predictions

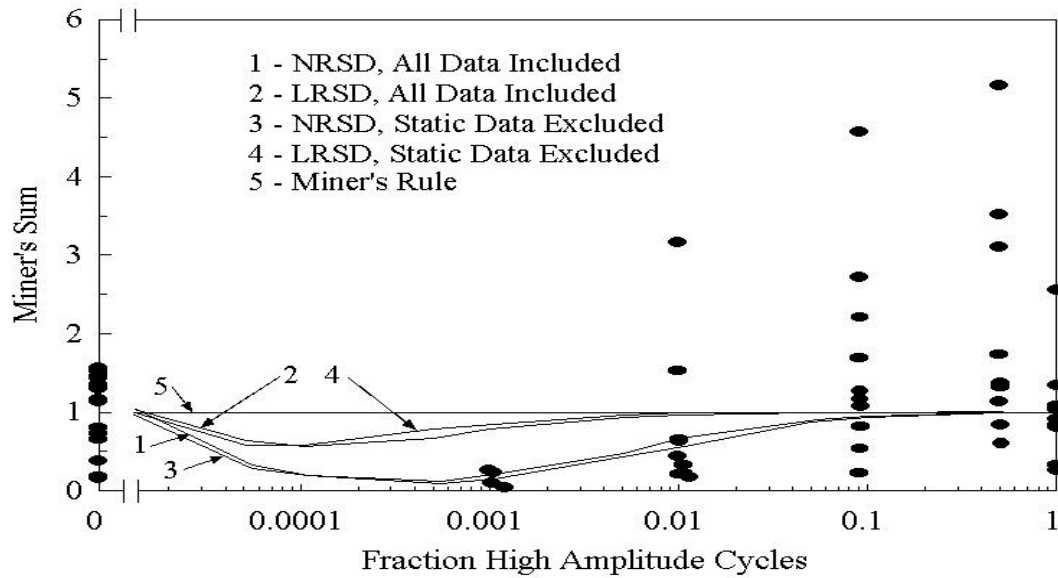


Figure 74. Two-Block Test Results for R = 10, -325 & -207 MPa; Exponential Fatigue Model With Linear and Nonlinear Residual Strength and Miner's Rule Lifetime Predictions

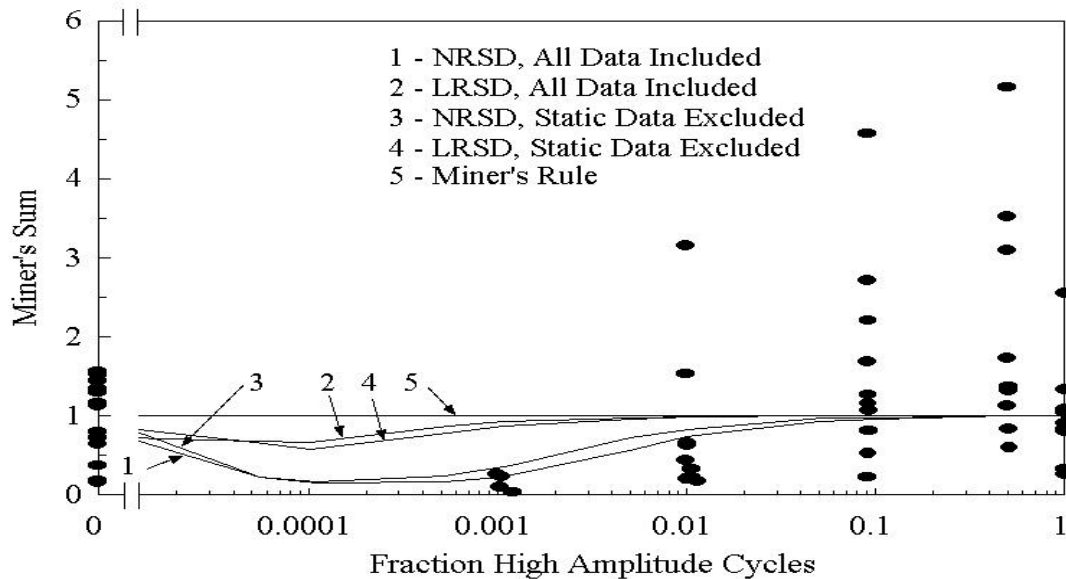


Figure 75. Two-Block Test Results for R = 10, -325 & -207 MPa; Power Law Fatigue Model With Linear and Nonlinear Residual Strength and Miner's Rule Lifetime Predictions

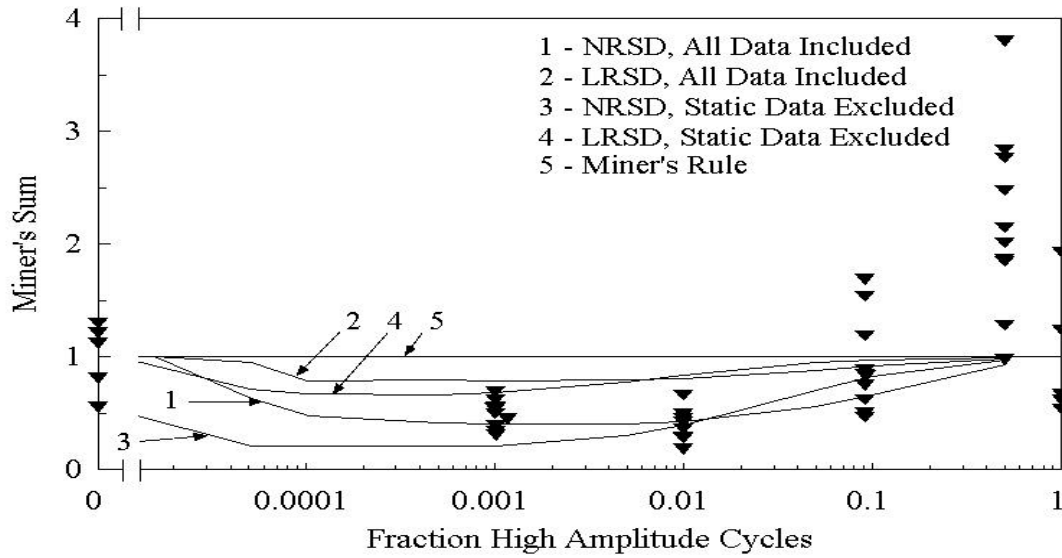


Figure 76. Two-Block Test Results for R = -1, 173 & 104 MPa; Exponential Fatigue Model With Linear and Nonlinear Residual Strength and Miner's Sum Lifetime Predictions

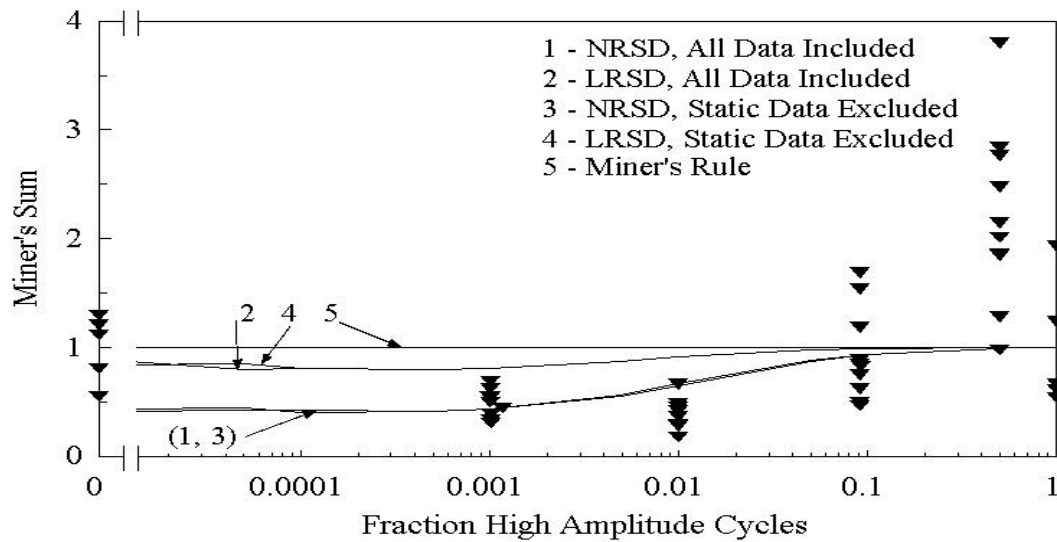


Figure 77. Two-Block Test Results for R = -1, 173 & 104 MPa; Power Law Fatigue Model With Linear and Nonlinear Residual Strength and Miner's Sum Lifetime Predictions

Multi-Block Fatigue Testing

Additional blocks were added to increase the complexity of the spectrum used in fatigue testing of the selected laminate. Testing of three and six blocks was performed. The three block test spectrum was generally comprised of ten cycles of 414 MPa maximum stress, ten cycles of 325 MPa, and 100 cycles of 235 MPa, all at an R-value of 0.1. The sequencing of the blocks was varied. Testing results were summarized and are shown in Table 7.

Table 7. Three-Block Test Results

Test No.	Block Cycles	Stress MPa	Actual Cycles to Specimen Failure	Miner's Sum at Failure
179	10	414	62	0.520
	100	325	600	
	1000	235	6000	
489	10	414	113	0.421
	10	325	110	
	100	235	1100	
490	10	325	180	0.653
	10	414	174	
	100	235	1700	
491	100	235	1600	0.576
	10	325	160	
	10	414	153	
492	10	414	123	0.458
	10	325	120	
	100	235	1200	
493	100	235	1634	0.599
	10	325	160	
	10	414	160	

The six block spectrum was arranged to the same format as that used by Echtermeyer, et. al., [48] and summarized in Table 8. Results of the six block testing are summarized in Table 9. Note, not all tests were conducted at the same maximum stress level.

Table 8. Six-Block Spectrum

Block #	Block Cycles	% Maximum Stress
1	1000	30
2	1000	50
3	400	75
4	10	100
5	400	75
6	1000	50

Table 9. Six-Block Test Results

Test No.	Block Cycles	Stress MPa	Actual Cycles to Specimen Failure	Miner's Sum at Failure
220	1000	97.5	26000	0.397
	1000	162.5	26000	
	400	243.75	10400	
	10	325	260	
	400	243.75	10337	
	1000	162.5	25000	
221	1000	103.5	8000	0.773
	1000	172.5	8000	
	400	258.75	3044	
	10	345	70	
	400	258.75	2800	
	1000	172.5	7000	
222	1000	124.2	2000	0.181
	1000	207	2000	
	400	310.5	654	
	10	414	10	
	400	310.5	400	
	1000	207	1000	
225	1000	103.5	5000	0.115
	1000	172.5	5000	
	400	258.75	2000	
	10	345	50	
	400	258.75	1857	
	1000	172.5	4000	

Table 9. Six-Block Test Results - continued

Test No.	Block Cycles	Stress MPa	Actual Cycles to Specimen Failure	Miner's Sum at Failure
226	1000	82.8	48000	0.203
	1000	138	48000	
	400	207	19200	
	10	276	480	
	400	207	18968	
	1000	138	47000	

The actual lifetime for each of the two, three and six block fatigue tests will be compared to the results of lifetime prediction models in Chapter 8. The actual Miner's sums for each of these multi-block tests were less than one.

## CHAPTER 7

## RANDOM SPECTRUM FATIGUE TESTING AND RESULTS

Fatigue testing of the selected laminate has covered constant amplitude and block spectra in the preceding Chapters 5 and 6. As loading of wind turbine blades is more random in nature, more random spectra also must be considered. Researchers in various industries have developed standard spectra for testing [15, 16]. The European wind research community developed WISPER (WInd turbine reference SPEctRum), a standardized variable amplitude loading history for wind turbine blades. Variations of this spectrum were created for use in this research.

WISPER and WISPERX

WISPER was developed from loading data collected from the root area of blades for wind turbines. The out-of-plane, or flap, loading was collected from nine horizontal axis wind turbines located in western Europe. The data were distilled into a sequence of 265,423 loading reversal points, or approximately 130,000 cycles. The reversal data are normalized to a maximum of 64 and a minimum of 1. In this form, the zero load level occurs at 25.

Analysis of WISPER revealed the spectrum has an average R-value of 0.4. The single largest peak and the single most extreme valley have an R-value of -0.67. The R-value for the adjacent largest spread between the peak and valley was -2.0.

Since the application of the WISPER spectrum at 10 Hertz would take nearly four



hours to make one pass, the authors of WISPER derived a shortened version to speed fatigue testing. The shortened version was created by filtering the smaller amplitude cycles, which resulted in one-tenth of the number of cycles, see Figure 78. Consequently the name applied to the new spectrum was WISPERX, the X representing the significance of the one-tenth size. Of the approximately 13,000 cycles in the WISPERX spectrum, only 143 are reversing.

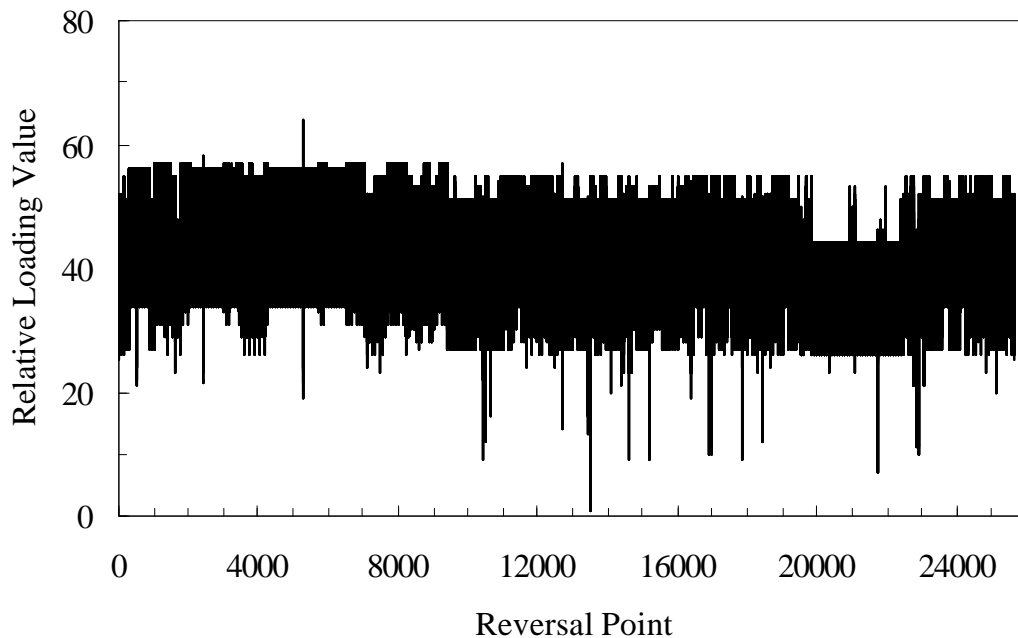


Figure 78. WISPERX Spectrum

The WISPER authors list several purposes [16] for the standard spectrum, including the evaluation of component design and the “assessment of models for the prediction of fatigue and crack propagation life by calculation, like Miner’s Rule.” The latter of these purposes was applied in this research.

WISPERX Modifications

WISPERX was re-scaled from its normalized form to a form compatible with the Instron software, RANDOM. The results are shown in Figure 79. The scaling followed the equation:

$$y = \frac{(x - 25)}{(64 - 25)} \quad (18)$$

where  $x$  are the published values for the reversal points and  $y$  is the scaled version. The convenience of forcing the spectrum reversal points to a maximum of one allowed the application of any maximum stress level by a simple multiplier of value equal to the

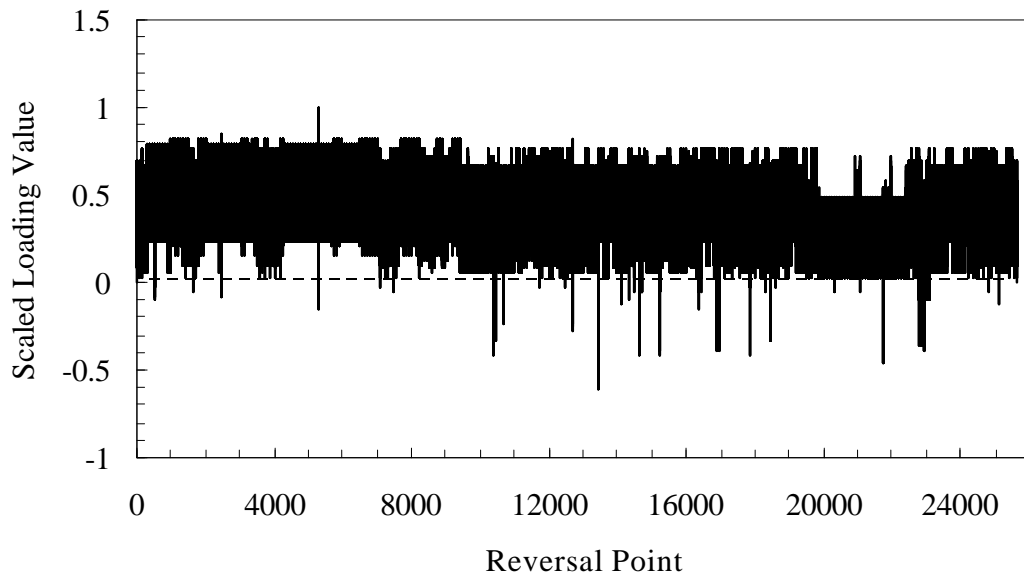


Figure 79. Scaled WISPERX Spectrum

maximum stress level. Each value was saved in a format of sign ( $\pm$ ) and the value to four significant figures (+#.####).

A wide range of R-values are present in WISPERX, yet only five R-values, other than the ultimate strengths, were tested in preparation of the base-line data. As a first step in applying this type of complex spectrum, it was decided to modify WISPERX to a constant R-value, thus avoiding both complex failure mode interactions and the need to interpolate between different R-values in the Goodman diagram. Two spectra were prepared, one for an R-value of 0.1 and one for 0.5. These modifications were accomplished by noting the peak reversal point and forcing the following valley (or trough) value to be either 0.1 or 0.5 times the peak value. A graphical version of these modifications is shown in Figure 80.

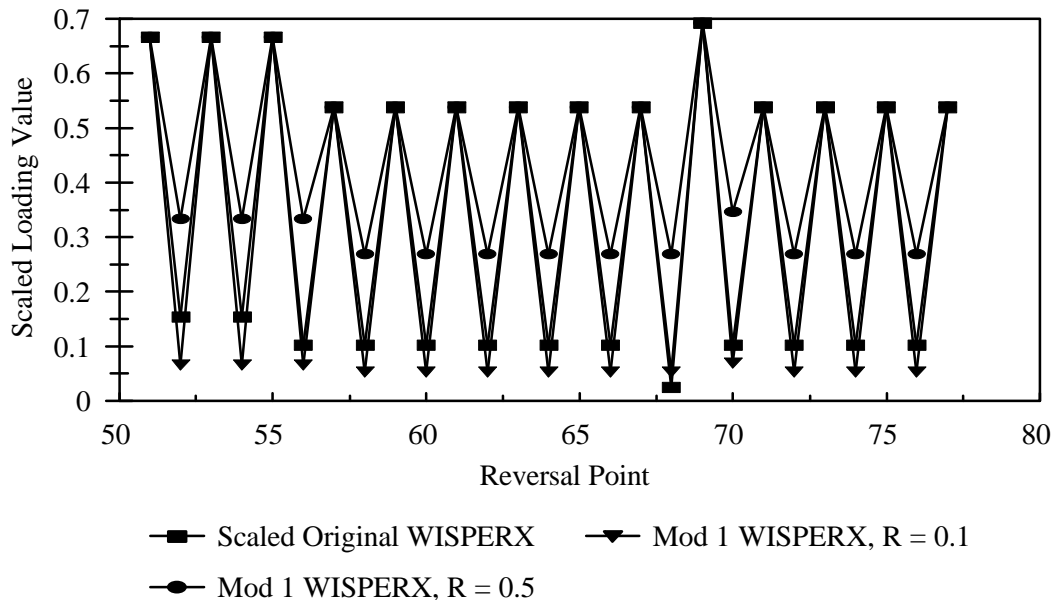


Figure 80. Modified WISPERX Spectrum Example

Two forms of the modified spectrum were created, both forced the constant R-values, but the first, termed Mod 1, retained only the tension-tension peak-valley reversal points, while the second, Mod 2, retained all reversal points. The first spectrum did not contain the one time extreme condition that was in the original WISPER and WISPERX spectra, while Mod 2 retained this one-time high-load event. Visual appreciation of these spectra can be gained from Figures 81, 82 and 83. Note the single relatively large event occurring at approximately the 5000<sup>th</sup> reversal point in the Mod 2 spectrum, Figure 83.

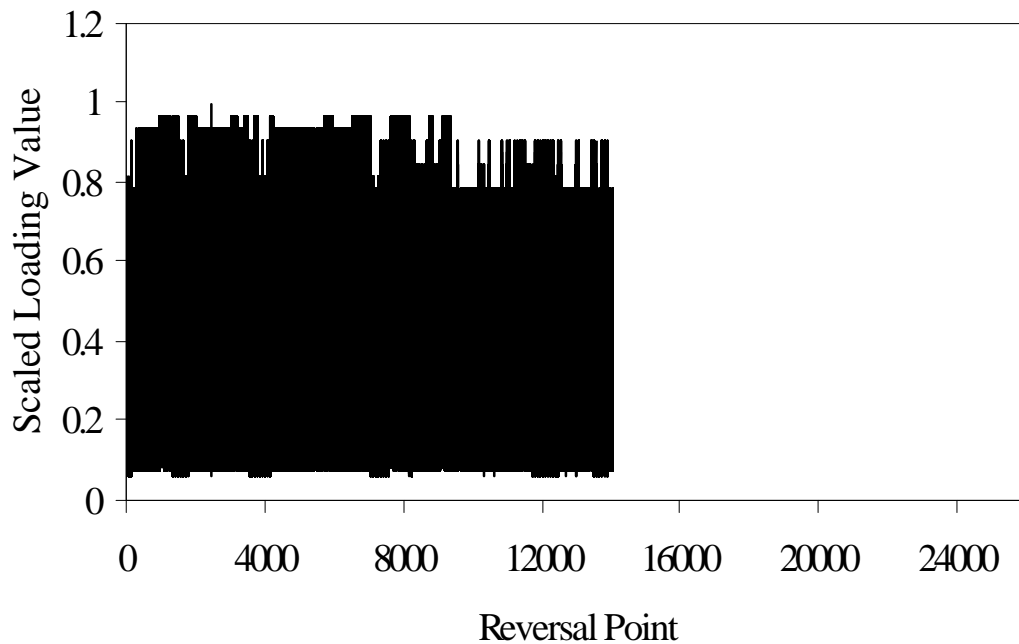


Figure 81. Mod 1 Spectrum for R = 0.1

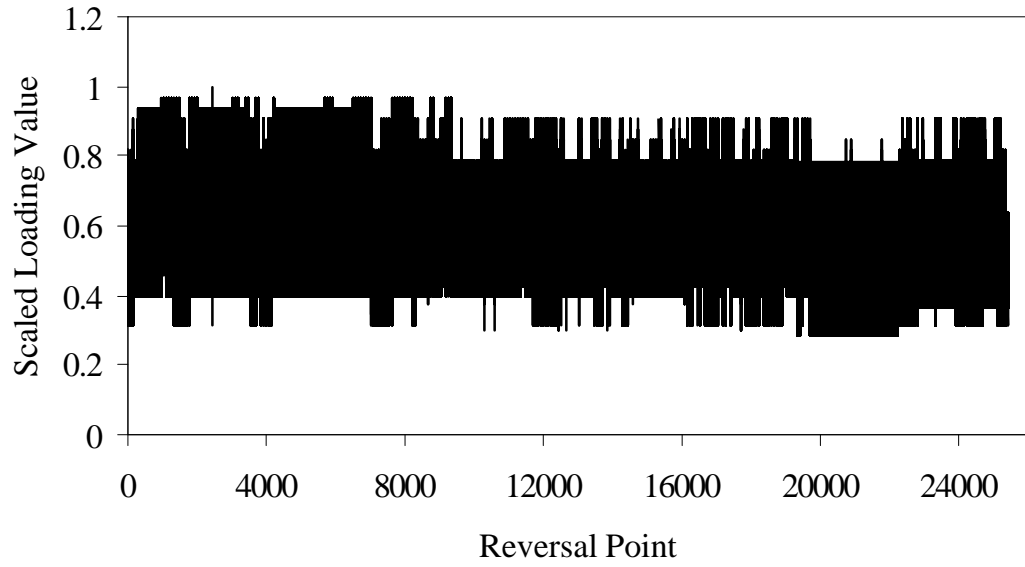


Figure 82. Mod 1 Spectrum for R = 0.5

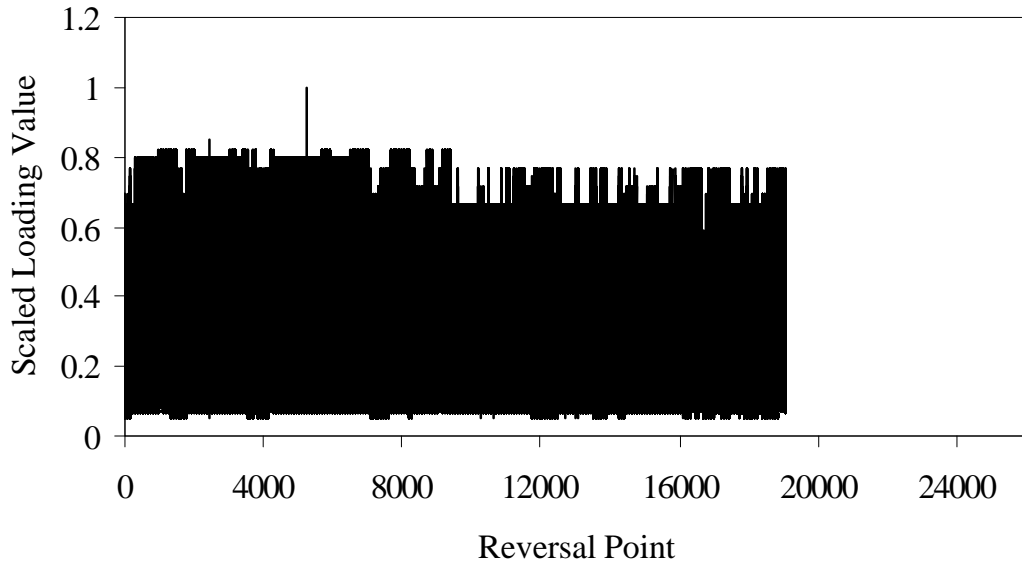


Figure 83. Mod 2 Spectrum for R = 0.1

Modified WISPERX Spectrum Test Results

Tests were run for these spectra with the loads taken as a multiples of the scaled values. The data are then represented in conventional S-N format where the stress coordinate is the maximum stress in the spectrum. The multiplier is varied to achieve relatively higher or lower stress cases having shorter or longer lifetimes, respectively.

The results for the Mod 1 and 2 spectra testing are summarized in Figures 84, 85 and 86. The trend of longer lifetimes for the R-value case of 0.5 were also experienced in the constant amplitude testing. Some high stress cases fail prior to completing one full pass through the spectrum. Tables 10 and 11 include a summary of the regression parameters for WISPERX test results for the exponential and power law regression analyses, respectively. These can be compared to the constant amplitude regression results presented in Tables 4 and 5. Reference equations 9 and 10 for definition of the terms  $C_1$ ,  $b$ ,  $C_2$  and  $m$ . For reference, approximately 13,000 cycles is equivalent to one block of the WISPERX spectra.

Table 10. Exponential Regression Analysis Parameters for WISPERX Fatigue

Range of Applicability	Regression Coefficients	Spectrum			
		Mod 1, R=0.1	Mod 1, R =0.5	Mod 2, R = 0.1	WISPERX
1 to $10^7$ Cycles	$C_1$	1.007	1.019	1.015	1.029
	$b$	0.121	0.107	0.106	0.107
10 to $10^7$ Cycles	$C_1$	0.879	0.941	0.891	0.872
	$b$	0.094	0.091	0.093	0.079

Table 11. Power Law Regression Analysis Parameters for WISPERX Fatigue

Range of Applicability	Regression Coefficients	Spectrum			
		Mod 1, R=0.1	Mod 1, R =0.5	Mod 2, R = 0.1	WISPERX
1 to 10 <sup>7</sup>	C <sub>2</sub>	1.048	1.056	1.075	1.041
Cycles	m	12.02	14.52	13.9	14.2
10 to 10 <sup>7</sup>	C <sub>2</sub>	1.111	1.179	1.126	1.21
Cycles	m	11.28	12.72	13.1	12.2

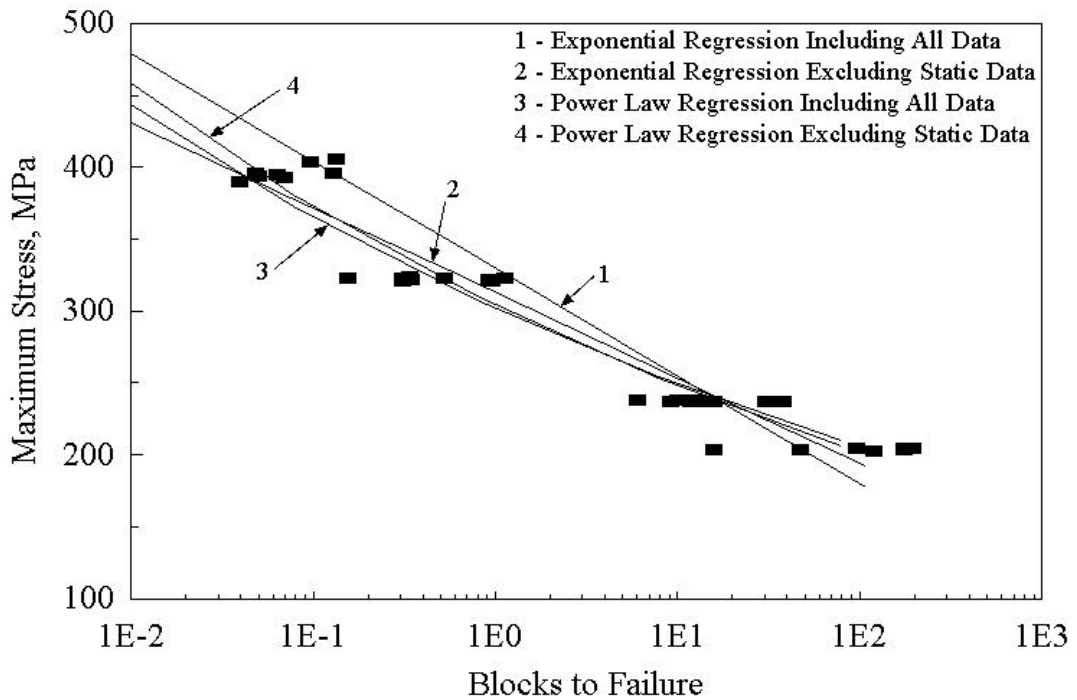


Figure 84. Mod 1 Spectrum Fatigue S-N Curve, R = 0.1

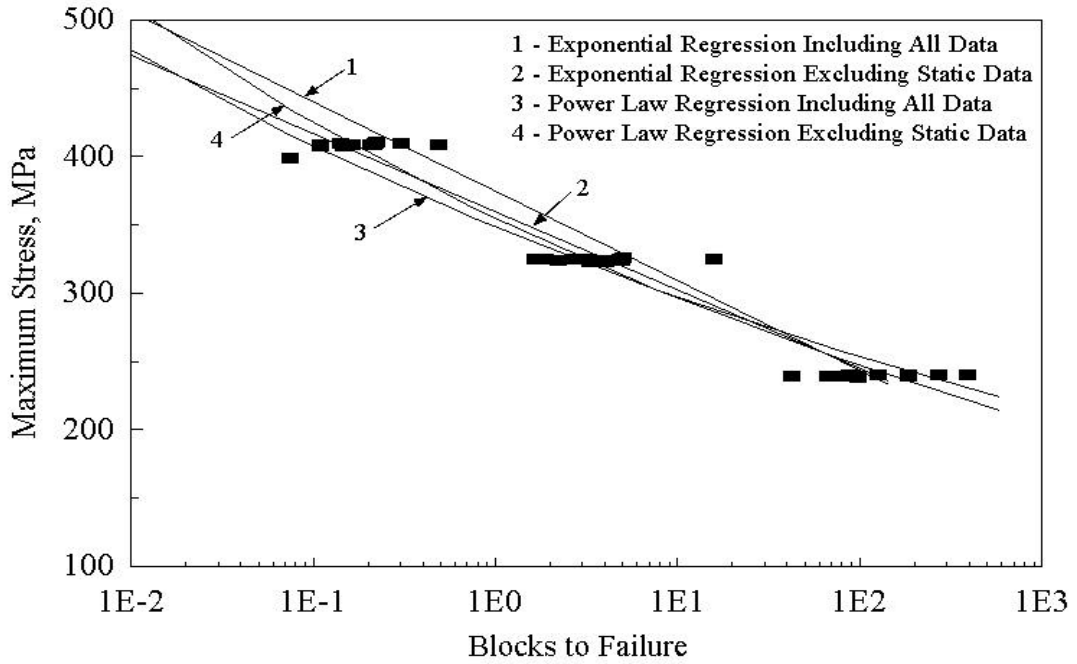


Figure 85. Mod 1 Spectrum Fatigue S-N Curve, R = 0.5

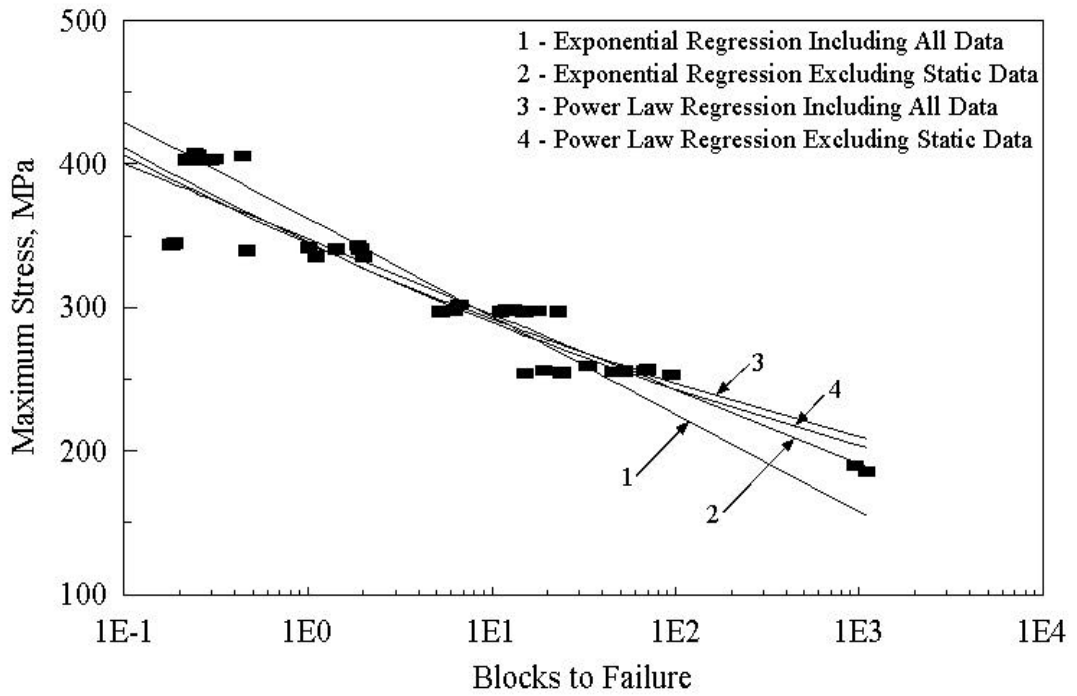


Figure 86. Mod 2 Spectrum Fatigue S-N Curve, R = 0.1



The slope or trend of the S-N curve in the Mod 2 case is less than that of the comparable case for the Mod 1 spectrum results. The maximum stress incurred in the Mod 2 spectrum tests was a once per pass event, while the maximum stress incurred in the Mod 1 spectrum tests was experienced several times per pass.

### Unmodified WISPERX Spectrum Test Results

Testing of coupons that were subjected to the original WISPERX spectrum, without modification for R-value, was also accomplished and summarized as exponential and power law S-N curves, Figure 87. The power law regression gives only slightly better correlation than the exponential regression. The regression analysis may be reviewed in Appendix D.

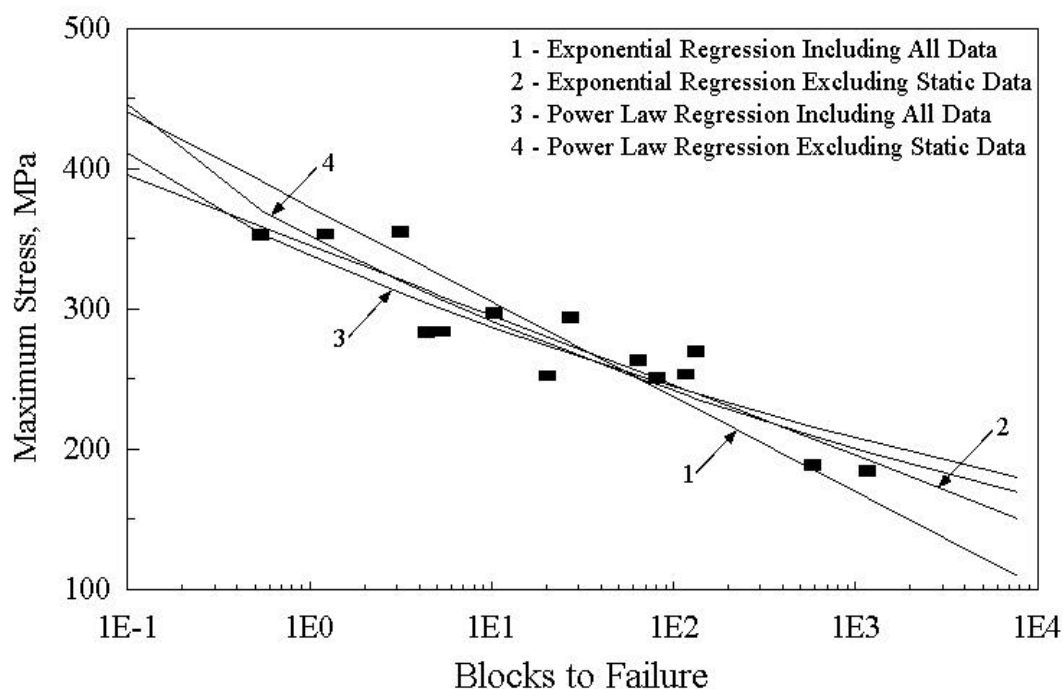


Figure 87. Unmodified WISPERX Spectrum Fatigue S-N Curve

The actual lifetime for the random tests will be compared to the results of lifetime prediction models in Chapter 8.

## CHAPTER 8

## LIFETIME PREDICTIONS

An accurate cumulative damage law is essential to efficient component design under fatigue loading. The fundamental and most widely applied damage law is that established by Palmgren [21] and Miner [5]. Under this law, damage is considered to develop linearly as a function of the number of cycles encountered at specific load levels. As reported earlier, Miner's sum is consistently less than unity, often on the order of 0.1, for tests using a spectrum of loads.

A component or specimen is considered to have failed when it can no longer support the load intended. One clear deficiency in Miner's sum is that it only accumulates damage and does not consider that the current strength may be exceeded by a particular high stress cycle, whereas residual strength based models inherently consider this event. Three models have been applied to lifetime predictions for theoretical specimens subjected to the various block and modified WISPERX spectra. Results of these predictions are compared to the actual lifetimes encountered during the testing. The three models considered are, 1) Miner's Rule, 2) linear residual strength degradation, and 3) nonlinear residual strength degradation. Constant amplitude fatigue models based upon exponential and power law regression analyses as well as the retention and omission of the static data were used in the residual strength based lifetime prediction rules. All results of predictions are reported in Miner's sum and compared to the actual Miner's sums from test results.

Constant Amplitude Fatigue Life Predictions

The base-line data of the constant amplitude testing was the starting point for the creation of lifetime predictions. The mean number of cycles to failure at each constant amplitude load level was used in all subsequent lifetime predictions; this would force the constant amplitude test Miner's sums to an average value of one. Therefore, the Miner's rule would reasonably accurately predict the lifetime for constant amplitude fatigue tests. Using either the linear or nonlinear residual strength lifetime prediction models for a constant amplitude test would reveal the same results as Miner's rule. Note the equations for the two residual strength degradation prediction methods, equations 15 and 16. Failure would be predicted by either of these equations when the residual strength was reduced to a level equivalent to the applied stress. This would happen when the number of cycles experienced,  $n$ , was equal to the number of cycles to failure,  $N$ , at that stress level. The constant amplitude test Miner's sum results are presented in Table 12. The "scatter" of Miner's sum for constant amplitude fatigue tests is greater than that experienced with metals.

Table 12. Descriptive Statistics for Constant Amplitude Miner's Sum

Case	Mean	Standard Deviation
414 MPa, R = 0.1	1	0.631
327 MPa, R = 0.1	1	0.692
245 MPa, r = 0.1	1	0.682

Table 12. Descriptive Statistics for Constant Amplitude Miner's Sum - continued

Case	Mean	Standard Deviation
207 MPa, R = 0.1	1	0.644
414 MPa, R = 0.5	1	0.486
327 MPa, R = 0.5	1	0.820
25 MPa, R = 0.5	1	0.840
-325 MPa, R = 10	1	0.638
-275 MPa, R = 10	1	0.681
-245 MPa, R = 10	1	1.942
-207 MPa, R = 10	1	0.484
-275 MPa, R = 2	1	1.686
173 MPa, R = -1	1	0.591
145 MPa, R = -1	1	0.281
104 MPa, R = -1	1	0.309

### Block Spectrum Fatigue Life Prediction Mechanics

#### Miner's Rule Lifetime Prediction Methodology

Miner's rule predictions are easily accomplished by accumulating the sums of each cycle ratio for each cycle of each block and repeating the sequence of blocks until this sum reaches unity. The cycle ratio for each cycle would be one (i.e. the single cycle) divided by the average number of cycles to failure at that cycle's stress level. This method is summarized in Figure 88.

#### Residual Strength Rule Based Lifetime Prediction Methodology

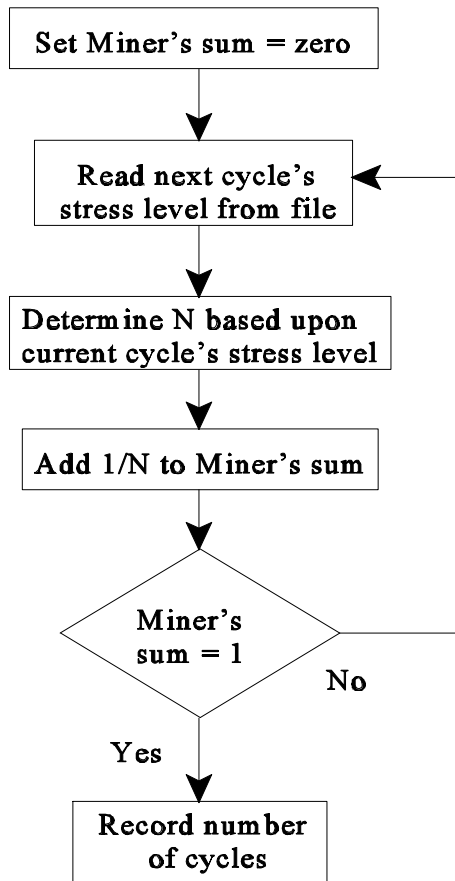


Figure 88. Miner's Sum Lifetime Prediction Methodology

Consider a life prediction based upon the linear residual strength model for a two block fatigue spectrum where the first block is  $n_1$  cycles long at a high stress level. The second block at a lower stress level is  $n_2$  cycles long. Trace the strength through the application of a succession of blocks as shown in Figure 89.

Starting with the ultimate strength, the strength decreases monotonically with each cycle in the first block until strength,  $s_1$ , is reached after  $n_1$  cycles of high stress. The residual

strength  $s_1$  would be the starting strength for fatigue at the stress level of the second block. The corresponding number of cycles theoretically experienced at this strength,  $s_1$ , would be  $n_2'$ . Fatigue for  $n_2$  cycles in the second block would extend the theoretically experienced cycles from  $n_2'$  to  $n_2''$  where  $n_2'' - n_2' = n_2$ , the number of cycles in the second block. The residual strength at this point in life is  $s_2$ , which would be the starting point for the next block, a repeat of the high stress cycle block. The corresponding number of theoretical cycles for at this stress level is  $n_3'$ . Fatigue at the high stress cycles would extend the number of cycles to  $n_3''$ . Since  $n_1$  is the number of cycles in the first high stress block, then  $n_3'' - n_3' = n_1 = n_3$ . This process would continue until the residual strength reduces to a value equal to the applied stress.

The calculation process is identical for both the linear and nonlinear residual strength degradation prediction models. The process is valid for blocks as short as one cycle; hence,

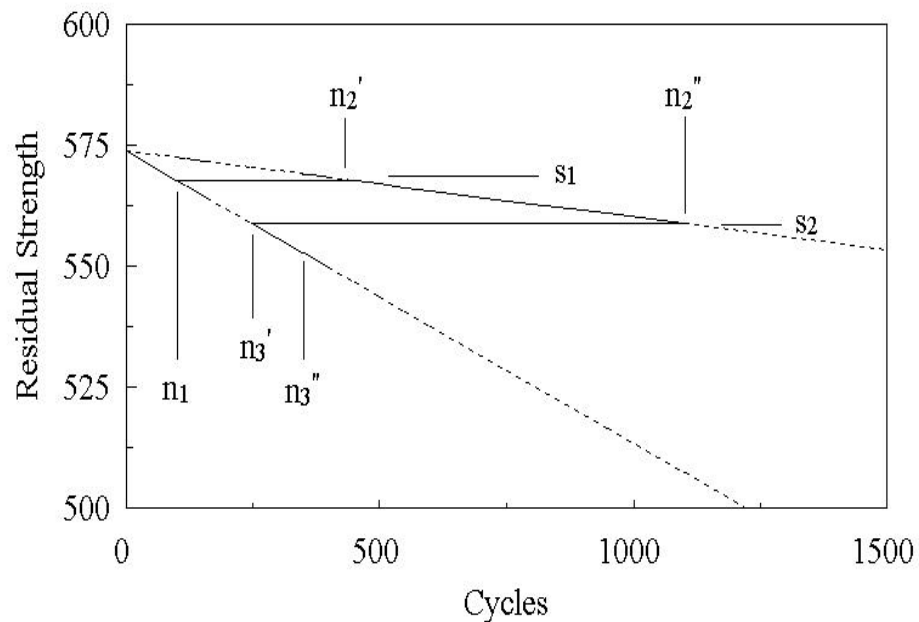


Figure 89. Lifetime Prediction Cycle Trace, Residual Strength Models

it is easily applied to random spectra as well as block spectra. The mechanics of these calculations were reduced to a computer algorithm to ease and speed data reduction. The algorithm is presented in Appendix F.

### Two-Block Spectrum Fatigue Life Predictions

The results of two-block spectrum fatigue tests were summarized in Figures 56 through 77 of Chapter 6 as a comparison of the Miner's sum related to the fraction of the high amplitude cycles experienced. The results of various lifetime prediction calculations were also shown on those figures. All but one of the multi-block fatigue test campaigns were performed in specific R-value regions where the mode of failure, tensile or compressive, was expected. This precluded the problem of lifetime predictions for mixed failure mode fatigue. The three prediction methods were applied in nine various configurations which are identified in Table 13 and applied for each load case.

Table 13. Lifetime Prediction Methods

1) Miner's linear rule
2) linear residual strength based with exponential fatigue model of all data
3) linear residual strength based with exponential fatigue model excluding static data
4) linear residual strength based with power law fatigue model of all data

Table 13. Lifetime Prediction Methods - continued

5) linear residual strength based with power law fatigue model excluding static data
6) nonlinear <sup>*</sup> residual strength based with exponential fatigue model of all data



7) nonlinear *	residual strength based with exponential fatigue model excluding static data
8) nonlinear *	residual strength based with power law fatigue model of all data
9) nonlinear *	residual strength based with power law fatigue model excluding static data

\* all nonlinear residual strength predictions assumed  $\dot{\epsilon} = 0.265$ .

### General Observations

The limit values for the fraction of high amplitude cycles for the two-block tests are zero and one. A zero fraction represents a constant amplitude fatigue test conducted at the lower stress level while a fraction of one represents the results of a constant amplitude fatigue test at the higher stress level. Consequently, the average of the Miner's sums at the limits must be one, as summarized in Table 12.

A general trend of Miner's sums of less than one is noted in the region between fractions of zero and one. The Miner's rule prediction is a constant value of 1.0 throughout the entire range of high amplitude cycle fractions, indicating the Miner's rule generally predicted a longer life than observed.

The relative magnitudes of the two stress levels had an effect on the variation of the Miner's sum over the range of the high cycle fraction. Test cases that had relatively close stress levels responded with a lesser variation in the Miner's sum whereas cases with a large difference in stress levels indicated a greater variation or dip in the Miner's sum. The former observation is logical when considering the limiting case of equal stress levels for each block. This would be a constant amplitude fatigue case for which the Miner's sum would be 1.0.

### Comparison of Residual Strength Based Lifetime Prediction Rules

The nonlinear rule with  $\hat{\alpha} = 0.265$  consistently provided Miner's sums less than those predicted by the linear residual strength degradation rule. This was assured by choosing the nonlinear parameter to be less than one, thereby forcing the predictions to more closely follow test results. Choosing a nonlinear parameter greater than unity would have caused the nonlinear Miner's sums to be greater than those calculated by the linear residual strength degradation method. Both methods trend towards unity at the limits of the high cycle fraction as shown in all Figures 56 through 77. In some cases such as that of Figures 62 and 66, the prediction stabilizes at unity for a range of cycle fractions above zero. In these cases, reducing the high cycle fraction below some value was not possible in that the predicted failure was always in the second low amplitude stress block, and the first high amplitude stress block was never repeated.

The linear and nonlinear methods produce converging Miner's sum predictions when the two block stress levels become closer. Typical examples of this latter observation are those in Figures 56 and 64 for R-values of 0.1 and Figures 72 and 74 for R-values of 10.

### Fatigue Model Selection Effect on Predictions

The fatigue models (equations 9 and 10) were based upon the regression analyses of the constant amplitude fatigue test results. There were four basic models prepared: 1) exponential regression analysis that included all fatigue data for each R-value; 2) exponential regression analysis that excluded the static data; 3) power law regression analysis that included all fatigue data; and 4) power law regression analysis that excluded the static data.

As there is some concern of possible differences in damage metrics that occur in high stress fatigue, including static tests, and the fatigue at lower stress levels, two fatigue models were prepared for consideration. This also allows breaking the regression results that represent the S-N fatigue data into a series of curves, each considered valid over a range of component life.

Generally, the nonlinear residual strength degradation based prediction models are sensitive to which of the four fatigue models is chosen, whereas the linear strength degradation based predictions models are insensitive. Consider Figure 33, the S-N diagram for constant amplitude fatigue at R-values of 0.1. The power law regression models for both cases of including and excluding the static data are nearly identical. This can also be seen in Figure 57 for the nonlinear lifetime predictions for the two-block case of block stresses of 414 and 325 MPa with R-values of 0.1. The exponential regression models represented in Figure 37 are quite different for the cases of including and excluding the static data. At the higher cycles, an equivalent higher stress is required to cause failure for the exponential fatigue model that excludes the static data than that which includes the static data. Again, this is borne out in the predictions summarized in Figure 56, where the Miner's sums at the low cycle fractions are greater for the exponential fatigue model that excluded the static data than for that which included the static data.

The nonlinear residual strength based prediction rules provided better agreement with test results than did the linear based rule. Generally, the selection of the fatigue model had little influence in the predictions, at least for the cases of two-block spectra.

Three and Six-Block Spectrum Fatigue Life Predictions

The actual Miner's sums for the three and six block tests (spectra shown in Tables 7 and 8 of Chapter 6) were consistently less than one, as summarized in Tables 14 and 15. The linear residual strength model predictions of the Miner's sum were always higher than the actual Miner's sums. The nonlinear residual strength model predictions of the Miner's sum were mostly higher than the actual.

Table 14. Three-Block Spectrum Fatigue Life Predictions

Test No.	Sequence Cycles	Load	Actual Cycles	Miner's Sum		
				Actual	Linear Prediction	Non-Linear Prediction
179	10	414	62	0.520	0.770	0.282
	100	325	600			
	1000	235	6000			
489	10	414	113	0.421	0.920	0.657
	10	325	110			
	100	235	1100			
490	10	325	180	0.653	0.918	0.651
	10	414	174			
	100	235	1700			
491	100	235	1600	0.576	0.916	0.648
	10	325	160			
	10	414	153			

Table 14. Three-Block Spectrum Fatigue Life Predictions - continued

Test No.	Sequence Cycles	Load	Actual Cycles	Miner's Sum		
				Actual	Linear Prediction	Non-Linear Prediction
492	10	414	123	0.458	0.920	0.657
	10	325	120			
	100	235	1200			
493	100	235	1634	0.599	0.916	0.648
	10	325	160			
	10	414	160			

Table 15. Six-Block Spectrum Fatigue Life Predictions

Test No.	Sequence		Actual Cycles	Miner's Sum		
	Cycles	Load		Actual	Linear Prediction	Non-Linear Prediction
220	1000	97.5	26000	0.397	0.758	0.335
	1000	162.5	26000			
	400	243.75	10400			
	10	325	260			
	400	243.75	10337			
	1000	162.5	25000			
221	1000	103.5	8000	0.173	0.747	0.296
	1000	172.5	8000			
	400	258.75	3044			
	10	345	70			
	400	258.75	2800			
	1000	172.5	7000			
222	1000	124.2	2000	0.181	0.677	0.203
	1000	207	2000			
	400	310.5	654			
	10	414	10			
	400	310.5	400			
	1000	207	1000			
225	1000	103.5	5000	0.115	0.747	0.296
	1000	172.5	5000			
	400	258.75	2000			
	10	345	50			
	400	258.75	1857			
	1000	172.5	4000			
226	1000	82.8	48000	0.203	0.814	0.406
	1000	138	48000			
	400	207	19200			
	10	276	480			
	400	207	18968			
	1000	138	47000			

Note the predictions for the both linear and nonlinear models are closer to the actual than what would have been predicted by Miner's rule. The nonlinear prediction is closer to the experimental value than the linear prediction in every case.

#### Modified WISPERX Spectra Fatigue Life Predictions

Predictions for the modified WISPERX spectra were made along the same lines as

for block spectra. Predictions based on the three models were reduced to a graphical form of the S-N curve type as in Figures 90 through 95 based upon the exponential and power law fatigue models. The shape of the curves in the higher stress region has abrupt changes in slope that occur at identifiable cycles in the spectrum. The incremental stress level used in the calculation of the lifetimes has an effect on the overall shape of these curves, yet the general trend can be ascertained from the presented figures. In general, the Miner's rule and the linear residual strength degradation models produce similar predictions, while the nonlinear residual strength degradation model is more conservative.

Figures 90 and 91 include the lifetime predictions for the Mod 1 WISPERX spectrum at an R-value of 0.1 for the exponential and power law fatigue models, respectively. The trend of this spectrum, shown in Figure 81, has a change in the average maximum stress level at around the 9,000<sup>th</sup> reversal point (4,500<sup>th</sup> cycle) and another at approximately the 19,000<sup>th</sup> reversal point (9,500<sup>th</sup> cycle). These are consistent with the changes in the slope in Figures 90 and 91. The scale compression of the logarithm prevents the observation of these slope changes for the higher cycle (greater number of blocks) regime. The power law fatigue model appears to provide a better correlation with the experimental data than the exponential fatigue model for the high cycle regime and for any of the three prediction models.

Figures 92 and 93 are a summary of the lifetime predictions for the Mod 1 WISPERX spectrum at an R-value of 0.5. The general slope of these prediction curves are less than those of the same spectrum at an R-value of 0.1, as might be expected based upon the results of the constant amplitude fatigue testing. The changes in slope of the predictions are again due to changes in the load values, as evident in Figure 82 for this spectrum. There is little

difference among the results for the three prediction models, although the power law fatigue model may provide a better overall correlation with the data at the high stress level. The exponential model appears to provide a better correlation at the low stress level, yet the trend at the lowest stress levels does require further investigation.

Figures 94 and 95 are the results of lifetime predictions for the Mod 2 WISPERX spectrum. The much more dramatic change in slope evident in these figures is a result of the single high load cycle present in this spectrum at approximately the 5,000<sup>th</sup> reversal point (2,500<sup>th</sup> cycle) as evident in Figure 83. In general, the lifetime predictions based upon the power law fatigue model provide better correlation with the experimental data than does the exponential fatigue model. The nonlinear strength degradation lifetime prediction method provides a closer correlation to the data than does the other two models. The greater differences in the stress levels created by the presence of the single high load cycle, seems to cause greater variability of the prediction produced by the three models.

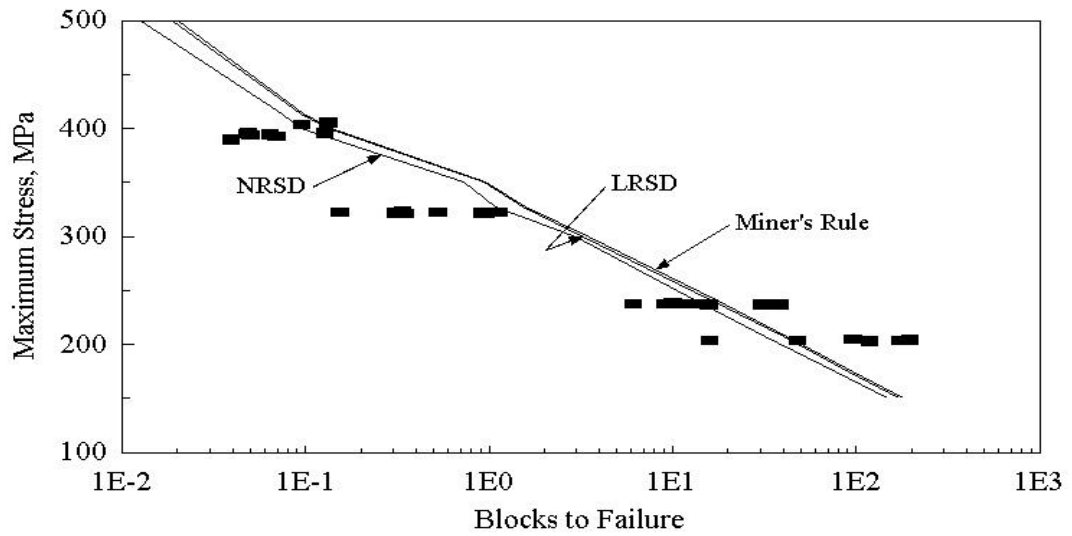


Figure 90. Mod 1 Spectrum Lifetime Predictions, R = 0.1  
Exponential Fatigue Model Including All Data

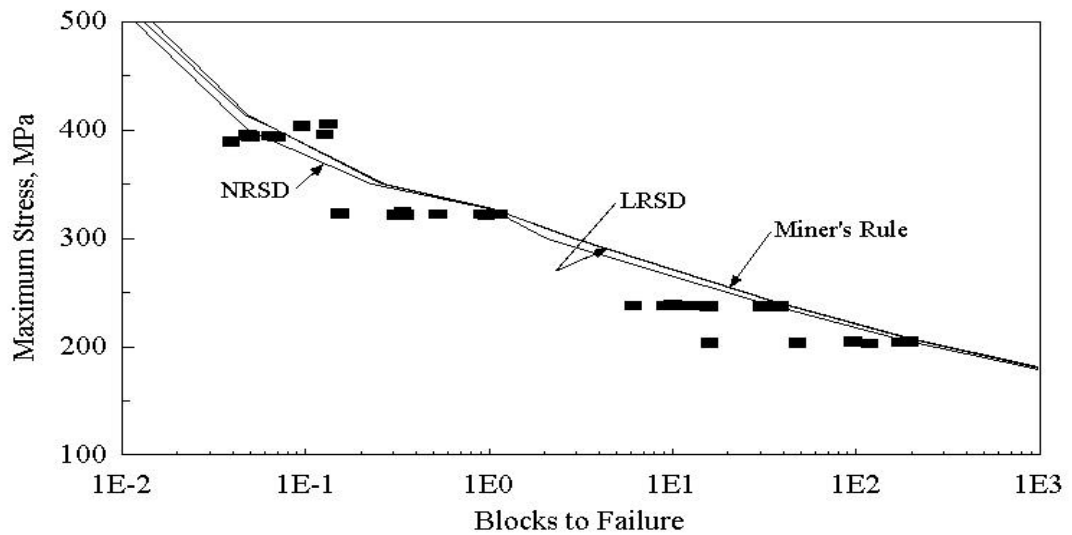


Figure 91. Mod 1 Spectrum Lifetime Predictions, R = 0.1  
Power Law Fatigue Model Including All Data



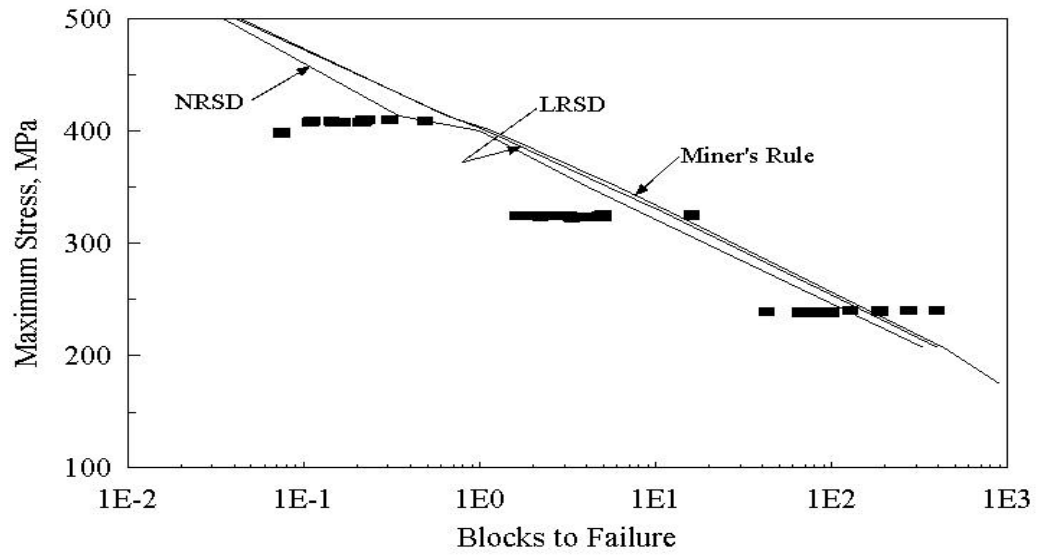


Figure 92. Mod 1 Spectrum Lifetime Predictions, R = 0.5  
Exponential Fatigue Model Including All Data

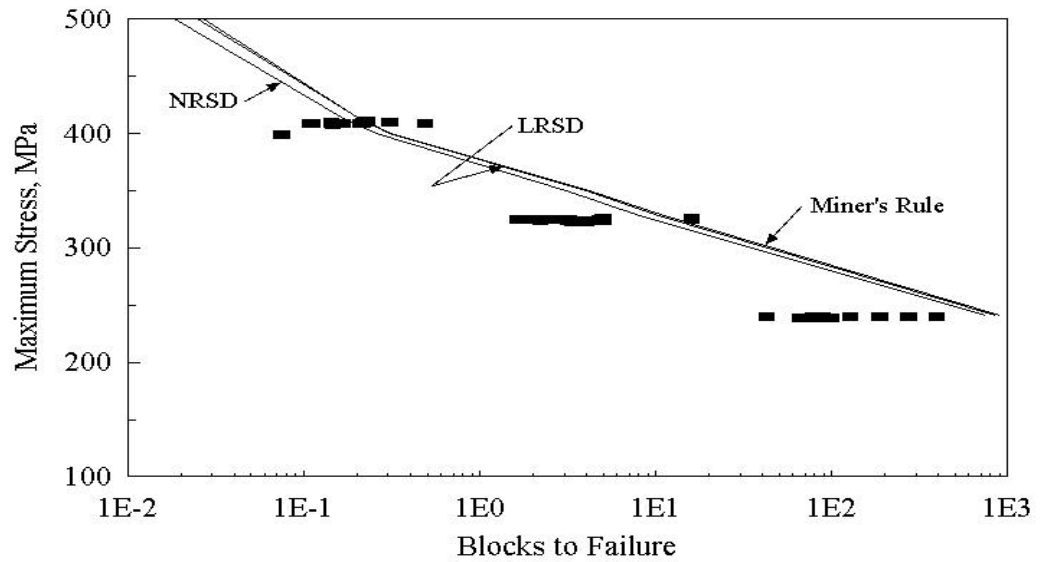


Figure 93. Mod 1 Spectrum Lifetime Predictions, R = 0.5  
Power Law Fatigue Model Including All Data

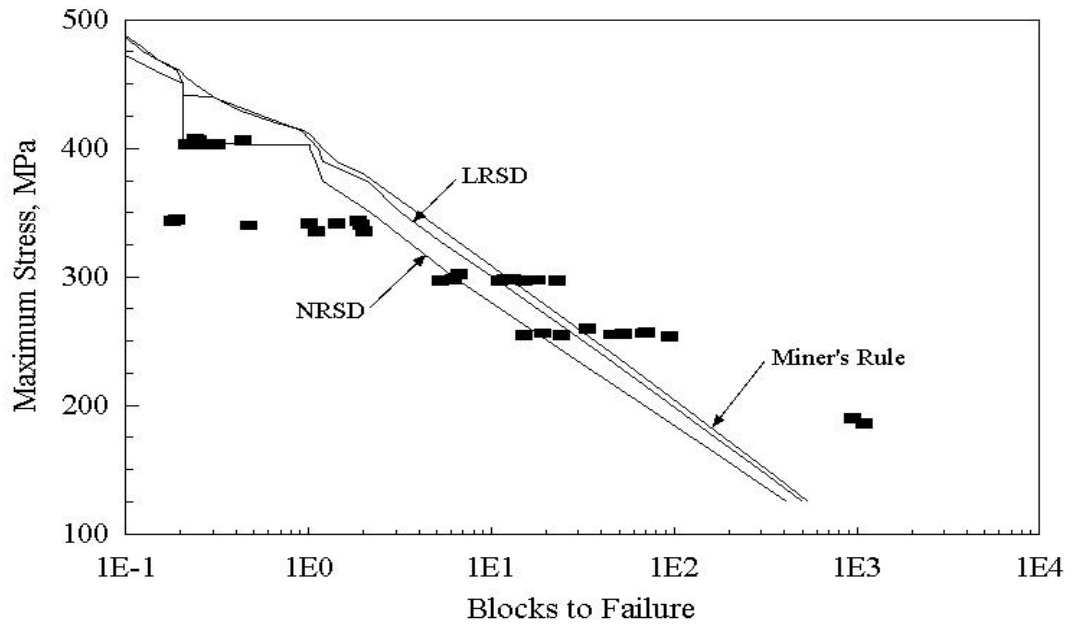


Figure 94. Mod 2 Spectrum Lifetime Predictions  
Exponential Fatigue Model Including All Data

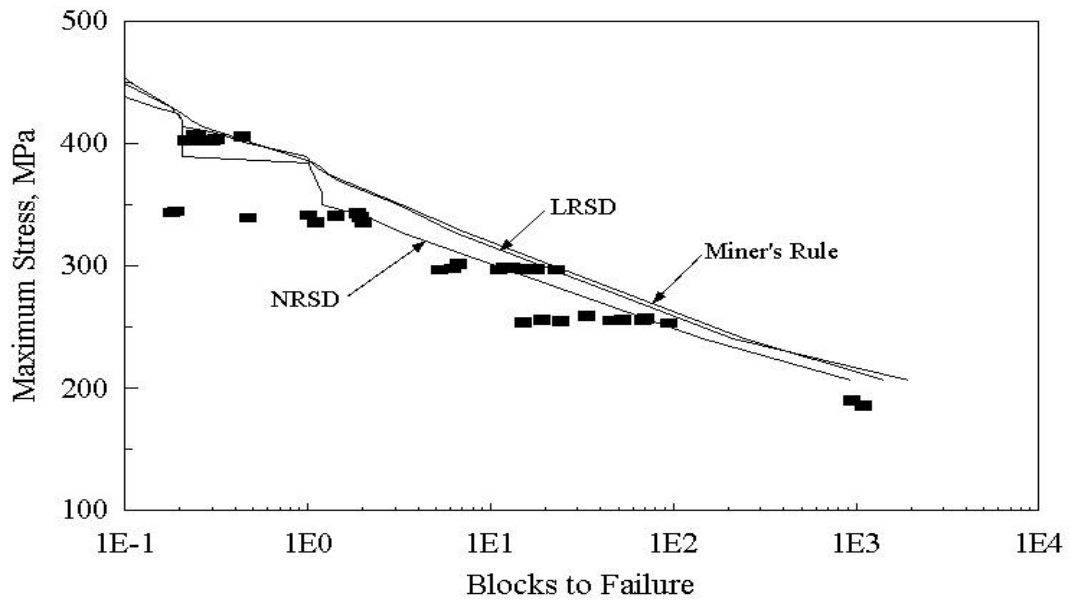


Figure 95. Mod 2 Spectrum Lifetime Predictions  
Power Law Fatigue Model Including All Data

It, therefore, seems that the selection of the prediction model becomes important when the variability of the stress levels in the spectrum becomes greater, as was the case in the Mod 2 spectrum.

The choice of the fatigue model becomes important for the case of a modified WISPERX spectrum fatigue predictions at the low stress/high cycle regime, where more of the cycles are at stress levels where the constant amplitude data must be extrapolated beyond the experimental data. The power law fatigue model provides a better correlation to data.

#### Block or Cycle Damage Contributions

Are all stress levels important in the fatigue of the laminate, or is one set of levels more damaging than others, to the point that all other stress cycles can be ignored? If the cycle ratio (the ratio of cycles experienced to cycles to failure, equation 3) is an indication of the damage contribution at each level, which is the premise of all three models investigated herein, then comparisons of the cycle ratio at each stress level can answer this question.

Consider the heavily tested two-block case of  $R = 0.1$  with the two maximum stress levels of 325 and 207 MPa. There were over 100 tests performed at the approximate high amplitude cycle fractional ratio of 0.01 (reference Figure 62, Chapter 6). The average tested Miner's sum for this case was 0.287, with a standard deviation of 0.222. Compare these statistics to the constant amplitude test results of Miner's sums of one. The average two-block Miner's sum was considerably less than one, while the standard deviation was also

less, indicating less scatter for the block testing. The average calculated damage contribution based on Miner's sum due to the higher stress cycles was 36 percent, with the remaining 64% due to the low amplitude cycles. This can better be summarized graphically, Figure 96, for this cycle fraction along with the other fractions. For a spectrum with 15 percent high amplitude stress cycles, the damage contribution is split equally between the two load levels. Notice, when the high amplitude stress spectrum content was roughly 50 percent or greater, all the damage essentially could be attributed to the high amplitude cycles. As the number of high amplitude cycles was reduced, the damage contribution from the low stress cycles was significant, greater than 10 percent, to 0.3 percent for the high amplitude cycles.

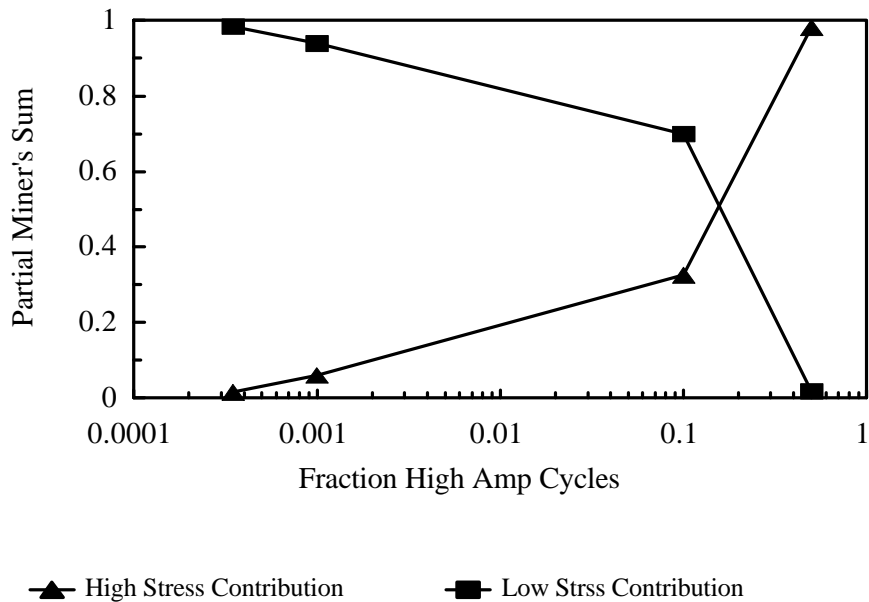


Figure 96. Two-Block Stress Level Damage Contributions

Analysis of the damage contribution for the more random spectra, such as the various

modified WISPERX cases, can be done similarly, provided the stress levels are properly handled. Since there is a multitude of stress levels in the WISPERX spectrum, segregating the levels into a series of increasing groups would produce a set of manageable size. Traditionally, this grouping is accomplished by rainflow counting methods [54, 55]. Here, each stress cycle is isolated, from which the range and mean values for that cycle are calculated. A matrix of bins for each of the groupings for range and mean is filled with the count of the number of cycles in each. A computer algorithm, Appendix F, was developed to perform the necessary calculations to rainflow count a spectrum. Figure 97, is a three dimensional representation of a rainflow count of the published WISPERX spectrum. For comparison, a rainflow count of a constant amplitude test would have a single peak at a

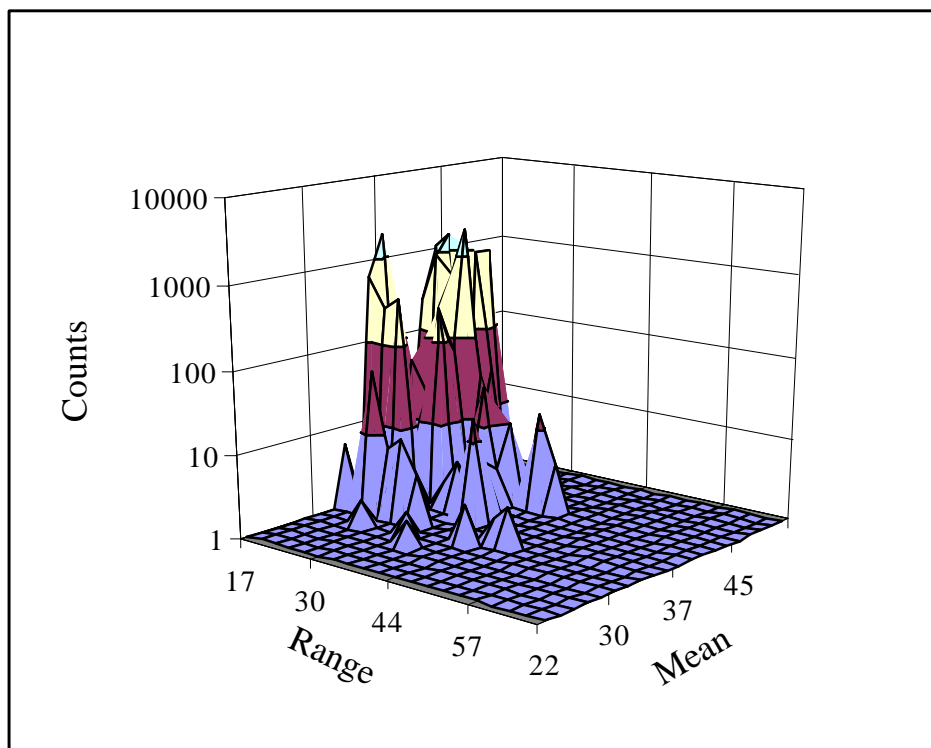


Figure 97. WISPERX Spectrum Cycle Count

unique bin. A rainflow count of a two-block test would display two peaks at two unique bins representative of the two stress levels. The Mod 1 or Mod 2 spectrum would appear as a series of peaks formed along a straight line on the plane of a rainflow count matrix. The slope of this line would be in accordance with that of equation 2,  $(1 - R)/(1 + R)$ .

Information from a matrix such as that in Figure 97 can be used along with the fatigue models, Tables 4 or 5, to develop a Miner's sum for theoretical tests performed with the spectrum represented. The comparisons in Figures 98 and 99 use the exponential fatigue model with static data included. The damage caused by each bin of stress cycles can also be

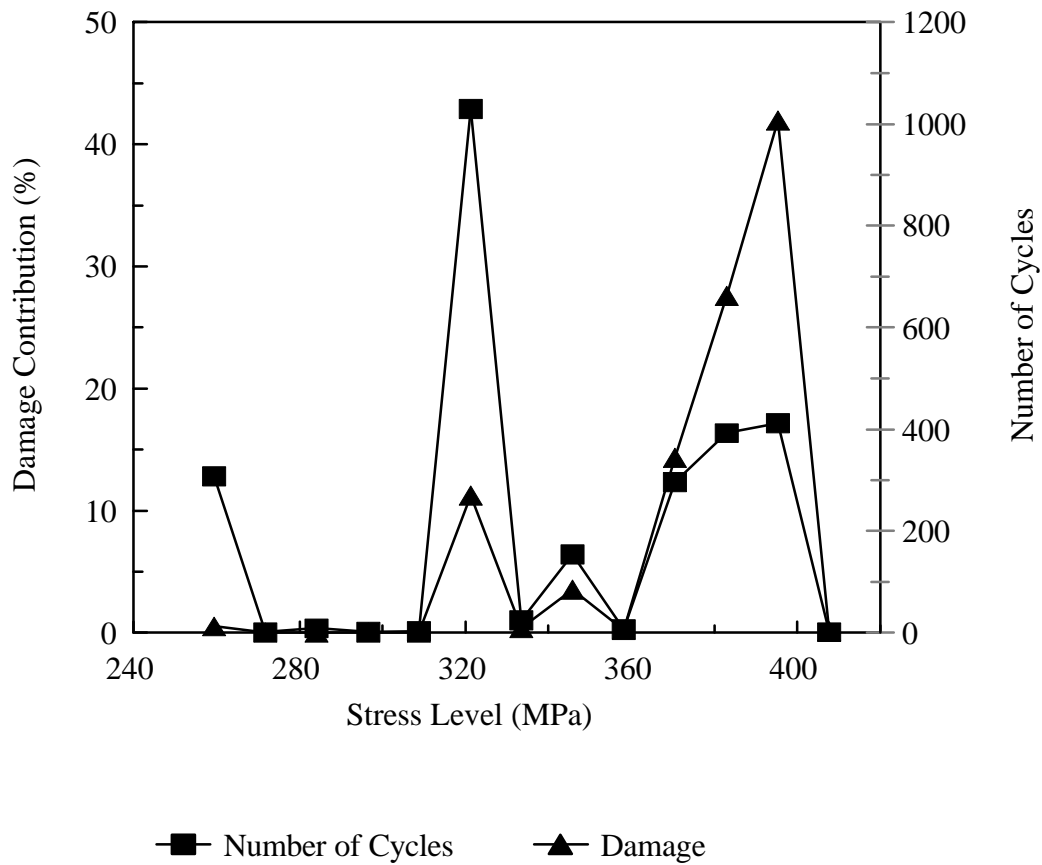


Figure 98. Stress Level Damage Contributions, Mod 1 Spectrum, R = 0.5, 414 MPa Maximum Stress

calculated, such as that shown in Figure 98. For the case shown in Figure 98, Mod 1 spectrum,  $R = 0.5$ , 414 MPa maximum stress, the relatively low number of high amplitude cycles caused the greatest amount of damage to the laminate. As the maximum stress level was decreased, the significance of the high amplitude cycles, although still significant, became less. Figure 99 displays results for a test similar to that of Figure 98, but with the maximum stress reduced.

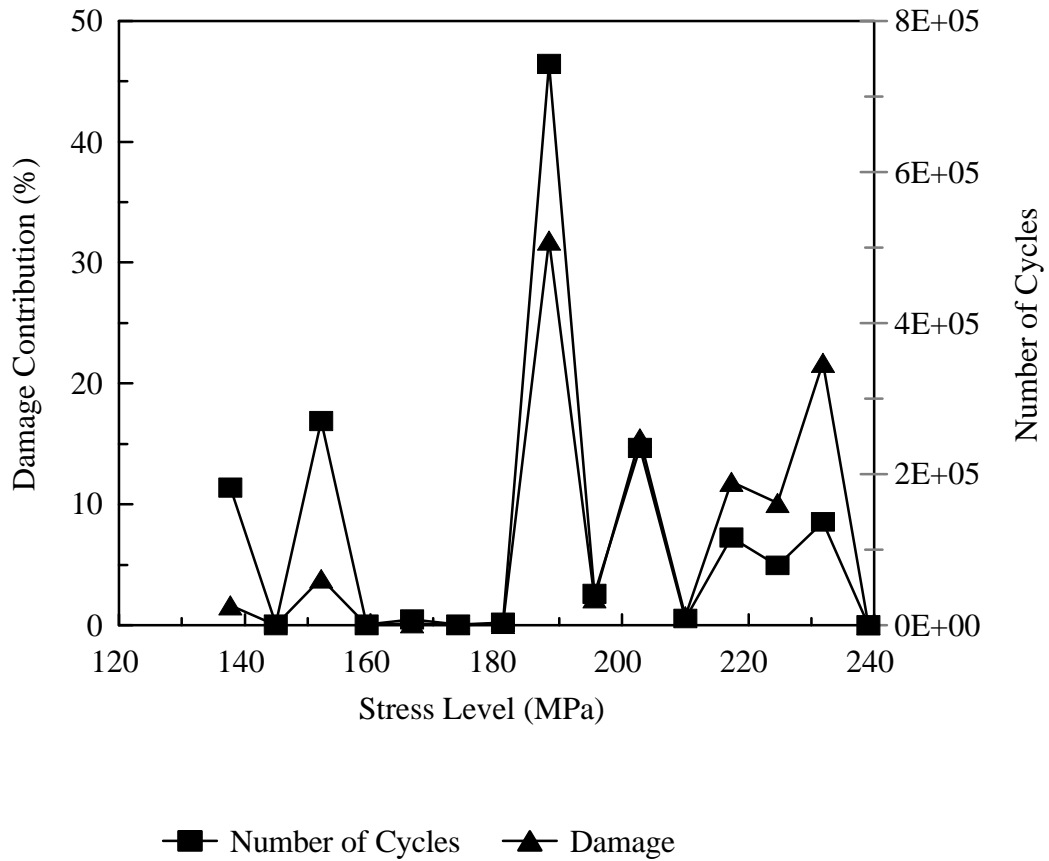


Figure 99. Stress Level Damage Contributions, Mod 1 Spectrum,  $R = 0.5$ , 241 MPa Maximum Stress

Generally, as a spectrum includes a greater difference in load levels, the life prediction model becomes more important. This is illustrated in Figure 100, which shows predictions for two-block repeated spectra with different ratios of low to high block amplitude. When the damage is mostly caused by low stresses, but occasional high stresses occur, then the residual strength models are more accurate and differ strongly from Miner's rule [56]. The 24 percent ratio is less than half of the any tested stress ratios shown in the two-block figures of Chapter 6. Continuing the fraction of high amplitude cycles to zero would cause the Miner's sum to trend to one, the low amplitude constant amplitude mean Miner's sum.

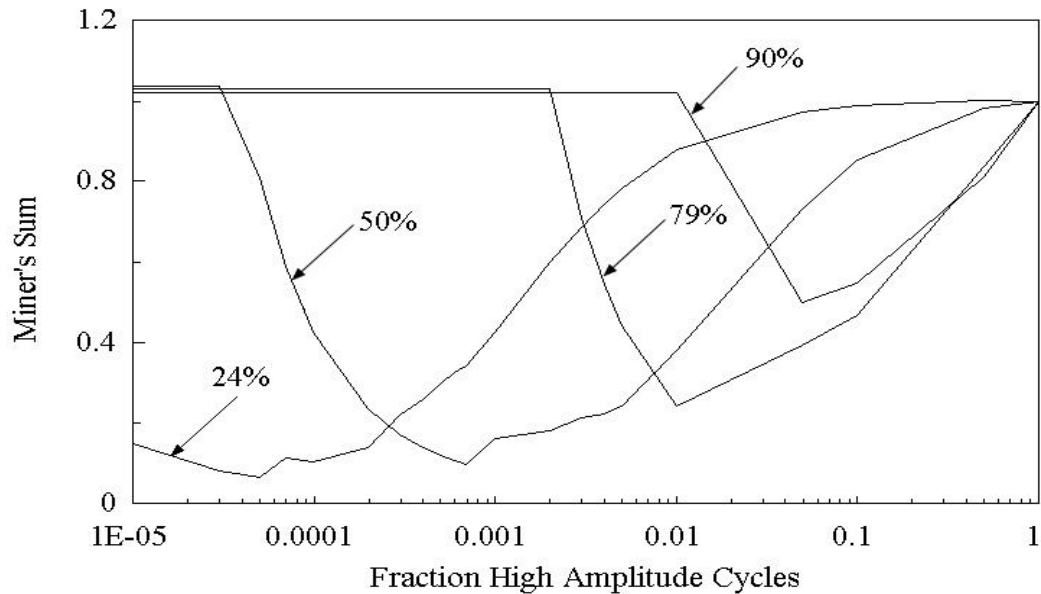


Figure 100. Two-Block Load Level Sensitivity, Low-Block Amplitude as Percent of High-Block Amplitude (nonlinear residual strength model prediction with  $\dot{\epsilon} = 0.265$ , exponential fatigue model)



Unmodified WISPERX Spectrum Fatigue Life Predictions

Fatigue lifetime predictions for a spectrum that contains a wide variety of R-values such that cycles of loading may be tensile, compressive or reversing require a consideration of the mode of failure. All previous discussions were restricted to tests and calculations that avoided this problem by forcing a consistent, known failure mode.

Consider that the failure mode must change from one that is tension dominated to one that is compression dominated as the R-value changes from 0.1 to -1 [9]. The R-values of 0.1 and -1 are listed, since they are the values for which tests have been conducted. Depending upon the laminate, the transition could occur between R-values of 0 and  $\infty$ , as is shown in Figure 101 (Figure 101 is a modification of Figure 5 to better illustrate the transition region). The fact of this transition is evident in analysis of the stress (y-axis)

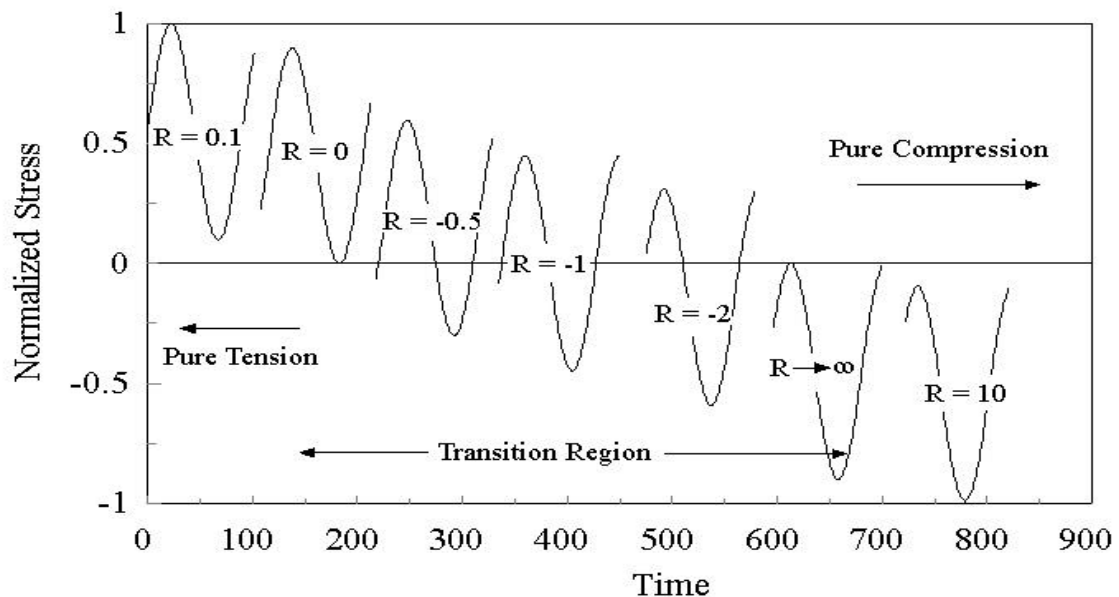


Figure 101. Transition From Tensile to Compressive Failure Mode,  
Constant Amplitude

intercept for the S-N curves for the constant amplitude fatigue tests, such as Figures 33 through 37. In order to apply the residual strength lifetime prediction models for this type of variable amplitude spectrum, the demarcation R-value must be known, as there are two distinct residual strength curves for compression and tension loading. This is not the case for application of Miner's rule in that the accepted interpolations from a Goodman diagram circumvent this need.

Lacking test information to allow determining this demarcation R-value, some logically developed value must be used. Hypothesize that the damage a laminate may suffer is dependent upon the ratio of the maximum stress to the ultimate strength for either tension or compression loading. If this were the case consider that the R-value that allows equal ratios of the tension maximum stress to the ultimate tensile stress and the compression minimum stress to the ultimate compressive stress would be the transition R-value. For equivalent damage from either the maximum tensile or compressive load then based upon the above hypothesis,

$$\sigma_{\min} / \sigma_{\text{ucs}} = \sigma_{\max} / \sigma_{\text{uts}} \quad (19)$$

Upon considering the same stress range (alternating stress), as shown in Figure 101, equation 19 reduces to:

$$R = \sigma_{\text{ucs}} / \sigma_{\text{uts}} \quad (20)$$

This R-value, for the tested laminate, was -0.63. This was then used as the demarcation R-value for the selection of the residual strength curve to be applied for any given cycle in a variable amplitude spectrum containing tensile, compressive and reversing loading cycles. A computer program was written to implement this method of lifetime prediction and is included in Appendix F.

The lifetime predictions based upon this method of failure mode demarcation are shown in Figures 102 and 103 for the exponential and power law fatigue models, respectively. Only the two lifetime prediction rules of NRSD and Miner's rule were employed as the LRSD and Miner's rule have yielded very similar results. The incremental value for the stress level was held coarse and hence any spectrum effects at the low cycles are not as evident as in previous Figures 90 through 95. The nonlinear residual strength rule was much more conservative than the Miner's rule. The prediction rules based upon the exponential fatigue model do not seem to follow the general slope of the experimental data. The predictions based upon the exponential fatigue model over-predict life at the low cycles and under-predict life at the high cycles. The rule predictions based upon the power law fatigue model over-predict life throughout the life, yet seem to follow the general slope much better.

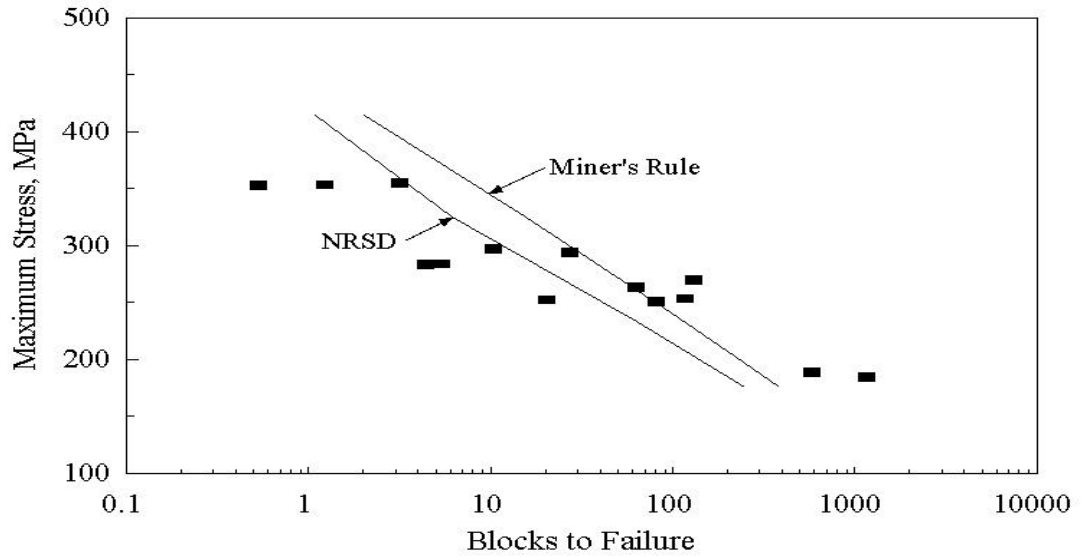


Figure 102. Unmodified WISPERX Spectrum Lifetime Predictions, Exponential Fatigue Model Including All Data

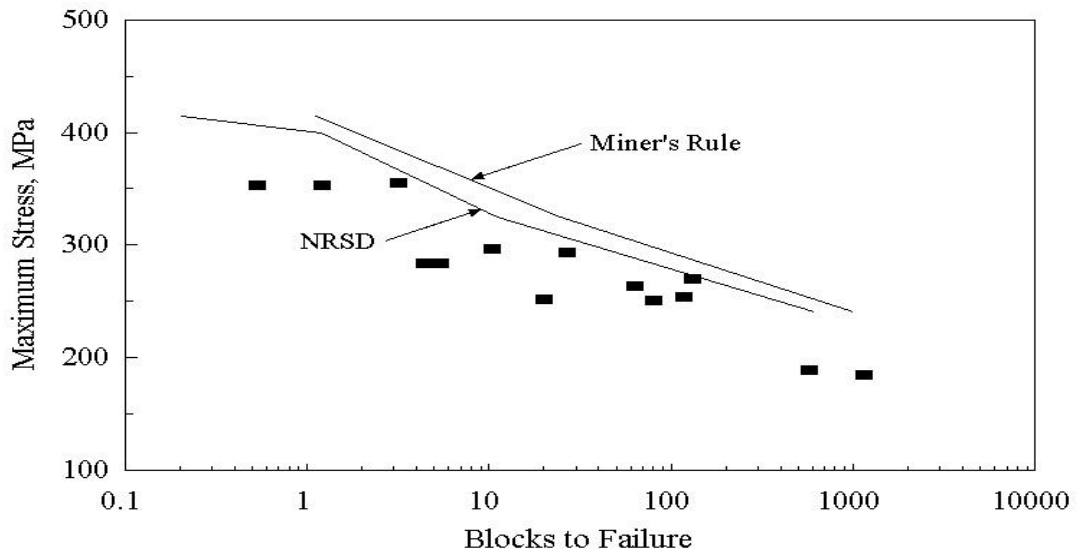


Figure 103. Unmodified WISPERX Spectrum Lifetime Predictions, Power Law Fatigue Model Including All Data

Comparisons between the WISPERX results of van Delft [4] and the present fatigue results for the WISPERX spectrum are shown in Figure 104. The lifetimes predicted by van Delft are much greater than those of the present research, similar to the results presented by Sutherland and Mandell [9]. Prediction rules employed by van Delft and during this present research over-predict the actual lifetimes.

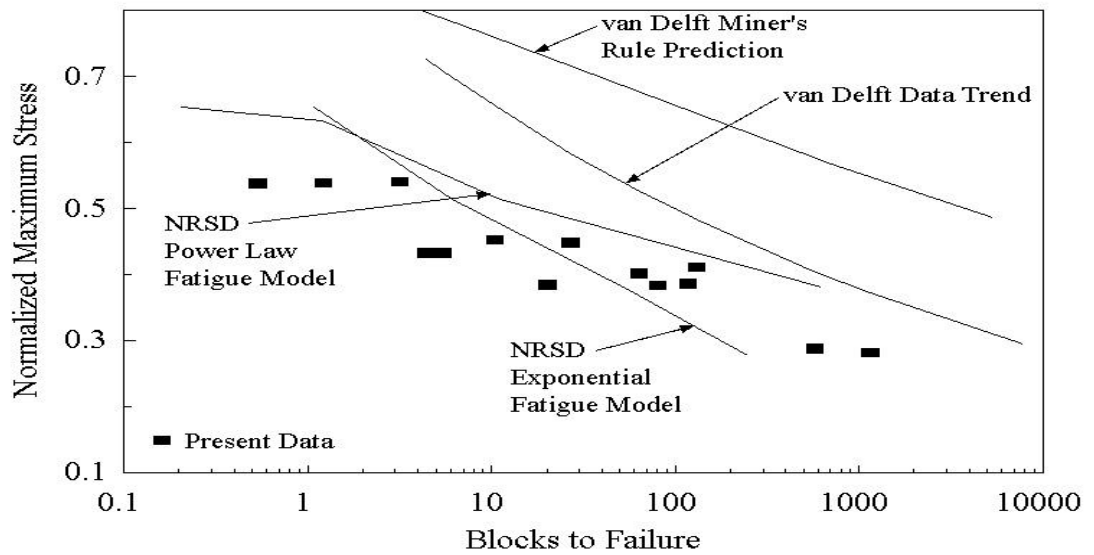


Figure 104. Comparison of WISPERX Lifetime Predictions

## CHAPTER 9

## SUMMARY, CONCLUSIONS AND RECOMMENDATIONS

The research conducted and reported here involved the development of an experimental program that, when implemented, generated a substantial quantity of fatigue data. Test methodologies, including material selection, test specimen geometry, data acquisition, and testing machine performance, were all held to unusually high standards, so that meaningful conclusions could be rendered relative to the accuracy of theoretical predictions in this and future studies. The data are those of the fatigue of specimens of the selected laminate, subjected to a variety of loads spectra and cycled until the specimens were sufficiently failed that they could not support loads. Other researchers have primarily investigated the response of laminates to either constant amplitude or simple two-block spectra. The present work extends the complexity to multi-block and random spectra.

Three fatigue life prediction models were employed to estimate the life of laminates subjected to a variety of loading spectra. Comparisons are made between the prediction models and the experimental data. While additional work with other models and loads spectra may be necessary to definitively prove the superiority of one prediction scheme over others, these results do allow limited conclusions to be drawn as to: (1.) the preferred methods of extrapolating the baseline constant amplitude S-N trends to higher cycles and (2.) the accuracy of cumulative damage models for particular spectrum characteristics.

### Lifetime Observations and Application to Blade Design

Spectra involving two or more different stress levels generally resulted in lifetimes less than predicted by Miner's rule. This was not entirely expected. Other researchers [41] have reported that, for the application of two blocks of stress levels, with the second block run to specimen failure, the actual lifetimes may be greater or lesser than predicted by Miner's rule. The conclusion that Miner's rule is non-conservative for nearly all spectra tested raised questions as to the current status of wind turbine blades designed using this method. Fortunately, blades appear to be generally over-designed in terms of strength and fatigue lifetime, with designs often driven by stiffness related factors.

Better agreement between predictions and data was found by the application of residual strength based rules than by the use of the linear Miner's rule. This was particularly notable where the spectra (repeated block spectra) had sufficient variations in stress levels to separate the prediction rules. Although the nonlinear residual strength degradation rule introduces an unknown parameter that must be determined experimentally, it does provide a better prediction of lifetimes than the linear residual strength rule. The exponential parameter in equation 16 has not been optimized; in fact the parameter may be a function of several factors, such as stress level, fatigue age and laminate selection. Presently the parameter has been given a value of 0.265, the result of a rudimentary error analysis of residual strength data and a mere visual fitting of the prediction results to experimental data. The choice of a nonlinear exponential parameter less than 1.0 indicates a relatively rapid decrease in residual strength early in the specimen or blade lifetime. This choice is supported

by all of the different types of spectra as well as direct residual strength measurements. Thus, not only is it practical to predict changes in material and blade strength at different fractions of test or service lifetime, it may be essential in designing against the occurrence of “hurricane” extreme load conditions.

#### Comments on Spectrum Effects

The Mod 1, Mod 2 and WISPERX spectra are rather benign and as such fatigue results for these spectra, do not differ greatly from the similar constant amplitude fatigue results. Regression results of the Mod 1 spectrum test results at an R-value of 0.1 produced a log-log inverse slope, regression parameter  $m$ , of 12.0, whereas, the constant amplitude equivalent was 11.5. Similarly for the Mod 1 spectrum at an R-value of 0.5, the inverse slope was 14.5 compared to the constant amplitude value of 14.4. The Mod 2 spectrum, which included the one large cycle, and was forced to an R-value of 0.1, produced an inverse slope of 13.9; compare this to the constant amplitude value of 11.5. It appears that for the case of the random spectrum of limited stress variation, such as the Mod 1 spectrum, the fatigue sensitivity of the laminate is little different from that achieved by a constant amplitude spectrum. The single large cycle of the Mod 2 spectrum does cause some effect and deviate the fatigue sensitivity of this spectrum from the constant amplitude equivalent.

The WISPERX spectrum has an average R-value of approximately 0.4. The fatigue inverse slope for these tests was 14.2, not much removed from the 14.4 of the constant amplitude (R-value = 0.5) fatigue results.



Spectra such as the two-block spectra reported in Chapter 6, have a greater variation in the cyclic load levels and have a greater effect on the fatigue lifetime predictions. This is born out by the difference seen in the lifetime predictions of the two-block as shown in the figures of Chapter 6. The differences among the Miner's rule, linear residual strength degradation rule and the nonlinear residual strength rule are more pronounced than those seen in the WISPERX spectra results. One may presume, and wish to investigate, that the greater variation in stress levels that a spectrum contains, the more important the selection of the fatigue lifetime prediction rule.

#### Stress Level Sequencing Effects

An investigation into the possibility of any stress level sequencing effects on lifetimes has not shown this to be a significant factor, at least for the sequences selected. The spectra of different sequences of cycles in repeated blocks did not have an effect on the life of the specimens. Yet, when the blocks are not repeated (the second block continued until failure), the sequencing does produce significantly different results. Upon comparing the results of the residual strength degradation lifetime predictions to the experimental results of other investigators [41], the fact that sequencing is important for this special case was confirmed both experimentally and theoretically. Consequently, it is believed that sequencing effects of the cycles experienced during the actual service of components subjected to realistic random spectra, is not significant. This observation allows for the possibility that relatively simple cumulative damage rules may be used (although load conditions where compressive

and tensile failure modes interact significantly may prove to cause complications).

### Fatigue Model Selection

The results of the constant amplitude fatigue testing were summarized into two fatigue models based upon exponential and power law regression curves representing the data. Generally, for the two-block fatigue testing, the selection of the fatigue model is immaterial. Application of either the exponential or the power law fatigue models caused little difference in the lifetime predictions for the two-block loading spectra. This appears to be due to a limit of the number of cycles that are placed within each of the two blocks. These tests were typically extending over a range of a few thousand to a million cycles, a range over which the two fatigue models differ only slightly, and extrapolation to lower stresses using the models is unnecessary. Testing at lower stress levels for each block would force the testing into greater numbers of cycles, at which point, the selection of the fatigue model may become significant if the constant amplitude input trends require extrapolation beyond the range of experimental data.

The significance of the higher number of cycles was evident in the modified and unmodified WISPERX fatigue testing. In fact, the power law fatigue model provided a better lifetime prediction than the exponential model when the number of cycles was extended by an order of magnitude to 10 million.

### Recommendations for Future Work

Many questions are still unanswered in regards to laminate response to spectrum loading; in fact work is still in progress in this research area. Items of ongoing work and areas of potential work are discussed below.

### Spectrum Considerations

Upon studying the relatively benign WISPERX spectrum as compared to some of the two-block spectra, and the various rule prediction accuracies for those spectra, testing of other more robust spectra may provide more insight into rule selection. Other random spectra have been collected; wind turbine start/stop sequences, WISPER, FALSTAFF, as well as spectrum based upon data collected from operational wind turbines in Montana. Lifetimes of the laminate when subjected to these varied spectra may provide more insight into fatigue prediction, since loads often are more variable than WISPERX.

### Compressive Residual Strength

There appears to be some differences in the response of the laminate to tensile and compressive loading as evidenced in the two-block testing. Residual strength testing of laminates was performed only for tensile loading case. This indicated the residual strength degradation lifetime prediction rule warrants use. Testing of the residual strength of the laminate subjected to compressive loading would be of interest.

### Failure Mode Transition

At some loading condition, the failure mode transitions from tensile to compressive. The application of the residual strength degradation lifetime prediction model is somewhat dependent upon this transition point for the selection of the proper strength degradation path. This warrants an investigation into the failure mode and the breakpoint between these two fundamental loading conditions. Testing at a finer grid of R-values in the region surrounding  $R = -1$  would be of interest.

#### Residual Strength Model Refinement

The nonlinear residual strength model was somewhat calibrated to the experimental data by selection of the exponent,  $\acute{1}$ , in equation 16. Adjustment of this single parameter causes a shifting of the predictions, in a manner similar to offset adjustment in instrumentation calibration. The introduction of a second variable of, as yet an unknown function, may allow better calibration of the model to fit the experimental data.

Simple magnitude shifting of the exponent can provide a better correlation with the experimental data for the unmodified WISPERX case that used the power law fatigue model. Unfortunately, this would not correct the lack of fit as observed in some of the two-block fatigue cases wherein the model is under-conservative for a spectrum of large high-amplitude cycle fractions and over-conservative for a spectrum with a smaller fraction. The second parameter may achieve a better calibration.

#### High Cycle Spectrum Fatigue Testing

Since the desired life of wind turbine blades can exceed 30 years or over  $10^9$  cycles, investigation of lifetimes of this magnitude, for laminates subjected to spectrum loading needs to be performed. It appears upon observation of the data in Figures 84 through 87, 90 through 95 and 102 and 103, the power law fatigue model provides a better correlation to the data than does the exponential fatigue model. Additional testing in the higher cycle region may provide more confidence for this conclusion.

REFERENCES CITED

1. Fuchs, H. O., Stephens, R. I., *Metal Fatigue in Engineering*, John Wiley & Sons publishers, 1980, pp. 1-5.
2. Anderson. T. L., *Fracture Mechanics, Fundamentals and Applications*, CRC Press, Inc. publishers, 1991, pp. 597-629.
3. Grover, H. J., *Fatigue of Aircraft Structures*, U.S. Government Printing Office, Washington, D.C., 1966, pp. 95-103.
4. Delft, D. R. V. van, de Winkel, G. D., Joosse, P. A., "Fatigue Behaviour of Fibreglass Wind Turbine Blade Material Under Variable Amplitude Loading," *Wind Energy 1997*, AIAA-97-0951, ASME/AIAA, (1997).
5. Miner, M. A., "Cumulative Damage in Fatigue," *Journal of Applied Mechanics*, Sept., 1945, pp. A-159 - A-164.
6. Kensche, Christoph, W., *High Cycle Fatigue of Glass Fibre Reinforced Epoxy Materials for Wind Turbines*, Institut für Bauweisen- und Konstruktionsforschung, DLR-Fb 92-17, 1992, pp. 14-15.
7. Schluter, L. L., Sutherland, H. J., *Reference Manual for the LIFE2 Computer Code*, Sandia National Laboratories, 1989, pp. 7-1.
8. Sutherland, H. J., Veers, P. S., Ashwill, T. D., "Fatigue Life Prediction for Wind Turbines: A Case Study on Loading Spectra and Parameter Sensitivity," American Society for Testing and Materials, 1995, pp.174-206.
9. Sutherland, H. J., Mandell, J. F., "Application of the U.S. High Cycle Fatigue Data Base to Wind Turbine Blade Lifetime Predictions," *Energy week 1996*, ASME, 1996.
10. Yang, J. N., Jones, D. L., "Effect of Load Sequence on the Statistical Fatigue of Composites," *AIAA Journal*, Vol. 18, No. 12, Dec, 1980, pp. 1525-1531.
11. Yang, J. N., Jones, D. L., "Load Sequence Effects on the Fatigue of Unnotched Composite Materials," *Fatigue of Fibrous Composite Materials, ASTM STP 723*, American Society for Testing and Materials, 1981, pp. 213-232.
12. Hwang, W., Han, K. S., "Cumulative Damage Models and Multi-Stress Fatigue Life Prediction," *Journal of Composite Materials*, Vol. 20, March, 1986, pp. 125-153.
13. Mandell, J. F., Samborsky, D. D., "DOE/MSU Composite Material Fatigue Database: Test Methods, Materials and Analysis," Contractor Report SAND97-3002, Sandia National Laboratories, Albuquerque, NM, 1997.

14. de Smet, B. J., Bach, P. W., *DATABASE FACT, FATigue of Composites for wind Turbines*, Netherlands Energy Research Foundation ECN, ECN-C--94-045, 1994.
15. ten Have, A. A., "WISPER and WISPERX: A Summary Paper Describing Their Backgrounds, Derivation and Statistics," *Wind Energy 1993*, SED-Vol. 14, ASME, (1993), pp. 169-178.
16. ten Have, A. A., "WISPER and WISPERX, Final Definition of Two Standardised Fatigue Loading Sequences for Wind Turbine Blades," NLR TP 91476 U, National Aerospace Laboratory NLR, the Netherlands.
17. Kelley, N. D., National Wind Technology Center, Golden, CO, Personal Communication, 2000.
18. National Research Council, *Assessment of Research Needs for Wind Turbine Rotor Materials Technology*, National Academy Press, pp. 59-60, (1991).
19. Sendeckyj, G. P. "Life Prediction for Resin-Matrix Composite Materials," *Fatigue of Composite Materials*, K. L. Reifsnider, Ed., Elsevier Sciences Publishers, 1990, pp. 431-483.
20. Bond, I. P., "Fatigue life prediction for GRP subjected to variable amplitude loading," *Composites, Part A: Applied Science and Manufacturing*, 1999, pp. 961-970.
21. Palmgren, A., "Die Lebensdauer von Kugellagern," *ZDVEDI*, Vol. 68, No. 14, 1924, pp. 339.
22. Broek, David, *Elementary Engineering Fracture Mechanics*, Martinus Nijhoff Publishers, 1982, pp. 13, 434-452.
23. Hertzberg, Richard, W., *Deformation and Fracture Mechanics of Engineering Materials*, John Wiley & Sons publishers, 1996, pp. 591-641.
24. Reifsnider, K. L., "Damage and Damage Mechanics (Chapter 2)," *The Fatigue Behavior of Composite Materials*, K. L. Reifsnider, Ed., Elsevier (1990), pp. 11-77.
25. Hertzberg, Richard W., Manson, John A., *Fatigue of Engineering Plastics*, Academic Press, Inc. publishers, 1980, pp. 239-256, 268-271.
26. Chawla, K. K., *Composite Materials Science and Engineering*, Springer-Verlag Publishers, New York, 1987, pp. 249-250.



27. Reed, Robert Michael, "Long Term Fatigue of Glass Fiber Reinforced Composite Materials for Wind Turbine Blades," Masters Thesis, Department of Chemical Engineering, Montana State University, 1991.
28. Sutherland, Herbert, J., "Damage Estimates for European and U.S. Sites Using the U.S. High-Cycle Fatigue Data Base," *IEA R&D Wind Annex XI, Symposium on Wind Turbine Fatigue*, DLR, Stuttgart, February 1-2, 1996.
29. Joosse, P. A., Delft, D. R. V. van, Bach, P. W., *Fatigue Design Curves Compared to Test Data of Fibreglass Blade Material*, Netherlands Energy Research Foundation ECN, ECN-RX--94-108, 1994, pp. 7.
30. Mandell, John F., Samborsky, Daniel, D., Sutherland, Herbert, J., "Effects of Materials Parameters and Design Details on the Fatigue of Composite Materials for Wind Turbine Blades," European Wind Energy Conference, 1999.
31. Sutherland, Herbert J., Carlin, Palmer W., "Damage Measurements on the NWTC Direct-Drive, Variable-Speed Test Bed," American Institute of Aeronautics and Astronautics, 1998.
32. Delft, D. R. V. van, Rink, H. D., Joosse, P. A., Bach, P. W., *Fatigue Behaviour of Fibreglass Wind Turbine Blade Material at the Very High Cycle Range*, Netherlands Energy Research Foundation ECN, ECN-RX-94-111, 1994.
33. Mandell, J. F., "Fatigue Behavior of Short Fiber Composite Materials," *The Fatigue Behavior of Composite Materials*, K. L. Reifsnider, Ed. Elsevier (1990), pp. 241-254.
34. Samborsky, Daniel, D., "Fatigue of E-Glass fiber Reinforced Composite Materials and Substructures," Masters Thesis, Department of Civil Engr. Montana State University, 1999.
35. Yang, J. N., Jones, D. L., Yang, S. H., Meskini, A., "A Stiffness Degradation Model for Graphite/Epoxy Laminates," *Journal of Composite Materials*, Vol. 24, July, 1990, pp. 753-769.
36. Bach, P. W., *High Cycle Fatigue Testing of Glass Fibre Reinforced Polyester and Welded Structural Details*, Netherlands Energy Research Foundation ECN, ECN-C--91-010, 1991, pp. 34.
37. Subramanian, S., Reifsnider, K. L., Stinchcomb, W. W., "A cumulative damage model to predict the fatigue life of composite laminates including the effect of a fibre-matrix interphase," *Int. J. Fatigue*, Vol. 17, No. 5, 1995, pp. 343-351.

38. Kung, D. N., Qi, G. Z., Yang, J. C. S., "Fatigue Life Prediction of Composite Materials," *Recent Advances in Structural Mechanics*, PVP-Vol. 225/NE-Vol. 7, American Society of Mechanical Engineers, 1991, pp. 41-50.
39. Rivière, A., "Damping Characterization of Composite Materials by Mechanical Spectrometry," Laboratoire de Mécanique et de Physique des Matériaux - URA CNRS n° 863 ENSMA, Rue Guillaume VII, 86034 Poitiers (France), pp. 316-322.
40. Revuelta, D., Cuartero, J., Miravele, A., Clemente, R., "A new approach to fatigue analysis in composites based on residual strength degradation," *Composite Structures* 48, Elsevier Science Ltd., 1999, pp. 183-186.
41. Broutman, L. J., Sahu, S., "A New Theory to Predict Cumulative Fatigue Damage in Fiberglass Reinforced Plastics," *Composite Materials: Testing and Design (Second Conference)*, ASTM STP 497, American Society for Testing and Materials, 1972, pp. 170-188.
42. Schaff, J. R., Davidson, B. D., "Life Prediction Methodology for Composite Structures. Part I - Constant Amplitude and Two-Stress Level Fatigue," *Journal of Composite Materials*, Vol. 31, No. 2, 1997, pp. 128-157.
43. Schaff, J. R., Davidson, B. D., "Life Prediction Methodology for Composite Structures. Part II - Spectrum Fatigue," *Journal of Composite Materials*, Vol. 31, No. 2, 1997, pp. 158-181.
44. Schaff, J. R., Davidson, B. D., "A Strength-Based Wearout Model for Predicting the Life of Composite Structures," *Composite Materials: Fatigue and Fracture (Sixth Volume)*, ASTM STP 1285, E. A. Armanious, Ed., American Society for Testing and Materials, 1997, pp. 179-200.
45. Whitworth, H. A., "Evaluation of the residual strength degradation in composite laminates under fatigue loading," *Composite Structures* 48, Elsevier Science Ltd., 2000, pp. 261-264.
46. Reifsnider, K. L., "Interpretation of Laboratory Test Information for Residual Strength and Life Prediction of Composite Systems," *Cyclic Deformation, Fracture and Nondestructive Evaluation of Advanced Materials*, ASTM STP 1157, M. R. Mitchell and O. Buck, Eds., American Society for Testing and Materials, Philadelphia, 1992, pp. 205-223.
47. O'Brien, T. K., "Characterization of Delamination Onset and Growth in a Composite Laminate," *Damage in Composite Materials*, ASTM STP 775, K. L. Reifsnider, Ed., American Society for Testing and Materials, 1982, pp. 140-167.

48. Echtermeyer, A. T., Kensche, C., Bach, P., Poppen, M., Lilholt, H., Andersen, S. I., Brøndsted, P., "Method to Predict Fatigue Lifetimes of GRP Wind Turbine Blades and Comparison With Experiments," *European Union Wind Energy Conference*, 1996, pp. 907-913.
49. Solin, J., "Methods for comparing fatigue lives for spectrum loading," *Int. J. Fatigue*, Vol., 12, No. 1, 1990, pp. 35-42.
50. Lee, L. J., Yang, J. N., Sheu, D. Y., "Prediction of Fatigue Life for Matrix-Dominated Composite Laminates," *Composites Science and Technology*, Elsevier Science Publishers Ltd., 1992, pp. 21-28.
51. Han, Patricia, Editor, *Tensile Testing*, ASM International, 1992, pp. 187-191.
52. Nichols, N. B., Ziegler, J. G., "Optimum Settings for Automatic Controllers," *ASME Transactions*, Vol. 64, No. 8, 1942, pp. 759-768.
53. Joosse, P. A., Delft, D. R. V. van, Bach, P. W., *Fatigue Design Curves Compared to Test Data of Fibreglass Blade Material*, Netherlands Energy Research Foundation ECN, ECN-RX---94-108, 1994, pp. 2.
54. Downing, S. D., Socie, D. F., "Simple Rainflow Counting Algorithms," *International Journal of Fatigue*, Vol. 4, No. 1, 1982, pp. 31-40.
55. Kelley, N. D., National Wind Technology Center, Golden, CO, Personal Communication, 1996.
56. Wahl, Neil. Samborsky, Daniel, Mandell, John, Cairns, Douglas, "Spectrum Fatigue Lifetime and Residual Strength for Fiberglass Laminates in Tension," *A Collection of the 2001 ASME Wind Energy Symposium*, American Institute of Aeronautics and Astronautics, Inc. and American Society of Mechanical Engineers, 2001, pp. 49- 59.

APPENDICES

APPENDIX A

SPECTRUM FATIGUE DATABASE

Nomenclature

Column 1: Test # is the unique identifying number for each test. Coupons were manufactured sequentially from plates and randomly selected from the stock and sequentially numbered. The tests were not conducted in this sequential number, but randomly in batches. An asterisk in this column indicates the test was not successful.

Residual strength tests are represented by two successive entries of the same identifying number. The first entry indicates the cyclic fatigue portion of the test, while the second entry with the letter "r" appended to the test number indicates the static test of the coupon.

Column 2: The comments for each test provide some insight as to the type of test or the success of the test.

DNF represents did not finish. Other entries such as tab or grip failure are self descriptive of the success of the test.

Dh/Dt is two-block spectrum test comment. This is an estimate of the expected ratio of the damage contribution of the high stress cycles and the total number of cycles expected. A Dh/Dt of unity would represent a constant amplitude test at the higher stress level. Tests identified with the Dh/Dt were conducted with the higher amplitude maximum stress of 414 MPa while the lower amplitude maximum stress was 235 MPa. These were based upon initial estimates of the constant amplitude cycles to failure of  $10^4$  and  $10^6$  for the two stress levels respectively.

An entry such as that of test number 154, "47.5/30-0.5" indicates that this test was conducted with a two-block spectrum with the first block's maximum stress equal to 47.5 ksi (325 MPa) and the second block's, 30 ksi (207 MPa). The damage contribution of the higher stress block was expected to be 50% (0.5).

Test 176 is listed as "47.5/30-10/1000" which represents a two-block test with stress levels of 47.5 and 30 ksi. The number of cycles in the first block, the high cyclic amplitude block is 10, while the second block contains 1000 cycles. Tests with the character(s) "r" or "r#" or "rand#" appended to the cycle numbers indicates the cycles were randomly ordered rather than in separate blocks; here the cycle numbers indicate an overall proportioning of the cycle numbers.

1 cycle indicates that this particular test was an ultimate strength test.

A listed stress, such as the “500 MPa” of test number 11 indicates the test is a constant amplitude test with the maximum stress equal to 500 MPa.

An entry such as “R=0.5” indicates the test was performed at a R-value of 0.5. The lack of an R-value implies the default value of 0.1 was used.

The descriptor “wvrnr” implies the Instron WaveRunner software package was used to control the hydraulic system. Descriptors such as “load#” indicate the Instron RANDOM software package was used for control.

Entries such as “Wisperx”, “WisxR05”, “WisxR01”, “Wisxmix”, or “Wispk” indicate that a modified WISPERX or original WISPERX spectrum was used to load the specimen.

- Column 3: The entries in this column indicate the type of coupon used and the material and batch used for the laminate.
- Column 4: The width of the gage section of the coupon is listed in inches.
- Column 5: The thickness of the gage section of the coupon is listed in inches.
- Column 6: The frequency of the test is documented in column six. Ultimate strength tests were conducted at the same rate as the cyclic tests. These tests are indicated by the entry “1 cycle”.
- Column 7: This column lists the number of cycles conducted at the high amplitude stress level.
- Column 8: The number of cycles conducted at the low amplitude stress level. Tests of more than two-blocks are summarized in Tables 6 and 7 of the text.
- Column 9: The total number of cycles of the test is listed in this column.
- Column 10: The maximum load encountered during the test is listed in pounds.

Test #	Comment	Coupon Style/Mat'l	Width in	Thick in	Freq Hz	# High Cycles	# Low Cycles	Total Cycles	Hi Block Max
Test #	Comment	Coupon Style/Mat'l	Width in	Thick in	Freq Hz	# High Cycles	# Low Cycles	Total Cycles	Hi Block Max
* 1	DNF	1/DD5	0.268	0.121					
2	Dh/Dt=1	1/DD5	0.266	0.124	10	4717		4717	1949.4
3	Dh/Dt=1	1/DD5	0.273	0.126	10	2711		2711	2037.3
4	Dh/Dt=1	1/DD5	0.276	0.133	10	1812		1812	2160.2
* 5	DNF	1/DD5	0.273	0.126					
6	1 cycle	1/DD5	0.273	0.127	1 cycle	1		1	3844.1
7	1 cycle	1/DD5	0.268	0.122	1 cycle	1		1	3853.5
8	1 cycle	1/DD5	0.274	0.119	1 cycle	1		1	3898.6
9	Dh/Dt=1	1/DD5	0.270	0.129		3711		3711	2072.4
* 10	DNF	1/DD5	0.270	0.123					
11	500 MPa	1/DD5	0.270	0.122	10	877		877	2353.4
* 12	Tab Fail	1/DD5	0.272	0.126					
13	500 MPa	1/DD5	0.266	0.126	10	584		584	2388.5
14	690 MPa	1/DD5	0.270	0.127	10	28		28	3366.8
* 15	DNF	1/DD5							
* 16	DNF	1/DD5	0.275	0.124					
17	Dh/Dt=0	1/DD5	0.269	0.127	10		3096821	3096821	1196.0
18	Dh/Dt=0	1/DD5	0.275	0.121	30		1709382	1709382	1142.0
19	Dh/Dt=0.1	1/DD5	0.267	0.125	10	670	594000	594670	1975.8
20	Dh/Dt=0.9	1/DD5	0.275	0.122	10	7950	88928	96878	2001.2
* 21	DNF	1/DD5	0.271	0.125					
22	Dh/Dt=0.1	1/DD5	0.265	0.128	10	1600	1435500	1437100	2001.2
23	Dh/Dt=0.25	1/DD5	0.268	0.122	10	2025	607500	609525	1957.1
24	Dh/Dt=0.25	1/DD5	0.271	0.122	10	3090	925500	928590	1949.4
25	Dh/Dt=0.75	1/DD5	0.270	0.124	10	6880	226061	232941	1983.5
26	Dh/Dt=0.75	1/DD5	0.270	0.124	10	6415	211530	217945	1983.5
27	Dh/Dt=0.5	1/DD5	0.276	0.126	10	2850	285000	287850	2018.8
28	Dh/Dt=0.9	1/DD5	0.271	0.126	10	7855	87808	95663	2027.6
29	Dh/Dt=0.1	1/DD5	0.271	0.119	10	400	1800000	1800400	1900.3
* 30	DNF	1/DD5	0.271	0.125					
31	Dh/Dt=0	1/DD5	0.274	0.122	10		4501339	4501339	1177.0
32	Dh/Dt=1	1/DD5	0.270	0.124	10	4221		4221	1975.8
33	690 MPa	1/DD5	0.270	0.120	10	67		67	3162.3
34	500 MPa	1/DD5	0.268	0.121	10	1113		1113	2316.4
35	690 MPa	1/DD5	0.271	0.126	10	39		39	3335.0
36	Dh/Dt=0.5	1/DD5	0.271	0.125	10	3270	327000	330270	2007.5
37	Dh/Dt=0.6	1/DD5	0.275	0.126	10	2860	189428	192288	2062.9
38	Dh/Dt=0.95	1/DD5	0.270	0.126	10	10100	52468	62568	2045.2
39	Dh/Dt=0.75	1/DD5	0.272	0.123	10	4340	144622	148962	1983.9
40	Dh/Dt=0.9	1/DD5	0.273	0.124	10	5040	56336	61376	2003.0
41	Dh/Dt=0.6	1/DD5	0.270	0.125	10	1727	114057	115784	2010.0
42	Dh/Dt=0.5	1/DD5	0.271	0.123	10	3670	366000	369670	1975.4
43	Dh/Dt=0.25	1/DD5	0.269	0.125	10	1960	588000	589960	1974.7
44	Dh/Dt=0.9	1/DD5	0.270	0.127	10	6440	72016	78456	2034.8
45	Dh/Dt=0.5	1/DD5	0.269	0.124	10	2780	277000	279780	1981.5
46	Dh/Dt=0.75	1/DD5	0.271	0.126	10	3920	130594	134514	2026.3
47	Dh/Dt=0.25	1/DD5	0.271	0.126	10	1330	399000	400330	2027.4
48	Dh/Dt=0.95	1/DD5	0.268	0.125	10	8610	44720	53330	1983.5
* 49	Tab Fail	2/DD5	0.625	0.138					
* 50	Tab Fail	2/DD5	0.643	0.132					
* 51	Tab Fail	2/DD5	0.646	0.131					
52	save for future	2/DD5	0.638	0.140					
53	save for future	2/DD5	0.646	0.127					
54	save for future	2/DD5	0.619	0.135					
55	save for future	2/DD5	0.648	0.132					
56	save for future	2/DD5	0.646	0.129					
57	save for future	2/DD5	0.647	0.135					
58	save for future	2/DD5	0.636	0.138					
59	save for future	2/DD5	0.631	0.124					
60	save for future	2/DD5	0.626	0.127					
61	save for future	2/DD5	0.646	0.137					



Test #	Comment	Coupon Style/Mat'l	Width in	Thick in	Freq Hz	# High Cycles	# Low Cycles	Total Cycles	Hi Block Max
62	save for future	2/DD5	0.635	0.124					
63	save for future	2/DD5	0.642	0.137					
64	save for future	2/DD5	0.643	0.132					
* 65	Grip fail	2x/DD5	0.613	0.117					
* 66	Grip fail	2x/DD5	0.593	0.119					
* 67	Tab fail	2x/DD5	0.607	0.124					
* 68	Grip fail	nt/DD5	0.581	0.118					
* 69	Grip fail	nt/DD5	0.586	0.125					
70	Dh/Dt=1	2t/DD5	0.445	0.122	10	1743		1743	3266.6
71	Dh/Dt=1	2t/DD5	0.469	0.119	10	1767		1767	3301.8
72	Dh/Dt=1	2t/DD5	0.465	0.122	10	1017		1017	3336.8
73	Dh/Dt=0.95	2t/DD5	0.467	0.121	10	1130	5824	6954	3336.9
74	Dh/Dt=0.95	2t/DD5	0.466	0.119	10	1980	10244	12224	3301.8
75	Dh/Dt=1	2t/DD5	0.425	0.125	10	1515		1515	3125.1
76	Dh/Dt=0.95	2t/DD5	0.448	0.120	10	1190	6188	7378	3196.4
77	Dh/Dt=0.9	2t/DD5	0.394	0.121	10	1080	11984	13064	2774.9
78	Dh/Dt=0.75	2t/DD5	0.404	0.122	10	1150	38076	39226	2880.3
79	Dh/Dt=0.5	2t/DD5	0.419	0.121	10	470	46000	46470	3020.8
* 80	Dh/Dt=0.25	2t/DD5	0.420	0.120					
81	Dh/Dt=0.1	2t/DD5	0.396	0.120	10	30	25918	25948	2851.2
82	Dh/Dt=0.6	2t/DD5	0.397	0.125	10	520	34017	34537	2977.5
83	Dh/Dt=0	2t/DD5	0.396	0.119	10		628444	628444	1642
84	Dh/Dt=1	2m/DD5	0.338	0.126	10	1697		1697	2555.3
85	1 cycle	2m/DD5	0.347	0.125	1 cycle	1		1	4507
86	500 MPa	2m/DD5	0.344	0.120	10	463		463	3055.9
87	500 MPa	2m/DD5	0.350	0.123	10	527		527	3091
* 88	Dh/Dt=0.0	2m/DD5	0.349	0.123					
89	Dh/Dt=0.5	2m/DD5	0.343	0.128	10	293	28527	28820	3110.7
90	Dh/Dt=0.9	2m/DD5	0.328	0.120	10	720	7952	8672	2852.2
91	Dh/Dt=0.1	2m/DD5	0.348	0.128	10	50	45000	45050	3227.8
92	Dh/Dt=0.25	2m/DD5	0.346	0.125	10	1102	330000	331102	2592.6
93	Dh/Dt=0.0	2m/DD5	0.343	0.122	10		1407916	1407916	1463
94	Dh/Dt=0.75	2m/DD5	0.347	0.124	10	782	26052	26834	2579.4
95	Dh/Dt=0.6	2m/DD5	0.350	0.130	10	903	60030	60933	2727.6
96	Dh/Dt=0.25	2m/DD5	0.339	0.129	10	710	213000	213710	2621.6
97	Dh/Dt=0.99	2m/DD5	0.345	0.126	10	4024	4020	8044	2605.9
98	Dh/Dt=0	2m/DD5	0.340	0.120	10		3403091	3403091	1427
99	Dh/Dt=0.99	2m/DD5	0.346	0.120	10	5956	5950	11906	2489.1
100	Dh/Dt=0.5	2m/DD5	0.327	0.119	10	2416	241000	243416	2314.1
101	Dh/Dt=0.9	2m/DD5	0.346	0.121	10	5337	59696	65033	2509.7
102	Dh/Dt=0.1	2m/DD5	0.342	0.126	10	795	711000	711795	2583.2
103	Dh/Dt=1.0	2m/DD5	0.345	0.118	10	1496		1496	2406
104	Dh/Dt=0.9	2m/DD5	0.345	0.126	10	2380	26544	28924	2605.9
105	1 cycle	2m/DD5	0.345	0.128	1 cycle	1		1	4744
106	Dh/Dt=1.0	2m/DD5	0.345	0.122	10	5660		5660	2523.1
107	Dh/Dt=0.1	2m/DD5	0.342	0.129	10	680	609298	609978	2644.7
108	Dh/Dt=1	2m/DD11B	0.362	0.145	10	97		97	3149.4
109	Dh/Dt=0	2m/DD11B	0.367	0.140	10		217518	217518	1798
110	Dh/Dt=0	2m/DD11B	0.369	0.148	10		208911	208911	1911
111	Dh/Dt=1	2m/DD11B	0.369	0.142	10	226		226	3143.9
112	Dh/Dt=0.75	2m/DD11B	0.370	0.151	10	21	668	689	3352.2
113	Dh/Dt=0.25	2m/DD11B	0.374	0.142	10	104	30000	30104	3186.5
114	1 cycle	2m/DD11B	0.372	0.153	1 cycle	1		1	4194.99
115	1 cycle	2m/DD11B	0.372	0.140	1 cycle	1		1	4358.46
116	475MPa	2m/DD11B	0.366	0.147	10	37		37	3682.78
117	350MPa	2m/DD11B	0.374	0.147	10	2729		2729	2716.24
118	475MPa	2m/DD11B	0.374	0.147	10	78		78	3685.34
119	Dh/Dt=1	2m/DD11B	0.364	0.148	10	29		29	3232.3
120	Dh/Dt=0.9	2m/DD11B	0.367	0.140	10	576	6384	6960	3051.63
121	Dh/Dt=0.5	2m/DD11B	0.373	0.144	10	88	8000	8088	3164.61
122	Dh/Dt=0.99	2m/DD11B	0.372	0.140	10	368	360	728	3071.09
123	Dh/Dt=1.0	2m/DD11B	0.371	0.150	10	801		801	3273.87
124	Dh/Dt=1.0	2m/DD11B	0.370	0.140	10	392		392	3032.22

Test #	Comment	Coupon Style/Mat'l	Width in	Thick in	Freq Hz	# High Cycles	# Low Cycles	Total Cycles	Hi Block Max
125	56ksi/32.6ksi	2m/DD11B	0.375	0.147	10	1228	13664	14892	3042.71
126	Dh/Dt=0.9	2m/DD11B	0.374	0.146	10	237	2576	2813	3212.53
127	Dh/Dt=0.0	2m/DD11B	0.375	0.143	10		107287	107287	
128	1 cycle	2m/DD16A	0.372	0.167	1 cycle	1		1	4437.82
129	Dh/Dt=1	2m/DD16A	0.390	0.161	10	78		78	3722.49
130	Dh/Dt=1	2m/DD16A	0.379	0.169	10	149		149	3765.45
131	Dh/Dt=0	2m/DD16A	0.329	0.163	10		141377	141377	1875
132	Dh/Dt=0.5	2m/DD16A	0.379	0.163	10	72	7000	7072	3707
133	Dh/Dt=0.75	2m/DD16A	0.378	0.166	10	40	1002	1042	3765
134	Dh/Dt=0.25	2m/DD16A	0.358	0.162	10	54	15000	15054	3480
135	Dh/Dt=0.9	2m/DD16A	0.386	0.166	10	230	2464	2694	3804.09
136	Dh/Dt=0.1	2m/DD16A	0.373	0.169	10	13	9000	9013	3782
137	Dh/Dt=0.99	2m/DD16A	0.368	0.169	10	130	120	250	3732
138	Dh/Dt=0	2m/DD16A	0.348	0.164	10		143456	143456	1999
139	328 MPa	2m/DD16A	0.357	0.164	10	2297		2297	2800.32
140	328 MPa	2m/DD16A	0.342	0.168	10	1914		1914	2690.32
141	1 cycle	2m/DD16A	0.379	0.167	1 cycle	1		1	4812.24
142	Dh/Dt=0.1	2m/DD16A	0.356	0.165	10	22	18000	18022	3476.29
143	Dh/Dt=0.5	2m/DD16A	0.359	0.162	10	60	5000	5060	3489.5
144	Dh/Dt=0.75	2m/DD16A	0.353	0.162	10	117	3674	3791	3431.2
145	Dh/Dt=0.9	2m/DD16A	0.372	0.163	10	91	1008	1099	3638.2
146	Dh/Dt=0.99	2m/DD16A	0.376	0.167	10	286	280	566	3767.5
147	Dh/Dt=0.0	2m/DD16A	0.361	0.171	10		31943	31943	3703.9
148	Dh/Dt=1	2m/DD16A	0.383	0.168	10	155		155	3860.6
149	Dh/Dt=0.95	2m/DD16A	0.36	0.164	10	182	936	1118	3542.4
150	Dh/Dt=0.95	2m/DD16A	0.392	0.163	10	195	988	1183	3833.8
151	207 MPa	2m/DD16A	0.397	0.163	10	274271		274271	1923.0
152	207 MPa	2m/DD16A	0.393	0.165	10	294549		294549	1902.0
153	207 MPa	2m/DD16A	0.355	0.168	10	382826		382826	1738.0
154	47.5/30-0.5	2m/DD16A	0.360	0.167	10	432	43000	43432	2855.7
155	47.5/30-0.9	2m/DD16A	0.384	0.164	10	1077	11984	13061	2991.4
156	47.5/30-0.1	2m/DD16A	0.379	0.162	10	120	92379	92499	2916.4
157	47.5/30-0.25	2m/DD16A	0.336	0.163	10	554	162287	162841	2601.5
158	47.5/30-0.99	2m/DD16A	0.359	0.161	10	1840	1830	3670	2745.5
159	47.5/30-0.75	2m/DD16A	0.358	0.160	10	1062	35404	36466	2720.8
160	30 ksi - 0.0	2m/DD16A	0.362	0.166	10		495397	495397	1770.0
161	47.5 ksi - 1.0	2m/DD16A	0.380	0.161	10	1722		1722	2906.1
162	47.5/30-0.5	2m/DD16A	0.334	0.160	10	1432	143000	144432	2538.4
163	47.5/30-0.9	2m/DD16A	0.357	0.159	10	2119	23632	25751	2696.2
164	47.5/30-0.1	2m/DD16A	0.362	0.162	10	270	239206	239476	2785.6
165	47.5/30-0.25	2m/DD16A	0.355	0.166	10	406	120000	120406	2799.2
166	47.5/30-0.99	2m/DD16A	0.391	0.160	10	4249	4240	8489	2971.6
167	47.5/30-0.75	2m/DD16A	0.351	0.163	10	932	31062	31994	2678.8
168	47.5 ksi - 1.0	2m/DD16A	0.365	0.171	10	744		744	2850.0
169	30 ksi - 0.0	2m/DD16A	0.335	0.162	10		588371	588371	
170	47.5/30-0.99	2m/DD16A	0.347	0.171	10	3552	3550	7102	2776.01
171	47.5ksi - 1.0	2m/DD16A	0.305	0.171	10	3152		3152	2439.05
172	60 ksi - 1.0	2m/DD16A	0.359	0.159	10	162		162	3367.15
173	1 cycle	2m/DD16A	0.358	0.169	1 cycle	1		1	4328.7
174	35ksi - 1.0	2m/DD16A	0.358	0.171	10		37855	37855	2097.23
175	47.5/30-10/667	2m/DD16A	0.360	0.160	10	987	65366	66353	2669.35
176	47.5/30-10/1000	2m/DD16A	0.358	0.172	10	349	34000	34349	2859.7
177	47.5/35-10/1000	2m/DD16A	0.317	0.168	10	656	65000	65656	2467.88
178	47.5/35-10/1000	2m/DD16A	0.314	0.172	10	197	19000	19197	2504.17
179	60/47.5/35	2m/DD16A	0.318	0.163	10	62	600	662	3010.01
180	47.5/30-20/10	2m/DD16A	0.355	0.170	10	2418	1200	3618	2814.1
181	47.5/30-10/250	2m/DD16A	0.360	0.161	10	2207	54750	56957	2705.6
182	47.5/30-10/40	2m/DD16A	0.359	0.159	10	2419	9640	12059	2654.3
183	47.5/30-10/1000	2m/DD16A	0.358	0.170	10	510	50906	51416	3085.71
184	47.5/30-10/667	2m/DD16A	0.355	0.172	10	359	23345	23704	2871.3
* 185	47.5/30 - 10/33K	2m/DD16A	0.358	0.169					
186	47.5/30-10/33000	2m/DD16A	0.355	0.164	10	106	330000	330106	2747.4
187	47.5/30-10/33000	2m/DD16A	0.357	0.172	10	42	165000	165042	2916.7

Test #	Comment	Coupon Style/Mat'l	Width in	Thick in	Freq Hz	# High Cycles	# Low Cycles	Total Cycles	Hi Block Max
188	47.5/30-10/50000	2m/DD16A	0.359	0.173	10	30	139982	140012	2950.1
189	47.5/30-10/60000	2m/DD16A	0.318	0.163	10	50	295894	295944	2462.1
190	47.5/30-10/20000	2m/DD16A	0.299	0.167	10	150	297672	297822	2371.8
191	47.5/30-10/50000	2m/DD16A	0.353	0.171	10	30	101013	101043	2867.2
192	47.5/30-10/33000	2m/DD16A	0.356	0.168	10	50	158561	158611	2840.9
193	47.5/30-10/60000	2m/DD16A	0.356	0.173	10	20	91339	91359	2925.4
194	47.5/35-10/1000	2m/DD16A	0.320	0.174	10	140	13016	13156	2589.09
195	47.5/35-10/3000	2m/DD16A	0.309	0.165	10	150	44460	44610	2371.42
196	47.5/35-10/5000	2m/DD16A	0.348	0.173	10	40	17361	17401	2805.31
* 197	47.5/35 ksi, 10/9K	2m/DD16A	0.354	0.171					
198	47.5/35-10/500	2m/DD16A	0.307	0.163	10	250	12114	12364	2313.91
199	47.5/35-10/100	2m/DD16A	0.352	0.169	10	364	3600	3964	2760.64
200	47.5/35-10/10	2m/DD16A	0.310	0.170	10	1357	1350	2707	2446.28
201	47.5/35-10/500	2m/DD16A	0.352	0.170	10	100	4774	4874	2782.18
202	47.5/35-10/1000	2m/DD16A	0.360	0.172	10	100	9359	9459	2872.17
203	47.5/35-10/5000	2m/DD16A	0.356	0.171	10	40	15564	15604	2835.05
204	47.5/35-10/3000	2m/DD16A	0.300	0.164	10	110	30522	30632	2284.75
205	35-0/100	2m/DD16A	0.313	0.171	10		15680	15680	1847
206	47.5-10/0	2m/DD16A	0.308	0.170	10	1339		1339	2440.36
207	47.5/30-10/10-N	2m/DD16A	0.334	0.164	10	2163	2160	4323	2540.58
208	47.5/30-10/10-D	2m/DD16A	0.337	0.171	10	2326	2320	4646	2678.83
209	47.5/35-10/10-N	2m/DD16A	0.332	0.177	10	583	580	1163	2721.06
210	47.5/35-10/10-D	2m/DD16A	0.321	0.164	10	1815	1810	3625	2440.87
211	60/35-10/10-N	2m/DD16A	0.335	0.170	10	98	90	188	3256.73
212	60/35-10/10-D	2m/DD16A	0.321	0.172	10	72	70	142	3177.86
213	47.5-10-N	2m/DD16A	0.331	0.163	10	3306		3306	2533.51
214	47.5-10-D	2m/DD16A	0.316	0.171	10	2078		2078	2496.13
215	60/35-10/9000	2m/DD16A	0.337	0.173	10	17	9000	9017	3328.89
216	47.5/30-10/9000	2m/DD16A	0.334	0.175	10	85	72000	72085	2704.92
217	47.5/35-10/3000	2m/DD16A	0.346	0.166	10	60	17063	17123	2665.75
218	47.5/30-10/3000	2m/DD16A	0.351	0.162	10	110	31739	31849	2634.8
219	47.5/30-10/5000	2m/DD16A	0.347	0.173	10	80	39441	39521	2800.37
220	6block-47.5 max	2m/DD16A	0.337	0.171	10			97997	2679.36
221	6block-50ksi max	2m/DD16A	0.338	0.173	10			28915	2923.7
222	6block-60ksi max	2m/DD16A	0.327	0.174	10			6064	3249.32
* 223	6block-40ksi max	2m/DD16A	0.320	0.162					
* 224	6block-30ksi max	2m/DD16A	0.348	0.170					
225	6block-50ksi max	2m/DD16A	0.333	0.175	10			20907	2906.52
226	6block-40ksi max	2m/DD16A	0.334	0.169	10			181648	2255.61
* 227	6block-30ksi max	2m/DD16A	0.323	0.168					
* 228	6block-60ksi max	2m/DD16A	0.338	0.172					
229	47.5/30-10/60000	2m/DD16A	0.346	0.173	10	20	61684	61704	2760.6
230	47.5/30-10/50000	2m/DD16A	0.333	0.164	10	70	319095	319165	2530.71
* 231	47.5/30-10/33000	2m/DD16A	0.324	0.169					
232	47.5/30-10/9000	2m/DD16A	0.333	0.174	10	100	81000	81100	2746.64
233	47.5/30-10/50000	2m/DD16A	0.330	0.168	10	50	202625	202675	2629.51
234	47.5/30-10/9000	2m/DD16A	0.338	0.158	10	210	180000	180210	2543.31
235	47.5/30-10/33000	2m/DD16A	0.330	0.173	10	30	82555	82585	2706.59
236	30 ksi residual/failed	2m/DD16A	0.341	0.161	10		446342	446342	1648.48
237	30 ksi residual	2m/DD16A	0.331	0.162	10		200016	200016	1608.42
237r	30 ksi residual	2m/DD16A	0.331	0.162	1 cycle				3240.29
238	30 ksi residual	2m/DD16A	0.328	0.165	10		100009	100009	1623.7
238r	30 ksi residual	2m/DD16A	0.328	0.165	1 cycle				3544.23
239	30 ksi residual/failed	2m/DD16A	0.358	0.170	10		111838	111838	1826.07
240	30 ksi residual	2m/DD16A	0.321	0.161	10		300010	300010	
240r	30 ksi residual	2m/DD16A	0.321	0.161	1 cycle				3381.21
241	30 ksi residual/failed	2m/DD16A	0.348	0.160	10		130521	130521	1669.74
242	30 ksi residual/failed	2m/DD16A	0.329	0.161	10		133659	133659	1587.5
243	30 ksi residual	2m/DD16A	0.331	0.175	10		100010	100010	1738.6
243r	30 ksi residual	2m/DD16A	0.331	0.175	1 cycle				3381.93
244	30 ksi residual/failed	2m/DD16A	0.360	0.174	10		38964	38964	1876.05
245	30 ksi residual	2m/DD16A	0.376	0.173			50008	50008	
245r	30 ksi residual	2m/DD16A	0.376	0.173	1 cycle				4243.84

Test #	Comment	Coupon Style/Mat'l	Width in	Thick in	Freq Hz	# High Cycles	# Low Cycles	Total Cycles	Hi Block Max
246	35/30 - 10/10	2m/DD16A	0.326	0.173	10	67370	67365	134735	1977.44
247	35/30 - 10/9000	2m/DD16A	0.319	0.167	10	600	535083	535683	1864.29
248	35/30 - 10/33000	2m/DD16A	0.319	0.175	10	100	307196	307296	1953.11
249	35/30 - 10/60000	2m/DD16A	0.323	0.175	10	30	137575	137605	1977.2
250	35/30 - 10/9000	2m/DD16A	0.323	0.174	10	580	518806	519386	1965.18
251	35/30 - 10/60000	2m/DD16A	0.320	0.159	10	40	198456	198496	1778.54
252	35/30 - 10/10	2m/DD16A	0.324	0.175	10	37306	37300	74606	1988.61
253	35/30 - 10/9000	2m/DD16A	0.327	0.162	10	410	366273	366683	1856.59
254	35/30 - 10/33000	2m/DD16A	0.325	0.172	10	90	274261	274351	1955.78
255	35/30 - 20/10	2m/DD16A	0.335	0.169	10	26342	13170	39512	1986.6
256	60/47.5 - 10/10	2m/DD16A	0.333	0.169	10	42	40	82	3287.55
257	60/47.5 - 10/1000	2m/DD16A	0.360	0.160	10	10	603	613	3361.38
258	60/47.5 - 10/100	2m/DD16A	0.330	0.172	10	20	145	165	3314
259	60/47.5 - 10/100	2m/DD16A	0.328	0.171	10	39	300	339	3280.92
260	60/47.5 - 1/1000	2m/DD16A	0.338	0.162	01/10	20	1268	1288	3235.15
261	47.5/30 - 10/10	2m/DD16A	0.328	0.163	10	519	510	1029	2545.34
* 262	+60/47.5, 1/1000	2m/DD16A	0.335	0.160					
263	47.5/30 - 1/100r	2m/DD16A	0.321	0.159	10	942	94100	95042	2482.68
264	47.5/30 - 1/100r	2m/DD16A	0.349	0.174	10	90	8900	8990	2784.82
265	47.5/30 - 10/10000	2m/DD16A	0.324	0.174	10	120	110187	110307	2672.65
* 266	25 ksi	2m/DD16A	0.333	0.169					
267	47.5/30 - 10/1000r	2m/DD16A	0.326	0.170	10	340	33037	33377	2468.92
268	1 cycle	2m/DD16A	0.357	0.165	1 cycle	1		1	4037.8
269	1 cycle	2m/DD16A	0.352	0.176	1 cycle	1		1	4202.54
270	1 cycle	2m/DD16A	0.328	0.172	1 cycle	1		1	3807.17
271	1 cycle	2m/DD16A	0.329	0.167	1 cycle	1		1	3894.48
272	1 cycle	2m/DD16A	0.332	0.171	1 cycle	1		1	3894.64
273	1 cycle	2m/DD16B	0.381	0.157	1 cycle	1		1	5606.75
274	1 cycle	2m/DD16B	0.361	0.157	1 cycle	1		1	5581.43
275	60/35 - 10/112	2m/DD16B	0.326	0.152	10	274	3024	3298	2976.95
276	47.5/30 - 10/1000	2m/DD16B	0.347	0.157	10	359	35000	35359	2585.1
277	35/30 - 10/1000	2m/DD16B	0.386	0.152	10	1320	131237	132557	2042.63
278	35/30 - 10/100	2m/DD16B	0.376	0.157	10	34940	349366	384306	2062.36
279	47.5/35 - 10/5000	2m/DD16B	0.338	0.159	10	150	71692	71842	2539.3
280	47.5/35 - 10/1000	2m/DD16B	0.383	0.168	10	80	7892	7972	3039.04
281	47.5/30 - 10/100	2m/DD16B	0.329	0.161	10	2543	25400	27943	2495.94
282	60 ksi	2m/DD16B	0.388	0.152	10	85		85	3521.28
283	1 cycle	2m/DD16B	0.382	0.161	1 cycle	1		1	5771.1
284	35	2m/DD16B	0.385	0.157	10	109547		109547	2110.65
285	35/30 - 10/1000	2m/DD16B	0.374	0.149	10	7060	706997	714057	1952.03
* 286	1 cycle (do not use)	2m/DD16B	0.355	0.153					
287	47.5/30 - 10/1000r	2m/DD16B	0.367	0.161	10	408	40800	41208	2796.03
288	47.5/30 - 10/1000r	2m/DD16B	0.409	0.152	10	288	28840	29128	2864.95
289	47.5/30 - 1/100r	2m/DD16B	0.349	0.174	10	81	8100	8181	2844.98
290	47.5/30 - 10/1000r	2m/DD16B	0.391	0.157	10	175	17448	17623	2894.05
291	47.5/30 - 10/1000	2m/DD16B	0.397	0.153	10	610	60710	61320	2887.81
* 292	47.5/30 - 10/1000r	2m/DD16B	0.392	0.156					
* 293	47.5/30 - 1/100r	2m/DD16B	0.391	0.157					
294	47.5/30 - 10/1000	2m/DD16B	0.33	0.162	10	540	53027	53567	2522.03
295	47.5/30 - 10/1000r	2m/DD16B	0.397	0.159	10	442	44166	44608	2986.16
296	1 cycle	2m/DD16B	0.375	0.172	1 cycle	1		1	4565.63
297	60 ksi	2m/DD16B	0.355	0.159	10	491		491	3380.67
298	60 ksi	2m/DD16B	0.394	0.156	10	356		356	3689.32
299	35/30 - 10/990	2m/DD16B	0.394	0.149	10	5970	590898	596868	2056.48
300	60/35 - 10/9000	2m/DD16B	0.367	0.159	10	40	27155	27195	3482.38
301	35/30 - 10/90	2m/DD16B	0.351	0.173	10	10170	91462	101632	2123.87
302	35 ksi	2m/DD16B	0.388	0.155	10	54487		54487	2095.99
303	35/30 - 10/49990	2m/DD16B	0.386	0.165	10	60	264911	264971	2225.73
304	60/35 - 10/112	2m/DD16B	0.387	0.156	10	312	3472	3784	3621.52
305	30 ksi	2m/DD16B	0.373	0.162	10		121190	121190	1809.8
306	1 cycle	2m/DD16B	0.379	0.158	1 cycle	1		1	5822.95
307	60/35 - 10/90	2m/DD16B	0.4	0.172	10	44	360	404	4109.19
308	60 ksi	2m/DD16B	0.39	0.152	10	91		91	3544.91

Test #	Comment	Coupon Style/Mat'l	Width in	Thick in	Freq Hz	# High Cycles	# Low Cycles	Total Cycles	Hi Block Max
309	30 ksi	2m/DD16B	0.375	0.152	10		373306	373306	1713.41
310	60/47.5 - 10/10	2m/DD16B	0.341	0.155	10	141	140	281	3164.41
311	60/47.5 - 10/90	2m/DD16B	0.387	0.152	10	173	1530	1703	3523.82
312	60/47.5 - 10/990	2m/DD16B	0.363	0.172	10	10	517	527	3714.7
313	60 ksi	2m/DD16B	0.373	0.152	10	429		429	3396.02
314	47.5/30 - 10/1000r	2m/DD16B	0.331	0.169	10	335	33528	33863	2642.82
315	47.5/30 - 10/10	2m/DD16B	0.392	0.158	10	2174	2170	4344	2928.99
316	47.5/30 - 10/90	2m/DD16B	0.396	0.151	10	1762	15840	17602	2836.87
317	47.5/30 - 10/1000r	2m/DD16B	0.393	0.154	10	464	46400	46864	2842.47
318	35/30 - 10/90	2m/DD16B	0.378	0.169	10	1610	14403	16013	2244.35
319	35/30 - 10/990	2m/DD16B	0.387	0.154	10	1980	195842	197822	2085.97
320	47.5/30 - 1/100r	2m/DD16B	0.407	0.155	10	301	30100	30401	2992.9
321	47.5	2m/DD16B	0.377	0.152	10	2611		2611	2717.21
322	47.5/30 - 10/1000r	2m/DD16B	0.363	0.161	10	441	44103	44544	2763.6
323	35	2m/DD16B	0.393	0.163	10	16884		16884	2245.69
324	47.5/30 - 1/100r	2m/DD16B	0.374	0.172	10	127	12700	12827	3051.5
325	47.5	2m/DD16B	0.371	0.154	10	8653		8653	2701.03
326	35	2m/DD16B	0.381	0.154	10	104679		104679	2045.16
327	47.5/30 - 10/1000r	2m/DD16B	0.379	0.155	10	480	48211	48691	2790.4
328	47.5/30 - 10/1000	2m/DD16B	0.388	0.153	10	799	79000	79799	2807.1
329	1 cycle	2m/DD16B	0.389	0.153	1 cycle	1		1	4665.19
330	47.5/30 - 10/1000r	2m/DD16B	0.342	0.171	10	379	37932	38311	2769.8
331	47.5/30 - 10/1000r3	2m/DD16B	0.397	0.149	10	980	98000	98980	2802.86
332	47.5/30 - 1/100r	2m/DD16B	0.383	0.17	10	278	27800	28078	3053.79
333	47.5/30 - 10/1000r3	2m/DD16B	0.379	0.17	10	510	51000	51510	3041.85
334	47.5/30 - 10/1000r2	2m/DD16B	0.374	0.153	10	591	59082	59673	2718
335	60 ksi - R=0.5	2m/DD16B	0.377	0.157	10	4701		4701	3541.86
336	47.5 ksi - R=0.5	2m/DD16B	0.377	0.154	10	32173		32173	2755.09
337	35 ksi - R=0.5	2m/DD16B	0.397	0.153	10	1469317		1469317	2119.49
* 338	30 ksi, R = 0.5	2m/DD16B	0.384	0.152					
339	47.5/30 - 10/1000 R=0.5	2m/DD16B	0.385	0.155	10	1630	16200	17830	2816.64
* 340	47.5/30 - 10/1000r3	2m/DD16B	0.386	0.152					
* 341	47.5/30 - 10/1000r2	2m/DD16B	0.376	0.155					
* 342	47.5/30 - 1/100r	2m/DD16B	0.336	0.171					
343	35 ksi - R=0.5	2m/DD16B	0.398	0.15	10	350682		350682	2086.9
344	30 ksi	2m/DD16B	0.391	0.172	10		run out		1784.94
345	35/30 ksi - 10/90 R=0.5	2m/DD16B	0.394	0.159	10	80180	721620	801800	2189.18
346	60 ksi R=0.5	2m/DD16B	0.355	0.164	10	3836		3836	3479.35
347	47.5 ksi R=0.5	2m/DD16B	0.399	0.156	10	20006		20006	2955.4
348	47.5/30 ksi - 10/1000 R=0.5	2m/DD16B	0.386	0.159	10	1790	179000	180790	2912.39
349	1 cycle	2m/DD16B	0.362	0.152	1 cycle	1		1	4454
350	47.5/35 - 10/10	2m/DD16B	0.387	0.152	10	5749	5740	11489	2801.54
351	47.5/35 - 10/90	2m/DD16B	0.39	0.152	10	1899	17010	18909	2813.94
352	47.5/30 - 10/1000 R=0.5	2m/DD16B	0.392	0.151	10	1710	171000	172710	2809.25
353	47.5/30 - 10/1000r3	2m/DD16B	0.376	0.161	10	350	35002	35352	2871.6
354	47.5/30 - 10/1000r2	2m/DD16B	0.387	0.153	10	832	83248	84080	2799.7
355	set aside for future	2m/DD16B	0.339	0.16					
356	set aside for future	2m/DD16B	0.385	0.149					
357	set aside for future	2m/DD16B	0.386	0.167					
358	set aside for future	2m/DD16B	0.372	0.148					
359	set aside for future	2m/DD16B	0.377	0.154					
* 360	47.5/30 - 1/100r	2m/DD16C	0.392	0.156					
* 361	1 cycle	2m/DD16C	0.388	0.154					
* 362	47.5/30 - 10/1000r	2m/DD16C	0.381	0.156					
363	47.5	2m/DD16C	0.392	0.156	10	3139		3139	2898.38
* 364	47.5/30 - 10/1000r	2m/DD16C	0.384	0.154					
* 365	30	2m/DD16C	0.400	0.154					
* 366	47.5/30 - 1/100r	2m/DD16C	0.386	0.155					
* 367	47.5/30 - 1/100r	2m/DD16C	0.399	0.156					
368	47.5/30 - 10/1000r	2m/DD16C	0.395	0.154	10	551	55063	55614	2885.79
369	47.5/30 - 10/1000	2m/DD16C	0.383	0.156	10	312	31000	31312	2839.56
370	47.5/30 - 1/100r	2m/DD16C	0.380	0.154	10	584	58400	58984	2775.38
371	47.5/30 - 1/100r	2m/DD16C	0.400	0.154	10	257	25700	25957	2915.66

Test #	Comment	Coupon Style/Mat'l	Width in	Thick in	Freq Hz	# High Cycles	# Low Cycles	Total Cycles	Hi Block Max
372	47.5/30 - 10/1000r3	2m/DD16C	0.393	0.155	10	750	75006	75756	2974.31
373	47.5/30 - 10/1000r3	2m/DD16C	0.380	0.156	10	479	47874	48353	2807.12
374	47.5/30 - 10/1000	2m/DD16C	0.379	0.153	10	1470	146350	147820	2758.23
375	47.5/30 - 10/1000r3	2m/DD16C	0.398	0.153	10	561	56122	56683	2889.09
376	47.5	2m/DD16C	0.392	0.160	10	1706		1706	2977.6
377	47.5/30 - 1/100r	2m/DD16C	0.398	0.153	10	670	67000	67670	2856.63
378	30	2m/DD16C	0.393	0.155	10		261287	261287	1829.27
379	47.5/30 - 1/100r	2m/DD16C	0.394	0.156	10	606	60600	61206	2913.22
380	47.5/30 - 10/1000r3	2m/DD16C	0.385	0.153	10	699	69875	70574	2793.85
381	47.5/30 - 10/1000r3	2m/DD16C	0.390	0.153	10	630	63002	63632	2815.22
382	47.5/30 - 1/100r	2m/DD16C	0.389	0.154	10	301	30100	30401	2841.01
383	1 cycle	2m/DD16C	0.387	0.151	1 cycle	1		1	5525.45
384	47.5/30 - 1/100r	2m/DD16C	0.383	0.154	10	681	68100	68781	2797.41
385	47.5/30 - 10/1000r3	2m/DD16C	0.400	0.157	10	364	36388	36752	2983
386	47.5/30 - 10/1000	2m/DD16C	0.394	0.154	10	454	45000	45454	2882.36
387	47.5/30 - 10/1000 random3	2m/DD16C	0.402	0.153	10	460	46001	46461	2908.67
388	47.5/30 - 1/100 onecycle	2m/DD16C	0.391	0.155	10	1698	169800	171498	2876.54
389	47.5/30 - 10/1000 random3	2m/DD16C	0.394	0.155	10	510	51005	51515	2897.25
390	47.5/30 - 10/1000 random3	2m/DD16C	0.405	0.151	10	869	86907	87776	2901.72
391	30 ksi	2m/DD16C	0.393	0.155	10		421272	421272	1827.33
392	47.5/30 - 1/100 onecycle	2m/DD16C	0.390	0.155	10	755	75500	76255	2860.48
393	47.5/30 - 1/100 onecycle	2m/DD16C	0.400	0.155	10	407	40700	41107	2933.72
394	47.5/30 - 10/1000	2m/DD16C	0.384	0.155	10	720	71039	71759	2824.34
395	47.5/30 - 1/100 onecycle	2m/DD16C	0.395	0.154	10	306	30600	30906	2877.72
396	47.5/30 - 10/1000 random3	2m/DD16C	0.382	0.153	10	800	80004	80804	2760.48
397	47.5/30 - 10/1000	2m/DD16C	0.398	0.159	10	993	99000	99993	3009.02
398	47.5/30 - 10/1000 random3	2m/DD16C	0.383	0.154	10	369	36860	37229	2811.16
399	47.5/30 - 1/100 onecycle	2m/DD16C	0.389	0.159	10	598	59800	60398	2897.88
400	60/47.5 - 10/10 R=0.5	2m/DD16C	0.366	0.153	10	1292	1290	2582	3352.9
401	60/47.5 - 10/50 R=0.5	2m/DD16C	0.343	0.156	10	879	4350	5229	3203.8
402	60/47.5 - 10/100 R=0.5	2m/DD16C	0.353	0.151	10	560	5576	6136	3192.61
403	60/47.5 - 10/1000 R=0.5	2m/DD16C	0.353	0.155	10	165	16000	16165	3281.11
404	60/47.5 - 10/10 R=0.5	2m/DD16C	0.374	0.154	10	2266	2260	4526	3450.83
405	60/47.5 - 10/50 R=0.5	2m/DD16C	0.343	0.158	10	2352	11750	14102	3251.65
406	60/47.5 - 10/100 R=0.5	2m/DD16C	0.354	0.162	10	872	8700	9572	3435.43
407	60/47.5 - 10/1000 R=0.5	2m/DD16C	0.354	0.158	10	240	23256	23496	3352.72
408	60 ksi R=0.5	2m/DD16C	0.361	0.160	10	2290		2290	3456.12
409	47.5 ksi R=0.5	2m/DD16C	0.350	0.156	10		49288	49288	2586.28
410	1 cycle	2m/DD16C	0.354	0.158	1 cycle	1		1	5173.99
411	47.5/30 - 10/1000 random3	2m/DD16C	0.348	0.157	10	460	46000	46460	2587.86
412	35 ksi R=0.5	2m/DD16C	0.358	0.154	10	829489		829489	1933.02
413	60/35 - 10/10 R=0.5	2m/DD16C	0.349	0.155	10	3233	3230	6463	3241.58
414	60/35 - 10/1000 R=0.5	2m/DD16C	0.351	0.163	10	267	26000	26267	3443.5
415	60/35 - 10/10000 R=0.5	2m/DD16C	0.358	0.149	10	175	170000	170175	3196.7
416	47.5 ksi R=0.5	2m/DD16C	0.343	0.153	10	74500		74500	2492.1
417	60 ksi R=0.5	2m/DD16C	0.355	0.155	10	4100		4100	3294.14
418	35 ksi R=0.5	2m/DD16C	0.347	0.154	10	1559097		1559097	1874.2
419	60/35 - 10/10000 R=0.5	2m/DD16C	0.357	0.160	10	91	90000	90091	3419.47
420	60/35 - 10/1000 R=0.5	2m/DD16C	0.361	0.160	10	258	25000	25258	3456
421	60/35 - 10/10 R=0.5	2m/DD16C	0.356	0.156	10	2800	2800	5600	3330.39
422	47.5/35 - 10/10 R=0.5	2m/DD16C	0.358	0.154	10	14325	14320	28645	2619.9
423	47.5/35 - 10/100 R=0.5	2m/DD16C	0.351	0.158	10	22439	224300	246739	2631.74
424	47.5/35 - 10/1000 R=0.5	2m/DD16C	0.347	0.156	10	1939	193000	194939	2566.85
425	47.5/35 - 10/1000 R=0.5	2m/DD16C	0.348	0.156	10	1481	148000	149481	2579.14
426	35 ksi R=0.5	2m/DD16C	0.348	0.154	10	808064		808064	1925.38
427	47.5/35 - 10/100 R=0.5	2m/DD16C	0.353	0.153	10	16397	163900	180297	2563.36
428	47.5/35 - 10/10 R=0.5	2m/DD16C	0.351	0.156	10	47833	47830	95663	2599.81
429	47.5 ksi R=0.5	2m/DD16C	0.361	0.153	10	33362		33362	2617.04
430	1 cycle	2m/DD16C	0.339	0.154	1 cycle	1		1	4531
431	60 ksi R=0.5	2m/DD16C	0.341	0.162	10	2469		2469	3303.09
432	47.5/30 - 1/100 R=0.1	2m/DD16C	0.353	0.157	01/10	447	44600	45047	2607.71
433	60 R=0.1	2m/DD16C	0.354	0.154	10	757		757	3274.23
434	47.5 R=0.1	2m/DD16C	0.344	0.155	10	3744		3744	2559.09

Test #	Comment	Coupon Style/Mat'l	Width in	Thick in	Freq Hz	# High Cycles	# Low Cycles	Total Cycles	Hi Block Max
435	35 R=0.1	2m/DD16C	0.354	0.157	10	181518		181518	1939.79
436	30 R=0.1	2m/DD16C	0.355	0.154	10	1137595		1137595	1636.53
437	47.5/30 - 10/1000	2m/DD16C	0.354	0.154	10	1282	128000	129282	2571.56
438	47.5/30 - 10/1000 random2	2m/DD16C	0.350	0.157	10	432	43206	43638	2600.21
439	60/47.5/35 - 10/10/100	2m/DD16C	0.350	0.157	10	394	390	4684	3291.36
440	47.5/60/35 - 10/10/100	2m/DD16C	0.343	0.155	10	820	811	9731	3194.78
441	60/35/47.5 - 10/100/10	2m/DD16C	0.357	0.155	10	219	2100	2529	3314.14
442	60/47.5/35 - 10/10/100	2m/DD16C	0.368	0.163	10	270	260	3130	3590.62
443	35/47.5/60 - 100/10/10	2m/DD16C	0.358	0.153	10	4200	420	5037	3281.91
444	60/37.9 - 10/1000 rand5	2m/DD16C	0.364	0.155	10	24	2383	2407	3357.47
445	47.5/30 - 10/1000 rand5	2m/DD16C	0.367	0.153	10	156	15629	15785	2657.69
446	47.5/30 - 10/1000 rand5	2m/DD16C	0.370	0.150	10	291	29134	29425	2625.09
447	47.5/30 - 10/1000 rand5	2m/DD16C	0.357	0.151	10	810	81086	81896	2549
448	47.5/30 - 10/1000 rand5	2m/DD16C	0.360	0.153	10	231	23134	23365	2603
449	47.5/30 - 10/1000 rand5	2m/DD16C	0.363	0.155	10	331	33134	33465	2660
450	47.5/30 - 10/1000 rand5	2m/DD16C	0.356	0.157	10	201	20127	20328	2646
451	47.5/30 - 10/1000 rand5	2m/DD16C	0.354	0.156	10	136	13576	13712	2615
452	47.5/30 - 10/1000 rand5	2m/DD16C	0.354	0.154	10	369	36851	37220	2576
453	47.5/30 - 10/1000 rand5	2m/DD16C	0.366	0.151	10	125	12469	12594	2613
454	47.5/30 - 10/1000 rand5	2m/DD16C	0.355	0.153	10	509	50912	51421	2570
455	47.5/30 - 10/1000 rand5	2m/DD16C	0.372	0.157	10	289	28912	29201	2760
456	47.5/30 - 10/1000 rand5	2m/DD16C	0.357	0.155	10	269	26851	27120	2615
457	47.5/30 - 10/1000 rand5	2m/DD16C	0.354	0.153	10	122	12209	12331	2559
* 458	47.5/30 - 10/1000 rand5	2m/DD16C	0.365	0.153					
459	60 ksi residual	2m/DD16C	0.364	0.148	10	100		100	3232.3
459r	60 ksi residual	2m/DD16C	0.364	0.148	1 cycle				5112
460	60 ksi residual	2m/DD16C	0.366	0.154	10	478		100	3381.8
461	60 ksi residual	2m/DD16C	0.364	0.153	10	810		100	3341.5
462	60 ksi residual	2m/DD16C	0.363	0.153	10	100		100	3332.3
462r	60 ksi residual	2m/DD16C	0.363	0.153	1 cycle				5324
463	60 ksi residual	2m/DD16C	0.354	0.156	10	100		100	3313.4
462r	60 ksi residual	2m/DD16C	0.354	0.156	1 cycle				5289
464	47.5 ksi residual	2m/DD16C	0.371	0.164	10	1000		100	2890.1
464r	47.5 ksi residual	2m/DD16C	0.371	0.164	1 cycle				5830
465	47.5 ksi residual	2m/DD16C	0.369	0.155	10	7752		100	2716.8
466	47.5 ksi residual	2m/DD16C	0.356	0.163	10	1000		100	2756.3
466r	47.5 ksi residual	2m/DD16C	0.356	0.163	1 cycle				4960
467	47.5 ksi residual	2m/DD16C	0.355	0.153	10	9811		100	2580
468	47.5 ksi residual	2m/DD16C	0.355	0.154	10	1000		100	2596.8
468r	47.5 ksi residual	2m/DD16C	0.355	0.154	1 cycle				4525
469	35 ksi residual	2m/DD16C	0.356	0.153	10	10000		100	1906.4
469r	35 ksi residual	2m/DD16C	0.356	0.153	1 cycle				5133
470	35 ksi residual	2m/DD16C	0.374	0.154	10	100000		100	2015.9
470r	35 ksi residual	2m/DD16C	0.374	0.154	1 cycle				4929
471	35 ksi residual	2m/DD16C	0.359	0.153	10	100000		100	1922.4
471r	35 ksi residual	2m/DD16C	0.359	0.153	1 cycle				5091
472	35 ksi residual	2m/DD16C	0.363	0.158	10	10000		100	2007.4
472r	35 ksi residual	2m/DD16C	0.363	0.158	1 cycle				5402
473	35 ksi residual	2m/DD16C	0.353	0.152	10	10000		100	1878
473r	35 ksi residual	2m/DD16C	0.353	0.152	1 cycle				5088
474	1 cycle	2m/DD16C	0.367	0.166	1 cycle	1		1	5558
475	47.5 ksi residual	2m/DD16C	0.364	0.158	10	10000			2731.8
475r	47.5 ksi residual	2m/DD16C	0.364	0.158	1 cycle				5282
476	35 ksi residual	2m/DD16C	0.359	0.153	10	100000			1922.4
476r	35 ksi residual	2m/DD16C	0.359	0.153	1 cycle				4772
477	60 ksi residual	2m/DD16C	0.351	0.154	10	1000			3243.2
477r	60 ksi residual	2m/DD16C	0.351	0.154	1 cycle				5189
* 478	1 cycle	2m/DD16C	0.361	0.154					
479	1 cycle	2m/DD16C	0.353	0.153	1 cycle	1		1	5146
480	47.5/30 - 1/100 onecycle	2m/DD16C	0.368	0.155	10	469	46900	47369	2710
481	47.5/30 - 10/1000 random2	2m/DD16C	0.358	0.153	10	528	52876	53404	2589
482	47.5/30 - 10/1000 block	2m/DD16C	0.354	0.156	10	320	32007	32327	2613
483	47.5/30 - 10/1000 rand5	2m/DD16C	0.358	0.155	10	349	34949	35298	2624

Test #	Comment	Coupon Style/Mat'l	Width in	Thick in	Freq Hz	# High Cycles	# Low Cycles	Total Cycles	Hi Block Max
484	47.5 ksi	2m/DD16C	0.356	0.153	10	936		936	2580.36
485	30 ksi, R=0.1	2m/DD16C	0.354	0.157	10	286613		286613	1664.3
486	60 ksi	2m/DD16C	0.356	0.154	10	1119		1119	3280.92
487	47.5 ksi, R=0.5	2m/DD16C	0.365	0.162	10	21452		21452	2799.74
488	35 ksi, R=0.5	2m/DD16C	0.358	0.151	10	156860		156860	1890.62
489	60/47.5/35 - 10/10/100	2m/DD16C	0.359	0.151	10	113	110		3240.84
490	47.5/60/35 - 10/10/100	2m/DD16C	0.364	0.154	10	180	174		3358.79
491	35/47.5/60 - 100/10/10	2m/DD16C	0.354	0.157	10	1600	160		3328.79
492	60/47.5/35 - 10/10/100	2m/DD16C	0.366	0.154	10	123	120		3376.95
493	35/47.5/60 - 100/10/10	2m/DD16C	0.365	0.152	10	1634	160		3315.79
494	47.5 ksi residual - R=0.5	2m/DD16C	0.364	0.152	10	9596		9596	2621.07
495	47.5 ksi residual - R=0.5	2m/DD16C	0.361	0.155	10	9872		9872	2650
496	47.5 ksi residual - R=0.5	2m/DD16C	0.359	0.163	10	12289		12289	2772.75
497	47.5 ksi residual - R=0.5	2m/DD16C	0.347	0.151	10	8981		8981	2479
498	47.5 ksi residual - R=0.5	2m/DD16C	0.358	0.160	10	8899		8899	2708
499	47.5 ksi residual - R=0.5	2m/DD16C	0.336	0.145	10	32810		32810	2304
500	47.5 ksi residual - R=0.5	2m/DD16C	0.343	0.149	10	20000		20000	2417
500r	47.5 ksi residual - R=0.5	2m/DD16C	0.343	0.149	1 cycle				4149
501	47.5 ksi residual - R=0.5	2m/DD16C	0.350	0.156	10	10000		10000	2583
501r	47.5 ksi residual - R=0.5	2m/DD16C	0.350	0.156	1 cycle				3969
502	47.5 ksi residual - R=0.5	2m/DD16C	0.349	0.151	10	12442		12442	2492
503	47.5 ksi residual - R=0.5	2m/DD16C	0.351	0.151	10	5336		5336	2517
504	47.5 ksi residual - R=0.5	2m/DD16C	0.353	0.149	10	10000		10000	2503
504r	47.5 ksi residual - R=0.5	2m/DD16C	0.353	0.149	1 cycle				4464
505	47.5 ksi residual - R=0.5	2m/DD16C	0.350	0.155	10	9800		9800	2572
506	47.5 ksi residual - R=0.5	2m/DD16C	0.360	0.153	10	11920		11920	2608
507	47.5 ksi residual - R=0.5	2m/DD16C	0.362	0.166	10	3769		3769	2843
508	47.5 ksi residual - R=0.5	2m/DD16C	0.362	0.155	10	8254		8254	2656
509	47.5 ksi residual - R=0.5	2m/DD16C	0.349	0.154	10	20000		20000	2543
509r	47.5 ksi residual - R=0.5	2m/DD16C	0.349	0.154	1 cycle				3659
510	47.5 ksi residual - R=0.5	2m/DD16C	0.364	0.156	10	10000		10000	2685
510r	47.5 ksi residual - R=0.5	2m/DD16C	0.364	0.156	1 cycle				4100
511	47.5 ksi residual - R=0.5	2m/DD16C	0.356	0.152	10	18330		18330	2559
512	47.5 ksi residual - R=0.5	2m/DD16C	0.360	0.156	10	8643		8643	2659
513	47.5 ksi residual - R=0.5	2m/DD16C	0.347	0.154	10	10000		10000	2529
513r	47.5 ksi residual - R=0.5	2m/DD16C	0.347	0.154	1 cycle				4570
514	47.5 ksi residual - R=0.5	2m/DD16C	0.346	0.155	10	11418		11418	2537
515	47.5 ksi residual - R=0.5	2m/DD16C	0.349	0.153	10	10814		10814	2536
516	47.5 ksi residual - R=0.5	2m/DD16C	0.377	0.154	10	7732		7732	2755
517	47.5 ksi residual - R=0.5	2m/DD16C	0.364	0.159	10	13968		13968	2741
518	47.5 ksi residual - R=0.5	2m/DD16C	0.355	0.154	10	8684		8684	2588
519	47.5 ksi residual - R=0.5	2m/DD16C	0.364	0.168	10	10000		10000	2892
519r	47.5 ksi residual - R=0.5	2m/DD16C	0.364	0.168	1 cycle				4793
520	47.5 ksi residual - R=0.5	2m/DD16C	0.363	0.153	10	7107		7107	2629
521	47.5 ksi residual - R=0.5	2m/DD16C	0.354	0.151	10	7189		7189	2530
522	47.5 ksi residual - R=0.5	2m/DD16C	0.359	0.150	10	10000		10000	2549
522r	47.5 ksi residual - R=0.5	2m/DD16C	0.359	0.150	1 cycle				3149
523	47.5 ksi residual - R=0.5	2m/DD16C	0.362	0.153	10	13784		13784	2619
524	47.5/30 ksi 1/100 block	2m/DD16C	0.361	0.151	10	227	22674	22901	2596.63
525	47.5/30 ksi 10/1000 block	2m/DD16C	0.354	0.153	10	340	34008	34348	2554.9
526	47.5/30 ksi 10/1000 rand5	2m/DD16C	0.355	0.152	10	470	46982	47452	2540.8
527	47.5/30 ksi 1/100 block	2m/DD16C	0.368	0.147	10	393	39300	39693	2545
528	47.5/30 ksi 10/1000 block	2m/DD16C	0.352	0.151	10	192	19209	19401	2506
529	47.5/30 ksi 10/1000 rand5	2m/DD16C	0.350	0.154	10	119	11851	11970	2537
530	47.5/30 ksi 1/100 block	2m/DD16C	0.368	0.155	10	233	23300	23533	2691
531	47.5/30 ksi 10/1000 block	2m/DD16C	0.353	0.153	10	1150	115005	116155	2545
532	47.5/30 ksi 10/1000 rand5	2m/DD16C	0.349	0.155	10	131	13134	13265	2544
533	47.5/30 ksi 1/100 block	2m/DD16C	0.361	0.154	10	550	55019	55569	2619
534	47.5/30 ksi 10/1000 block	2m/DD16C	0.348	0.150	10	240	24008	24248	2460.48
535	47.5/30 ksi 10/1000 rand5	2m/DD16C	0.368	0.153	10	105	10548	10653	2652
536	47.5/30 ksi 1/100 block	2m/DD16C	0.361	0.156	10	261	26153	26414	2657
537	47.5/30 ksi 10/1000 block	2m/DD16C	0.349	0.150	10	220	22001	22221	2476
538	47.5/30 ksi 10/1000 rand5	2m/DD16C	0.348	0.152	10	141	14087	14228	2499



Test #	Comment	Coupon Style/Mat'l	Width in	Thick in	Freq Hz	# High Cycles	# Low Cycles	Total Cycles	Hi Block Max
539	47.5/30 ksi 1/100 block	2m/DD16C	0.342	0.151	10	469	46900	47369	2436
540	47.5/30 ksi 10/1000 block	2m/DD16C	0.367	0.155	10	58	5834	5892	2693
541	47.5/30 ksi 10/1000 rand5	2m/DD16C	0.357	0.154	10	122	12209	12331	2596
542	47.5/30 ksi 1/100 block	2m/DD16C	0.359	0.155	10	239	23900	24139	2622
543	47.5/30 ksi 10/1000 block	2m/DD16C	0.362	0.169	10	260	25951	26211	2882
544	47.5/30 ksi 10/1000 rand5	2m/DD16C	0.372	0.153	10	53	5342	5395	2685
545	47.5/30 ksi 1/100 block	2m/DD16C	0.357	0.150	10	241	24060	24301	2525
546	47.5/30 ksi 10/1000 block	2m/DD16C	0.350	0.162	10	179	17908	18087	2672
547	47.5/30 ksi 10/1000 rand5	2m/DD16C	0.356	0.153	10	463	46342	46805	2565
548	47.5/30 ksi 1/100 block	2m/DD16C	0.355	0.151	10	198	19800	19998	2527
549	47.5/30 ksi 10/1000 block	2m/DD16C	0.342	0.149	10	310	31007	31317	2406
550	47.5/30 ksi 10/1000 rand5	2m/DD16C	0.361	0.161	10	70	6982	7052	2740
551	47.5/30 ksi 1/100 block	2m/DD16C	0.358	0.154	10	138	13767	13905	2599
552	47.5/30 ksi 10/1000 block	2m/DD16C	0.355	0.152	10	254	25393	25647	2543
553	47.5/30 ksi 10/1000 rand5	2m/DD16C	0.356	0.147	10	206	20576	20782	2467
554	47.5 ksi, R=0.1	2m/DD16C	0.352	0.156	10	763		763	2594.81
* 555	30 ksi, R=0.1	2m/DD16C	0.360	0.153					
556	47.5 ksi, R=0.5	2m/DD16C	0.344	0.156	10	15905		15905	2539.77
557	47.5 ksi, R=0.5	2m/DD16C	0.329	0.149	10	38319		38319	2316.68
558	47.5 ksi, R=0.5	2m/DD16C	0.324	0.148	10	8357		8357	2275.79
559	47.5 ksi, R=0.5	2m/DD16C	0.339	0.159	10	31685		31685	2551.46
560	47.5 ksi, R=0.5	2m/DD16C	0.332	0.156	10	21025		21025	2448.47
561	47.5 ksi, R=0.5	2m/DD16C	0.338	0.154	10	48516		48516	2460.01
562	47.5 ksi, R=0.5	2m/DD16C	0.337	0.154	10	24391		24391	2455.88
563	35 ksi, R=0.5	2m/DD16C	0.326	0.152	10	1051280		1051280	1731.45
564	35 ksi, R=0.5	2m/DD16C	0.348	0.166	10	1988538		1988538	2015.7
565	35 ksi, R=0.5	2m/DD16C	0.318	0.153	10	1119777		1119777	1698.24
566	35 ksi, R=0.5	2m/DD16C	0.33	0.153	10	280171		280171	1761.4
* 567	35 ksi, R=0.5	2m/DD16C	0.316	0.151					
568	35 ksi, R=0.5	2m/DD16C	0.324	0.155	10	1749635		1749635	1749.63
569	35 ksi, R=0.5	2m/DD16C	0.323	0.154	10	763276		763276	1737.04
570	35 ksi, R=0.5	2m/DD16C	0.312	0.154	10	2470072		2470072	1677.74
571	60 ksi, R=0.5	2m/DD16C	0.328	0.164	10	1652		1652	3211.11
572	60 ksi, R=0.5	2m/DD16C	0.316	0.152	10	2513		2513	2864.1
573	60 ksi, R=0.5	2m/DD16C	0.333	0.153	10	2519		2519	3037.96
* 574	60 ksi, R=0.5	2m/DD16C	0.32	0.151					
* 575	60 ksi, R=0.5	2m/DD16C	0.336	0.163					
576	60 ksi, R=0.5	2m/DD16C	0.322	0.153	10	2755		2755	2940.94
577	60 ksi, R=0.1	2m/DD16C	0.34	0.152	10	310		310	3072.45
578	60 ksi, R=0.1	2m/DD16C	0.328	0.154	10	274		274	3005.79
579	60 ksi, R=0.1	2m/DD16C	0.34	0.155	10	283		283	3132.99
580	60 ksi, R=0.1	2m/DD16C	0.342	0.155	10	334		334	3153.61
581	47.5 ksi, R=0.1	2m/DD16C	0.329	0.157	10	4375		4375	2430.48
582	47.5 ksi, R=0.1	2m/DD16C	0.337	0.152	10	4190		4190	2414.31
583	47.5 ksi, R=0.1	2m/DD16C	0.324	0.154	10	2620		2620	2349.53
584	47.5 ksi, R=0.1	2m/DD16C	0.323	0.156	10	1306		1306	2375.71
585	35 ksi, R=0.1	2m/DD16C	0.333	0.154	10	186268		186268	1781.97
586	35 ksi, R=0.1	2m/DD16C	0.332	0.152	10	89527		89527	1755.48
587	35 ksi, R=0.1	2m/DD16C	0.335	0.154	10	35109		35109	1796.3
588	35 ksi, R=0.1	2m/DD16C	0.336	0.153	10	187293		187293	1787
589	30 ksi, R=0.1	2m/DD16C	0.33	0.165	10	697446		697446	1624.3
590	30 ksi, R=0.1	2m/DD16C	0.329	0.15	10	436185		436185	1474.89
591	30 ksi, R=0.1	2m/DD16C	0.327	0.151	10	732874		732874	1475.84
592	30 ksi, R=0.1	2m/DD16C	0.339	0.157	10	366748		366748	1586.97
593	47.5/30 ksi, R=0.1, load5	2m/DD16D	0.315	0.148	10	1020	102006	103026	2196
594	47.5/30 ksi, R=0.1, wvrnr	2m/DD16D	0.32	0.157	01/10	379	37000	37379	2361.9
595	47.5/30 ksi, R=0.1, load5	2m/DD16D	0.325	0.155	10	410	41006	41416	2368
596	47.5/30 ksi, R=0.1, wvrnr	2m/DD16D	0.338	0.153	10	310	30570	30880	2453.09
597	47.5/30 ksi, R=0.1, load5	2m/DD16D	0.377	0.148	10	1850	185004	186854	2627
598	47.5/30 ksi, R=0.1, wvrnr	2m/DD16D	0.319	0.154	01/10	324	32000	32324	2317.24
599	47.5/30 ksi, R=0.1, load5	2m/DD16D	0.34	0.156	10	2120	212007	214127	2493
600	47.5/30 ksi, R=0.1, wvrnr	2m/DD16D	0.333	0.152	01/10	853	85000	85853	2372.8
601	47.5/30 ksi, R=0.1, load5	2m/DD16D	0.312	0.147	10	490	49001	49491	2157

Test #	Comment	Coupon Style/Mat'l	Width in	Thick in	Freq Hz	# High Cycles	# Low Cycles	Total Cycles	Hi Block Max
602	47.5/30 ksi, R=0.1, wvrnr	2m/DD16D	0.396	0.153	10	310	30952	31262	2858.07
603	47.5/30 ksi, R=0.1, load5	2m/DD16D	0.317	0.148	10	500	50008	50508	2222
604	47.5/30 ksi, R=0.1, wvrnr	2m/DD16D	0.379	0.154	10	390	38919	39309	2747.33
605	60 ksi, R=0.1, wvrnr	2m/DD16D	0.387	0.145	10	783		783	3331.67
606	60 ksi, R=0.1, load10	2m/DD16D	0.394	0.146	10	286		286	3424.79
607	47.5 ksi, R=0.1	2m/DD16D	0.418	0.153	10	1690		1690	3019.63
608	47.5 ksi, R=0.1, load10	2m/DD16D	0.410	0.156	10	1794		1794	3016.14
609	35 ksi, R=0.1	2m/DD16D	0.391	0.152	10	58826		58826	2071.51
610	35 ksi, R=0.1, load10	2m/DD16D	0.396	0.150	10	43618		43618	2064
611	30 ksi, R=0.1	2m/DD16D	0.376	0.147	10	318890		318890	1645.87
612	30 ksi, R=0.1, load10	2m/DD16D	0.435	0.145	10	418886		418886	1875
* 613	47.5/30 ksi, R=0.1, wvrnr	2m/DD16D	0.402	0.149					
* 614	47.5/30 ksi, R=0.1, load5	2m/DD16D	0.398	0.143					
* 615	1 cycle	2m/DD16D	0.396	0.156					
616	47.5 ksi, R=0.1, wvrnr	2m/DD16D	0.392	0.151	10	1081		1081	2782.88
617	47.5 ksi, R=0.1, load10	2m/DD16D	0.386	0.154	10	2433		2433	2802
618	47.5 ksi, R=0.1, wvrnr, ??	2m/DD16D	0.416	0.156	10	769		769	3051.93
619	47.5 ksi, R=0.1, load10	2m/DD16D	0.404	0.146	10	2329		2329	2770.93
620	60 ksi, R=0.1, wvrnr	2m/DD16D	0.397	0.152	10	234		234	3573.93
621	60 ksi, R=0.1, load10	2m/DD16D	0.401	0.155	10	180		180	3697.7
622	60 ksi, R=0.1, wvrnr	2m/DD16D	0.402	0.155	10	290		290	3690.38
623	60 ksi, R=0.1, load10	2m/DD16D	0.400	0.147	10	311		311	3495
624	60 ksi, R=0.1, wvrnr	2m/DD16D	0.414	0.152	10	161		161	3755.65
625	30 ksi, R=0.1, load10	2m/DD16D	0.405	0.155	10	41493		41493	1870
626	30 ksi, R=0.1, wvrnr	2m/DD16D	0.399	0.154	10	496355		496355	1830.83
627	30 ksi, R=0.1, load10	2m/DD16D	0.400	0.147	10	598609		598609	1744
628	30 ksi, R=0.1, wvrnr	2m/DD16D	0.400	0.148	10	129134		129134	1756.4
629	30 ksi, R=0.1, load10	2m/DD16D	0.396	0.153	10	78888		78888	1806.65
630	35 ksi, R=0.1, wvrnr	2m/DD16D	0.428	0.150	10	57742		57742	2216.93
* 631	1 cycle, do not use	2m/DD16D	0.394	0.150					
632	35 ksi, R=0.1, load10	2m/DD16D	0.421	0.155	10	37576			2262
633	35 ksi, R=0.1, wvrnr	2m/DD16D	0.390	0.154	10	43491			2080.33
634	35 ksi, R=0.1, load10	2m/DD16D	0.394	0.149	10	163745			2031
635	1 cycle	2m/DD16D	0.392	0.155	1 cycle	1		1	5901
636	35 ksi, R=0.5, wvrnr	2m/DD16D	0.39	0.151	10	464516			2074
* 637	35 ksi, R=0.5, load11	2m/DD16D	0.401	0.153					
638	35 ksi, R=0.5, wvrnr	2m/DD16D	0.382	0.148	10	460884			1972.8
* 639	35 ksi, R=0.5, load11	2m/DD16D	0.399	0.149					
640	35 ksi, R=0.5, wvrnr	2m/DD16D	0.402	0.146	10	98521			2040.64
641	47.5 ksi, R=0.5, load11	2m/DD16D	0.397	0.148	10	7421			2768
642	47.5 ksi, R=0.5, wvrnr	2m/DD16D	0.388	0.152	10	5801			2783.96
643	47.5 ksi, R=0.5, load11	2m/DD16D	0.406	0.146	10	6548			2977
644	47.5 ksi, R=0.5, wvrnr	2m/DD16D	0.434	0.154	10	24381			3158.01
645	47.5 ksi, R=0.5, load11	2m/DD16D	0.386	0.153	10	19568			2775
646	1 cycle	2m/DD16D	0.414	0.145	1 cycle	1		1	4953
647	60 ksi, R=0.5, load11	2m/DD16D	0.399	0.153	10	2609			3615
648	60 ksi, R=0.5, wvrnr	2m/DD16D	0.375	0.154	10	438			3428
649	60 ksi, R=0.5, load11	2m/DD16D	0.394	0.154	10	2507			3607
650	60 ksi, R=0.5, wvrnr	2m/DD16D	0.405	0.148	10	1169			3558.67
651	60 ksi, R=0.5, load11	2m/DD16D	0.418	0.156	10	1475			3858
652	1 cycle	2m/DD16D	0.308	0.155	1 cycle	1		1	4285
653	1 cycle	2m/DD16D	0.404	0.142	1 cycle	1		1	5624
654	60 ksi max, Wisperx	2m/DD16D	0.407	0.151	10	14090		14090	3656
655	1 cycle	2m/DD16D	0.39	0.151	1 cycle	1		1	5879
656	60 ksi max, Wisperx	2m/DD16D	0.402	0.145	10	13404		13404	2981
657	60/35 ksi, R=0.5, load12	2m/DD16D	0.398	0.151	10	490	4411	4901	3568
658	60/35 ksi, R=0.5, load12	2m/DD16D	0.383	0.153	10	1130	10178	11308	3462
659	60/35 ksi, R=0.5, load13	2m/DD16D	0.387	0.154	10	310	30695	31005	3520
660	60/35 ksi, R=0.5, load13	2m/DD16D	0.432	0.148	10	440	43565	44005	3788
661	47.5 ksi max, Wisperx	2m/DD16D	0.407	0.154	10	160725		160725	2965
662	47.5/35 ksi, R=0.5, load14	2m/DD16D	0.394	0.147	10	2800	277206	280006	2719
663	47.5/35 ksi, R=0.5, load14	2m/DD16D	0.386	0.148	10	3360	332645	336005	2699
* 664	47.5/35 ksi, R=0.5, load15	2m/DD16D	0.403	0.149					

Test #	Comment	Coupon Style/Mat'l	Width in	Thick in	Freq Hz	# High Cycles	# Low Cycles	Total Cycles	Hi Block Max
665	47.5/35 ksi, R=0.5, load15	2m/DD16D	0.397	0.153	10	3230	29073	32303	2858
666	1 cycle	2m/DD16D	0.39	0.151	1 cycle	1		1	5726
667	60/35 ksi, R=0.5, load16	2m/DD16D	0.398	0.154	10	120	119888	120008	3627
668	60/35 ksi, R=0.5, load16	2m/DD16D	0.418	0.156	10	41	41388	41429	3885
669	60/35 ksi, R=0.5, load18	2m/DD16D	0.41	0.157	10	70	6934	7004	3807
670	60/35 ksi, R=0.5, load16	2m/DD16D	0.395	0.147	10	70	69935	70005	3429
671	1 cycle	2m/DD16D	0.377	0.15	1 cycle	1		1	5633
672	47.5 ksi, R=0.5, load11	2m/DD16D	0.393	0.151	10	1400		1400	2799
673	35 ksi, R=0.5, load11	2m/DD16D	0.387	0.147	10	100193		100193	1977
674	47.5/35 ksi, R=0.5, load17	2m/DD16D	0.39	0.155	10	350	349656	350006	2837
675	47.5/35 ksi, R=0.5, load17	2m/DD16D	0.389	0.149	10	160	160773	160933	2724
676	60 ksi max, Wisxperx	2m/DD16D	0.4	0.152	10	12832		12832	3621.27
677	60 ksi max, WisxR05	2m/DD16D	0.427	0.153	10	1874		1874	3861.51
678	60 ksi max, WisxR05	2m/DD16D	0.403	0.153	10	2812		2812	3659.54
679	60 ksi max, WisxR05	2m/DD16D	0.408	0.153	10	6270		6270	3697
680	60 ksi max, WisxR05	2m/DD16D	0.437	0.155	10	2768		2768	4006
* 681	60 ksi max, WisxR05	2m/DD16D	0.402	0.156					
682	60 ksi max, WisxR05	2m/DD16D	0.391	0.155	10	2680		2680	3584
683	60 ksi max, WisxR05	2m/DD16D	0.403	0.154	10	2102		2102	3671
684	60 ksi max, WisxR05	2m/DD16D	0.389	0.153	10	1397		1397	3519
685	60 ksi max, WisxR05	2m/DD16D	0.412	0.143	10	956		956	3401
686	60 ksi max, WisxR05	2m/DD16D	0.401	0.151	10	3915		3915	3596
687	47.5 ksi max, WisxR05	2m/DD16D	0.397	0.151	10	40997		40997	2816
688	47.5 ksi max, WisxR05	2m/DD16D	0.397	0.147	10	51690		51690	2732.02
689	47.5 ksi max, WisxR05	2m/DD16D	0.378	0.154	10	28166		28166	2733
690	47.5 ksi max, WisxR05	2m/DD16D	0.407	0.142	10	34678		34678	2717
691	47.5 ksi max, WisxR05	2m/DD16D	0.420	0.144	10	42728		42728	2831
692	47.5 ksi max, WisxR05	2m/DD16D	0.394	0.154	10	42077		42077	2842
693	47.5 ksi max, WisxR05	2m/DD16D	0.392	0.153	10	204617		204617	2825
694	47.5 ksi max, WisxR05	2m/DD16D	0.407	0.147	10	64030		64030	2819
695	47.5 ksi max, WisxR05	2m/DD16D	0.405	0.157	10	61941		61941	2989.32
696	47.5 ksi max, WisxR05	2m/DD16D	0.396	0.155	10	24102		24102	2888
697	35 ksi max, WisxR05	2m/DD16D	0.392	0.153	10	1268170		1268170	2072
698	35 ksi max, WisxR05	2m/DD16D	0.390	0.152	10	851414		851414	2049
* 699	35 ksi max, WisxR05	2m/DD16D	0.379	0.153					
700	35 ksi max, WisxR05	2m/DD16D	0.419	0.154	10	5040003		5040003	2242
701	35 ksi max, WisxR05	2m/DD16D	0.396	0.154	10	3466288		3466288	2119
702	35 ksi max, WisxR05	2m/DD16D	0.396	0.149	10	1620900		1620900	2051
703	35 ksi max, WisxR05	2m/DD16D	0.406	0.142	10	1002695		1002695	1992
704	35 ksi max, WisxR05	2m/DD16D	0.394	0.147	10	993446		993446	2005
705	35 ksi max, WisxR05	2m/DD16D	0.429	0.155	10	1130037		1130037	2306
706	35 ksi max, WisxR05	2m/DD16D	0.421	0.155	10	2387020		2387020	2264
707	30 ksi max, WisxR01	2m/DD16D	0.400	0.146	10	2502591		2502591	1728
708	30 ksi max, WisxR01	2m/DD16D	0.398	0.153	10	1523103		1523103	1790
709	35 ksi max, WisxR01	2m/DD16D	0.399	0.154	10	392963		392963	2110
710	35 ksi max, WisxR01	2m/DD16D	0.407	0.156	10	77859		77859	2186
711	47.5 ksi max, WisxR01	2m/DD16D	0.385	0.153	10	3963		3963	2741
712	47.5 ksi max, WisxR01	2m/DD16D	0.411	0.156	10	4457		4457	2986
713	60 ksi max, WisxR01	2m/DD16D	0.393	0.150	10	893		893	3356
714	60 ksi max, WisxR01	2m/DD16D	0.411	0.157	10	504		504	3640
715	30 ksi max, WisxR01	2m/DD16D	0.440	0.155	10	1231745		1231745	2020
716	35 ksi max, WisxR01	2m/DD16D	0.395	0.155	10	201697		201697	2103
717	60 ksi max, Load11	2m/DD16D	0.407	0.152	10	2886		2886	3677
718	60 ksi max, Load11	2m/DD16D	0.394	0.148	10	1412		1412	3453
719	47.5 ksi max, Load11	2m/DD16D	0.373	0.156	10	21037		21037	2736
720	47.5 ksi, Load11, R=0.5	2m/DD16D	0.390	0.149	10	120101		120101	2728
721	35 ksi max, Load11	2m/DD16D	0.400	0.150	10	272818		272818	2077
722	35 ksi max, Load11	2m/DD16D	0.408	0.150	10	545546		545546	2121
723	60 ksi max, WisxR01	2m/DD16D	0.398	0.146	10	1227		1227	3398
724	47.5 ksi max, WisxR01	2m/DD16D	0.410	0.156	10	4330		4330	3000
725	35 ksi max, WisxR01	2m/DD16D	0.387	0.145	10	128215		128215	1937
726	47.5 ksi max, WisxR01	2m/DD16D	0.423	0.153	10	3973		3973	3023.5
726a	1 cycle	2m/DD16D	0.404	0.152	1 cycle	1		1	5765

Test #	Comment	Coupon Style/Mat'l	Width in	Thick in	Freq Hz	# High Cycles	# Low Cycles	Total Cycles	Hi Block Max
727	35 ksi max, WisxR01	2m/DD16D	0.395	0.154	10	491135		491135	2089
728	35 ksi max, WisxR01	2m/DD16D	0.396	0.147	10	116302		116302	2001
729	35 ksi max, WisxR01	2m/DD16D	0.390	0.150	10	153229		153229	2013
730	35 ksi max, WisxR01	2m/DD16D	0.407	0.155	10	165568		165568	2170
* 731	30 ksi max, WisxR01	2m/DD16D	0.411	0.143					
732	30 ksi max, WisxR01	2m/DD16D	0.406	0.147	10	609578		609578	1758
733	30 ksi max, WisxR01	2m/DD16D	0.411	0.141	10	202727		202727	1707
734	30 ksi max, WisxR01	2m/DD16D	0.391	0.151	10	2231997		2231997	1744
735	47.5 ksi max, WisxR01	2m/DD16D	0.414	0.153	10	1977		1977	2960
736	47.5 ksi max, WisxR01	2m/DD16D	0.389	0.148	10	11721		11721	2684
737	47.5 ksi max, WisxR01	2m/DD16D	0.384	0.148	10	6742		6742	2655
738	47.5 ksi max, WisxR01	2m/DD16D	0.387	0.148	10	14445		14445	2673
739	1 cycle	2m/DD16D	0.404	0.152	1 cycle	1		1	5734
740	60 ksi max, WisxR01	2m/DD16D	0.398	0.153	10	620		620	3485
741	60 ksi max, WisxR01	2m/DD16D	0.384	0.149	10	1120		1120	3282
742	60 ksi max, WisxR01	2m/DD16D	0.421	0.154	10	818		818	3706
743	60 ksi max, WisxR01	2m/DD16D	0.415	0.154	10	624		624	3661
744	60 ksi max, Load10	2m/DD16D	0.390	0.150	10	642		642	3339
745	47.5 ksi max, Load10	2m/DD16D	0.410	0.153	10	1290		1290	2936
746	35 ksi max, Load10	2m/DD16D	0.397	0.147	10	31733		31733	2012
747	30 ksi max, Load10	2m/DD16D	0.382	0.146	10	544532		544532	1649
748	60 ksi max, Wisxmix	2m/DD16D	0.398	0.153	10	2211		2211	3597
749	60 ksi max, Wisxmix	2m/DD16D	0.388	0.150	10	3313		3313	3437
750	60 ksi max, Wisxmix	2m/DD16D	0.409	0.148	10	1744		1744	3576
751	60 ksi max, Wisxmix	2m/DD16D	0.389	0.152	10	2260		2260	3497
752	60 ksi max, Wisxmix	2m/DD16D	0.392	0.147	10	2058		2058	3405
753	60 ksi max, Wisxmix	2m/DD16D	0.402	0.154	10	5679		5679	3657
754	60 ksi max, Wisxmix	2m/DD16D	0.393	0.148	10	3634		3634	3440
755	60 ksi max, Wisxmix	2m/DD16D	0.386	0.153	10	1705		1705	3488
756	1 cycle	2m/DD16D	0.398	0.155	1 cycle	1		1	5940
757	47.5 ksi max, Wisxmix	2m/DD16D	0.429	0.152	10	8425		8425	3057
758	47.5 ksi max, Wisxmix	2m/DD16D	0.393	0.146	10	17202		17202	2687
759	47.5 ksi max, Wisxmix	2m/DD16D	0.417	0.153	10	17170		17170	2991
760	47.5 ksi max, Wisxmix	2m/DD16D	0.389	0.150	10	49795		49795	2732
761	47.5 ksi max, Wisxmix	2m/DD16D	0.397	0.155	10	15763		15763	2878
762	47.5 ksi max, Wisxmix	2m/DD16D	0.404	0.154	10	29281		29281	2908
763	47.5 ksi max, Wisxmix	2m/DD16D	0.432	0.152	10	9075		9075	3075
764	47.5 ksi max, Wisxmix	2m/DD16D	0.415	0.153	10	45756		45756	2974
765	1 cycle	2m/DD16D	0.416	0.156	1 cycle	1		1	5849
766	35 ksi max, Wisxmix	2m/DD16D	0.407	0.148	10	259709		259709	2071
767	35 ksi max, Wisxmix	2m/DD16D	0.394	0.156	10	625695		625695	2111
768	35 ksi max, Wisxmix	2m/DD16D	0.389	0.151	10	157203		157203	2022
769	35 ksi max, Wisxmix	2m/DD16D	0.396	0.144	10	373607		373607	1959
770	35 ksi max, Wisxmix	2m/DD16D	0.398	0.153	10	477747		477747	2091
771	35 ksi max, Wisxmix	2m/DD16D	0.405	0.155	10	165811		165811	2156
772	35 ksi max, Wisxmix	2m/DD16D	0.413	0.144	10	534391		534391	2040
773	35 ksi max, Wisxmix	2m/DD16D	0.382	0.152	10	763579		763579	1994
774	1 cycle	2m/DD16D	0.395	0.150	1 cycle	1		1	5893
775	30 ksi max, Wisxmix	2m/DD16D	0.406	0.155	10	2883840		2883840	1859
776	30 ksi max, Wisxmix	2m/DD16D	0.401	0.148	10	1085994		1085994	1740
777	30 ksi max, Wisxmix	2m/DD16D	0.386	0.154	10	1803131		1803131	1757
778	30 ksi max, Wisxmix	2m/DD16D	0.394	0.156	10	1005992		1005992	1816
779	30 ksi max, Wisxmix	2m/DD16D	0.408	0.158	10	496982		496982	1913
780	30 ksi max, Wisxmix	2m/DD16D	0.405	0.156	10	1701443		1701443	1864
781	30 ksi max, Wisxmix	2m/DD16D	0.407	0.157	10	2392836		2392836	1889.42
782	30 ksi max, Wisxmix	2m/DD16D	0.404	0.154	10	2079241		2079241	1834
783	1 cycle	2m/DD16D	0.399	0.151	1 cycle	1		1	6086
784	60 ksi max, Load10	2m/DD16D	0.395	0.148	10	343		343	3445
785	60 ksi max, Load11	2m/DD16D	0.413	0.156	10	400		400	3809
786	60 ksi max, WisxR01	2m/DD16D	0.388	0.150	10	1713		1713	3419
787	60 ksi max, WisxR05	2m/DD16D	0.427	0.144	10	1349		1349	3645
788	47.5 ksi max, Load10	2m/DD16D	0.375	0.152	10	815		815	2677
789	47.5 ksi max, Load11	2m/DD16D	0.405	0.155	10	11812		11812	2961

Test #	Comment	Coupon Style/Mat'l	Width in	Thick in	Freq Hz	# High Cycles	# Low Cycles	Total Cycles	Hi Block Max
790	47.5 ksi max, WisxR01	2m/DD16D	0.399	0.154	10	12294		12294	2860
791	47.5 ksi max, WisxR05	2m/DD16D	0.412	0.155	10	63945		63945	2992
792	35 ksi max, Load10	2m/DD16D	0.408	0.155	10	115525		115525	2178
793	35 ksi, R = 0.5	2m/DD16D	0.407	0.155	10	334060		334060	2185
794	35 ksi max, WisxR01	2m/DD16D	0.404	0.147	10	104636		104636	2032
795	35 ksi max, WisxR05	2m/DD16D	0.419	0.155	10	862547		862547	2238
796	-40 ksi, R=10	c/DD16D	0.654	0.154	10	11608		11608	-4040.94
797	-40 ksi, R=10	c/DD16D	0.638	0.154	10	2463		2463	-3941.61
798	-40 ksi, R=10	c/DD16D	0.648	0.158	10	2727		2727	-4100.65
799	-40 ksi, R=10	c/DD16D	0.653	0.152	10	5904		5904	-4024
800	-40 ksi, R=10	c/DD16D	0.65	0.153	10	5123		5123	-3996.29
801	-35 ksi, R=10	c/DD16D	0.648	0.155	10	379064		379064	-3531.43
802	-35 ksi, R=10	c/DD16D	0.649	0.159	10	54873		54873	-3636
803	-35 ksi, R=10	c/DD16D	0.647	0.161	10	11145		11145	-3666
804	-35 ksi, R=10	c/DD16D	0.637	0.154	10	11738		11738	-3454
805	-35 ksi, R=10	c/DD16D	0.643	0.164	10	21240		21240	-3746
806	-40 ksi, R=10	c/DD16D	0.642	0.165	10	5010		5010	-3962.41
807	-30 ksi, R=10	c/DD16D	0.644	0.157	10	487946		487946	-3099
808	-30 ksi, R=10	c/DD16D	0.643	0.153	10	993821		993821	-3045.37
809	-30 ksi, R=10	c/DD16D	0.639	0.152	10	1859843		1859843	-2927
810	-30 ksi, R=10	c/DD16D	0.653	0.152	10	1747111		1747111	-2991
811	-30 ksi, R=10	c/DD16D	0.636	0.153	10	1464645		1464645	-2949
812	1 cycle	c/DD16D	0.648	0.155	1 cycle	1		1	-5815
813	-40 ksi, R=10	c/DD16D	0.645	0.158	10	2469		2469	-4077
814	-40 ksi, R=10	c/DD16D	0.645	0.155	10	4353		4353	-4002
815	-40 ksi, R=10		0.633	0.167					
816	-40 ksi, R=10	c/DD16D	0.65	0.153	10	3850		3850	-3979
817	-40 ksi, R=10	c/DD16D	0.643	0.15	10	15393		15393	-3875
818	1 cycle	c/DD16D	0.641	0.153	1 cycle	1		1	-5626
819	-35 ksi, R=10	c/DD16D	0.642	0.16	10	14172		14172	-3616.61
820	-35 ksi, R=10	c/DD16D	0.646	0.155	10	36657		36657	-3526
821	-35 ksi, R=10	c/DD16D	0.632	0.167	10	6704		6704	-3692
822	-35 ksi, R=10	c/DD16D	0.629	0.156	10	9235		9235	-3448
823	-35 ksi, R=10	c/DD16D	0.642	0.154	10	67973		67973	-3484
824	1 cycle	c/DD16D	0.653	0.155	1 cycle	1		1	-5948
825	-30 ksi, R=10	c/DD16D	0.649	0.152	10	1505733		1505733	-2976
826	-30 ksi, R=10	c/DD16D	0.646	0.155	10	1980344		1980344	-3017
827	-30 ksi, R=10	c/DD16D	0.651	0.155	10	1037244		1037244	-3069
828	-30 ksi, R=10	c/DD16D	0.642	0.152	10	1508674		1508674	-3043
829	-30 ksi, R=10	c/DD16D	0.645	0.158	10	842537		842537	-3078.48
830	1 cycle	c/DD16D	0.653	0.16	1 cycle	1		1	-5560
831	1 cycle	c/DD16D	0.64	0.152	1 cycle	1		1	-5769
832	1 cycle	c/DD16D	0.646	0.157	1 cycle	1		1	-5395
833	1 cycle	c/DD16D	0.632	0.16	1 cycle	1		1	-6103
834	1 cycle	c/DD16D	0.632	0.158	1 cycle	1		1	-5485
835	1 cycle	c/DD16D	0.645	0.152	1 cycle	1		1	-6182
836	-40/-30 ksi,10/1000/R=10	c/DD16D	0.644	0.155	10	3030	303000	306030	-3994
837	-40/-30 ksi,10/1000/R=10	c/DD16D	0.637	0.154	10	2500	250000	252500	-3917
838	-40/-30 ksi,10/1000/R=10	c/DD16D	0.652	0.156	10	2200	220005	222205	-4039.7
839	-40/-30 ksi,10/1000/R=10	c/DD16D	0.644	0.152	10	4590	459006	463596	-3915.5
840	-40/-30 ksi,10/100/R=10	c/DD16D	0.644	0.152	10	2651	26508	29159	-3896.06
841	-40/-30 ksi,10/100/R=10	c/DD16D	0.639	0.152	10	8311	83107	91418	-3880.48
842	-40/-30 ksi,10/100/R=10	c/DD16D	0.644	0.151	10	9890	98903	108793	-3891
843	-40/-30 ksi,10/100/R=10	c/DD16D	0.639	0.152	10	10920	109206	120126	-3879
844	-40/-30 ksi,10/10/R=10	c/DD16D	0.653	0.155	10	1684	1684	3368	-4042.33
845	-40/-30 ksi,10/10/R=10	c/DD16D	0.64	0.152	10	11151	11151	22302	-3901
846	-40/-30 ksi,10/10/R=10	c/DD16D	0.65	0.157	10	4374	4374	8748	-4086
847	-40/-30 ksi,10,000/10/R=10	c/DD16D	0.651	0.156	10	290	290007	290297	-4066
848	-40/-30 ksi,10,000/10/R=10	c/DD16D	0.643	0.156	10	330	330003	330333	-4059
849	-40/-30 ksi,10,000/10/R=10	c/DD16D	0.644	0.151	10	2030	2030002	2032032	-3918
850	-40/-30 ksi,1000/10/R=10	c/DD16D	0.645	0.157	10	630	63000	63630	-4027
851	-40/-30 ksi,1000/10/R=10	c/DD16D	0.646	0.15	10	7430	743010	750440	-3937
852	-40/-30 ksi,1000/10/R=10	c/DD16D	0.647	0.151	10	4780	478000	482780	-3921

Test #	Comment	Coupon Style/Mat'l	Width in	Thick in	Freq Hz	# High Cycles	# Low Cycles	Total Cycles	Hi Block Max
853	-40/-30 ksi,1000/10/R=10	c/DD16D	0.639	0.164	10	400	40007	40407	-4184
854	-40/-30 ksi,1000/10/R=10	c/DD16D	0.641	0.155	10	680	68001	68681	-3985
855	-40 ksi, R=10	c/DD16D	0.649	0.151	10	4063		4063	-3942
856	-40 ksi, R=10	c/DD16D	0.639	0.152	10	4410		4410	-3909
857	-40 ksi, R=10	c/DD16D	0.654	0.158	10	1957		1957	-4121
858	-40 ksi, R=10	c/DD16D	0.643	0.152	10	8288		8288	-3910
859	-40 ksi, R=10	c/DD16D	0.644	0.153	10	10692		10692	-3949
860	-30 ksi, R=10	c/DD16D	0.647	0.152	10	2021912		2021912	-2965
861	-30 ksi, R=10	c/DD16D	0.646	0.152	10	943072		943072	-3077
862	-30 ksi, R=10	c/DD16D	0.641	0.161	10	205084		205084	-3110
863	-30 ksi, R=10	c/DD16D	0.648	0.154	10	1884110		1884110	-3131
864	-30 ksi, R=10	c/DD16D	0.653	0.154	10	235297		235297	-3024
865	1 cycle	c/DD16D	0.649	0.152	1 cycle	1		1	-6107
866	1 cycle	c/DD16D	0.641	0.151	1 cycle	1		1	-5727
867	1 cycle	c/DD16D	0.659	0.154	1 cycle	1		1	-5982
868	1 cycle	c/DD16D	0.642	0.155	1 cycle	1		1	-5574
869	1 cycle	c/DD16D	0.643	0.152	1 cycle	1		1	-5941
870	-40/-30 ksi,10/10/R=10	c/DD16D	0.642	0.16	10	1171	1170	2341	-4084
871	-40/-30 ksi,10/10/R=10	c/DD16D	0.638	0.16	10	2675	2674	5349	-4061
872	-40/-30 ksi,10/10/R=10	c/DD16D	0.652	0.157	10	1685	1684	3369	-4070
873	-40/-30 ksi,10/10/R=10	c/DD16D	0.651	0.156	10	3362	3362	6724	-4038
874	-40/-30 ksi,10/10/R=10	c/DD16D	0.645	0.151	10	9812	9812	19624	-3893
875	-40/-30 ksi,10,000/10/R=10	c/DD16D	0.644	0.151	10	990	990000	990990	-3899
876	-40/-30 ksi,10,000/10/R=10	c/DD16D	0.643	0.153	10	1398	1397653	1399051	-3934
877	-40/-30 ksi,10,000/10/R=10	c/DD16D	0.651	0.158	10	153	155364	155517	-4056
878	-40/-30 ksi,10,000/10/R=10	c/DD16D	0.65	0.153	10	728	727806	728534	-3948
879	-40/-30 ksi,10,000/10/R=10	c/DD16D	0.648	0.152	10	640	640008	640648	-3907
880	1 cycle	c/DD16D	0.632	0.161	1 cycle	1		1	-5469
881	1 cycle	c/DD16D	0.638	0.152	1 cycle	1		1	-5689
882	1 cycle	c/DD16D	0.64	0.151	1 cycle	1		1	-5980
883	1 cycle	c/DD16D	0.636	0.153	1 cycle	1		1	-5601
884	1 cycle	c/DD16D	0.639	0.154	1 cycle	1		1	-6011
885	1 cycle	c/DD16D	0.642	0.153	1 cycle	1		1	-5618
886	1 cycle	c/DD16D	0.654	0.151	1 cycle	1		1	-5880
887	1 cycle	c/DD16D	0.636	0.156	1 cycle	1		1	-5380
888	1 cycle	c/DD16D	0.635	0.153	1 cycle	1		1	-5848
889	1 cycle	c/DD16D	0.656	0.151	1 cycle	1		1	-5939
890	-40 ksi, R=2		0.654	0.15					
891	-40 ksi, R=2		0.642	0.152					
892	-40 ksi, R=2	c/DD16D	0.641	0.155	10	130733		130733	-3973
893	-40 ksi, R=2, Pwr Failure	c/DD16D	0.638	0.156	8	62258		62258	-3962
894	-40 ksi, R=2	c/DD16D	0.635	0.154	10	158396		158396	-3957.9
895	-40 ksi, R=2	c/DD16D	0.654	0.152	10	1442932		1442932	-3939
896	-40 ksi, R=2	c/DD16D	0.649	0.157	10	162400		162400	-4135
897	-40 ksi, R=2	c/DD16D	0.641	0.153	10	46304		46304	-3988
898	-40 ksi, R=2	c/DD16D	0.64	0.154	10	192595		192595	-3928
899	-40 ksi, R=2	c/DD16D	0.653	0.155	10	48990		48990	-4004
900	-35 ksi, R=2		0.649	0.155					
901	-35 ksi, R=2		0.652	0.154					
902	-35 ksi, R=2		0.654	0.152					
903	-35 ksi, R=2		0.639	0.152					
904	-35 ksi, R=2		0.646	0.153					
905	-35 ksi, R=2	c/DD16D	0.637	0.152	10	1190152		1190152	-3546
906	-35 ksi, R=2		0.638	0.152					
907	-35 ksi, R=2, coupon runout	c/DD16D	0.632	0.157	10	4950838		4950838	-3498
908	-35 ksi, R=2, load11.prn, run	c/DD16D	0.633	0.153	10	11829100		11829100	-3435
909	-35 ksi, R=2	c/DD16D	0.65	0.154	10	2738468		2738468	-3516
910	-47.5, R=2	c/DD16D	0.64	0.151	10	4297		4297	-4550
911	-47.5, R=2		0.632	0.155					
912	-47.5, R=2		0.631	0.154					
913	-47.5, R=2		0.639	0.152					
914	-47.5, R=2		0.654	0.153					
915	-47.5, R=2		0.647	0.158					

Test #	Comment	Coupon Style/Mat'l	Width in	Thick in	Freq Hz	# High Cycles	# Low Cycles	Total Cycles	Hi Block Max
916	-47.5, R=2		0.641	0.154					
917	-47.5, R=2		0.64	0.158					
918	-47.5, R=2		0.65	0.152					
919	-30 ksi, R=2, has not failed	c/DD16D	0.64	0.161	10	4013900		4013900	-3109
920	-47.5 ksi, R=10	c/DD16D	0.632	0.153	10	131		131	-4534
921	-47.5 ksi, R=10	c/DD16D	0.635	0.153	10	364		364	-4521
922	-47.5 ksi, R=10	c/DD16D	0.643	0.154	10	415		415	-4630
923	-47.5 ksi, R=10	c/DD16D	0.639	0.154	10	334		334	-4783
924	-47.5 ksi, R=10	c/DD16D	0.631	0.154	10	533		533	-4548
925	-47.5 ksi, R=10	c/DD16D	0.65	0.152	10	1019		1019	-4621
926	-47.5 ksi, R=10	c/DD16D	0.648	0.155	10	327		327	-4697
927	-47.5 ksi, R=10	c/DD16D	0.651	0.154	10	322		322	-4845
928	-47.5 ksi, R=10	c/DD16D	0.639	0.155	10	433		433	-4634
929	-47.5 ksi, R=10	c/DD16D	0.656	0.156	10	104		104	-4823
930	-47.5/-30 ksi,10/100/R=10	c/DD16D	0.651	0.155	8	324	3200	3524	-4715
931	-47.5/-30 ksi,10/100/R=10	c/DD16D	0.637	0.153	8	1080	10800	11880	-4567
932	-47.5/-30 ksi,10/100/R=10	c/DD16D	0.641	0.153	8	670	6700	7370	-4569
933	-47.5/-30 ksi,10/100/R=10	c/DD16D	0.638	0.161	8	212	2100	2312	-4781
934	-47.5/-30 ksi,10/100/R=10	c/DD16D	0.636	0.151	8	1815	18100	19915	-4502
935	-47.5/-30 ksi,10/100/R=10	c/DD16D	0.647	0.154	8	427	4200	4627	-4814
936	-47.5/-30 ksi,10/100/R=10	c/DD16D	0.639	0.155	8	462	4600	5062	-4632
937	-47.5/-30 ksi,10/100/R=10	c/DD16D	0.643	0.152	8	877	8700	9577	-4575
938	-47.5/-30 ksi,10/100/R=10	c/DD16D	0.636	0.158	8	90	900	990	-4692
939	-47.5/-30 ksi,10/100/R=10	c/DD16D	0.641	0.153	8	505	5000	5505	-4570
940	-47.5/-30 ksi,10/10/R=10	c/DD16D	0.641	0.155	8	546	540	1086	-4628
941	-47.5/-30 ksi,10/10/R=10	c/DD16D	0.643	0.152	8	2053	2050	4103	-4556
942	-47.5/-30 ksi,10/10/R=10	c/DD16D	0.641	0.151	8	1235	1230	2465	-4534
943	-47.5/-30 ksi,10/10/R=10	c/DD16D	0.64	0.153	8	452	450	902	-4563
944	-47.5/-30 ksi,10/10/R=10	c/DD16D	0.653	0.151	8	1402	1400	2802	-4707
945	-47.5/-30 ksi,10/10/R=10	c/DD16D	0.63	0.157	8	334	330	664	-4633
946	-47.5/-30 ksi,10/10/R=10	c/DD16D	0.634	0.157	8	525	520	1045	-4656
947	-47.5/-30 ksi,10/10/R=10	c/DD16D	0.639	0.156	8	239	230	469	-4664
948	-47.5/-30 ksi,10/10/R=10	c/DD16D	0.638	0.154	8	690	690	1380	-4624
* 949	failed test	c/DD16D	0.641	0.157					
950	-47.5/-30 ksi, 10/10K, R = 10	c/DD16D	0.636	0.162	8	21	20000	20021	-4707
951	-47.5/-30 ksi, 10/10K, R = 10	c/DD16D	0.65	0.154	8	139	130000	130139	-4750
952	-47.5/-30 ksi, 10/10K, R = 10	c/DD16D	0.647	0.151	8	688	680000	680688	-4622
953	-47.5/-30 ksi, 10/10K, R = 10	c/DD16D	0.649	0.158	8	272	270000	270272	-4732
* 954	-47.5/-30 ksi, 10/10K, R = 10	c/DD16D	0.632	0.162					
* 955	-47.5/-30 ksi, autotune error		0.634	0.163					
956	-47.5/-30 ksi,10/10,000/R=10	c/DD16D	0.643	0.155	8	73	70000	70073	-4636
957	-47.5/-30 ksi,10/10,000/R=10	c/DD16D	0.63	0.159	8	12	10000	10012	-4674
958	-47.5/-30 ksi,10/10,000/R=10	c/DD16D	0.65	0.158	8	31	30000	30031	-4795.9
959	-47.5/-30 ksi,10/10,000/R=10	c/DD16D	0.644	0.159	8	80	80004	80084	-4779
960	-47.5/-30 ksi,10/1000/R=10	c/DD16D	0.644	0.157	8	171	17000	17171	-4719
961	-47.5/-30 ksi,10/1000/R=10	c/DD16D	0.647	0.157	8	128	12000	12128	-4744
962	-47.5/-30 ksi,10/1000/R=10	c/DD16D	0.64	0.161	8	84	8000	8084	-4813
963	-47.5/-30 ksi,10/1000/R=10	c/DD16D	0.642	0.155	8	244	24000	24244	-4644
964	-47.5/-30 ksi,10/1000/R=10	c/DD16D	0.645	0.156	8	87	8000	8087	-4774
965	-47.5/-30 ksi,10/1000/R=10	c/DD16D	0.64	0.155	8	254	25000	25254	-4637
966	-47.5/-30 ksi,10/1000/R=10	c/DD16D	0.648	0.155	8	69	6000	6069	-4696
967	-47.5/-30 ksi,10/1000/R=10	c/DD16D	0.644	0.155	8	81	8000	8081	-4648
968	-47.5/-30 ksi,10/1000/R=10	c/DD16D	0.647	0.153	8	1220	122000	123220	-4609
969	-47.5/-30 ksi,10/1000/R=10	c/DD16D	0.645	0.152	8	591	590000	590591	-4656.9
970	Wispk	2m/DD16D	0.322	0.155	10	3844		3844	2914
971	Wispk	2m/DD16D	0.366	0.159	10	1276		1276	2875
972	Wispk	2m/DD16D	0.384	0.155	10	2325		2325	2960
973	Wispk	2m/DD16D	0.378	0.153	10	2448		2448	2889
974	Wispk	2m/DD16D	0.374	0.152	10	3130		3130	3352
975	Wispk	2m/DD16D	0.338	0.156	10	4044		4044	3081
976	Wispk	2m/DD16D	0.342	0.156	10	2806		2806	3115
977	Wispk	2m/DD16D	0.302	0.153	10	5722		5722	2716
978	Wispk	2m/DD16D	0.376	0.153	10	3233		3233	3387

Test #	Comment	Coupon Style/Mat'l	Width in	Thick in	Freq Hz	# High Cycles	# Low Cycles	Total Cycles	Hi Block Max
979	Wispk	2m/DD16D	0.414	0.152	10	3203		3203	3669
980	Wispk	2m/DD16D	0.338	0.153	10	167885		167885	2232.87
981	Wispk	2m/DD16D	0.377	0.152	10	155850		155850	2475
982	Wispk	2m/DD16D	0.376	0.152	10	195616		195616	2462
983	Wispk	2m/DD16D	0.384	0.159	10	86293		86293	2669
984	Wispk	2m/DD16D	0.346	0.153	10	298800		298800	2270
985	Wispk	2m/DD16D	0.339	0.157	10	169839		169839	2299
986	Wispk	2m/DD16D	0.379	0.155	10	68426		68426	2524
987	Wispk	2m/DD16D	0.346	0.156	10	231019		231019	2319
988	Wispk	2m/DD16D	0.39	0.152	10	144430		144430	2543
989	Wispk	2m/DD16D	0.375	0.152	10	80980		80980	2458
990	Wispk	2m/DD16D	0.407	0.156	10	195751		195751	2338
991	Wispk	2m/DD16D	0.38	0.157	10	598438		598438	2202
992	Wispk	2m/DD16D	0.332	0.153	10	876955		876955	1878
993	Wispk	2m/DD16D	0.339	0.151	10	1231928		1231928	1878
* 994	Wispk, bad test	2m/DD16D	0.383	0.151					
995	Wispk	2m/DD16D	0.391	0.154	10	312744		312744	2222
996	Wispk	2m/DD16D	0.373	0.155	10	432307		432307	2164
997	Wispk	2m/DD16D	0.35	0.152	10	912240		912240	1979
998	Wispk	2m/DD16D	0.374	0.157	10	680774		680774	2175
999	Wispk	2m/DD16D	0.381	0.158	10	248429		248429	2227
1000	Wispk	2m/DD16D	0.381	0.159	10	14371		14371	2945
1001	Wispk	2m/DD16D	0.379	0.153	10	26045		26045	2810
1002	Wispk	2m/DD16D	0.343	0.153	10	18334		18334	2593
1003	Wispk	2m/DD16D	0.379	0.157	10	24906		24906	2934
1004	Wispk	2m/DD16D	0.382	0.161	10	6048		6048	3026
1005	Wispk	2m/DD16D	0.342	0.155	10	13058		13058	2613
1006	Wispk	2m/DD16D	0.35	0.155	10	24196		24196	2698
1007	Wispk	2mDD16C	0.373	0.155	10	14130978		14130978	1550
1008	sample never tested & missing		0.379	0.16					
1009	WISPERX	2mDD16C	0.384	0.153					
1010	WISPERX	2mDD16C	0.373	0.158					
1011	WISPERX	2mDD16C	0.38	0.154					
1012	WISPERX	2mDD16C	0.375	0.152					
1013	WISPERX	2mDD16C	0.367	0.153					
1014	WISPERX	2mDD16C	0.379	0.155					
1015	WISPERX	2mDD16C	0.377	0.154					
1016	Wispk	2mDD16C	0.371	0.152	10	12289518		12289518	1513
1017	WISPERX	2mDD16D	0.364	0.152					
1018	WISPERX	2mDD16D	0.373	0.147					
1019	WISPERX	2mDD16D	0.37	0.147					
1020	WISPERX	2mDD16D	0.376	0.154					
1021	WISPERX	2mDD16D	0.368	0.155					
1022	WISPERX	2mDD16D	0.371	0.155					
1023	WISPERX	2mDD16D	0.368	0.152					
1024	WISPERX	2mDD16D	0.374	0.149					
1025	WISPERX	2mDD16D	0.368	0.149					
1026	WISPERX	2mDD16D	0.368	0.152					
* 1027	47.5 ksi, R = -1, buckling evl	2mDD16E	0.373	0.155					
* 1028	47.5 ksi, R = -1, buckling evl	2mDD16E	0.37	0.152					
* 1029	47.5 ksi, R = -1, tabs removed	2mDD16E	0.379	0.156					
* 1030	30 ksi, R = -1, tabs removed	2mDD16E	0.379	0.149					
* 1031	20 ksi, R = -1, tab removed,	2mDD16E	0.379	0.157					
1032	sample never tested & missing		0.379	0.149					
1033	25 ksi, R=-1	2mDD16E	0.376	0.152					
1034	25/15 ksi, 10/10, R=-1	2mDD16E	0.376	0.156					
1035	15 ksi, R=-1	2mDD16E	0.375	0.155					
1036	25/15 ksi, 10/10, R=-1	2mDD16E	0.375	0.152					
1037	25 ksi, R = -1	2mDD16E	0.365	0.152	5	11189		11189	1464
1038	25 ksi, R = -1	2mDD16E	0.369	0.151	5	5556		5556	1474
1039	20 ksi, R = -1	2mDD16E	0.375	0.154	5	93249		93249	1220
1040	20 ksi, R = -1	2mDD16E	0.367	0.154	5	74482		74482	1197
1041	15 ksi, R = -1	2mDD16E	0.367	0.161	5	1313993		1313993	950



Test #	Comment	Coupon Style/Mat'l	Width in	Thick in	Freq Hz	# High Cycles	# Low Cycles	Total Cycles	Hi Block Max
1042	15 ksi, R = -1	2mDD16E	0.368	0.158	5	902103		902103	929
1043	15 ksi, R = -1	2mDD16E	0.37	0.155	5	1814761		1814761	924
1044	25 ksi, R = -1	2mDD16E	0.371	0.155	5	4861		4861	1487
1045	20 ksi, R = -1	2mDD16E	0.364	0.156	5	62837		62837	1222
1046	15 ksi, R = -1	2mDD16E	0.368	0.154	5	785091		785091	914
1047	20 ksi, R = -1	2mDD16E	0.372	0.152	5	93636		93636	1199
1048	25 ksi, R = -1	2mDD16E	0.364	0.153	5	17397		17397	1258
1049	15 ksi, R = -1	2mDD16E	0.371	0.151	5	2108317		2108317	928
1050	25 ksi, R = -1	2mDD16E	0.365	0.151	5	6004		6004	1424
1051	20 ksi, R = -1	2mDD16E	0.367	0.159	5	57737		57737	1225
1052	25/15 ksi, 10/100, R=-1		0.371	0.153					
1053	25 ksi, R=-1		0.372	0.156					
1054	25/15 ksi, 10/100, R=-1		0.37	0.156					
1055	15 ksi, R=-1		0.373	0.157					
1056	shaped, not tabbed		0.371	0.152					
1057	25/15 ksi, 10/1000, R=-1		0.369	0.152					
1058	25/15 ksi, 10/10, R=-1		0.368	0.152					
1059	25/15 ksi, 10/100, R=-1		0.367	0.153					
1060	15 ksi, R=-1		0.378	0.154					
1061	shaped, not tabbed		0.369	0.15					
1062	shaped, not tabbed		0.366	0.152					
1063	shaped, not tabbed		0.368	0.153					
1064	shaped, not tabbed		0.371	0.157					
1065	shaped, not tabbed		0.369	0.151					
1066	shaped, not tabbed		0.372	0.15					
1067	shaped, not tabbed		0.375	0.154					
1068	shaped, not tabbed		0.373	0.156					
1069	shaped, not tabbed		0.371	0.15					
1070	shaped, not tabbed		0.36	0.15					
1071	shaped, not tabbed		0.372	0.154					
1072	shaped, not tabbed		0.37	0.149					
1073	shaped, not tabbed		0.376	0.149					
1074	25/15 ksi, 10/1000, R=-1		0.369	0.152					
1075	shaped, not tabbed		0.366	0.151					
1076	shaped, not tabbed		0.369	0.158					
1077	shaped, not tabbed		0.351	0.152					
1078	shaped, not tabbed		0.371	0.152					
1079	shaped, not tabbed		0.371	0.157					
1080	shaped, not tabbed		0.365	0.15					
1081	shaped, not tabbed		0.368	0.152					
1082	shaped, not tabbed		0.373	0.149					
1083	shaped, not tabbed		0.369	0.151					
1084	25/15 ksi, 10/10K, R=-1		0.37	0.152					
1085	shaped, not tabbed		0.374	0.15					
1086	shaped, not tabbed		0.364	0.152					
1087	-25/-15 ksi, 10/10, R=-1	2mDD16E	0.449	0.15	5	25430	25420	50850	1741
1088	-25/-15 ksi, 10/10, R=-1	2mDD16E	0.432	0.151	5	16536	16530	33066	1703
1089	-25/-15 ksi, 10/10, R=-1	2mDD16E	0.438	0.151	5	11467	11460	22927	1722
1090	-25/-15 ksi, 10/10, R=-1	2mDD16E	0.443	0.15	5	8779	8770	17549	1748
1091	-25/-15 ksi, 10/10, R=-1	2mDD16E	0.432	0.155	5	18018	18010	36028	1749
1092	-25/-15 ksi, 10/10, R=-1	2mDD16E	0.427	0.153	5	16674	16670	33344	1697
1093	-25/-15 ksi, 10/10, R=-1	2mDD16E	0.45	0.15	5	24781	24780	49561	1751
1094	-25/-15 ksi, 10/10, R=-1	2mDD16E	0.435	0.152	5	34040	34030	68070	1722
1095	-25/-15 ksi, 10/10, R=-1	2mDD16E	0.429	0.15	5	19245	19240	38485	1657
1096	-25/-15 ksi, 10/10, R=-1	2mDD16E	0.447	0.15	5	22190	22180	44370	1747
1097	-25/-15, 10 / 100, R=-1	2mDD16E	0.435	0.153	5	7581	75800	83381	1730
1098	-25/-15, 10 / 100, R=-1	2mDD16E	0.44	0.148	5	14380	143781	158161	1698
1099	-25/-15, 10 / 100, R=-1	2mDD16E	0.444	0.154	5	6405	64000	70405	1769
1100	-25/-15, 10 / 100, R=-1	2mDD16E	0.43	0.153	5	13142	131400	144542	1713
1101	-25/-15, 10 / 100, R=-1	2mDD16E	0.438	0.15	5	7191	71900	79091	1706
1102	-25/-15, 10 / 100, R=-1	2mDD16E	0.437	0.152	5	5291	52900	58191	1746
1103	-25/-15, 10 / 100, R=-1	2mDD16E	0.437	0.155	5	10150	101488	111638	1775
1104	-25/-15, 10 / 100, R=-1	2mDD16E	0.433	0.156	5	4283	42800	47083	1779



APPENDIX B

CONSTANT AMPLITUDE FATIGUE TEST SUMMARY

	Total	Log	MPa, Max	Log	Exponent	Power	Power
Test #	Cycles	Cycles	Stress	Stress	All Data	All Data	-Static
	Total	Log	MPa, Max	Log	Exponent	Power	Power
Test #	Cycles	Cycles	Stress	Stress	All Data	All Data	-Static
R=0.1							
274	1	0	680.44	2.833	603.95	635.34	648.64
283	1	0	649.49	2.813	603.95	635.34	648.64
296	1	0	489.07	2.689	603.95	635.34	648.64
306	1	0	673.09	2.828	603.95	635.34	648.64
329	1	0	542.62	2.734	603.95	635.34	648.64
349	1	0	558.53	2.747	603.95	635.34	648.64
383	1	0	652.42	2.815	603.95	635.34	648.64
410	1	0	638.28	2.805	603.95	635.34	648.64
430	1	0	598.86	2.777	603.95	635.34	648.64
474	1	0	629.50	2.799	603.95	635.34	648.64
479	1	0	657.43	2.818	603.95	635.34	648.64
635	1	0	670.13	2.826	603.95	635.34	648.64
646	1	0	569.31	2.755	603.95	635.34	648.64
652	1	0	619.32	2.792	603.95	635.34	648.64
653	1	0	676.43	2.830	603.95	635.34	648.64
655	1	0	688.83	2.838	603.95	635.34	648.64
666	1	0	670.90	2.827	603.95	635.34	648.64
671	1	0	687.32	2.837	603.95	635.34	648.64
739	1	0	644.29	2.809	603.95	635.34	648.64
726a	1	0	647.77	2.811	603.95	635.34	648.64
129	78	1.8921	409.06	2.612	460.75	434.67	439.82
282	85	1.9294	413.34	2.616	457.92	431.43	436.46
308	91	1.9590	412.62	2.616	455.68	428.87	433.81
130	149	2.1732	405.64	2.608	439.47	410.84	415.15
148	155	2.1903	414.00	2.617	438.17	409.43	413.69
624	161	2.2068	411.80	2.615	436.93	408.07	412.29
172	162	2.2095	407.02	2.610	436.72	407.85	412.06
621	180	2.2553	410.49	2.613	433.26	404.13	408.21
620	234	2.3692	410.01	2.613	424.64	394.99	398.77
578	274	2.4378	410.59	2.613	419.45	389.60	393.20
579	283	2.4518	410.20	2.613	418.39	388.50	392.07
606	286	2.4564	412.22	2.615	418.04	388.15	391.70
622	290	2.4624	409.98	2.613	417.58	387.68	391.21
577	310	2.4914	410.21	2.613	415.39	385.43	388.89
623	311	2.4928	410.13	2.613	415.28	385.32	388.78
580	334	2.5237	410.49	2.613	412.94	382.94	386.32
784	342.5	2.5347	406.61	2.609	412.11	382.10	385.45
298	356	2.5514	414.17	2.617	410.84	380.81	384.12
313	429	2.6325	414.67	2.618	404.71	374.68	377.79
297	491	2.6911	413.85	2.617	400.27	370.30	373.27
744	641.5	2.8072	393.83	2.595	391.49	361.77	364.47
168	744	2.8716	315.07	2.498	386.61	357.13	359.69
433	757	2.8791	414.41	2.617	386.04	356.59	359.13
554	763	2.8825	326.05	2.513	385.79	356.34	358.88
618	769	2.8859	324.88	2.512	385.53	356.10	358.63

Test #	Total Cycles	Log Cycles	MPa, Max Stress	Log Stress	Exponent All Data	Power All Data	Power -Static
605	783	2.8938	411.09	2.614	384.93	355.54	358.05
788	814.5	2.9109	324.06	2.511	383.64	354.32	356.79
616	1081	3.0338	324.81	2.512	374.33	345.69	347.90
745	1289.5	3.1104	322.95	2.509	368.54	340.42	342.47
584	1306	3.1159	325.32	2.512	368.12	340.04	342.08
206	1339	3.1268	321.59	2.507	367.30	339.30	341.32
607	1690	3.2279	325.79	2.513	359.65	332.49	334.31
376	1706	3.2320	327.57	2.515	359.34	332.22	334.03
161	1722	3.2360	327.76	2.516	359.03	331.95	333.75
608	1794	3.2538	325.38	2.512	357.68	330.77	332.53
140	1914	3.2819	323.09	2.509	355.55	328.90	330.62
214	2078	3.3176	318.74	2.503	352.85	326.56	328.20
139	2297	3.3612	330.02	2.519	349.56	323.72	325.29
619	2329	3.3672	325.66	2.513	349.10	323.33	324.88
617	2433	3.3861	325.24	2.512	347.67	322.10	323.62
321	2611	3.4168	328.26	2.516	345.35	320.13	321.59
583	2620	3.4183	324.91	2.512	345.23	320.03	321.49
363	3139	3.4968	327.03	2.515	339.29	315.03	316.35
171	3152	3.4986	322.68	2.509	339.16	314.92	316.23
213	3306	3.5193	324.01	2.511	337.59	313.61	314.89
434	3744	3.5733	331.17	2.520	333.50	310.23	311.42
582	4190	3.6222	325.21	2.512	329.80	307.20	308.31
581	4375	3.6410	324.67	2.511	328.38	306.05	307.12
325	8653	3.9372	327.26	2.515	305.96	288.39	289.00
205	15680	4.1953	238.11	2.377	286.42	273.84	274.08
323	16884	4.2275	242.20	2.384	283.99	272.08	272.28
746	31732.5	4.5015	237.89	2.376	263.25	257.52	257.38
147	31943	4.5044	241.55	2.383	263.03	257.38	257.23
587	35109	4.5454	240.25	2.381	259.93	255.27	255.07
632	37576	4.5749	239.47	2.379	257.70	253.76	253.53
632	37576	4.5749	239.47	2.379	257.70	253.76	253.53
174	37855	4.5781	236.38	2.374	257.45	253.60	253.36
625	41493	4.6180	205.54	2.313	254.44	251.58	251.30
633	43491	4.6384	239.78	2.380	252.89	250.55	250.24
610	43618	4.6397	240.06	2.380	252.79	250.48	250.18
302	54487	4.7363	241.57	2.383	245.48	245.68	245.26
630	57742	4.7615	239.34	2.379	243.57	244.44	244.00
609	58826	4.7696	240.50	2.381	242.96	244.04	243.59
629	78888	4.8970	205.75	2.313	233.32	237.88	237.30
586	89527	4.9520	240.03	2.380	229.16	235.27	234.64
326	104679	5.0199	241.29	2.383	224.02	232.09	231.39
284	109547	5.0396	241.71	2.383	222.53	231.17	230.45
792	115524.5	5.0627	237.64	2.376	220.78	230.11	229.36
305	121190	5.0835	206.66	2.315	219.21	229.15	228.39
305	121190	5.0835	206.66	2.315	219.21	229.15	228.39
628	129134	5.1110	205.41	2.313	217.12	227.88	227.10
131	141377	5.1504	241.28	2.383	214.14	226.09	225.27
138	143456	5.1567	241.56	2.383	213.66	225.80	224.98
634	163745	5.2142	239.82	2.380	209.31	223.22	222.34

Test #	Total Cycles	Log Cycles	MPa, Max Stress	Log Stress	Exponent All Data	Power All Data	Power -Static
634	163745	5.2142	239.82	2.380	209.31	223.22	222.34
435	181518	5.2589	240.82	2.382	205.93	221.22	220.31
585	186268	5.2701	239.76	2.380	205.08	220.73	219.80
588	187293	5.2725	239.85	2.380	204.90	220.62	219.69
378	261287	5.4171	207.21	2.316	193.95	214.31	213.26
151	274271	5.4382	205.05	2.312	192.36	213.41	212.34
485	286613	5.4573	206.62	2.315	190.91	212.59	211.51
152	294549	5.4692	202.39	2.306	190.01	212.09	211.00
611	318890	5.5036	206.17	2.314	187.40	210.62	209.51
309	373306	5.5721	207.41	2.317	182.23	207.75	206.59
153	382826	5.5830	201.08	2.303	181.40	207.30	206.12
612	418886	5.6221	206.06	2.314	178.44	205.68	204.47
391	421272	5.6246	206.99	2.316	178.25	205.58	204.37
590	436185	5.6397	206.22	2.314	177.11	204.95	203.74
160	495397	5.6950	207.00	2.316	172.92	202.69	201.44
626	496355	5.6958	205.59	2.313	172.86	202.66	201.40
747	544531.5	5.7360	204.01	2.310	169.82	201.03	199.75
169	588371	5.7697	207.00	2.316	167.27	199.68	198.37
627	598609	5.7771	205.61	2.313	166.70	199.38	198.07
589	697446	5.8435	205.83	2.314	161.68	196.74	195.39
591	732874	5.8650	206.24	2.314	160.05	195.89	194.52
436	1137595	6.0560	206.55	2.315	145.60	188.53	187.04
	1E+07	7			74.15	156.01	154.08
	1E+08	8			-1.54	127.65	125.48
<b>Exponential Regression Output Including All Data:</b>						Avg Static	
Constant			603.95	C =	0.9553143	Stress	
Std Err of Y Est			37.02			632.20	MPa
R Squared			0.94				
No. of Observations			116				
Degrees of Freedom			114				
No. of Observations			122				
X Coefficient(s)		-75.6858	120				
Std Err of Coef.		1.82368		b =	0.1197		
<b>Exponential Regression Output Excluding Static:</b>							
Constant			536.99	C =	0.8494037		
Std Err of Y Est			22.21				
R Squared			0.92				
No. of Observations			96				
Degrees of Freedom			94				
X Coefficient(s)		-60.4033					
Std Err of Coef.		1.82695		b =	0.0955		

Test #	Total Cycles	Log Cycles	MPa, Max Stress	Log Stress	Exponent All Data	Power All Data	Power -Static
<b>Power Law Regression Output Including All Data:</b>							
Constant			2.8030045		635.3375		
Std Err of Y Est			0.0312122				
R Squared			0.9657102	C =	1.00496		
No. of Observations			116				
Degrees of Freedom			114				
X Coefficient(s)		-0.08712		m =	11.477961		
Std Err of (Lin-Log Re		0.00154					
<b>Power Law Regression Output Excluding Static Data:</b>							
Constant			2.8120052		648.64214		
Std Err of Y Est			0.0292205				
R Squared			0.9360578	C =	1.0260049		
No. of Observations			96				
Degrees of Freedom			94				
X Coefficient(s)		-0.08918		m =	11.213549		
Std Err of Coef.		0.0024					
<b>R=0.5</b>							
274	1	0	680.44	2.833	625.84	640.20	717.51
283	1	0	649.49	2.813	625.84	640.20	717.51
296	1	0	489.07	2.689	625.84	640.20	717.51
306	1	0	673.09	2.828	625.84	640.20	717.51
329	1	0	542.62	2.734	625.84	640.20	717.51
349	1	0	558.53	2.747	625.84	640.20	717.51
383	1	0	652.42	2.815	625.84	640.20	717.51
410	1	0	638.28	2.805	625.84	640.20	717.51
430	1	0	598.86	2.777	625.84	640.20	717.51
474	1	0	629.50	2.799	625.84	640.20	717.51
479	1	0	657.43	2.818	625.84	640.20	717.51
635	1	0	670.13	2.826	625.84	640.20	717.51
646	1	0	569.31	2.755	625.84	640.20	717.51
652	1	0	619.32	2.792	625.84	640.20	717.51
653	1	0	676.43	2.830	625.84	640.20	717.51
655	1	0	688.83	2.838	625.84	640.20	717.51
666	1	0	670.90	2.827	625.84	640.20	717.51
671	1	0	687.32	2.837	625.84	640.20	717.51
739	1	0	644.29	2.809	625.84	640.20	717.51
726a	1	0	647.77	2.811	625.84	640.20	717.51
785	399.5	2.6015	407.93	2.611	450.00	422.33	444.16
648	438	2.6415	409.58	2.612	447.30	419.65	440.90

Test #	Total Cycles	Log Cycles	MPa, Max Stress	Log Stress	Exponent All Data	Power All Data	Power -Static
486	1119	3.0488	412.93	2.616	419.76	393.18	409.01
650	1169	3.0678	409.66	2.612	418.48	391.99	407.58
672	1400	3.1461	325.45	2.512	413.19	387.11	401.73
718	1412	3.1498	409.98	2.613	412.94	386.88	401.46
651	1475	3.1688	408.24	2.611	411.66	385.71	400.06
571	1652	3.2180	411.90	2.615	408.33	382.69	396.45
408	2290	3.3598	412.87	2.616	398.74	374.11	386.22
431	2469	3.3925	412.57	2.616	396.53	372.16	383.89
649	2507	3.3992	410.18	2.613	396.08	371.76	383.43
572	2513	3.4002	411.44	2.614	396.01	371.70	383.35
573	2519	3.4012	411.43	2.614	395.94	371.64	383.28
647	2609	3.4165	408.60	2.611	394.91	370.74	382.20
576	2755	3.4401	411.90	2.615	393.32	369.34	380.54
717	2885.5	3.4602	410.62	2.613	391.96	368.15	379.13
417	4100	3.6128	413.08	2.616	381.65	359.28	368.62
642	5801	3.7635	325.71	2.513	371.46	350.72	358.52
643	6548	3.8161	324.42	2.511	367.90	347.79	355.06
641	7421	3.8705	325.06	2.512	364.23	344.78	351.52
558	8357	3.9221	327.47	2.515	360.74	341.94	348.19
789	11811.5	4.0723	325.46	2.513	350.59	333.83	338.68
556	15905	4.2015	326.56	2.514	341.85	327.00	330.70
645	19568	4.2915	324.22	2.511	335.77	322.33	325.26
347	20006	4.3012	327.62	2.515	335.12	321.83	324.69
560	21025	4.3227	326.20	2.513	333.66	320.72	323.40
719	21036.5	4.3230	325.48	2.513	333.64	320.71	323.38
487	21452	4.3315	326.71	2.514	333.07	320.28	322.88
644	24381	4.3871	326.03	2.513	329.31	317.44	319.59
562	24391	4.3872	326.52	2.514	329.30	317.43	319.57
559	31685	4.5009	326.62	2.514	321.62	311.72	312.95
557	38319	4.5834	326.09	2.513	316.04	307.63	308.22
561	48516	4.6859	326.10	2.513	309.11	302.63	302.46
409	49288	4.6927	326.84	2.514	308.65	302.30	302.07
416	74500	4.8722	327.66	2.515	296.52	293.75	292.25
640	98521	4.9935	239.90	2.380	288.32	288.10	285.78
673	100193	5.0008	239.79	2.380	287.82	287.77	285.39
488	156860	5.1955	241.32	2.383	274.67	278.95	275.33
721	272817.5	5.4359	239.95	2.380	258.42	268.43	263.40
566	280171	5.4474	240.71	2.382	257.64	267.93	262.84
638	460884	5.6636	240.77	2.382	243.03	258.83	252.57
636	464516	5.6670	243.01	2.386	242.80	258.69	252.41
722	545545.5	5.7368	240.23	2.381	238.08	255.82	249.18
569	763276	5.8827	240.95	2.382	228.22	249.92	242.57
412	829489	5.9188	241.93	2.384	225.78	248.48	240.96
563	1051280	6.0217	241.10	2.382	218.82	244.43	236.43
565	1119777	6.0491	240.84	2.382	216.97	243.36	235.24
418	1559097	6.1929	242.00	2.384	207.25	237.83	229.09
568	1749635	6.2429	240.39	2.381	203.87	235.93	226.98
564	1988538	6.2985	240.76	2.382	200.11	233.84	224.67
570	2470072	6.3927	240.93	2.382	193.74	230.35	220.80



Test #	Total Cycles	Log Cycles	MPa, Max Stress	Log Stress	Exponent All Data	Power All Data	Power -Static
	1E+07	7			152.70	209.03	197.42
	1E+08	8			85.10	178.14	164.18
<b>Exponential Regression Output Including All Data:</b>						Avg Static	
Constant			625.84156	C =	0.9899396	Stress	
Std Err of Y Est			37.072151			632.20	MPa
R Squared			0.9419801				
No. of Observations			71				
Degrees of Freedom			69				
X Coefficient(s)	-67.5923			b =	0.1069157		
Std Err of Coef.	2.01948						
<b>Exponential Regression Output Excluding Static Data:</b>							
Constant			581.52815	C =	0.9198458		
Std Err of Y Est			25.674422				
R Squared			0.8601635				
No. of Observations			51				
Degrees of Freedom			49				
X Coefficient(s)	-58.0875			b =	0.0918813		
Std Err of Coef.	3.34583						
<b>Power Law Regression Output Including All Data:</b>							
Constant			2.8063138		640.19729		
Std Err of Y Est			0.0367539				
R Squared			0.9457545	C =	1.0126471		
No. of Observations			71				
Degrees of Freedom			69				
X Coefficient(s)	-0.06944			m =	14.40032		
Std Err of Coef.	0.002						
<b>Power Law Regression Output Excluding Static Data:</b>							
Constant			2.8558296		717.51277		
Std Err of Y Est			0.0336047				
R Squared			0.8721437	C =	1.1349427		
No. of Observations			51				
Degrees of Freedom			49				
X Coefficient(s)	-0.08006			m =	12.490079		
Std Err of Coef.	0.00438						
R=-1							
812	1	0.0000	399.48	2.601	400.08	401.87	394.95
818	1	0.0000	395.82	2.597	400.08	401.87	394.95
824	1	0.0000	405.49	2.608	400.08	401.87	394.95

Test #	Total Cycles	Log Cycles	MPa, Max Stress	Log Stress	Exponent All Data	Power All Data	Power -Static
830	1	0.0000	368.34	2.566	400.08	401.87	394.95
831	1	0.0000	410.54	2.613	400.08	401.87	394.95
832	1	0.0000	368.21	2.566	400.08	401.87	394.95
833	1	0.0000	416.44	2.620	400.08	401.87	394.95
834	1	0.0000	379.01	2.579	400.08	401.87	394.95
835	1	0.0000	435.09	2.639	400.08	401.87	394.95
865	1	0.0000	427.49	2.631	400.08	401.87	394.95
866	1	0.0000	408.58	2.611	400.08	401.87	394.95
867	1	0.0000	406.71	2.609	400.08	401.87	394.95
868	1	0.0000	387.75	2.589	400.08	401.87	394.95
869	1	0.0000	419.75	2.623	400.08	401.87	394.95
880	1	0.0000	370.86	2.569	400.08	401.87	394.95
881	1	0.0000	404.78	2.607	400.08	401.87	394.95
882	1	0.0000	426.97	2.630	400.08	401.87	394.95
883	1	0.0000	397.16	2.599	400.08	401.87	394.95
884	1	0.0000	421.48	2.625	400.08	401.87	394.95
885	1	0.0000	394.64	2.596	400.08	401.87	394.95
886	1	0.0000	411.15	2.614	400.08	401.87	394.95
887	1	0.0000	374.45	2.573	400.08	401.87	394.95
888	1	0.0000	415.66	2.619	400.08	401.87	394.95
889	1	0.0000	413.70	2.617	400.08	401.87	394.95
1044	4861	3.6867	178.42	2.251	215.30	187.79	186.86
1038	5555.5	3.7447	182.78	2.262	212.39	185.56	184.67
1050	6003.5	3.7784	178.27	2.251	210.70	184.27	183.41
1037	11188.5	4.0488	182.08	2.260	197.15	174.27	173.62
1048	17396.5	4.2405	180.64	2.257	187.55	167.51	166.99
1051	57736.5	4.7615	144.85	2.161	161.43	150.44	150.23
1045	62837	4.7982	148.49	2.172	159.59	149.30	149.12
1040	74481.5	4.8720	146.81	2.167	155.89	147.04	146.90
1039	93249	4.9696	146.24	2.165	151.00	144.11	144.02
1047	93635.5	4.9714	146.31	2.165	150.91	144.06	143.96
1042	902103	5.9553	110.25	2.042	101.60	117.59	117.90
1041	1313992.5	6.1186	110.94	2.045	93.41	113.69	114.06
1043	1814760.5	6.2588	111.68	2.048	86.38	110.45	110.85
1046	1962727	6.2929	111.28	2.046	84.68	109.68	110.09
1049	2108316.5	6.3239	114.45	2.059	83.12	108.98	109.40
	1E+07	7.0000			49.24	94.78	95.37
	1E+08	8.0000			-0.89	77.11	77.85
<b>Exponential Regression Output Including All Data:</b>							<b>Avg Compi</b>
Constant			400.08	C =	0.9940	<b>Static Stres</b>	
Std Err of Y Est			20.55			402.48	
R Squared			0.975				
No. of Observations			39.00				
Degrees of Freedom			37.00				
X Coefficient(s)		-50.121					
Std Err of Coef.		1.3176		b =	0.1245		

Test #	Total Cycles	Log Cycles	MPa, Max Stress	Log Stress	Exponent All Data	Power All Data	Power -Static
<b>Exponential Regression Output Excluding Static Data:</b>							
Constant			290.55	C =	0.7218954		
Std Err of Y Est			6.14				
R Squared			0.959				
No. of Observations			15.00				
Degrees of Freedom			13.00				
X Coefficient(s)	-28.9321			b =	0.0719		
Std Err of Coef.	1.66654						
<b>Power Law Regression Output Including All Data:</b>							
Constant			2.60		401.8718		
Std Err of Y Est			0.02				
R Squared			0.993	C =	0.9985		
No. of Observations			39.00				
Degrees of Freedom			37.00				
X Coefficient(s)	-0.0896			m =	11.1580		
Std Err of Coef.	0.0013						
<b>Power Law Regression Output Excluding Static Data:</b>							
Constant			2.60		394.9484		
Std Err of Y Est			0.02				
R Squared			0.964	C =	0.9813		
No. of Observations			15.00				
Degrees of Freedom			13.00				
X Coefficient(s)	-0.0882			m =	11.3428		
Std Err of Coef.	0.0047						
R=10							
812	1	0	399.48	2.601	400.17	404.69	419.77
818	1	0	395.82	2.597	400.17	404.69	419.77
824	1	0	405.49	2.608	400.17	404.69	419.77
830	1	0	368.34	2.566	400.17	404.69	419.77
831	1	0	410.54	2.613	400.17	404.69	419.77
832	1	0	368.21	2.566	400.17	404.69	419.77
833	1	0	416.44	2.620	400.17	404.69	419.77
834	1	0	379.01	2.579	400.17	404.69	419.77
835	1	0	435.09	2.639	400.17	404.69	419.77
865	1	0	427.49	2.631	400.17	404.69	419.77
866	1	0	408.58	2.611	400.17	404.69	419.77
867	1	0	406.71	2.609	400.17	404.69	419.77
868	1	0	387.75	2.589	400.17	404.69	419.77

Test #	Total Cycles	Log Cycles	MPa, Max Stress	Log Stress	Exponent All Data	Power All Data	Power -Static
869	1	0	419.75	2.623	400.17	404.69	419.77
880	1	0	370.86	2.569	400.17	404.69	419.77
881	1	0	404.78	2.607	400.17	404.69	419.77
882	1	0	426.97	2.630	400.17	404.69	419.77
883	1	0	397.16	2.599	400.17	404.69	419.77
884	1	0	421.48	2.625	400.17	404.69	419.77
885	1	0	394.64	2.596	400.17	404.69	419.77
886	1	0	411.15	2.614	400.17	404.69	419.77
887	1	0	374.45	2.573	400.17	404.69	419.77
888	1	0	415.66	2.619	400.17	404.69	419.77
889	1	0	413.70	2.617	400.17	404.69	419.77
923	333.5	2.5231	335.37	2.526	318.42	309.06	314.35
927	321.5	2.50718	333.46	2.523	318.93	309.58	314.93
929	103.5	2.01494	325.19	2.512	334.88	326.30	333.21
920	130.5	2.11561	323.79	2.510	331.62	322.81	329.38
924	532.5	2.72632	322.94	2.509	311.83	302.42	307.12
922	414.5	2.61752	322.88	2.509	315.36	305.95	310.97
928	432.5	2.63599	322.83	2.509	314.76	305.35	310.31
925	1018.5	3.00796	322.72	2.509	302.71	293.45	297.36
926	326.5	2.51388	322.67	2.509	318.72	309.36	314.69
921	363.5	2.5605	322.39	2.508	317.21	307.82	313.01
796	11607.5	4.06474	280.47	2.448	268.46	262.12	263.44
799	5903.5	3.77111	279.74	2.447	277.98	270.47	272.45
855	4062.5	3.60879	277.77	2.444	283.24	275.21	277.57
856	4409.5	3.64439	277.70	2.444	282.08	274.16	276.44
800	5122.5	3.70948	277.27	2.443	279.98	272.26	274.39
817	15392.5	4.18731	277.22	2.443	264.49	258.71	259.76
816	3849.5	3.5854	277.19	2.443	284.00	275.89	278.32
858	8287.5	3.91842	276.95	2.442	273.20	266.25	267.89
797	2462.5	3.39138	276.81	2.442	290.28	281.67	284.58
859	10691.5	4.02904	276.54	2.442	269.62	263.12	264.52
814	4352.5	3.63874	276.42	2.442	282.27	274.33	276.62
798	2726.5	3.43561	276.36	2.441	288.85	280.35	283.14
813	2468.5	3.39243	276.04	2.441	290.25	281.64	284.54
857	1956.5	3.29148	275.39	2.440	293.52	284.70	287.85
806	5009.5	3.69979	259.09	2.413	280.29	272.54	274.69
805	21240	4.32715	245.30	2.390	259.96	254.87	255.63
802	54872.5	4.73935	243.89	2.387	246.60	243.89	243.84
823	67972.5	4.83233	243.15	2.386	243.59	241.48	241.25
804	11737.5	4.06958	243.14	2.386	268.31	261.98	263.29
820	36656.5	4.56415	242.98	2.386	252.28	248.50	248.78
819	14172	4.15143	242.94	2.385	265.65	259.70	260.83
803	11145	4.04708	242.84	2.385	269.04	262.61	263.97
801	379063.5	5.57871	242.60	2.385	219.41	222.97	221.47
822	9234.5	3.96541	242.46	2.385	271.68	264.92	266.45
821	6703.5	3.8263	241.37	2.383	276.19	268.88	270.74
863	1884109.5	6.27511	216.49	2.335	196.84	206.98	204.48
861	933071.5	5.96991	216.39	2.335	206.73	213.84	211.76
828	1508673.5	6.1786	215.17	2.333	199.97	209.13	206.75



Test #	Total Cycles	Log Cycles	MPa, Max Stress	Log Stress	Exponent All Data	Power All Data	Power -Static
<b>Power Law Regression Output Excluding Static Data:</b>							
Constant			2.6230149		419.7734		
Std Err of Y Est			0.0216765				
R Squared			0.906	C =	1.0430		
No. of Observations			50				
Degrees of Freedom			48				
X Coefficient(s)		-0.04978		m =	20.0889		
Std Err of Coef.		0.00231					
R=2							
812	1	0	399.48	2.601	402.50	402.41	465.00
818	1	0	395.82	2.597	402.50	402.41	465.00
824	1	0	405.49	2.608	402.50	402.41	465.00
830	1	0	368.34	2.566	402.50	402.41	465.00
831	1	0	410.54	2.613	402.50	402.41	465.00
832	1	0	368.21	2.566	402.50	402.41	465.00
833	1	0	416.44	2.620	402.50	402.41	465.00
834	1	0	379.01	2.579	402.50	402.41	465.00
835	1	0	435.09	2.639	402.50	402.41	465.00
865	1	0	427.49	2.631	402.50	402.41	465.00
866	1	0	408.58	2.611	402.50	402.41	465.00
867	1	0	406.71	2.609	402.50	402.41	465.00
868	1	0	387.75	2.589	402.50	402.41	465.00
869	1	0	419.75	2.623	402.50	402.41	465.00
880	1	0	370.86	2.569	402.50	402.41	465.00
881	1	0	404.78	2.607	402.50	402.41	465.00
882	1	0	426.97	2.630	402.50	402.41	465.00
883	1	0	397.16	2.599	402.50	402.41	465.00
884	1	0	421.48	2.625	402.50	402.41	465.00
885	1	0	394.64	2.596	402.50	402.41	465.00
886	1	0	411.15	2.614	402.50	402.41	465.00
887	1	0	374.45	2.573	402.50	402.41	465.00
888	1	0	415.66	2.619	402.50	402.41	465.00
889	1	0	413.70	2.617	402.50	402.41	465.00
897	46303.5	4.6656	280.58	2.448	285.32	280.68	286.92
899	48989.5	4.6901	273.84	2.438	284.70	280.15	286.19
893	62258.0	4.7942	274.67	2.439	282.09	277.90	283.12
892	130732.5	5.1164	275.92	2.441	274.00	271.07	273.84
894	158395.5	5.1997	279.27	2.446	271.90	269.34	271.49
896	162399.5	5.2106	280.91	2.449	271.63	269.11	271.18
898	192595.0	5.2846	275.89	2.441	269.77	267.58	269.11
895	1.4E+06	6.1592	273.41	2.437	247.80	250.10	245.82
909	2.7E+06	6.4375	242.36	2.384	240.82	244.79	238.85

Test #	Total Cycles	Log Cycles	MPa, Max Stress	Log Stress	Exponent All Data	Power All Data	Power -Static
919	4.0E+06	6.6036	208.19	2.318	236.64	241.67	234.78
	1E+07	7			226.69	234.38	225.34
	1E+08	8			201.57	216.96	203.18
<b>Exponential Regression Output Including All Data:</b>						Avg Static	
Constant			402.50	C =	1.00	Stress	
Std Err of Y Est			18.14			402.48	MPa
R Squared			0.927				
No. of Observations			34.00				
Degrees of Freedom			32.00				
X Coefficient(s)	-25.1155						
Std Err of Coef.	1.24672			b =	0.0624017		
<b>Exponential Regression Output Excluding Static Data:</b>							
Constant			404.85807	C =	1.0059059		
Std Err of Y Est			15.18018				
R Squared			0.624				
No. of Observations			10				
Degrees of Freedom			8				
X Coefficient(s)	-25.5447						
Std Err of Coef.	7.01791			b =	0.0634681		
<b>Power Law Regression Output Including All Data:</b>							
Constant			2.60		402.41		
Std Err of Y Est			0.02				
R Squared			0.933	C =	0.9998		
No. of Observations			34.00				
Degrees of Freedom			32.00				
X Coefficient(s)	-0.03353			m =	29.8200		
Std Err of Coef.	0.00158						
<b>Power Law Regression Output Excluding Static Data:</b>							
Constant			2.67		465.00		
Std Err of Y Est			0.03				
R Squared			0.610	C =	1.1553		
No. of Observations			10.00				
Degrees of Freedom			8.00				
X Coefficient(s)	-0.04495			m =	22.2493		
Std Err of Coef.	0.01271						

APPENDIX C

MULTI-BLOCK FATIGUE TEST SUMMARY



			NRSD	LRS D	NRSD	LRS D	NRSD	LRS D	NRSD	LRS D
	actual		exponent	exponent	exponent	exponent	power	power	power	power
Test #	Miner's #	Frac Hi	all data	all data	-static	-static	all data	all data	-static	-static
+60/47.5	ksi	R=0.1								
		0.505					0.871			
		0.102					0.579			
		0.052					0.487			
		0.011					0.531			
		0.005					0.987			
		0.005					1.053			
		0.005					1.053			
		0.005					1.053			
		0.005					1.053			
		0.514						0.985		
		0.101						0.921		
		0.054						0.828		
		0.010						1.043		
		0.005						0.987		
		0.005						1.021		
		0.005						1.021		
		0.005						1.021		
		0.005						1.021		
		0.005						1.021		
		0.510							0.865	
		0.102							0.526	
		0.052							0.447	
		0.011							0.498	
		0.005							0.929	
		0.004							1.047	
		0.004							1.047	
		0.004							1.047	
		0.004							1.047	
		0.004							1.047	
		0.502								0.978
		0.108								0.876
		0.051								0.888
		0.010								0.99
		0.005								0.929
		0.004								1.019
		0.004								1.019
		0.004								1.019
		0.004								1.019
		0.004								1.019
		0.509	0.836							
		0.101	0.458							
		0.051	0.362							
		0.010	0.485							
		0.005	0.456							



			NRSD	LRS D	NRSD	LRS D	NRSD	LRS D	NRSD	LRS D
	actual		exponent	exponent	exponent	exponent	power	power	power	power
Test #	Miner's #	Frac Hi	all data	all data	-static	-static	all data	all data	-static	-static
621	1.664	1.000								
620	0.610	1.000								
578	0.793	1.000								
606	0.929	1.000								
129	0.969	1.000								
130	0.264	1.000								
148	0.505	1.000								
172	0.525	1.000								
623	0.549	1.000								
624	1.054	1.000								
605	0.546	1.000								
433	2.654	1.000								
580	2.566	1.000								
308	1.132	1.000								
282	0.308	1.000								
313	0.288	1.000								
622	1.454	1.000								
298	0.983	1.000								
213	1.207	0.000								
161	1.343	0.000								
171	0.699	0.000								
139	1.280	0.000								
168	0.933	0.000								
582	0.302	0.000								
434	1.702	0.000								
583	1.521	0.000								
214	1.064	0.000								
140	0.844	0.000								
617	0.777	0.000								
619	0.988	0.000								
608	0.946	0.000								
607	0.729	0.000								
616	0.686	0.000								
206	0.439	0.000								
581	0.544	0.000								
376	1.777	0.000								
554	0.693	0.000								
584	0.310	0.000								
321	0.530	0.000								
325	1.061	0.000								
618	3.515	0.000								
60/35	ksi	R=0.1								
		0.50943					0.99			
		0.10075					0.898			
		0.05473					0.827			

			NRSD	LRS D	NRSD	LRS D	NRSD	LRS D	NRSD	LRS D
	actual		exponent	exponent	exponent	exponent	power	power	power	power
Test #	Miner's #	Frac Hi	all data	all data	-static	-static	all data	all data	-static	-static
		0.01017					0.512			
		0.00512					0.388			
		0.0011					0.191			
		0.00055					0.301			
		0.00011					1.066			
		0.00011					1.066			
		0.00011					1.066			
		0.51311						1.005		
		0.10276						0.995		
		0.05037						0.987		
		0.01099						0.915		
		0.00506						0.864		
		0.00103						0.741		
		0.0007						0.646		
		0.00012						1.033		
		0.00012						1.033		
		0.00012						1.033		
		0.50331							0.99	
		0.10345							0.891	
		0.05387							0.798	
		0.01017							0.464	
		0.00512							0.357	
		0.0011							0.185	
		0.00055							0.299	
		0.00011							1.058	
		0.00011							1.058	
		0.00011							1.058	
		0.50658								1.003
		0.10638								0.99
		0.05203								0.98
		0.0109								0.904
		0.00539								0.834
		0.00103								0.721
		0.00068								0.63
		0.00012								1.029
		0.00012								1.029
		0.00012								1.029
		0.50166	0.957							
		0.10256	0.707							
		0.0503	0.55							
		0.0104	0.232							
		0.00517	0.18							
		0.0011	0.172							
		0.00055	0.31							
		0.00014	1.029							
		0.00014	1.029							















APPENDIX D

WISPERX FATIGUE TEST SUMMARY

Mod2 WisperX Spectrum, R=0.1					LRSD	NRSD		NRSD	LRSD
Test	Max Load	Max Stress	Cycles	Regress	Exponent	Exponent	Miner's	Power	Power
					Predict	Predict	Predict	Predict	Predict
615	5544	622.0	1	641.4					
635	5901	670.1	1	641.4					
646	4953	569.3	1	641.4					
652	4285	619.3	1	641.4					
653	5624	676.4	1	641.4					
655	5879	688.8	1	641.4					
666	5726	670.9	1	641.4					
739	5734	696.9	1	641.4					
726	5765	647.8	1	641.4					
671	5633	687.3	1	641.4					
971	2875	340.9	1275.5	430.2					
972	2960	343.6	2324.5	412.4					
973	2889	344.7	2447.5	410.9					
976	3115	402.9	2805.5	406.9					
974	3352	406.9	3129.5	403.6					
979	3669	402.3	3202.5	403.0					
978	3387	406.2	3232.5	402.7					
970	2914	402.9	3843.5	397.6					
975	3081	403.2	4043.5	396.1					
977	2716	405.6	5722	385.8					
1004	3026	339.5	6047.5	384.2					
1005	2613	341.2	13057.5	361.4					
1000	2945	335.4	14370.5	358.6					
1002	2593	340.9	18333.5	351.4					
1006	2698	343.2	24195.5	343.2					
1003	2934	340.2	24905.5	342.4					
1001	2810	335.5	26044.5	341.0					
986	2524	296.9	68425.5	312.5					
989	2458	297.5	80979.5	307.5					
983	2669	301.6	86292.5	305.7					
988	2543	297.0	144430	290.4					
981	2475	298.0	155850	288.2					
980	2233	297.9	167885	286.0					
985	2299	298.0	169839	285.7					
982	2462	297.2	195616	281.5					
990	2338	254.1	195751	281.5					
987	2319	297.4	231019	276.6					
999	2227	256.1	248429	274.4					
984	2270	296.8	298800	269.0					
995	2222	254.6	312744	267.6					
996	2164	259.1	432307	258.1					
991	2202	255.0	598438	248.5					
998	2175	255.6	680774	244.6					

Mod2 WisperX Spectrum, R=0.1					LRSD	NRSD		NRSD	LRSD
Test	Max Load	Max Stress	Cycles	Regress	Exponent	Exponent	Miner's	Power	Power
					Predict	Predict	Predict	Predict	Predict
992	1878	255.9	876955	237.2					
997	1979	256.7	912240	236.0					
993	1878	253.1	1231928	227.1					
1016	1550	189.7	1.2E+07	159.2					
1007	1550	185.6	1.4E+07	155.0					
			12983		414				
			92466		327.75				
			836664		241.5				
			1952961		207				
			2649			414			
			41142			327.75			
			503058			241.5			
			1298580			207			
			13409				414		
			117716				327.75		
			984459				241.5		
			2284731				207		
			2649					414	
			41142					327.75	
			1863144					241.5	
			1E+07					207	
			1497						414
	644		28311						327.75
	31		1118946						241.5
	1		6777417						207

APPENDIX E

WIND TURBINE BLADE STRAIN DATA ACQUISITION SYSTEM

## Wind Turbine Data Acquisition Project

Summary

Two ten-kilowatt wind turbine have been installed, at a southwestern Montana wind rich location, for the purpose of testing blade designs and blade materials. This testing required the collection of certain operational data; namely, strain due to fiberglass blade loading, wind speed, wind direction and generator rotor speed. The collection of strain data from rotating blades posed the greatest challenge and will be documented here.

Data acquisition systems employed by the National Wind Technology Center, NWTC, in Golden, Colorado, the National Earthquake Center, and the University of Texas at El Paso, UTEP, were studied. These systems were rejected for reasons of lack of desired speed and high cost. The system chosen by NWTC was based upon data collection via a microprocessor controlled system that was mounted upon the rotating hub of the wind turbine generator. The strain data was collected, digitized, manipulated and periodically transmitted to a ground recording station. The data available was not "real time" and in fact was presented in a compressed format of ranged and averaged data placed in "bins". The system employed by UTEP was very similar in operation as the one chosen by NWTC. The system used by the National Earthquake Center was designed to handled the relatively low frequencies of earthquakes and found not capable of modification for higher frequencies experienced in wind turbine operation.

The final system designed and produced for this project, provided "real time" data. This data could then be manipulated into any desired format for analysis. The "home-built"

data acquisition system involved the collection of strain data, analog signal manipulation of filtering, zeroing and scaling, digitizing and serial transmission to a ground station for recording. The system had eight channels of data acquisition.

Software was written in Visual Basic to facilitate the collection and manipulation of data. Specific programs covered, a) collection of raw data, b) routines for play back of raw data, c) manipulation of data into successive cycles of strain represented by a range and average strain, d) placement of the range and average strain data into bins; the accepted format. Plotting of the results of the fourth program was accomplished by the use of spreadsheet software.

### Data Acquisition System Design

The data acquisition system was comprised of a power supply, strain gage bridge amplifiers, microprocessor based signal conditioning, analog to digital conversion and serial data preparation for transmission. and a wireless modem. Several of these components are carried on printed circuit boards (PCB's). Figure 105 depicts the component arrangement.

This DAQ system is attached to the rotating hub of the wind turbine generator and covered by the original machine nose cone. AC power is supplied to this system via two sets of slip rings, one to pass power over the turbine yaw shaft and one to pass power over the rotating generator. The delivered AC power is used to energize a battery charger, thereby keeping the 12 V battery charged and ready. The battery in turn supplies energy to a power conditioning board where supply voltages of 5 and 12 VDC are produced.



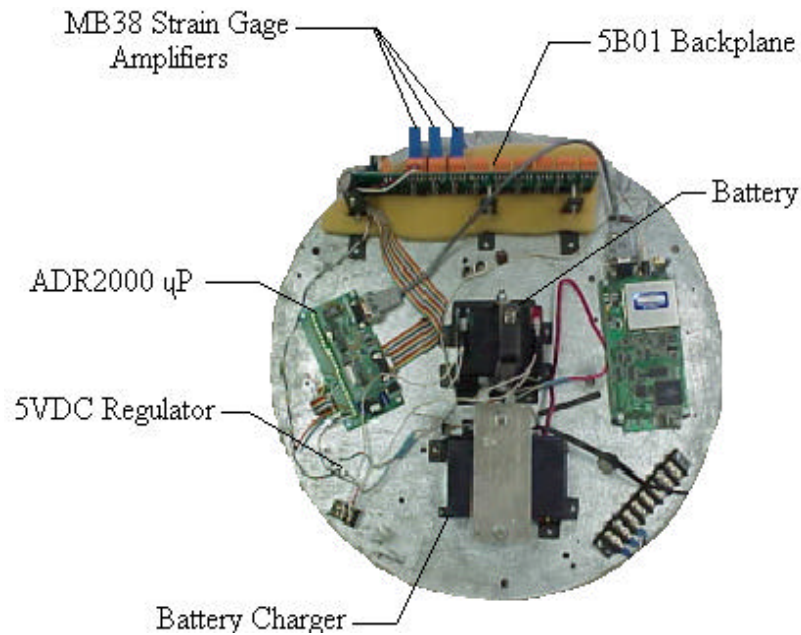


Figure 105. Data Acquisition System

Up to eight strain gages can be mounted on rotating components of the wind turbine. The number of channels is selected by appropriate microprocessor commands. A 22 gage ribbon cable is used to carry excitation power to the strain gage bridges and return the electronic strain signals to the strain gage amplifiers. The output voltage signals from the amplifiers are delivered to a microprocessor board for filtering and scaling. The -5 to +5 VDC signals are scaled to 0 to +5 VDC for compatible application to the microprocessor analog to digital converter. The digitized signals are sequentially passed to the wireless modem for 900 MHz frequency telemetering to a ground receiver.

The ground receiving station is comprised of a 486DX2 66 MHz computer and wireless modem. The signal transmitted from the DAQ wireless modem is received at the ground station wireless modem and provided to a computer serial port.

Software Design

Two computer programs were written to accomplish specific tasks. These two tasks involved the collection of the data to mass digital storage, and the playback of the previously collected data. Figures 106 and 107 are copies of the graphic user interface prepared for the data acquisition and playback respectively. The Visual BASIC code for each of these programs follows.

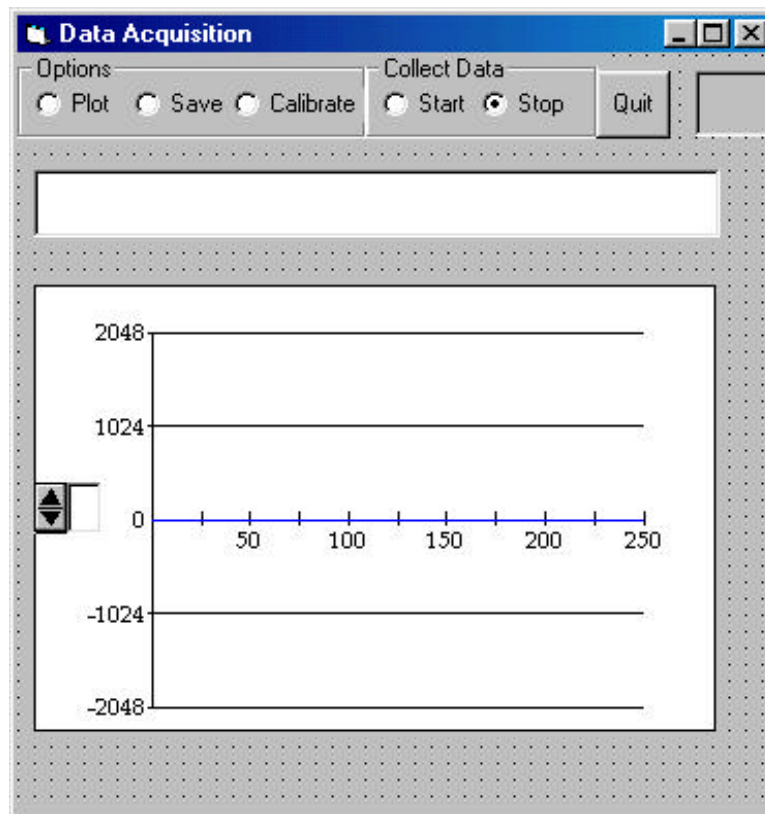


Figure 106. Data Acquisition GUI

```

VERSION 4.00
Begin VB.Form Form2
    Caption       = "Data Acquisition"
    ClientHeight  = 5520
    ClientLeft    = 1530
    ClientTop     = 1800
    ClientWidth   = 5475
    Height        = 5925
    Left          = 1470
    LinkTopic     = "Form2"
    ScaleHeight   = 5520
    ScaleWidth    = 5475
    Top           = 1455
    Width         = 5595
    Begin VB.TextBox Text10
        BeginProperty Font
            {0BE35203-8F91-11CE-9DE3-00AA004BB851}
            Name       = "MS Sans Serif"
            Size        = 9.75
            Charset     = 0
            Weight      = 400
            Underline   = 0 'False
            Italic       = 0 'False
            Strikethrough = 0 'False
        EndProperty
        Height       = 375
        Left         = 360
        TabIndex     = 10
        Top          = 3120
        Width        = 255
    End
    Begin VB.CommandButton Command1
        Caption     = "Quit"
        Height      = 495
        Left        = 4200
        TabIndex    = 6
        Top         = 125
        Width       = 540
    End
    Begin VB.TextBox Text1
        Height      = 495
        Left        = 120
        TabIndex    = 5
        Top         = 840
        Width       = 4980
    End
    Begin VB.Frame Frame3
        Caption     = "Options"
        Height      = 615
        Left        = 0
        TabIndex    = 2
        Top         = 0
        Width       = 2535
    End
    Begin VB.OptionButton Option5
        Caption     = "Plot"
        Height      = 255
        Left        = 120
        TabIndex    = 11
        Top         = 240
        Width       = 615
    End
    Begin VB.OptionButton Option4
        Caption     = "Calibrate"
        Height      = 255
        Left        = 1560
        TabIndex    = 4
        Top         = 240
        Width       = 960
    End
    Begin VB.OptionButton Option3
        Caption     = "Save"
        Height      = 255
        Left        = 840
        TabIndex    = 3
        Top         = 240
        Width       = 750
    End
    End
    Begin VB.Frame Frame2
        Caption     = "Collect Data"
        Height      = 615
        Left        = 2520
        TabIndex    = 1
        Top         = 0
        Width       = 1695
    End
    Begin VB.OptionButton Option2
        Caption     = "Stop"
        Height      = 255
        Left        = 840
        TabIndex    = 8
        Top         = 240
        Value       = -1 'True
        Width       = 735
    End
    End
    Begin VB.OptionButton Option1
        Caption     = "Start"
        Height      = 255
        Left        = 120
        TabIndex    = 7
        Top         = 240
        Width       = 645
    End
    End
    Begin VB.PictureBox MSCComm1

```

```

Height      = 480
Left        = 4920
ScaleHeight = 420
ScaleWidth  = 1140
TabIndex    = 12
Top         = 120
Width       = 1200
End
Begin Spin.SpinButton SpinButton1
Height      = 375
Left        = 120
TabIndex    = 9
Top         = 3120
Width       = 255
_Version    = 65536
_ExtentX    = 450
_ExtentY    = 661
_StockProps = 73
MousePointer = 1
ShadowThickness = 1
TdThickness = 1
End
Begin GraphLib.Graph Graph1
Height      = 3255
Left        = 120
TabIndex    = 0
Top         = 1680
Width       = 4950
_Version    = 65536
_ExtentX    = 8731
_ExtentY    = 5741
_StockProps = 96
BorderStyle = 1
GraphCaption = "Strain"
GraphType   = 6
GridStyle   = 1
LabelEvery  = 50
NumPoints   = 251
PatternedLines = 1
PrintStyle  = 1
RandomData  = 0
ThickLines  = 0
TickEvery   = 25
YAxisMax    = 2048
YAxisMin    = -2048
YAxisStyle  = 2
YAxisTicks  = 2
ColorData   = 0
ExtraData   = 0
ExtraData[] = 0
FontFamily  = 4
FontSize    = 4
FontSize[0] = 100
FontSize[1] = 150
FontSize[2] = 100
FontSize[3] = 100
FontStyle   = 4
GraphData   = 1
GraphData[] = 251
GraphData[0,0] = 0
GraphData[0,1] = 0
GraphData[0,2] = 0
GraphData[0,3] = 0
GraphData[0,4] = 0
GraphData[0,5] = 0
GraphData[0,6] = 0
GraphData[0,7] = 0
GraphData[0,8] = 0
GraphData[0,9] = 0
GraphData[0,10] = 0
GraphData[0,11] = 0
GraphData[0,12] = 0
GraphData[0,13] = 0
GraphData[0,14] = 0
GraphData[0,15] = 0
GraphData[0,16] = 0
GraphData[0,17] = 0
GraphData[0,18] = 0
GraphData[0,19] = 0
GraphData[0,20] = 0
GraphData[0,21] = 0
GraphData[0,22] = 0
GraphData[0,23] = 0
GraphData[0,24] = 0
GraphData[0,25] = 0
GraphData[0,26] = 0
GraphData[0,27] = 0
GraphData[0,28] = 0
GraphData[0,29] = 0
GraphData[0,30] = 0
GraphData[0,31] = 0
GraphData[0,32] = 0
GraphData[0,33] = 0
GraphData[0,34] = 0
GraphData[0,35] = 0
GraphData[0,36] = 0
GraphData[0,37] = 0
GraphData[0,38] = 0
GraphData[0,39] = 0
GraphData[0,40] = 0
GraphData[0,41] = 0
GraphData[0,42] = 0
GraphData[0,43] = 0
GraphData[0,44] = 0

```

GraphData[0,45] = 0  
GraphData[0,46] = 0  
GraphData[0,47] = 0  
GraphData[0,48] = 0  
GraphData[0,49] = 0  
GraphData[0,50] = 0  
GraphData[0,51] = 0  
GraphData[0,52] = 0  
GraphData[0,53] = 0  
GraphData[0,54] = 0  
GraphData[0,55] = 0  
GraphData[0,56] = 0  
GraphData[0,57] = 0  
GraphData[0,58] = 0  
GraphData[0,59] = 0  
GraphData[0,60] = 0  
GraphData[0,61] = 0  
GraphData[0,62] = 0  
GraphData[0,63] = 0  
GraphData[0,64] = 0  
GraphData[0,65] = 0  
GraphData[0,66] = 0  
GraphData[0,67] = 0  
GraphData[0,68] = 0  
GraphData[0,69] = 0  
GraphData[0,70] = 0  
GraphData[0,71] = 0  
GraphData[0,72] = 0  
GraphData[0,73] = 0  
GraphData[0,74] = 0  
GraphData[0,75] = 0  
GraphData[0,76] = 0  
GraphData[0,77] = 0  
GraphData[0,78] = 0  
GraphData[0,79] = 0  
GraphData[0,80] = 0  
GraphData[0,81] = 0  
GraphData[0,82] = 0  
GraphData[0,83] = 0  
GraphData[0,84] = 0  
GraphData[0,85] = 0  
GraphData[0,86] = 0  
GraphData[0,87] = 0  
GraphData[0,88] = 0  
GraphData[0,89] = 0  
GraphData[0,90] = 0  
GraphData[0,91] = 0  
GraphData[0,92] = 0  
GraphData[0,93] = 0  
GraphData[0,94] = 0  
GraphData[0,95] = 0  
GraphData[0,96] = 0  
GraphData[0,97] = 0  
GraphData[0,98] = 0  
GraphData[0,99] = 0  
GraphData[0,100]= 0  
GraphData[0,101]= 0  
GraphData[0,102]= 0  
GraphData[0,103]= 0  
GraphData[0,104]= 0  
GraphData[0,105]= 0  
GraphData[0,106]= 0  
GraphData[0,107]= 0  
GraphData[0,108]= 0  
GraphData[0,109]= 0  
GraphData[0,110]= 0  
GraphData[0,111]= 0  
GraphData[0,112]= 0  
GraphData[0,113]= 0  
GraphData[0,114]= 0  
GraphData[0,115]= 0  
GraphData[0,116]= 0  
GraphData[0,117]= 0  
GraphData[0,118]= 0  
GraphData[0,119]= 0  
GraphData[0,120]= 0  
GraphData[0,121]= 0  
GraphData[0,122]= 0  
GraphData[0,123]= 0  
GraphData[0,124]= 0  
GraphData[0,125]= 0  
GraphData[0,126]= 0  
GraphData[0,127]= 0  
GraphData[0,128]= 0  
GraphData[0,129]= 0  
GraphData[0,130]= 0  
GraphData[0,131]= 0  
GraphData[0,132]= 0  
GraphData[0,133]= 0  
GraphData[0,134]= 0  
GraphData[0,135]= 0  
GraphData[0,136]= 0  
GraphData[0,137]= 0  
GraphData[0,138]= 0  
GraphData[0,139]= 0  
GraphData[0,140]= 0  
GraphData[0,141]= 0  
GraphData[0,142]= 0  
GraphData[0,143]= 0  
GraphData[0,144]= 0  
GraphData[0,145]= 0  
GraphData[0,146]= 0  
GraphData[0,147]= 0  
GraphData[0,148]= 0

GraphData[0,149]= 0	GraphData[0,201]= 0
GraphData[0,150]= 0	GraphData[0,202]= 0
GraphData[0,151]= 0	GraphData[0,203]= 0
GraphData[0,152]= 0	GraphData[0,204]= 0
GraphData[0,153]= 0	GraphData[0,205]= 0
GraphData[0,154]= 0	GraphData[0,206]= 0
GraphData[0,155]= 0	GraphData[0,207]= 0
GraphData[0,156]= 0	GraphData[0,208]= 0
GraphData[0,157]= 0	GraphData[0,209]= 0
GraphData[0,158]= 0	GraphData[0,210]= 0
GraphData[0,159]= 0	GraphData[0,211]= 0
GraphData[0,160]= 0	GraphData[0,212]= 0
GraphData[0,161]= 0	GraphData[0,213]= 0
GraphData[0,162]= 0	GraphData[0,214]= 0
GraphData[0,163]= 0	GraphData[0,215]= 0
GraphData[0,164]= 0	GraphData[0,216]= 0
GraphData[0,165]= 0	GraphData[0,217]= 0
GraphData[0,166]= 0	GraphData[0,218]= 0
GraphData[0,167]= 0	GraphData[0,219]= 0
GraphData[0,168]= 0	GraphData[0,220]= 0
GraphData[0,169]= 0	GraphData[0,221]= 0
GraphData[0,170]= 0	GraphData[0,222]= 0
GraphData[0,171]= 0	GraphData[0,223]= 0
GraphData[0,172]= 0	GraphData[0,224]= 0
GraphData[0,173]= 0	GraphData[0,225]= 0
GraphData[0,174]= 0	GraphData[0,226]= 0
GraphData[0,175]= 0	GraphData[0,227]= 0
GraphData[0,176]= 0	GraphData[0,228]= 0
GraphData[0,177]= 0	GraphData[0,229]= 0
GraphData[0,178]= 0	GraphData[0,230]= 0
GraphData[0,179]= 0	GraphData[0,231]= 0
GraphData[0,180]= 0	GraphData[0,232]= 0
GraphData[0,181]= 0	GraphData[0,233]= 0
GraphData[0,182]= 0	GraphData[0,234]= 0
GraphData[0,183]= 0	GraphData[0,235]= 0
GraphData[0,184]= 0	GraphData[0,236]= 0
GraphData[0,185]= 0	GraphData[0,237]= 0
GraphData[0,186]= 0	GraphData[0,238]= 0
GraphData[0,187]= 0	GraphData[0,239]= 0
GraphData[0,188]= 0	GraphData[0,240]= 0
GraphData[0,189]= 0	GraphData[0,241]= 0
GraphData[0,190]= 0	GraphData[0,242]= 0
GraphData[0,191]= 0	GraphData[0,243]= 0
GraphData[0,192]= 0	GraphData[0,244]= 0
GraphData[0,193]= 0	GraphData[0,245]= 0
GraphData[0,194]= 0	GraphData[0,246]= 0
GraphData[0,195]= 0	GraphData[0,247]= 0
GraphData[0,196]= 0	GraphData[0,248]= 0
GraphData[0,197]= 0	GraphData[0,249]= 0
GraphData[0,198]= 0	GraphData[0,250]= 0
GraphData[0,199]= 0	LabelText = 0
GraphData[0,200]= 0	LegendText = 0

```

    PatternData = 0
    SymbolData = 0
    XPosData = 0
    XPosData[] = 0
End
End
Attribute VB_Name = "Form2"
Attribute VB_Creatable = False
Attribute VB_Exposed = False

Public strain1 As Integer

Public ij As Integer

Public strain As Integer

Public chn As Integer

Public plt As Integer

Private Sub Check2_Click()

If Check2 Then
    Message = "Channel 2 Label"
    Title = "Get Channe2 Label"
    Default = "Channel 2"
    myvalue = InputBox(Message, Title, Default)
    If myvalue = "" Then myvalue = Default
    Text3.Text = myvalue
End If

If Check2 = False Then
    Text3.Text = ""
End If

End Sub

Private Sub Check3_Click()
ij = 2
If Check3 Then
    Message = "Channel 3 Label"
    Title = "Get Channe3 Label"
    Default = "Channel 3"
    myvalue = InputBox(Message, Title, Default)
    If myvalue = "" Then myvalue = Default
    Text4.Text = myvalue
End If

If Check3 = False Then
    Text4.Text = ""
End If

End If

End Sub

Private Sub Check4_Click()

If Check4 Then
    Message = "Channel 4 Label"
    Title = "Get Channe4 Label"
    Default = "Channel 4"
    myvalue = InputBox(Message, Title, Default)
    If myvalue = "" Then myvalue = Default
    Text5.Text = myvalue
End If

If Check4 = False Then
    Text5.Text = ""
End If

End Sub

Private Sub Check5_Click()

If Check5 Then
    Message = "Channel 5 Label"
    Title = "Get Channel 5 Label"
    Default = "Channel 5"
    myvalue = InputBox(Message, Title, Default)
    If myvalue = "" Then myvalue = Default
    Text6.Text = myvalue
End If

If Check5 = False Then
    Text6.Text = ""
End If

End Sub

Private Sub Check6_Click()

If Check6 Then
    Message = "Channel 6 Label"
    Title = "Get Channe6 Label"
    Default = "Channel 6"
    myvalue = InputBox(Message, Title, Default)
    If myvalue = "" Then myvalue = Default

```

```

    Text7.Text = myvalue
End If

If Check6 = False Then
    Text7.Text = ""
End If

End Sub

Private Sub Check7_Click()

If Check7 Then
    Message = "Channel 7 Label"
    Title = "Get Channel 7 Label"
    Default = "Channel 7"
    myvalue = InputBox(Message, Title, Default)
    If myvalue = "" Then myvalue = Default
    Text8.Text = myvalue
End If

If Check7 = False Then
    Text8.Text = ""
End If

End Sub

Private Sub Check8_Click()

If Check8 Then
    Message = "Channel 8 Label"
    Title = "Get Channe8 Label"
    Default = "Channel 8"
    myvalue = InputBox(Message, Title, Default)
    If myvalue = "" Then myvalue = Default
    Text9.Text = myvalue
End If

If Check8 = False Then
    Text9.Text = ""
End If

End Sub

Private Sub Check9_Click()
If Option1 = False Then Check9 = False

End Sub

Private Sub Command1_Click()
Close #1
If MSComm1.PortOpen = True Then
MSComm1.PortOpen = False
End
End Sub

Private Sub Option1_Click()
If chn < 1 Then
    chn = 1
    Text10.Text = chn
End If

MSComm1.PortOpen = True
labela:

If Option5 Then plt = 1 Else plt = 0
If Option3 Then sav = 1 Else sav = 0
If Option4 Then cal = 1 Else cal = 0
If plt <> 1 And sav <> 1 And cal <> 1 Then
    Option1 = False
    Option2 = True
    Exit Sub
End If
If Option3 Then Text1.Text = "Saving Data"

While plt = 1
If Option3 Or Option4 Then
    plt = 0
    GoTo labela
End If
Graph1.ThisSet = 1
Graph1.NumSets = 1
Graph1.ThisPoint = 1

For kk = 1 To 250

    A$ = "rb" + Str$(chn - 1)
    MSComm1.Output = A$ + Chr$(13)
    Do
        dummy = DoEvents()

    Loop Until MSComm1.InBufferCount >= 5

    strain = Val(MSComm1.Input) - 2048

    Graph1.GraphData = strain

Next kk

Graph1.DrawMode = 2

```



```

Graph1.DrawMode = 3

Wend

While sav = 1
  If Option5 Or Option4 Then
    sav = 0
    GoTo labela
  End If
  MSComm1.Output = "rb" + Chr$(13)
  Do
    dummy = DoEvents()

  Loop Until MSComm1.InBufferCount >= 40

  Write #1, MSComm1.Input,

Wend

While cal = 1
  If Option3 Or Option5 Then
    cal = 0
    GoTo labela
  End If
  MSComm1.Output = "rb" + Chr$(13)

  Do
    dummy = DoEvents()
    Loop Until MSComm1.InBufferCount >= 40
    Text1.Text = MSComm1.Input

Wend

End Sub

Private Sub Option2_Click()
  Close #1
  Graph1.DrawMode = 1
  If MSComm1.PortOpen = True Then
    MSComm1.PortOpen = False
  If Option2 Then Text1.Text = ""
  If Option2 = True Then Option3 = False
  If Option2 = True Then Option4 = False
  If Option2 = True Then Option5 = False
  End Sub

Private Sub Option3_Click()

Title = "GetFileName"
Default = "c:\strain.dat"
myvalue = InputBox(Message, Title, Default)
If myvalue = "" Then myvalue = Default
Open myvalue For Output As #1
Text1.Text = "Ready to Save Data"
If Option3 Then sav = 1
End Sub

Private Sub Option4_Click()

If Option1 = False Then Option4 = False
If Option4 Then Text1.Text = "Calibration Mode"
'Load Calibrate
'Calibrate.Show
If Option4 Then cal = 1
End Sub

Private Sub Option5_Click()

If chn < 1 Then
  chn = 1
  Text10.Text = chn
End If
If Option5 Then
  b$ = "Plotting Channel " + Chr$(chn + 48)
  Text1.Text = b$
  plt = 1
End If
End Sub

Private Sub SpinButton1_SpinDown()
  chn = chn - 1
  If chn < 1 Then chn = 1
  Text10.Text = chn
  Text1.Text = "Plotting Channel " + Chr$(48 +
  chn)
End Sub

Private Sub SpinButton1_SpinUp()
  chn = chn + 1
  If chn > 8 Then chn = 8
  Text10.Text = chn
  Text1.Text = "Plotting Channel " + Chr$(48 +
  chn)
End Sub

Message = "Enter a filename with path"

```

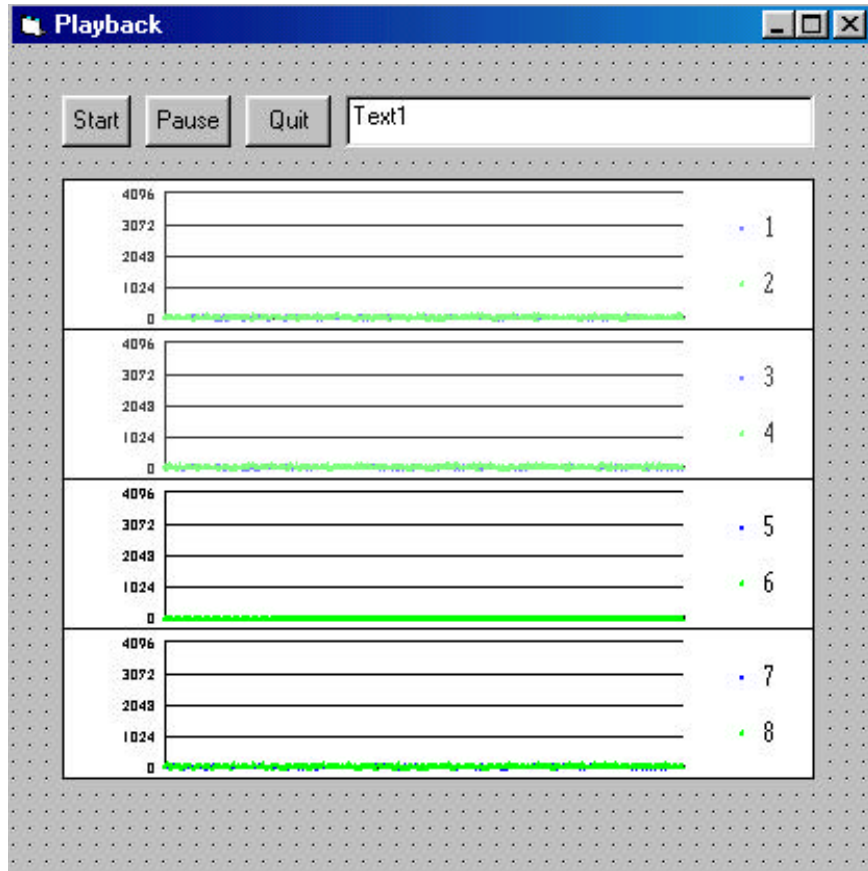


Figure 107. Playback Software Screen

```

VERSION 4.00
Begin VB.Form Form1
    Caption       = "Playback"
    ClientHeight  = 5940
    ClientLeft    = 3810
    ClientTop     = 1695
    ClientWidth   = 6180
    Height        = 6345
    Left          = 3750
    LinkTopic     = "Form1"
    ScaleHeight   = 5940
    ScaleWidth    = 6180
    Top           = 1350
    Width         = 6300
    Begin VB.CommandButton Command3
        Caption     = "Quit"
        Height      = 375
        Left        = 1680
        TabIndex    = 7
        Top         = 360
        Width       = 615
    End
    Begin VB.CommandButton Command2
        Caption     = "Pause"
        Height      = 375
        Left        = 960
        TabIndex    = 4
        Top         = 360
        Width       = 615
    End
    Begin VB.TextBox Text1
        Height      = 375
        Left        = 2400
        TabIndex    = 1
        Text        = "Text1"
        Top         = 360
    End
End

```

```

Width      = 3375
End
Begin VB.CommandButton Command1
Caption    = "Start"
Height    = 375
Left      = 360
TabIndex  = 0
Top       = 360
Width     = 495
End
Begin GraphLib.Graph Graph4
Height    = 1095
Left      = 360
TabIndex  = 6
Top       = 4200
Width     = 5415
_Version  = 65536
_ExtentX = 9551
_ExtentY = 1931
_StockProps = 96
BorderStyle = 1
GraphStyle = 5
GraphType = 6
GridStyle = 1
LabelEvery = 100
Labels    = 3
NumPoints = 250
NumSets   = 2
PatternedLines = 1
RandomData = 1
ThickLines = 0
TickEvery = 50
Ticks     = 2
YAxisMax  = 4096
YAxisStyle = 2
YAxisTicks = 4
ColorData = 0
ExtraData = 0
ExtraData[] = 0
FontFamily = 4
FontSize   = 4
FontSize[0] = 200
FontSize[1] = 150
FontSize[2] = 100
FontSize[3] = 100
FontStyle = 4
GraphData = 0
GraphData[] = 0
LabelText = 0
LegendText = 2
LegendText[0] = "7"
LegendText[1] = "8"
PatternData = 0
SymbolData = 0
XPosData = 0
XPosData[] = 0
End
Begin GraphLib.Graph Graph3
Height    = 1095
Left      = 360
TabIndex  = 5
Top       = 3120
Width     = 5415
_Version  = 65536
_ExtentX = 9551
_ExtentY = 1931
_StockProps = 96
BorderStyle = 1
GraphStyle = 5
GraphType = 6
GridStyle = 1
LabelEvery = 1000
Labels    = 3
NumPoints = 250
NumSets   = 2
PatternedLines = 1
RandomData = 0
ThickLines = 0
TickEvery = 50
Ticks     = 2
YAxisMax  = 4096
YAxisStyle = 2
YAxisTicks = 4
ColorData = 0
ExtraData = 0
ExtraData[] = 0
FontFamily = 4
FontSize   = 4
FontSize[0] = 200
FontSize[1] = 150
FontSize[2] = 100
FontSize[3] = 100
FontStyle = 4
GraphData = 2
GraphData[] = 250
GraphData[0,0] = 0
GraphData[0,1] = 0
GraphData[0,2] = 0
GraphData[0,3] = 0
GraphData[0,4] = 0
GraphData[0,5] = 0
GraphData[0,6] = 0
GraphData[0,7] = 0
GraphData[0,8] = 0

```

GraphData[0,9] = 0  
GraphData[0,10] = 0  
GraphData[0,11] = 0  
GraphData[0,12] = 0  
GraphData[0,13] = 0  
GraphData[0,14] = 0  
GraphData[0,15] = 0  
GraphData[0,16] = 0  
GraphData[0,17] = 0  
GraphData[0,18] = 0  
GraphData[0,19] = 0  
GraphData[0,20] = 0  
GraphData[0,21] = 0  
GraphData[0,22] = 0  
GraphData[0,23] = 0  
GraphData[0,24] = 0  
GraphData[0,25] = 0  
GraphData[0,26] = 0  
GraphData[0,27] = 0  
GraphData[0,28] = 0  
GraphData[0,29] = 0  
GraphData[0,30] = 0  
GraphData[0,31] = 0  
GraphData[0,32] = 0  
GraphData[0,33] = 0  
GraphData[0,34] = 0  
GraphData[0,35] = 0  
GraphData[0,36] = 0  
GraphData[0,37] = 0  
GraphData[0,38] = 0  
GraphData[0,39] = 0  
GraphData[0,40] = 0  
GraphData[0,41] = 0  
GraphData[0,42] = 0  
GraphData[0,43] = 0  
GraphData[0,44] = 0  
GraphData[0,45] = 0  
GraphData[0,46] = 0  
GraphData[0,47] = 0  
GraphData[0,48] = 0  
GraphData[0,49] = 0  
GraphData[0,50] = 0  
GraphData[0,51] = 0  
GraphData[0,52] = 0  
GraphData[0,53] = 0  
GraphData[0,54] = 0  
GraphData[0,55] = 0  
GraphData[0,56] = 0  
GraphData[0,57] = 0  
GraphData[0,58] = 0  
GraphData[0,59] = 0  
GraphData[0,60] = 0  
GraphData[0,61] = 0  
GraphData[0,62] = 0  
GraphData[0,63] = 0  
GraphData[0,64] = 0  
GraphData[0,65] = 0  
GraphData[0,66] = 0  
GraphData[0,67] = 0  
GraphData[0,68] = 0  
GraphData[0,69] = 0  
GraphData[0,70] = 0  
GraphData[0,71] = 0  
GraphData[0,72] = 0  
GraphData[0,73] = 0  
GraphData[0,74] = 0  
GraphData[0,75] = 0  
GraphData[0,76] = 0  
GraphData[0,77] = 0  
GraphData[0,78] = 0  
GraphData[0,79] = 0  
GraphData[0,80] = 0  
GraphData[0,81] = 0  
GraphData[0,82] = 0  
GraphData[0,83] = 0  
GraphData[0,84] = 0  
GraphData[0,85] = 0  
GraphData[0,86] = 0  
GraphData[0,87] = 0  
GraphData[0,88] = 0  
GraphData[0,89] = 0  
GraphData[0,90] = 0  
GraphData[0,91] = 0  
GraphData[0,92] = 0  
GraphData[0,93] = 0  
GraphData[0,94] = 0  
GraphData[0,95] = 0  
GraphData[0,96] = 0  
GraphData[0,97] = 0  
GraphData[0,98] = 0  
GraphData[0,99] = 0  
GraphData[0,100]= 0  
GraphData[0,101]= 0  
GraphData[0,102]= 0  
GraphData[0,103]= 0  
GraphData[0,104]= 0  
GraphData[0,105]= 0  
GraphData[0,106]= 0  
GraphData[0,107]= 0  
GraphData[0,108]= 0  
GraphData[0,109]= 0  
GraphData[0,110]= 0  
GraphData[0,111]= 0  
GraphData[0,112]= 0

GraphData[0,113]= 0	GraphData[0,165]= 0
GraphData[0,114]= 0	GraphData[0,166]= 0
GraphData[0,115]= 0	GraphData[0,167]= 0
GraphData[0,116]= 0	GraphData[0,168]= 0
GraphData[0,117]= 0	GraphData[0,169]= 0
GraphData[0,118]= 0	GraphData[0,170]= 0
GraphData[0,119]= 0	GraphData[0,171]= 0
GraphData[0,120]= 0	GraphData[0,172]= 0
GraphData[0,121]= 0	GraphData[0,173]= 0
GraphData[0,122]= 0	GraphData[0,174]= 0
GraphData[0,123]= 0	GraphData[0,175]= 0
GraphData[0,124]= 0	GraphData[0,176]= 0
GraphData[0,125]= 0	GraphData[0,177]= 0
GraphData[0,126]= 0	GraphData[0,178]= 0
GraphData[0,127]= 0	GraphData[0,179]= 0
GraphData[0,128]= 0	GraphData[0,180]= 0
GraphData[0,129]= 0	GraphData[0,181]= 0
GraphData[0,130]= 0	GraphData[0,182]= 0
GraphData[0,131]= 0	GraphData[0,183]= 0
GraphData[0,132]= 0	GraphData[0,184]= 0
GraphData[0,133]= 0	GraphData[0,185]= 0
GraphData[0,134]= 0	GraphData[0,186]= 0
GraphData[0,135]= 0	GraphData[0,187]= 0
GraphData[0,136]= 0	GraphData[0,188]= 0
GraphData[0,137]= 0	GraphData[0,189]= 0
GraphData[0,138]= 0	GraphData[0,190]= 0
GraphData[0,139]= 0	GraphData[0,191]= 0
GraphData[0,140]= 0	GraphData[0,192]= 0
GraphData[0,141]= 0	GraphData[0,193]= 0
GraphData[0,142]= 0	GraphData[0,194]= 0
GraphData[0,143]= 0	GraphData[0,195]= 0
GraphData[0,144]= 0	GraphData[0,196]= 0
GraphData[0,145]= 0	GraphData[0,197]= 0
GraphData[0,146]= 0	GraphData[0,198]= 0
GraphData[0,147]= 0	GraphData[0,199]= 0
GraphData[0,148]= 0	GraphData[0,200]= 0
GraphData[0,149]= 0	GraphData[0,201]= 0
GraphData[0,150]= 0	GraphData[0,202]= 0
GraphData[0,151]= 0	GraphData[0,203]= 0
GraphData[0,152]= 0	GraphData[0,204]= 0
GraphData[0,153]= 0	GraphData[0,205]= 0
GraphData[0,154]= 0	GraphData[0,206]= 0
GraphData[0,155]= 0	GraphData[0,207]= 0
GraphData[0,156]= 0	GraphData[0,208]= 0
GraphData[0,157]= 0	GraphData[0,209]= 0
GraphData[0,158]= 0	GraphData[0,210]= 0
GraphData[0,159]= 0	GraphData[0,211]= 0
GraphData[0,160]= 0	GraphData[0,212]= 0
GraphData[0,161]= 0	GraphData[0,213]= 0
GraphData[0,162]= 0	GraphData[0,214]= 0
GraphData[0,163]= 0	GraphData[0,215]= 0
GraphData[0,164]= 0	GraphData[0,216]= 0

GraphData[0,217]= 0	GraphData[1,19] = 0
GraphData[0,218]= 0	GraphData[1,20] = 0
GraphData[0,219]= 0	GraphData[1,21] = 0
GraphData[0,220]= 0	GraphData[1,22] = 0
GraphData[0,221]= 0	GraphData[1,23] = 0
GraphData[0,222]= 0	GraphData[1,24] = 0
GraphData[0,223]= 0	GraphData[1,25] = 0
GraphData[0,224]= 0	GraphData[1,26] = 0
GraphData[0,225]= 0	GraphData[1,27] = 0
GraphData[0,226]= 0	GraphData[1,28] = 0
GraphData[0,227]= 0	GraphData[1,29] = 0
GraphData[0,228]= 0	GraphData[1,30] = 0
GraphData[0,229]= 0	GraphData[1,31] = 0
GraphData[0,230]= 0	GraphData[1,32] = 0
GraphData[0,231]= 0	GraphData[1,33] = 0
GraphData[0,232]= 0	GraphData[1,34] = 0
GraphData[0,233]= 0	GraphData[1,35] = 0
GraphData[0,234]= 0	GraphData[1,36] = 0
GraphData[0,235]= 0	GraphData[1,37] = 0
GraphData[0,236]= 0	GraphData[1,38] = 0
GraphData[0,237]= 0	GraphData[1,39] = 0
GraphData[0,238]= 0	GraphData[1,40] = 0
GraphData[0,239]= 0	GraphData[1,41] = 0
GraphData[0,240]= 0	GraphData[1,42] = 0
GraphData[0,241]= 0	GraphData[1,43] = 0
GraphData[0,242]= 0	GraphData[1,44] = 0
GraphData[0,243]= 0	GraphData[1,45] = 0
GraphData[0,244]= 0	GraphData[1,46] = 0
GraphData[0,245]= 0	GraphData[1,47] = 0
GraphData[0,246]= 0	GraphData[1,48] = 0
GraphData[0,247]= 0	GraphData[1,49] = 0
GraphData[0,248]= 0	GraphData[1,50] = 0
GraphData[0,249]= 0	GraphData[1,51] = 0
GraphData[1,0] = 0	GraphData[1,52] = 0
GraphData[1,1] = 0	GraphData[1,53] = 0
GraphData[1,2] = 0	GraphData[1,54] = 0
GraphData[1,3] = 0	GraphData[1,55] = 0
GraphData[1,4] = 0	GraphData[1,56] = 0
GraphData[1,5] = 0	GraphData[1,57] = 0
GraphData[1,6] = 0	GraphData[1,58] = 0
GraphData[1,7] = 0	GraphData[1,59] = 0
GraphData[1,8] = 0	GraphData[1,60] = 0
GraphData[1,9] = 0	GraphData[1,61] = 0
GraphData[1,10] = 0	GraphData[1,62] = 0
GraphData[1,11] = 0	GraphData[1,63] = 0
GraphData[1,12] = 0	GraphData[1,64] = 0
GraphData[1,13] = 0	GraphData[1,65] = 0
GraphData[1,14] = 0	GraphData[1,66] = 0
GraphData[1,15] = 0	GraphData[1,67] = 0
GraphData[1,16] = 0	GraphData[1,68] = 0
GraphData[1,17] = 0	GraphData[1,69] = 0
GraphData[1,18] = 0	GraphData[1,70] = 0

GraphData[1,71] = 0	GraphData[1,123]= 0
GraphData[1,72] = 0	GraphData[1,124]= 0
GraphData[1,73] = 0	GraphData[1,125]= 0
GraphData[1,74] = 0	GraphData[1,126]= 0
GraphData[1,75] = 0	GraphData[1,127]= 0
GraphData[1,76] = 0	GraphData[1,128]= 0
GraphData[1,77] = 0	GraphData[1,129]= 0
GraphData[1,78] = 0	GraphData[1,130]= 0
GraphData[1,79] = 0	GraphData[1,131]= 0
GraphData[1,80] = 0	GraphData[1,132]= 0
GraphData[1,81] = 0	GraphData[1,133]= 0
GraphData[1,82] = 0	GraphData[1,134]= 0
GraphData[1,83] = 0	GraphData[1,135]= 0
GraphData[1,84] = 0	GraphData[1,136]= 0
GraphData[1,85] = 0	GraphData[1,137]= 0
GraphData[1,86] = 0	GraphData[1,138]= 0
GraphData[1,87] = 0	GraphData[1,139]= 0
GraphData[1,88] = 0	GraphData[1,140]= 0
GraphData[1,89] = 0	GraphData[1,141]= 0
GraphData[1,90] = 0	GraphData[1,142]= 0
GraphData[1,91] = 0	GraphData[1,143]= 0
GraphData[1,92] = 0	GraphData[1,144]= 0
GraphData[1,93] = 0	GraphData[1,145]= 0
GraphData[1,94] = 0	GraphData[1,146]= 0
GraphData[1,95] = 0	GraphData[1,147]= 0
GraphData[1,96] = 0	GraphData[1,148]= 0
GraphData[1,97] = 0	GraphData[1,149]= 0
GraphData[1,98] = 0	GraphData[1,150]= 0
GraphData[1,99] = 0	GraphData[1,151]= 0
GraphData[1,100]= 0	GraphData[1,152]= 0
GraphData[1,101]= 0	GraphData[1,153]= 0
GraphData[1,102]= 0	GraphData[1,154]= 0
GraphData[1,103]= 0	GraphData[1,155]= 0
GraphData[1,104]= 0	GraphData[1,156]= 0
GraphData[1,105]= 0	GraphData[1,157]= 0
GraphData[1,106]= 0	GraphData[1,158]= 0
GraphData[1,107]= 0	GraphData[1,159]= 0
GraphData[1,108]= 0	GraphData[1,160]= 0
GraphData[1,109]= 0	GraphData[1,161]= 0
GraphData[1,110]= 0	GraphData[1,162]= 0
GraphData[1,111]= 0	GraphData[1,163]= 0
GraphData[1,112]= 0	GraphData[1,164]= 0
GraphData[1,113]= 0	GraphData[1,165]= 0
GraphData[1,114]= 0	GraphData[1,166]= 0
GraphData[1,115]= 0	GraphData[1,167]= 0
GraphData[1,116]= 0	GraphData[1,168]= 0
GraphData[1,117]= 0	GraphData[1,169]= 0
GraphData[1,118]= 0	GraphData[1,170]= 0
GraphData[1,119]= 0	GraphData[1,171]= 0
GraphData[1,120]= 0	GraphData[1,172]= 0
GraphData[1,121]= 0	GraphData[1,173]= 0
GraphData[1,122]= 0	GraphData[1,174]= 0

```

GraphData[1,175]= 0
GraphData[1,176]= 0
GraphData[1,177]= 0
GraphData[1,178]= 0
GraphData[1,179]= 0
GraphData[1,180]= 0
GraphData[1,181]= 0
GraphData[1,182]= 0
GraphData[1,183]= 0
GraphData[1,184]= 0
GraphData[1,185]= 0
GraphData[1,186]= 0
GraphData[1,187]= 0
GraphData[1,188]= 0
GraphData[1,189]= 0
GraphData[1,190]= 0
GraphData[1,191]= 0
GraphData[1,192]= 0
GraphData[1,193]= 0
GraphData[1,194]= 0
GraphData[1,195]= 0
GraphData[1,196]= 0
GraphData[1,197]= 0
GraphData[1,198]= 0
GraphData[1,199]= 0
GraphData[1,200]= 0
GraphData[1,201]= 0
GraphData[1,202]= 0
GraphData[1,203]= 0
GraphData[1,204]= 0
GraphData[1,205]= 0
GraphData[1,206]= 0
GraphData[1,207]= 0
GraphData[1,208]= 0
GraphData[1,209]= 0
GraphData[1,210]= 0
GraphData[1,211]= 0
GraphData[1,212]= 0
GraphData[1,213]= 0
GraphData[1,214]= 0
GraphData[1,215]= 0
GraphData[1,216]= 0
GraphData[1,217]= 0
GraphData[1,218]= 0
GraphData[1,219]= 0
GraphData[1,220]= 0
GraphData[1,221]= 0
GraphData[1,222]= 0
GraphData[1,223]= 0
GraphData[1,224]= 0
GraphData[1,225]= 0
GraphData[1,226]= 0
GraphData[1,227]= 0
GraphData[1,228]= 0
GraphData[1,229]= 0
GraphData[1,230]= 0
GraphData[1,231]= 0
GraphData[1,232]= 0
GraphData[1,233]= 0
GraphData[1,234]= 0
GraphData[1,235]= 0
GraphData[1,236]= 0
GraphData[1,237]= 0
GraphData[1,238]= 0
GraphData[1,239]= 0
GraphData[1,240]= 0
GraphData[1,241]= 0
GraphData[1,242]= 0
GraphData[1,243]= 0
GraphData[1,244]= 0
GraphData[1,245]= 0
GraphData[1,246]= 0
GraphData[1,247]= 0
GraphData[1,248]= 0
GraphData[1,249]= 0
LabelText = 0
LegendText = 2
LegendText[0] = "5"
LegendText[1] = "6"
PatternData = 0
SymbolData = 0
XPosData = 0
XPosData[] = 0
End
Begin GraphLib.Graph Graph2
Height = 1095
Left = 360
TabIndex = 3
Top = 2040
Width = 5415
_Version = 65536
_ExtentX = 9551
_ExtentY = 1931
_StockProps = 96
BorderStyle = 1
GraphStyle = 5
GraphType = 6
GridStyle = 1
LabelEvery = 100
Labels = 3
NumPoints = 250
NumSets = 2
Palette = 1
PatternedLines = 1

```



```

RandomData      = 1
ThickLines      = 0
TickEvery       = 50
Ticks           = 2
YAxisMax        = 4096
YAxisStyle      = 2
YAxisTicks      = 4
ColorData       = 0
ExtraData       = 0
ExtraData[]     = 0
FontFamily      = 4
FontSize        = 4
FontSize[0]     = 50
FontSize[1]     = 100
FontSize[2]     = 100
FontSize[3]     = 100
FontStyle       = 4
GraphData       = 1
GraphData[]     = 250
GraphData[0,0] = 0
GraphData[0,1] = 0
GraphData[0,2] = 0
GraphData[0,3] = 0
GraphData[0,4] = 0
GraphData[0,5] = 0
GraphData[0,6] = 0
GraphData[0,7] = 0
GraphData[0,8] = 0
GraphData[0,9] = 0
GraphData[0,10] = 0
GraphData[0,11] = 0
GraphData[0,12] = 0
GraphData[0,13] = 0
GraphData[0,14] = 0
GraphData[0,15] = 0
GraphData[0,16] = 0
GraphData[0,17] = 0
GraphData[0,18] = 0
GraphData[0,19] = 0
GraphData[0,20] = 0
GraphData[0,21] = 0
GraphData[0,22] = 0
GraphData[0,23] = 0
GraphData[0,24] = 0
GraphData[0,25] = 0
GraphData[0,26] = 0
GraphData[0,27] = 0
GraphData[0,28] = 0
GraphData[0,29] = 0
GraphData[0,30] = 0
GraphData[0,31] = 0
GraphData[0,32] = 0
GraphData[0,33] = 0
GraphData[0,34] = 0
GraphData[0,35] = 0
GraphData[0,36] = 0
GraphData[0,37] = 0
GraphData[0,38] = 0
GraphData[0,39] = 0
GraphData[0,40] = 0
GraphData[0,41] = 0
GraphData[0,42] = 0
GraphData[0,43] = 0
GraphData[0,44] = 0
GraphData[0,45] = 0
GraphData[0,46] = 0
GraphData[0,47] = 0
GraphData[0,48] = 0
GraphData[0,49] = 0
GraphData[0,50] = 0
GraphData[0,51] = 0
GraphData[0,52] = 0
GraphData[0,53] = 0
GraphData[0,54] = 0
GraphData[0,55] = 0
GraphData[0,56] = 0
GraphData[0,57] = 0
GraphData[0,58] = 0
GraphData[0,59] = 0
GraphData[0,60] = 0
GraphData[0,61] = 0
GraphData[0,62] = 0
GraphData[0,63] = 0
GraphData[0,64] = 0
GraphData[0,65] = 0
GraphData[0,66] = 0
GraphData[0,67] = 0
GraphData[0,68] = 0
GraphData[0,69] = 0
GraphData[0,70] = 0
GraphData[0,71] = 0
GraphData[0,72] = 0
GraphData[0,73] = 0
GraphData[0,74] = 0
GraphData[0,75] = 0
GraphData[0,76] = 0
GraphData[0,77] = 0
GraphData[0,78] = 0
GraphData[0,79] = 0
GraphData[0,80] = 0
GraphData[0,81] = 0
GraphData[0,82] = 0
GraphData[0,83] = 0
GraphData[0,84] = 0

```

GraphData[0,85] = 0  
GraphData[0,86] = 0  
GraphData[0,87] = 0  
GraphData[0,88] = 0  
GraphData[0,89] = 0  
GraphData[0,90] = 0  
GraphData[0,91] = 0  
GraphData[0,92] = 0  
GraphData[0,93] = 0  
GraphData[0,94] = 0  
GraphData[0,95] = 0  
GraphData[0,96] = 0  
GraphData[0,97] = 0  
GraphData[0,98] = 0  
GraphData[0,99] = 0  
GraphData[0,100]= 0  
GraphData[0,101]= 0  
GraphData[0,102]= 0  
GraphData[0,103]= 0  
GraphData[0,104]= 0  
GraphData[0,105]= 0  
GraphData[0,106]= 0  
GraphData[0,107]= 0  
GraphData[0,108]= 0  
GraphData[0,109]= 0  
GraphData[0,110]= 0  
GraphData[0,111]= 0  
GraphData[0,112]= 0  
GraphData[0,113]= 0  
GraphData[0,114]= 0  
GraphData[0,115]= 0  
GraphData[0,116]= 0  
GraphData[0,117]= 0  
GraphData[0,118]= 0  
GraphData[0,119]= 0  
GraphData[0,120]= 0  
GraphData[0,121]= 0  
GraphData[0,122]= 0  
GraphData[0,123]= 0  
GraphData[0,124]= 0  
GraphData[0,125]= 0  
GraphData[0,126]= 0  
GraphData[0,127]= 0  
GraphData[0,128]= 0  
GraphData[0,129]= 0  
GraphData[0,130]= 0  
GraphData[0,131]= 0  
GraphData[0,132]= 0  
GraphData[0,133]= 0  
GraphData[0,134]= 0  
GraphData[0,135]= 0  
GraphData[0,136]= 0  
GraphData[0,137]= 0  
GraphData[0,138]= 0  
GraphData[0,139]= 0  
GraphData[0,140]= 0  
GraphData[0,141]= 0  
GraphData[0,142]= 0  
GraphData[0,143]= 0  
GraphData[0,144]= 0  
GraphData[0,145]= 0  
GraphData[0,146]= 0  
GraphData[0,147]= 0  
GraphData[0,148]= 0  
GraphData[0,149]= 0  
GraphData[0,150]= 0  
GraphData[0,151]= 0  
GraphData[0,152]= 0  
GraphData[0,153]= 0  
GraphData[0,154]= 0  
GraphData[0,155]= 0  
GraphData[0,156]= 0  
GraphData[0,157]= 0  
GraphData[0,158]= 0  
GraphData[0,159]= 0  
GraphData[0,160]= 0  
GraphData[0,161]= 0  
GraphData[0,162]= 0  
GraphData[0,163]= 0  
GraphData[0,164]= 0  
GraphData[0,165]= 0  
GraphData[0,166]= 0  
GraphData[0,167]= 0  
GraphData[0,168]= 0  
GraphData[0,169]= 0  
GraphData[0,170]= 0  
GraphData[0,171]= 0  
GraphData[0,172]= 0  
GraphData[0,173]= 0  
GraphData[0,174]= 0  
GraphData[0,175]= 0  
GraphData[0,176]= 0  
GraphData[0,177]= 0  
GraphData[0,178]= 0  
GraphData[0,179]= 0  
GraphData[0,180]= 0  
GraphData[0,181]= 0  
GraphData[0,182]= 0  
GraphData[0,183]= 0  
GraphData[0,184]= 0  
GraphData[0,185]= 0  
GraphData[0,186]= 0  
GraphData[0,187]= 0  
GraphData[0,188]= 0

```

GraphData[0,189]= 0
GraphData[0,190]= 0
GraphData[0,191]= 0
GraphData[0,192]= 0
GraphData[0,193]= 0
GraphData[0,194]= 0
GraphData[0,195]= 0
GraphData[0,196]= 0
GraphData[0,197]= 0
GraphData[0,198]= 0
GraphData[0,199]= 0
GraphData[0,200]= 0
GraphData[0,201]= 0
GraphData[0,202]= 0
GraphData[0,203]= 0
GraphData[0,204]= 0
GraphData[0,205]= 0
GraphData[0,206]= 0
GraphData[0,207]= 0
GraphData[0,208]= 0
GraphData[0,209]= 0
GraphData[0,210]= 0
GraphData[0,211]= 0
GraphData[0,212]= 0
GraphData[0,213]= 0
GraphData[0,214]= 0
GraphData[0,215]= 0
GraphData[0,216]= 0
GraphData[0,217]= 0
GraphData[0,218]= 0
GraphData[0,219]= 0
GraphData[0,220]= 0
GraphData[0,221]= 0
GraphData[0,222]= 0
GraphData[0,223]= 0
GraphData[0,224]= 0
GraphData[0,225]= 0
GraphData[0,226]= 0
GraphData[0,227]= 0
GraphData[0,228]= 0
GraphData[0,229]= 0
GraphData[0,230]= 0
GraphData[0,231]= 0
GraphData[0,232]= 0
GraphData[0,233]= 0
GraphData[0,234]= 0
GraphData[0,235]= 0
GraphData[0,236]= 0
GraphData[0,237]= 0
GraphData[0,238]= 0
GraphData[0,239]= 0
GraphData[0,240]= 0
GraphData[0,241]= 0
GraphData[0,242]= 0
GraphData[0,243]= 0
GraphData[0,244]= 0
GraphData[0,245]= 0
GraphData[0,246]= 0
GraphData[0,247]= 0
GraphData[0,248]= 0
GraphData[0,249]= 0
LabelText = 0
LegendText = 2
LegendText[0] = "3"
LegendText[1] = "4"
PatternData = 0
SymbolData = 0
XPosData = 0
XPosData[] = 0
End
Begin GraphLib.Graph Graph1
Height = 1095
Left = 360
TabIndex = 2
Top = 960
Width = 5415
_Version = 65536
_ExtentX = 9551
_ExtentY = 1931
_StockProps = 96
BorderStyle = 1
GraphStyle = 5
GraphType = 6
GridStyle = 1
LabelEvery = 100
Labels = 3
NumPoints = 250
NumSets = 2
Palette = 1
PatternedLines = 1
RandomData = 1
ThickLines = 0
TickEvery = 50
Ticks = 2
YAxisMax = 4096
YAxisPos = 1
YAxisStyle = 2
YAxisTicks = 4
ColorData = 0
ExtraData = 0
ExtraData[] = 0
FontFamily = 4
FontSize = 4
FontSize[0] = 100

```

```
FontSize[1] = 150
FontSize[2] = 100
FontSize[3] = 100
FontStyle   = 4
GraphData   = 2
GraphData[] = 250
GraphData[0,0] = 0
GraphData[0,1] = 0
GraphData[0,2] = 0
GraphData[0,3] = 0
GraphData[0,4] = 0
GraphData[0,5] = 0
GraphData[0,6] = 0
GraphData[0,7] = 0
GraphData[0,8] = 0
GraphData[0,9] = 0
GraphData[0,10] = 0
GraphData[0,11] = 0
GraphData[0,12] = 0
GraphData[0,13] = 0
GraphData[0,14] = 0
GraphData[0,15] = 0
GraphData[0,16] = 0
GraphData[0,17] = 0
GraphData[0,18] = 0
GraphData[0,19] = 0
GraphData[0,20] = 0
GraphData[0,21] = 0
GraphData[0,22] = 0
GraphData[0,23] = 0
GraphData[0,24] = 0
GraphData[0,25] = 0
GraphData[0,26] = 0
GraphData[0,27] = 0
GraphData[0,28] = 0
GraphData[0,29] = 0
GraphData[0,30] = 0
GraphData[0,31] = 0
GraphData[0,32] = 0
GraphData[0,33] = 0
GraphData[0,34] = 0
GraphData[0,35] = 0
GraphData[0,36] = 0
GraphData[0,37] = 0
GraphData[0,38] = 0
GraphData[0,39] = 0
GraphData[0,40] = 0
GraphData[0,41] = 0
GraphData[0,42] = 0
GraphData[0,43] = 0
GraphData[0,44] = 0
GraphData[0,45] = 0
GraphData[0,46] = 0
GraphData[0,47] = 0
GraphData[0,48] = 0
GraphData[0,49] = 0
GraphData[0,50] = 0
GraphData[0,51] = 0
GraphData[0,52] = 0
GraphData[0,53] = 0
GraphData[0,54] = 0
GraphData[0,55] = 0
GraphData[0,56] = 0
GraphData[0,57] = 0
GraphData[0,58] = 0
GraphData[0,59] = 0
GraphData[0,60] = 0
GraphData[0,61] = 0
GraphData[0,62] = 0
GraphData[0,63] = 0
GraphData[0,64] = 0
GraphData[0,65] = 0
GraphData[0,66] = 0
GraphData[0,67] = 0
GraphData[0,68] = 0
GraphData[0,69] = 0
GraphData[0,70] = 0
GraphData[0,71] = 0
GraphData[0,72] = 0
GraphData[0,73] = 0
GraphData[0,74] = 0
GraphData[0,75] = 0
GraphData[0,76] = 0
GraphData[0,77] = 0
GraphData[0,78] = 0
GraphData[0,79] = 0
GraphData[0,80] = 0
GraphData[0,81] = 0
GraphData[0,82] = 0
GraphData[0,83] = 0
GraphData[0,84] = 0
GraphData[0,85] = 0
GraphData[0,86] = 0
GraphData[0,87] = 0
GraphData[0,88] = 0
GraphData[0,89] = 0
GraphData[0,90] = 0
GraphData[0,91] = 0
GraphData[0,92] = 0
GraphData[0,93] = 0
GraphData[0,94] = 0
GraphData[0,95] = 0
GraphData[0,96] = 0
GraphData[0,97] = 0
```

GraphData[0,98] = 0	GraphData[0,150]= 0
GraphData[0,99] = 0	GraphData[0,151]= 0
GraphData[0,100]= 0	GraphData[0,152]= 0
GraphData[0,101]= 0	GraphData[0,153]= 0
GraphData[0,102]= 0	GraphData[0,154]= 0
GraphData[0,103]= 0	GraphData[0,155]= 0
GraphData[0,104]= 0	GraphData[0,156]= 0
GraphData[0,105]= 0	GraphData[0,157]= 0
GraphData[0,106]= 0	GraphData[0,158]= 0
GraphData[0,107]= 0	GraphData[0,159]= 0
GraphData[0,108]= 0	GraphData[0,160]= 0
GraphData[0,109]= 0	GraphData[0,161]= 0
GraphData[0,110]= 0	GraphData[0,162]= 0
GraphData[0,111]= 0	GraphData[0,163]= 0
GraphData[0,112]= 0	GraphData[0,164]= 0
GraphData[0,113]= 0	GraphData[0,165]= 0
GraphData[0,114]= 0	GraphData[0,166]= 0
GraphData[0,115]= 0	GraphData[0,167]= 0
GraphData[0,116]= 0	GraphData[0,168]= 0
GraphData[0,117]= 0	GraphData[0,169]= 0
GraphData[0,118]= 0	GraphData[0,170]= 0
GraphData[0,119]= 0	GraphData[0,171]= 0
GraphData[0,120]= 0	GraphData[0,172]= 0
GraphData[0,121]= 0	GraphData[0,173]= 0
GraphData[0,122]= 0	GraphData[0,174]= 0
GraphData[0,123]= 0	GraphData[0,175]= 0
GraphData[0,124]= 0	GraphData[0,176]= 0
GraphData[0,125]= 0	GraphData[0,177]= 0
GraphData[0,126]= 0	GraphData[0,178]= 0
GraphData[0,127]= 0	GraphData[0,179]= 0
GraphData[0,128]= 0	GraphData[0,180]= 0
GraphData[0,129]= 0	GraphData[0,181]= 0
GraphData[0,130]= 0	GraphData[0,182]= 0
GraphData[0,131]= 0	GraphData[0,183]= 0
GraphData[0,132]= 0	GraphData[0,184]= 0
GraphData[0,133]= 0	GraphData[0,185]= 0
GraphData[0,134]= 0	GraphData[0,186]= 0
GraphData[0,135]= 0	GraphData[0,187]= 0
GraphData[0,136]= 0	GraphData[0,188]= 0
GraphData[0,137]= 0	GraphData[0,189]= 0
GraphData[0,138]= 0	GraphData[0,190]= 0
GraphData[0,139]= 0	GraphData[0,191]= 0
GraphData[0,140]= 0	GraphData[0,192]= 0
GraphData[0,141]= 0	GraphData[0,193]= 0
GraphData[0,142]= 0	GraphData[0,194]= 0
GraphData[0,143]= 0	GraphData[0,195]= 0
GraphData[0,144]= 0	GraphData[0,196]= 0
GraphData[0,145]= 0	GraphData[0,197]= 0
GraphData[0,146]= 0	GraphData[0,198]= 0
GraphData[0,147]= 0	GraphData[0,199]= 0
GraphData[0,148]= 0	GraphData[0,200]= 0
GraphData[0,149]= 0	GraphData[0,201]= 0

GraphData[0,202]= 0	GraphData[1,4] = 0
GraphData[0,203]= 0	GraphData[1,5] = 0
GraphData[0,204]= 0	GraphData[1,6] = 0
GraphData[0,205]= 0	GraphData[1,7] = 0
GraphData[0,206]= 0	GraphData[1,8] = 0
GraphData[0,207]= 0	GraphData[1,9] = 0
GraphData[0,208]= 0	GraphData[1,10] = 0
GraphData[0,209]= 0	GraphData[1,11] = 0
GraphData[0,210]= 0	GraphData[1,12] = 0
GraphData[0,211]= 0	GraphData[1,13] = 0
GraphData[0,212]= 0	GraphData[1,14] = 0
GraphData[0,213]= 0	GraphData[1,15] = 0
GraphData[0,214]= 0	GraphData[1,16] = 0
GraphData[0,215]= 0	GraphData[1,17] = 0
GraphData[0,216]= 0	GraphData[1,18] = 0
GraphData[0,217]= 0	GraphData[1,19] = 0
GraphData[0,218]= 0	GraphData[1,20] = 0
GraphData[0,219]= 0	GraphData[1,21] = 0
GraphData[0,220]= 0	GraphData[1,22] = 0
GraphData[0,221]= 0	GraphData[1,23] = 0
GraphData[0,222]= 0	GraphData[1,24] = 0
GraphData[0,223]= 0	GraphData[1,25] = 0
GraphData[0,224]= 0	GraphData[1,26] = 0
GraphData[0,225]= 0	GraphData[1,27] = 0
GraphData[0,226]= 0	GraphData[1,28] = 0
GraphData[0,227]= 0	GraphData[1,29] = 0
GraphData[0,228]= 0	GraphData[1,30] = 0
GraphData[0,229]= 0	GraphData[1,31] = 0
GraphData[0,230]= 0	GraphData[1,32] = 0
GraphData[0,231]= 0	GraphData[1,33] = 0
GraphData[0,232]= 0	GraphData[1,34] = 0
GraphData[0,233]= 0	GraphData[1,35] = 0
GraphData[0,234]= 0	GraphData[1,36] = 0
GraphData[0,235]= 0	GraphData[1,37] = 0
GraphData[0,236]= 0	GraphData[1,38] = 0
GraphData[0,237]= 0	GraphData[1,39] = 0
GraphData[0,238]= 0	GraphData[1,40] = 0
GraphData[0,239]= 0	GraphData[1,41] = 0
GraphData[0,240]= 0	GraphData[1,42] = 0
GraphData[0,241]= 0	GraphData[1,43] = 0
GraphData[0,242]= 0	GraphData[1,44] = 0
GraphData[0,243]= 0	GraphData[1,45] = 0
GraphData[0,244]= 0	GraphData[1,46] = 0
GraphData[0,245]= 0	GraphData[1,47] = 0
GraphData[0,246]= 0	GraphData[1,48] = 0
GraphData[0,247]= 0	GraphData[1,49] = 0
GraphData[0,248]= 0	GraphData[1,50] = 0
GraphData[0,249]= 0	GraphData[1,51] = 0
GraphData[1,0] = 0	GraphData[1,52] = 0
GraphData[1,1] = 0	GraphData[1,53] = 0
GraphData[1,2] = 0	GraphData[1,54] = 0
GraphData[1,3] = 0	GraphData[1,55] = 0

GraphData[1,56] = 0	GraphData[1,108]= 0
GraphData[1,57] = 0	GraphData[1,109]= 0
GraphData[1,58] = 0	GraphData[1,110]= 0
GraphData[1,59] = 0	GraphData[1,111]= 0
GraphData[1,60] = 0	GraphData[1,112]= 0
GraphData[1,61] = 0	GraphData[1,113]= 0
GraphData[1,62] = 0	GraphData[1,114]= 0
GraphData[1,63] = 0	GraphData[1,115]= 0
GraphData[1,64] = 0	GraphData[1,116]= 0
GraphData[1,65] = 0	GraphData[1,117]= 0
GraphData[1,66] = 0	GraphData[1,118]= 0
GraphData[1,67] = 0	GraphData[1,119]= 0
GraphData[1,68] = 0	GraphData[1,120]= 0
GraphData[1,69] = 0	GraphData[1,121]= 0
GraphData[1,70] = 0	GraphData[1,122]= 0
GraphData[1,71] = 0	GraphData[1,123]= 0
GraphData[1,72] = 0	GraphData[1,124]= 0
GraphData[1,73] = 0	GraphData[1,125]= 0
GraphData[1,74] = 0	GraphData[1,126]= 0
GraphData[1,75] = 0	GraphData[1,127]= 0
GraphData[1,76] = 0	GraphData[1,128]= 0
GraphData[1,77] = 0	GraphData[1,129]= 0
GraphData[1,78] = 0	GraphData[1,130]= 0
GraphData[1,79] = 0	GraphData[1,131]= 0
GraphData[1,80] = 0	GraphData[1,132]= 0
GraphData[1,81] = 0	GraphData[1,133]= 0
GraphData[1,82] = 0	GraphData[1,134]= 0
GraphData[1,83] = 0	GraphData[1,135]= 0
GraphData[1,84] = 0	GraphData[1,136]= 0
GraphData[1,85] = 0	GraphData[1,137]= 0
GraphData[1,86] = 0	GraphData[1,138]= 0
GraphData[1,87] = 0	GraphData[1,139]= 0
GraphData[1,88] = 0	GraphData[1,140]= 0
GraphData[1,89] = 0	GraphData[1,141]= 0
GraphData[1,90] = 0	GraphData[1,142]= 0
GraphData[1,91] = 0	GraphData[1,143]= 0
GraphData[1,92] = 0	GraphData[1,144]= 0
GraphData[1,93] = 0	GraphData[1,145]= 0
GraphData[1,94] = 0	GraphData[1,146]= 0
GraphData[1,95] = 0	GraphData[1,147]= 0
GraphData[1,96] = 0	GraphData[1,148]= 0
GraphData[1,97] = 0	GraphData[1,149]= 0
GraphData[1,98] = 0	GraphData[1,150]= 0
GraphData[1,99] = 0	GraphData[1,151]= 0
GraphData[1,100]= 0	GraphData[1,152]= 0
GraphData[1,101]= 0	GraphData[1,153]= 0
GraphData[1,102]= 0	GraphData[1,154]= 0
GraphData[1,103]= 0	GraphData[1,155]= 0
GraphData[1,104]= 0	GraphData[1,156]= 0
GraphData[1,105]= 0	GraphData[1,157]= 0
GraphData[1,106]= 0	GraphData[1,158]= 0
GraphData[1,107]= 0	GraphData[1,159]= 0

```

GraphData[1,160]= 0
GraphData[1,161]= 0
GraphData[1,162]= 0
GraphData[1,163]= 0
GraphData[1,164]= 0
GraphData[1,165]= 0
GraphData[1,166]= 0
GraphData[1,167]= 0
GraphData[1,168]= 0
GraphData[1,169]= 0
GraphData[1,170]= 0
GraphData[1,171]= 0
GraphData[1,172]= 0
GraphData[1,173]= 0
GraphData[1,174]= 0
GraphData[1,175]= 0
GraphData[1,176]= 0
GraphData[1,177]= 0
GraphData[1,178]= 0
GraphData[1,179]= 0
GraphData[1,180]= 0
GraphData[1,181]= 0
GraphData[1,182]= 0
GraphData[1,183]= 0
GraphData[1,184]= 0
GraphData[1,185]= 0
GraphData[1,186]= 0
GraphData[1,187]= 0
GraphData[1,188]= 0
GraphData[1,189]= 0
GraphData[1,190]= 0
GraphData[1,191]= 0
GraphData[1,192]= 0
GraphData[1,193]= 0
GraphData[1,194]= 0
GraphData[1,195]= 0
GraphData[1,196]= 0
GraphData[1,197]= 0
GraphData[1,198]= 0
GraphData[1,199]= 0
GraphData[1,200]= 0
GraphData[1,201]= 0
GraphData[1,202]= 0
GraphData[1,203]= 0
GraphData[1,204]= 0
GraphData[1,205]= 0
GraphData[1,206]= 0
GraphData[1,207]= 0
GraphData[1,208]= 0
GraphData[1,209]= 0
GraphData[1,210]= 0
GraphData[1,211]= 0
GraphData[1,212]= 0
GraphData[1,213]= 0
GraphData[1,214]= 0
GraphData[1,215]= 0
GraphData[1,216]= 0
GraphData[1,217]= 0
GraphData[1,218]= 0
GraphData[1,219]= 0
GraphData[1,220]= 0
GraphData[1,221]= 0
GraphData[1,222]= 0
GraphData[1,223]= 0
GraphData[1,224]= 0
GraphData[1,225]= 0
GraphData[1,226]= 0
GraphData[1,227]= 0
GraphData[1,228]= 0
GraphData[1,229]= 0
GraphData[1,230]= 0
GraphData[1,231]= 0
GraphData[1,232]= 0
GraphData[1,233]= 0
GraphData[1,234]= 0
GraphData[1,235]= 0
GraphData[1,236]= 0
GraphData[1,237]= 0
GraphData[1,238]= 0
GraphData[1,239]= 0
GraphData[1,240]= 0
GraphData[1,241]= 0
GraphData[1,242]= 0
GraphData[1,243]= 0
GraphData[1,244]= 0
GraphData[1,245]= 0
GraphData[1,246]= 0
GraphData[1,247]= 0
GraphData[1,248]= 0
GraphData[1,249]= 0
LabelText = 0
LegendText = 8
LegendText[0] = "1"
LegendText[1] = "2"
LegendText[2] = "3"
LegendText[3] = "4"
LegendText[4] = "5"
LegendText[5] = "6"
LegendText[6] = "7"
LegendText[7] = "8"
PatternData = 0
SymbolData = 0
XPosData = 0
XPosData[] = 0

```



```

End
End
Attribute VB_Name = "Form1"
Attribute VB_Creatable = False
Attribute VB_Exposed = False
Dim chn(8)
Private Sub Command1_Click()
Open "c:\strain.dat" For Input As #1
  lf = LOF(1)

  Graph1.ThisSet = 1
  Graph1.NumSets = 2
  Graph1.ThisPoint = 1
  Graph1.AutoInc = 1

  Graph2.ThisSet = 1
  Graph2.NumSets = 2
  Graph2.ThisPoint = 1
  Graph2.AutoInc = 1

  Graph3.ThisSet = 1
  Graph3.NumSets = 2
  Graph3.ThisPoint = 1
  Graph3.AutoInc = 1

  Graph4.ThisSet = 1
  Graph4.NumSets = 2
  Graph4.ThisPoint = 1
  Graph4.AutoInc = 1

While Not (EOF(1))
  For j = 1 To 250
  If EOF(1) Then Exit Sub
  Input #1, a$

  text1.Text = a$
    Graph1.ThisPoint = j
    Graph2.ThisPoint = j
    Graph3.ThisPoint = j
    Graph4.ThisPoint = j

  For i = 0 To 7

    chn(i + 1) = Val(Mid(a$, i * 5 + 1, 4))

  Next i

  Graph1.ThisSet = 1
  Graph1.GraphData = chn(1)

  Graph1.ThisSet = 2
  Graph1.GraphData = chn(2)

  Graph2.ThisSet = 1
  Graph2.GraphData = chn(3)
  Graph2.ThisSet = 2
  Graph2.GraphData = chn(4)

  Graph3.ThisSet = 1
  Graph3.GraphData = chn(5)
  Graph3.ThisSet = 2
  Graph3.GraphData = chn(6)

  Graph4.ThisSet = 1
  Graph4.GraphData = chn(7)
  Graph4.ThisSet = 2
  Graph4.GraphData = chn(8)

  text1.Text = chn(1) & Chr$(32) & chn(2) &
Chr$(32) & chn(3) & Chr$(32) & chn(4) &
Chr$(32) & chn(5) & Chr$(32) & chn(6) &
Chr$(32) & chn(7) & Chr$(32) & chn(8)
  start = Timer
  'Do While Timer < start + 0.002
  '  DoEvents
  'Loop

  Next j

  Graph1.DrawMode = 2
  Graph1.DrawMode = 3
  Graph2.DrawMode = 2
  Graph2.DrawMode = 3
  Graph3.DrawMode = 2
  Graph3.DrawMode = 3
  Graph4.DrawMode = 2
  Graph4.DrawMode = 3
Wend
Close #1

End Sub

Private Sub Command2_Click()

Do While 1
  DoEvents

```

```
Loop  
End Sub
```

```
Private Sub Command3_Click()  
Close #1  
End  
End Sub
```

APPENDIX F

PROGRAMS FOR LIFETIME PREDICTION

### Goodman Diagram Interpolation

The following is a summary of the method used to allow calculations of the number of constant amplitude cycles to failure at any given loading cycle. Consider a Goodman diagram's radial line of constant R-value,  $R_3$ , that is bounded by two radial lines,  $R_1$  and  $R_2$ , from tested R-values as shown in Figure 108. A line of constant cycles to failure,  $N$ , is shown connecting the two known R-value radial lines. This line is between the points  $(S_{\text{mean1}}, S_{\text{alt1}})$  and  $(S_{\text{mean2}}, S_{\text{alt2}})$  and passes through the point  $(S_{\text{mean3}}, S_{\text{alt3}})$  and must be of constant slope to satisfy the Goodman failure criterion. The slope of this line can be determined as

$$\frac{S_{\text{alt2}} - S_{\text{alt3}}}{S_{\text{mean2}} - S_{\text{mean3}}} = \frac{S_{\text{alt1}} - S_{\text{alt3}}}{S_{\text{mean1}} - S_{\text{mean3}}}$$

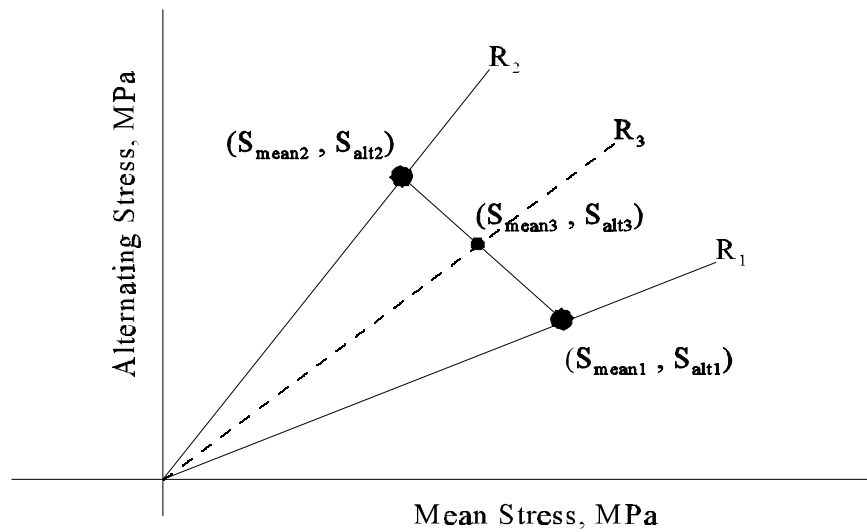


Figure 108. Goodman Diagram

$R_3$  is determined from the loading cycle being investigated, probably saved in a file as the cycle peak and valley (maximum and minimum) values,  $S_{\max}$  and  $S_{\min}$ . The relationships among the various means of representing the loading cycles are:

$$S_{alt} = \frac{S_{\max} - S_{\min}}{2}, \quad S_{mean} = \frac{S_{\max} + S_{\min}}{2}, \quad R = \frac{S_{\min}}{S_{\max}}$$

$R_1$  and  $R_2$  are taken as the values of tested R-values, from which the fatigue models can be determined from the general regression equations

$$\frac{S}{S_0} = C_1 - b \cdot \log(N) \quad \text{for the exponential regression fatigue model and}$$

$$\frac{S}{S_0} = C_2 N^{-1/m} \quad \text{for the power law regression fatigue model.}$$

Here  $S$  represents the maximum stress level for this particular fatigue model.  $S_0$  is the ultimate strength, either compressive or tensile.  $C_1$ ,  $b$ ,  $C_2$  and  $m$  are regression constants.  $N$  is the number of constant amplitude cycles to failure at the stress level  $S$ .

Exponential Algorithm

The solution for the number of cycles to failure that utilizes the exponential fatigue model is of closed form solution. Use the fatigue models for the two radial lines of tested R-values to determine the maximum stresses

$$S_{alt1} = \frac{S_0 * \left( C_{1,1} - b_1 * \log(N) \right) * (1 - R_1)}{2} \quad S_{alt2} = \frac{S_0 * \left( C_{1,2} - b_2 * \log(N) \right) * (1 - R_2)}{2}$$

$$S_{mean1} = \frac{S_0 * \left( C_{1,1} - b_1 * \log(N) \right) * (1 + R_1)}{2} \quad S_{mean2} = \frac{S_0 * \left( C_{1,2} - b_2 * \log(N) \right) * (1 + R_2)}{2}$$

Here  $C_{1,1}$  represents the exponential regression constant  $C_1$  and  $b_1$  represents the exponential regression constant  $b$  for the Goodman diagram radial line identified as  $R_1$ , etc. Substitute these expressions into the equations for the slopes of the constant cycle line.

$$\frac{\frac{S_0 * \left( C_{1,2} - b_2 * \log(N) \right) * (1 - R_2)}{2} - S_{alt3}}{\frac{S_0 * \left( C_{1,2} - b_2 * \log(N) \right) * (1 + R_2)}{2} - S_{mean3}} = \frac{\frac{S_0 * \left( C_{1,1} - b_1 * \log(N) \right) * (1 - R_1)}{2} - S_{alt3}}{\frac{S_0 * \left( C_{1,1} - b_1 * \log(N) \right) * (1 + R_1)}{2} - S_{mean3}}$$

Allow some simplifying substitutions:  $x = \log(N)$

$$K_1 = S_0 * C_{1,2} * \frac{(1-R_2)}{2} - S_{alt3}$$

$$K_2 = -S_0 * b_2 * \left( \frac{1-R_2}{2} \right)$$

$$K_3 = S_0 * C_{1,2} * \frac{(1+R_2)}{2} - S_{mean3}$$

$$K_4 = -S_0 * b_2 * \left( \frac{1+R_2}{2} \right)$$

$$K_5 = S_0 * C_{1,1} * \frac{(1-R_1)}{2} - S_{alt3}$$

$$K_6 = -S_0 * b_1 * \left( \frac{1-R_1}{2} \right)$$

$$K_7 = S_0 * C_{1,1} * \frac{(1+R_1)}{2} - S_{mean3}$$

$$K_8 = -S_0 * b_1 * \left( \frac{1+R_1}{2} \right)$$

The expression is now simplified as:

$$\frac{K_1 + K_2 * x}{K_3 + K_4 * x} = \frac{K_5 + K_6 * x}{K_7 + K_8 * x}$$

which becomes upon cross multiplication

$$K_1 K_7 + (K_2 K_7 + K_1 K_8) * x + K_2 K_8 * x^2 = K_3 K_5 + (K_3 K_6 + K_4 K_5) * x + K_4 K_6 * x^2$$

which rearranges to

$$(K_1 K_7 - K_3 K_5) + (K_2 K_7 + K_1 K_8 - K_3 K_6 - K_4 K_5) * x + (K_2 K_8 - K_4 K_6) * x^2 = 0$$

simplify this as

$$D_1 * x^2 + D_2 * x + D_3 = 0 \text{ which can be solved by use of the quadratic equation. Once}$$

the solution for x is known than N, the number of cycles to failure =  $10^x$ .

### Power Law Algorithm

The solution method for the number of cycles to failure when using the power law fatigue model is similar. The only major difference is that the solution is not in closed form. When following the same steps as outlined in the Exponential Algorithm section, the equations reduce as follows.



$$\frac{S_{alt2} - S_{alt3}}{S_{mean2} - S_{mean3}} = \frac{S_{alt1} - S_{alt3}}{S_{mean1} - S_{mean3}} \quad \text{The equal slope equation}$$

$$S_{alt1} = \frac{1-R_1}{2} * C_{2,1} * S_0 * N^{-1/m_1} \quad S_{mean1} = \frac{1+R_1}{2} * C_{2,1} * S_0 * N^{-1/m_1}$$

$$S_{mean2} = \frac{1+R_2}{2} * C_{2,2} * S_0 * N^{-1/m_2} \quad S_{alt2} = \frac{1-R_2}{2} * C_{2,2} * S_0 * N^{-1/m_2}$$

For simplification, define the following terms  $a = -\frac{1}{m_1}$  and  $b = -\frac{1}{m_2}$

$$A_1 = \frac{1-R_1}{2} * C_{2,1} * S_0 \quad A_2 = \frac{1+R_1}{2} * C_{2,1} * S_0 \quad B_1 = S_{alt3}$$

$$A_3 = \frac{1-R_2}{2} * C_{2,2} * S_0 \quad A_4 = \frac{1+R_2}{2} * C_{2,2} * S_0 \quad B_2 = S_{mean3}$$

Then the slope equation becomes simplified as

$$\frac{A_1 N^a - B_1}{A_2 N^a - B_2} = \frac{A_3 N^b - B_1}{A_4 N^b - B_2}$$

Which becomes the following upon cross multiplication

$$A_1 A_4 N^{a+b} - A_1 B_2 N^a - A_4 B_1 N^b + B_1 B_2 = A_2 A_3 N^{a+b} - A_2 B_1 N^a - A_3 B_2 N^b + B_1 B_2$$

which simplifies to

$$\left( A_1 A_4 - A_2 A_3 \right) N^{a+b} + \left( A_2 B_1 - A_1 B_2 \right) N^a + \left( A_3 B_2 - A_4 B_1 \right) N^b = 0$$

or as

$$D_1 N^{a+b} + D_2 N^a + D_3 N^b = 0$$

which is transcendental in form, but can be solved by successive substitution numerical methods. Rearrange the last equation as

$$N = \left( \frac{-D_2 N^a - D_3 N^b}{D_1} \right)^{1/(a+b)} \quad \text{here guess a value for N, calculate a new value}$$

of N using this equation, keep repeating until the percent difference between the last two calculated values of N, the number of cycles to failure is acceptable. Plotting the left hand and right hand side of the last equation against N revealed that the method would converge quite rapidly.

These methods were implemented in BASIC language computer algorithms, documented as follows.

Residual Strength Lifetime Prediction Program Based Upon the  
Exponential Fatigue Model

CLS	Clear screen
ON ERROR GOTO erhdlr	Specify subroutine for error handler
OPEN "c:\thesis\wisprx.dat" FOR OUTPUT AS #2	Open output file for depositing results of calculations
maxs = 414	Specify the maximum stress encountered in the spectrum
uts = 632: s = uts: s0 = uts	Specify the ultimate tensile strength and the initial residual strength
ucs = -400	Specify the ultimate compressive strength
cyc = 0: miners = 0	Zero total cycle counter and Miner's sum
nu = .265	Specify the nonlinear parameter in the residual strength equation
OPEN "c:\data\wisprx.dat" FOR INPUT AS #1	Open input file containing the desired spectrum
WHILE 1	Infinite loop, only exit is when applied stress exceeds the residual strength
WHILE NOT EOF(1)	Read until the end of the spectrum
INPUT #1, a\$	Input the peak value for the first cycle
INPUT #1, b\$	Input the valley value for the first cycle
smax3 = VAL(a\$) * maxs	Calculate the maximum stress, MPa
sl = smax3	Set the applied load to this stress
smin3 = VAL(b\$) * maxs	Calculate the minimum stress, MPa
r3 = smin3 / smax3	Calculate this cycle's R-value
GOSUB getn	Route to subroutine to calculate the number of cycles to failure at the current stress level
$c = ((s - s0) / (sl - s0)) ^ (1 / nu) * n$	Calculate the number of cycles required at this stress level based upon the residuals strength degradation curve for this stress level
cyc = cyc + 1	Increment the total cycle counter
c = c + 1	Increment the residual strength cycle counter for the present stress level
s = s0 + (sl - s0) * (c / n) ^ nu	Calculate the residual strength

<pre> miners = miners + 1 / n IF s &lt; sl THEN GOTO rept  'PRINT cyc; s; smax3 PRINT #2, USING "+#####;+###.##"; cyc; s WEND PRINT cyc, smax3 SEEK #1, 1  WEND rept: PRINT miners, cyc, maxs CLOSE END  getn: </pre>	<pre> Adjust Miner' sum If the applied stress is greater than the residual strength, exit Print intermediate results to screen Print intermediate results to file End of first sweep through spectrum Print intermediate results to screen Reset input file pointer to the beginning to allow another sweep through the spectrum End of infinite loop Infinite loop exit flag Print results to screen Close all open files End of program </pre>
<pre> IF r3 &gt; 1 AND r3 &lt; 2 THEN region = 1 'print "case 1, 1 &lt; r3 &lt; 2" c2 = 1 * ucs: b2 = .062 * ucs: r2 = 2 salt3 = (smax3 - smin3) / 2 smean3 = (smax3 + smin3) / 2 k1 = -2 * salt3 * ucs k1 = k1 / (-salt3 * (1 + r2) / r2 - (ucs - smean3) * (1 - r2) / r2) n = 10 ^ ((c2 - k1) / b2) END IF </pre>	<pre> Subroutine to calculate number of cycles to failure  R-value region between 1 and 2  specify fatigue model constants Intermediate calculations  Calculate number of cycles to failure </pre>
<pre> IF r3 &gt; 2 AND r3 &lt; 10 THEN region = 2 'PRINT TAB(5); "case 2, 2 &lt; r3 &lt; 10" c2 = .994 * ucs: b2 = .081 * ucs c1 = 1 * ucs: b1 = .062 * ucs r2 = 10 r1 = 2 salt3 = (smax3 - smin3) / 2 smean3 = (smax3 + smin3) / 2 k1 = c2 * (1 - r2) / (2 * r2) - salt3 k2 = -b2 * (1 - r2) / (2 * r2) k3 = smean3 - c1 * (1 + r1) / (2 * r1) k4 = b1 * (1 + r1) / (2 * r1) k5 = salt3 - c1 * (1 - r1) / (2 * r1) k6 = b1 * (1 - r1) / (2 * r1) k7 = c2 * (1 + r2) / (2 * r2) - smean3 k8 = -b2 * (1 + r2) / (2 * r2) a = k2 * k4 - k6 * k8 b = k1 * k4 + k2 * k3 - k5 * k8 - k6 * k7 c = k1 * k3 - k5 * k7 rt = b ^ 2 - 4 * a * c n = (-b - rt ^ .5) / (2 * a) </pre>	

```

      n = 10 ^ n
END IF

IF r3 > 10 OR r3 < -1 THEN
region = 3
  'PRINT TAB(10); "case 3, r3 > 10 or r3 < -1"
  c1 = .994 * ucs: b1 = .125 * ucs: r1 = -1
  c2 = .994 * ucs: b2 = .081 * ucs: r2 = 10
  salt3 = (smax3 - smin3) / 2
  smean3 = (smax3 + smin3) / 2
  k1 = c2 * (1 - r2) / (2 * r2) - salt3
  k2 = -b2 * (1 - r2) / (2 * r2)
  k3 = smean3
  k5 = c2 * (1 + r2) / (2 * r2) - smean3
  k6 = -b2 * (1 + r2) / (2 * r2)
  k7 = salt3 - c1 * (1 - r1) / (2 * r1)
  k8 = b1 * (1 - r1) / (2 * r1)
  a = k6 * k8
  b = k5 * k8 + k6 * k7 - k2 * k3
  c = k5 * k7 - k1 * k3
  n = (-b - (b ^ 2 - 4 * a * c) ^ .5) / (2 * a)
  n = 10 ^ n
END IF

```

```

IF r3 > -1 AND r3 < .1 THEN
region = 4
  'PRINT TAB(15); "case 4, -1 < r3 < 0.1"
  c1 = .955 * uts: b1 = .12 * uts: r1 = .1
  c2 = .994 * ucs: b2 = .125 * ucs: r2 = -1
  salt3 = (smax3 - smin3) / 2
  smean3 = (smax3 + smin3) / 2
  k1 = c2 * (1 - r2) / (2 * r2) - salt3
  k2 = -b2 * (1 - r2) / (2 * r2)
  k3 = smean3 - c1 * (1 + r1) / 2
  k4 = b1 * (1 + r1) / 2
  k5 = -smean3
  k7 = salt3 - c1 * (1 - r1) / 2
  k8 = b1 * (1 - r1) / 2
  a = k2 * k4
  b = k1 * k4 + k2 * k3 - k5 * k8
  c = k1 * k3 - k5 * k7
  n = (-b + (b ^ 2 - 4 * a * c) ^ .5) / (2 * a)
  n = 10 ^ n
END IF

```

```

IF r3 > .1 AND r3 < .5 THEN
region = 5
  'PRINT TAB(20); "case 5, 0.1 < r3 < 0.5"
  c1 = .955 * uts: b1 = .12 * uts
  c2 = .99 * uts: b2 = .107 * uts
  r1 = .1
  r2 = .5

```

```

salt3 = (smax3 - smin3) / 2
smean3 = (smax3 + smin3) / 2
k1 = c2 * (1 - r2) / 2 - salt3
k2 = -b2 * (1 - r2) / 2
k3 = smean3 - c1 * (1 + r1) / 2
k4 = b1 * (1 + r1) / 2
k5 = salt3 - c1 * (1 - r1) / 2
k6 = b1 * (1 - r1) / 2
k7 = c2 * (1 + r2) / 2 - smean3
k8 = -b2 * (1 + r2) / 2
a = k2 * k4 - k6 * k8
b = k1 * k4 + k2 * k3 - k5 * k8 - k6 * k7
c = k1 * k3 - k5 * k7
rt = b ^ 2 - 4 * a * c
n = (-b - rt ^ .5) / (2 * a)
n = 10 ^ n
END IF

IF r3 < 1 AND r3 > .5 THEN
region = 6
  PRINT TAB(25); "case 6, 0.5 < r3 < 1"
  c1 = .99 * uts: b1 = .107 * uts: r1 = .5
  salt3 = (smax3 - smin3) / 2
  smean3 = (smax3 + smin3) / 2
  k1 = (-2 * uts * salt3)
  k1 = k1 / ((1 - r1) * (smean3 - uts) - (1 + r1) * salt3)
  n = 10 ^ ((c1 - k1) / b1)
END IF

IF r3 = 2 THEN
region = 7
  c3 = 1! * ucs: b3 = .062 * ucs
  n = 10 ^ ((c3 - smin3) / b3)
END IF

IF r3 = 10 THEN
region = 8
  c3 = .994 * ucs: b3 = .081 * ucs
  n = 10 ^ ((c3 - smin3) / b3)
END IF

IF r3 = -1 THEN
region = 9
  c3 = .994 * ucs: b3 = .125 * ucs
  n = 10 ^ ((c3 - smin3) / b3)
END IF

IF r3 = .1 THEN
region = 10
  c3 = .955 * uts: b3 = .12 * uts
  n = 10 ^ ((c3 - smax3) / b3)
END IF

```

```

IF r3 = .5 THEN
region = 11
  c3 = .99 * uts: b3 = .107 * uts
  n = 10 ^ ((c3 - smax3) / b3)
END IF

```

```
RETURN
```

```

erhdlr:
PRINT r3; smax3; c; cyc; a; s; s0
END

```

### Residual Strength Lifetime Prediction Program Based Upon the Power Law Fatigue Model

<pre> CLS ON ERROR GOTO erhdlr maxs = 414  uts = 632  s0 = uts: ra# = 1: s = uts  ucs = -400  cyc = 0: miners = 0  nu = .265  OPEN "c:\data\wisprx.dat" FOR INPUT AS #1  OPEN "c:\data\resid.dat" FOR OUTPUT AS #2  WHILE 1  WHILE NOT EOF(1)    INPUT #1, a\$   INPUT #1, b\$    smax = VAL(a\$) * maxs   smin = VAL(b\$) * maxs </pre>	<pre> Clear screen Direction to error handler subroutine Maximum stress in the spectrum, MPa Define ultimate tensile strength, MPa Initialize values. Assumes initial load in spectrum is tensile and sets the normalized residual strength to one and initial strength to the uts Define ultimate compressive strength, MPa Initialize total cycle counter and Mianer's sum Specify the exponent in the nonlinear residual strength calculations Open an input file containing the spectrum for which this run is being made Open an output file for which calculated results can be deposited Begin infinite loop. Only exit is when the applied stress exceeds the residual strength Read input file until the end. Will be repeated if necessary  Read the peak value of the first cycle Read the valley value of the first cycle Calculate the maximum stress, MPa Calculate the minimum stress, MPa </pre>
--	--

r = smin / smax	Calculate the R-value for the current cycle
IF r < ucs / uts THEN rl# = smin / ucs ELSE rl# = smax / uts	Determine if the failure mode for this cycle is dominated by tensile or compressive behavior
GOSUB getn	Get the number of cycles to failure at the current stress level
c = ((ra# - 1) / (rl# - 1)) ^ (1 / nu) * n	Calculate the number of cycles to get to the present stress level on the residual strength curve for the present stress level
cyc = cyc + 1	Increment the total number of cycles
c = c + 1	Increment the cycles of this stress level by one
ra# = 1 - (1 - rl#) * (c / n) ^ nu	Calculate the normalized residual strength
miners = miners + 1 / n	Increment the Miner's sum by the contribution of one cycle at the present stress level
IF ra# < rl# THEN GOTO rept	Exit the infinite loop if the present stress exceeds the residual strength
'PRINT USING "smax=+####.# cyc=##### rl=+##.### ra=+##.###"; smax; cyc; rl#; ra#	Print intermediate calculated results
to screen	
'PRINT #2, USING "+##### , +####.###"; cyc; ra#	print intermediate calculated results to file
WEND	End of loop reading the input file
PRINT miners, cyc, ra#, rl#	Print intermediate calculated results
SEEK #1, 1	Reset input file pointer to the beginning of file. Necessary if spectrum if swept more than once
WEND	End of infinite loop, only exit is if applied stress is greater than residual strength
rept:	Flag for routing control of program upon calculated specimen failure
PRINT miners, cyc, maxs, ra#, rl#	Print final results to screen
CLOSE	Close any open files
END	End of routine
getn:	Subroutine to calculate number of cycles to failure at the current stress level if a constant amplitude test

The following are calculation modules depending upon the R-value range.

IF r > 1 AND r3 < 2 THEN	R-value must be between 1 and 2
'region = 1	
r1 = 2: c1 = 1: m1 = 29.82	Specify the R-value limits for this region and the fatigue model's constants



<pre> a1 = (-c1 * ucs * (1 - r1)) / r1 a2 = (-c1 * ucs * (1 + r1)) / r1 a3 = (smin * (1 - r) / r) / (2 * ucs - smin * (1 + r) / r) x = (b1 * a3) / (a1 - a2 * a3) n = x ^ -m1 END IF  IF r &gt; 2 AND r &lt; 10 THEN 'region = 2  END IF  IF r &gt; 10 OR r &lt; -1 THEN  'region = 3 c1 = 1.005: c2 = .998  m1 = 21.55: m2 = 11.158  r1 = 10: r2 = -1  a1 = (1 - r1) / (2 * r1) * c1 * ucs a2 = (1 + r1) / (2 * r1) * c1 * ucs a3 = (1 - r2) / (2 * r2) * c2 * ucs a4 = (1 + r2) / (2 * r2) * c2 * ucs a = -1 / m1: b = -1 / m2 b1 = (smax - smin) / 2: b2 = (smax + smin) / 2 d1 = a2 * a3 - a1 * a4 d2 = a1 * b2 - a2 * b1 d3 = a4 * b1 - a3 * b2 x1 = 6000  i = 0 WHILE 1      i = i + 1     x = ((-d2 * x1 ^ a - d3 * x1 ^ b) / d1) ^ (1 / (a + b))     lx = LOG(x) / LOG(10): lxl = LOG(x1) / LOG(10)      IF ABS((lx - lxl) / lx) * 100 &lt; .01 THEN GOTO rept3      x1 = x  WEND rept3: n = x  END IF  IF r &gt; -1 AND r3 &lt; .1 THEN 'region = 4 </pre>	<p>Calculate intermediate results</p> <p>Calculate number of cycles to failure End of calculations for this region</p> <p>R-values must be between 2 and 10 This region is never encountered for the WISPERX spectrum, hence no equations. End of calculations for this region</p> <p>R-values must be between -1 and 10 (through infinity)</p> <p>Specify the fatigue models' constants Specify the fatigue models' constants Specify the R-value limits for this region Calculate intermediate results</p> <p>Gaussian solution is implemented, this is the initial guess at the solution Zero pass counter Infinite pass loop, exit is allowed upon acceptable percent error Increment counter Gaussian solution equation Specify intermediate results in log scale Check percent error is less than 0.01 % Redefine the last calculated result to be the present End of infinite loop Infinite loop exit flag Specify the number of cycles to failure End of calculations for this region</p> <p>R-values must be between -1 and 0.1</p>
---	--

r1 = -1: r2 = .1	Specify the R-value limits for this region
c1 = .998: c2 = 1.005	Specify the fatigue model's constants
m1 = 11.158: m2 = 11.478	Specify the fatigue model's constants
a1 = (1 - r1) / (2 * r1) * c1 * ucs	Intermediate calculations
a2 = (1 + r1) / (2 * r1) * c1 * ucs	
a3 = (1 - r2) / 2 * c2 * uts	
a4 = (1 + r2) / 2 * c2 * uts	
b1 = (smax - smin) / 2: b2 = (smax + smin) / 2	
d1 = a2 * a3 - a1 * a4	
d2 = a1 * b2 - a2 * b1	
d3 = a4 * b1 - a3 * b2	
a = -1 / m1: b = -1 / m2	
x1 = 6000	Initial guess at solution
i = 0	Zero pass counter
WHILE 1	Infinite pass loop, exit is allowed upon acceptable percent error
i = i + 1	Increment pass counter
x = ((-d2 * x1 ^ a - d3 * x1 ^ b) / d1) ^ (1 / (a + b))	Gaussian solution equation
lx = LOG(x) / LOG(10): lx1 = LOG(x1) / LOG(10)	Place solution in log form
IF ABS((lx - lx1) / lx) * 100 < .01 THEN GOTO rept1	Check percent error
x1 = x	Redefine last calculated value
WEND	End of infinite loop
rept1:	Infinite loop exit flag
n = x	Specify the number of cycles to failure
END IF	End of calculations for this region
IF r > .1 AND r3 < .5 THEN	R-values must be between 0.1 and 0.5
'region = 5	
r1 = .1: r2 = .5	Specify the R-value limits for this region
c1 = 1.005: c2 = 1.013	Specify fatigue models' constants
m1 = 11.478: m2 = 14.4	Specify fatigue models' constants
a1 = c1 * uts * (1 - r1)	Intermediate calculations
a2 = c2 * uts * (1 - r2)	
a3 = c1 * uts * (1 + r1)	
a4 = c2 * uts * (1 + r2)	
b1 = smax * (1 - r)	
b2 = smax * (1 + r)	
d1 = a1 * a4 - a2 * a3	
d2 = a3 * b1 - a1 * b2	
d3 = -a4 * b1 + a2 * b2	
a = -1 / m1: b = -1 / m2	
x1 = 6000	Initial guess
i = 0	Zero counter
WHILE 1	Gaussian solution loop
i = i + 1	Increment counter
x = ((-d2 * x1 ^ a - d3 * x1 ^ b) / d1) ^ (1 / (a + b))	Gaussian equation

lx = LOG(x) / LOG(10): lx1 = LOG(x1) / LOG(10)	Log form
IF ABS((lx - lx1) / lx) * 100 < .00001 THEN GOTO rept2	Check percent error
x1 = x	Redefine last value
WEND	End of loop
rept2:	Infinite loop exit flag
n = x	Specify the number of cycles to failure
END IF	End of calculations for this region
IF r < 1 AND r3 > .5 THEN	R-values must be between 1 and 0.5
'region = 6	There are no R-values in this range in WISPERX
END IF	End of this region's calculations
IF r3 = 2 THEN	R-value must be 2
'region = 7	Specify fatigue model's constants
c1 = 1!: m1 = 29.82	Closed form calculation of number of cycles to failure
n = (smin / (c1 * ucs)) ^ -m1	End of calculations for this region
END IF	
IF r = 10 THEN	R-value must be 10
'region = 8	Specify fatigue model's constants
c1 = 1.005: m1 = 21.55	Closed form calculation of number of cycles to failure
n = (smin / (c1 * ucs)) ^ -m1	End of calculations for this region
END IF	
IF r = -1 THEN	R-value must be -1
'region = 9	Specify fatigue model's constants
c1 = .998: m1 = 11.158	Closed form calculation of number of cycles to failure
n = (smax / (c1 * uts)) ^ -m1	End of calculations for this region
END IF	
IF r = .1 THEN	R-value must be 0.1
'region = 10	Specify fatigue model's constants
c1 = 1.005: m1 = 11.478	Closed form calculation of number of cycles to failure
n = (smax / (c1 * uts)) ^ -m1	End of calculations for this region
END IF	
IF r = .5 THEN	R-value must be 0.5
'region = 11	Specify fatigue model's constants
c1 = 1.013: m1 = 14.4	Closed form calculation of number of cycles to failure
n = (smax / (c1 * uts)) ^ -m1	End of calculations for this region
END IF	
RETURN	End of number of cycle calculation subroutine

```

erhdlr:
PRINT r3; smax3; c; cyc; a; s; s0
END

```

```

Error handler subroutine flag
Print results at point of error
End of program

```

### Linear Elastic Fracture Mechanics Algorithm

Software was also developed to allow the implementation of linear elastic fracture mechanic methods for comparison between predicted metals and laminate lifetimes. The following LEFM BASIC program was prepared including retardation and for two blocks of load levels.

CLS	Clear screen
OPEN "c:\temp.dat" FOR OUTPUT AS #1	Open a file for storing calculation results
co = 3 * 10 ^ -10	Define the constant coefficient in $da/dn = C \Delta K^n$
ad# = 5	Minimum detectable crack size, mm
Sa = 13.5	First block maximum stress, kg/mm <sup>2</sup>
Sb = 5	Second block maximum stress, kg/mm <sup>2</sup>
sys = 51	Yield stress, kg/mm <sup>2</sup>
k1c = 104	K <sub>1C</sub> , kg/mm <sup>3/2</sup>
pi = 3.1415926#	
ac1# = k1c ^ 2 / pi / Sa ^ 2	calculate the critical crack size for the stress Sa
ac2# = k1c ^ 2 / pi / Sb ^ 2	calculate the critical crack size for the stress Sb
n1 = 10	number of cycles in the first block
n2 = 100	number of cycles in the second block
nn1 = 1495	number of cycles to failure at constant amp of max stress Sa
nn2 = 76643	number of cycles to failure at constant amp of max stress Sb
a# = ad#	initial crack size set to minimum detectable crack size
miners = 0	zero the Miner's number accumulator
j = 0: jh = 0: jl = 0	zero the total and individual block cycle counters
WHILE 1	begin infinite fatigue loop, only exit is when critical crack size is reached
FOR i = 1 TO n1	beginning of loop for first block
j = j + 1: jh = jh + 1	increment the total and first block cycle counters

<pre> k# = Sa * (pi * a#) ^ .5 dadn# = co * k# ^ 4 a# = a# + dadn# 'PRINT #1, USING "##### , ###.###"; j; a# miners = miners + 1 / nn1 IF a# &gt;= ac1# THEN GOTO rept  NEXT i  rp0# = k# ^ 2 / (6 * pi * sys ^ 2)  ap0# = a# + rp0#  k# = Sb * (pi * a#) ^ .5 rp# = k# ^ 2 / (6 * pi * sys ^ 2) 'PRINT rp0#, rp#  FOR i = 1 TO n2 k# = Sb * (pi * a#) ^ .5 dadn# = co * k# ^ 4  IF ap0# - a# &lt;= 0 THEN phi = 1 ELSE phi = (rp# / (ap0# - a#)) ^ 1.3  IF Sa = Sb THEN phi = 1  'PRINT phi; a#; j; dadn# j = j + 1; jl = jl + 1 a# = a# + phi * dadn#  'PRINT #1, USING "##### , ###.###"; j; a# miners = miners + 1 / nn2 IF a# &gt;= ac2# THEN GOTO rept  NEXT i WEND  rept: CLOSE #1   PRINT "miners  n1    n2    ac1    ac2    a    j    jh    jl" PRINT USING "#.### #####  #####  ##.###  ###.###  ##.###  #####  #####  #####"; miners; n1; n2; ac1#; ac2#; a#; j; jh; jl  END </pre>	<pre> calculate the current stress intensity factor calculate the crack growth rate for this cycle calculate the new crack size print results to file update the Miner's number accumulator compare the current crack size to the critical crack size  end of loop for the first block  calculate the plastic zone size for the last cycle of the first block calculate the extent the crack size must be to grow through the plastic zone calculate the current stress intensity factor calculate the plastic zone size at the present load value debug print statement  beginning of the loop for the second block calculate the current stress intensity factor calculate the crack growth rate for this cycle  determine the retardation factor if the blocks have the same load there can be no retardation factor debug print statement increment the total and second block cycle counters calculate the new crack size  print results to file update the Miner's number accumulator compare the current crack size to the critical crack size  end of loop for second block end of infinite fatigue loop  label for exit of fatigue loop close the open file print header information to screen for observation print calculation results to screen for observation end of program </pre>
--	---

Rainflow counting program was based upon the work of Socie and Downing [48]

```

WINDOW (0, 0)-(100, 100)
CLS
  INPUT "ENTER DRIVE:\FILENAME.EXT"; AA$
  OPEN AA$ FOR INPUT AS #1
max = -1000000!: min = 1000000!: i = 0
WHILE NOT EOF(1)
  INPUT #1, val1
  i = i + 1
  IF val1 > max THEN
    max = val1
    imax = i
  END IF
  IF val1 < min THEN
    min = val1
    imin = i
  END IF
WEND
SEEK #1, 1
numrec = i
PRINT USING "Number of records is #####."; numrec

PRINT USING "Maximum of +###.## occurs at #####."; max; imax
PRINT USING "Minimum of +###.## occurs at #####."; min; imin

OPEN "c:\ranavg.dat" FOR OUTPUT AS #2
IF NOT EOF(1) THEN INPUT #1, val1
val2 = val1: val3 = val2: val4 = val3: val5 = val4
val6 = val5: val7 = val6: val8 = val7

DIM e(1000)
n = 2
j = 0
istart = 1
GOSUB getdata
e(1) = vvv
100 GOSUB getdata
e(2) = vvv
IF e(1) = e(2) GOTO 100
slope = 1
IF e(1) > e(2) THEN slope = -1
1 GOSUB getdata
p = vvv
IF (v = 1) THEN GOTO 6
n = n + 1
slope = slope * -1
e(n) = p
2 IF (n < istart + 1) THEN GOTO 1
x = slope * (e(n) - e(n - 1))
IF x <= 0 THEN GOTO 200
IF (n < istart + 2) THEN GOTO 1
y = slope * (e(n - 2) - e(n - 1))
3 IF x < y THEN GOTO 1

```

```

IF x = y AND irstart = n - 2 THEN GOTO 1
IF x > y AND irstart = n - 2 THEN GOTO 4
IF x >= y AND irstart <> n - 2 THEN GOTO 5
4  irstart = irstart + 1
   GOTO 1
5  range = y
   xmean = (e(n - 1) + e(n - 2)) / 2
   PRINT #2, range, xmean
   n = n - 2
   e(n) = e(n + 2)
   GOTO 2
6  j = j + 1
   IF j > irstart THEN GOTO skip1
   n = n + 1
   slope = slope * -1
   e(n) = e(j)
7  IF n < irstart + 1 THEN GOTO 6
   x = slope * (e(n) - e(n - 1))
   IF x <= 0 THEN GOTO 300
   IF n < irstart + 2 THEN GOTO 6
   y = slope * (e(n - 2) - e(n - 1))
8  IF x < y THEN GOTO 6
   IF x >= y THEN GOTO 9
9  range = y
   xmean = (e(n - 1) + e(n - 2)) / 2
   PRINT #2, range, xmean
   n = n - 2
   e(n) = e(n + 2)
   GOTO 7
200 n = n - 1
    e(n) = e(n + 1)
    slope = slope * -1
    GOTO 2
300 n = n - 1
    e(n) = e(n + 1)
    slope = slope * -1
    GOTO 7
skip1:
  CLOSE
  GOSUB count
  END

getdata:

repeat:
  IF NOT EOF(1) THEN INPUT #1, val1 ELSE v = 1: RETURN
  vvv = val1
  xx = xx + .01
  PSET (xx, vvv), 2
  IF xx > 100 THEN
    xx = 0

```

```

      CLS
    END IF
    IF a$ = "valid" THEN
      PSET (xx, vvv + 10)
      v = 0
      lastval4 = val4
      RETURN
    END IF
    IF a$ = "invalid" THEN GOTO repeat
  RETURN

```

count:

```

OPEN "c:\ranavg.dat" FOR INPUT AS #1
maxran = -1000000: minran = 1000000
maxavg = -1000000: minavg = 1000000
WHILE NOT EOF(1)
INPUT #1, ran, avg
  IF ran > maxran THEN maxran = ran
  IF ran < minran THEN minran = ran
  IF avg > maxavg THEN maxavg = avg
  IF avg < minavg THEN minavg = avg

```

```

WEND
PRINT maxran, minran, maxavg, minavg
SEEK #1, 1

```

```

'PRINT "maxran", maxran, "minran", minran, "maxavg", maxavg, "minavg", minavg
'END

```

rpt1:

```

INPUT "auto range (y or n)"; a$
  IF a$ = "N" OR a$ = "n" THEN
skip2:
    INPUT "enter range upper and lower limits."; ranup, ranlw
    INPUT "enter mean upper and lower limits."; avgup, avglw
    IF ranup < maxran OR ranlw > minran OR avgup < maxavg OR avglw > minavg THEN
      PRINT "data max or min exceed specified limits. Try again."
      GOTO skip2
    END IF
  END IF

```

```

IF a$ = "Y" OR a$ = "y" THEN
  avgup = 1.1 * maxavg: avglw = .9 * minavg
  ranup = 1.1 * maxran: ranlw = .9 * minran
END IF

```

```

IF a$ <> "N" AND a$ <> "n" AND a$ <> "Y" AND a$ <> "y" THEN GOTO rpt1

```

rpt2:



```

INPUT "enter number of range bins."; rann
INPUT "enter number of mean bins."; avgn
IF rann = 0 OR avgn = 0 THEN GOTO rpt2
DIM rancenter(rann), avgcenter(avgn), count(rann, avgn)
'find bin size and spacing

delavgbin = (avgup - avglw) / avgn
delranbin = delavgbin
delranbin = (ranup - ranlw) / rann

FOR i = 1 TO rann
  rancenter(i) = ranlw + (i - .5) * delranbin
NEXT i
FOR i = 1 TO avgn
  avgcenter(i) = avglw + (i - .5) * delavgbin
NEXT i

FOR i = 1 TO rann
  FOR j = 1 TO avgn
    count(i, j) = 0
  NEXT j
NEXT i

WHILE NOT EOF(1)

INPUT #1, ran, avg

FOR i = 1 TO rann
  IF ran <= rancenter(i) + .5 * delranbin AND ran >= rancenter(i) - .5 * delranbin THEN
    tempi = i
    GOTO skip3
  END IF
NEXT i

skip3:

FOR j = 1 TO avgn
  IF avg <= avgcenter(j) + .5 * delavgbin AND avg >= avgcenter(j) - .5 * delavgbin THEN
    tempj = j
    GOTO skip4
  END IF
NEXT j

skip4:

count(tempi, tempj) = count(tempi, tempj) + 1

WEND

CLOSE

OPEN "c:\binned.dat" FOR OUTPUT AS #1

```

```

OPEN "d:\cycnt.dat" FOR OUTPUT AS #2
  PRINT #1, USING "Number of records is #####."; numrec
  PRINT #1, USING "Maximum of +###.## occurs at #####."; max; imax
  PRINT #1, USING "Minimum of +###.## occurs at #####."; min; imin

PRINT "Range Bin   Mean Bin"
PRINT " Center     Center   Count"
PRINT #1, "Range Bin   Mean Bin"
PRINT #1, " Center     Center   Count"

k = 0
FOR i = 1 TO rann
  FOR j = 1 TO avgn
    IF count(i, j) <> 0 THEN
      PRINT USING "+###.### +###.### #####"; rancenter(i); avgcenter(j); count(i, j)
      PRINT #1, USING "+###.### +###.### #####"; rancenter(i); avgcenter(j); count(i, j)
      PRINT #2, rancenter(i), ",", avgcenter(j), ",", count(i, j)
    END IF

    k = k + count(i, j)
  NEXT j
NEXT i
PRINT "total cycles = "; k
PRINT #1, "total cycles = "; k

CLOSE
OPEN "c:\mat.dat" FOR OUTPUT AS #1
PRINT #1, 0
FOR i = 1 TO avgn - 1
  PRINT #1, avgcenter(i);
NEXT i
PRINT #1, avgcenter(avgn)

FOR i = 1 TO rann
  PRINT #1, rancenter(i);
  FOR j = 1 TO avgn - 1
    PRINT #1, count(i, j);
  NEXT j
  PRINT #1, count(i, avgn)
NEXT i

CLOSE

```